ABSTRACT

Azuma, Chieko. Evaluation of tumor hypoxia and proliferation in canine spontaneous solid tumors (Under the direction of Donald E. Thrall)

Tumor hypoxia and proliferation have been shown to be related to malignant tumor progression and treatment resistance. Studying tumor hypoxia and proliferation is important to address the biology of tumors and problems which may limit successful therapy. Tumor oxygenation is directly affected by oxygen consumption of tumors. Oxygen consumption is increased in actively proliferating cells. In this study the primary aim was to study the relationship between tumor hypoxia and proliferation in canine spontaneous solid tumors using immunohistochemical methods. Hypoxia was determined by detecting exsogenous hypoxia marker, pimonidazole adducts and proliferation was determined by the fraction of cells labeled with proliferating cell nuclear antigen. We hypothesized that hypoxia may be more pronounced in rapidly proliferating tumors due to increased oxygen consumption.

Pimonidazole adduct formation occurred within 20 minutes after intravenous administration and cells with adducts were stable for several days in canine spontaneous tumors. Rapid and stable adduct formation *in vivo* are the important characteristics of using pimonidazole as a clinically useful hypoxia marker. There was no association between tumor hypoxia and proliferation evaluated by immunohistochemistry. The clinical outcome of the dogs studied in the project is unknown at this time, but these results to date suggest that tumor hypoxia and proliferation measurements are independent and may be potentially complementary predictive factors in canine spontaneous tumors.

Classic diffusion limited hypoxia may be more related to intensive areas of pimonidazole labeling and transient perfusion limited hypoxia may not have been detected with our

technique. Perfusion limited hypoxia being related to proliferation might be more complex because the areas of hypoxia are transient and such areas still might be actively proliferating under the transient hypoxic conditions. Methods need to be developed to differentiate acute versus chronic hypoxia to know the true hypoxic fractions and their effects on tumor biology. The type of cells may affect estimates of hypoxia by pimonidazole labeling and it is necessary to evaluate histologic features before designing a study. The hypoxia marker pimonidazole is a powerful tool that can be used in a clinical setting to study tumor biology with minimum invasiveness.

EVALUATION OF TUMOR HYPOXIA AND PROLIFERATION IN CANINE SPONTANEOUS SOLID TUMORS

by

CHIEKO AZUMA

A dissertation submitted to the Graduate Faculty of
North Carolina State University
in partial fulfillment of the
requirements for the Degree of
Doctor of Philosophy

COMPARATIVE BIOMEDICAL SCIENCES

Raleigh

2004

APPROVED BY:

Donald E. Thrall Chair of Advisory Committee	**James A. Raleigh**
Marlene L. Hauck	**Philip L. Sannes**

BIOGRAPHY

Chieko Azuma was born August 19, 1966 in Aichi-ken, Japan to Hiroko and Kunio Shimizu. She graduated from Yakuendai High School, Chiba, Japan in 1985. In 1992, Chieko graduated from Nippon Veterinary and Animal Science University, Japan with a Bachelor of Veterinary Medicine degree. An opportunity to expand her education in came 1994 and Chieko entered a Ph.D. program at North Carolina State University, College of Veterinary Medicine. In 1996, she joined NCSU as a research associate in Anatomy, Pathology and Radiology. In 1998, she completed the clinical radiation oncology training program at NCSU. In 2000, she became a Clinical Assistant Professor in Anatomy, Pathology and Radiology. She joined Tufts University School of Veterinary Medicine as an Assistant Professor in department of Clinical Sciences in March of 2001 and she successfully completed her board certification in Veterinary Radiation Oncology and became a member of the American College of Veterinary Radiology (Radiation Oncology) in September of 2001. She directs the clinical program and residency program in radiation oncology at Tufts University School of Veterinary Medicine. She married Yoshihiro Azuma in 1992 and they have two beautiful children, Youki born in 1997 and Miki born in 1999.

ACKNOWLEDGEMENTS

I would like to thank Dr. Don Thrall for the tremendous support that he has given me during my Ph.D. program and all activities I have done at NCSU. He is the best teacher I have ever had and a friend. I could not have done it without him and I do intend to pay it forward. My special thanks goes to Drs. Jim Raleigh and Gary Rosner for their help to move it forward.

I appreciate the strong background in radiation biology that I received under the tutelage of Drs. Zeman and Dewhirst. A big thank you goes to the members of my Ph.D. committee who are not already thanked above, Drs. Rod Page, Marlene Hauck and Phil Sannes.

I also would like to give thanks generous support provided by Drs. Kawamura and Nagata from Japan.

On a personal note, I would like to thank my parents, Hiroko and Kunio Shimizu, who always encouraged me to pursue my career goals and who helped support me, financially and otherwise, throughout the many years that I have been in school. I also acknowledge my brother, Dr. Takeshi Shimizu for his support. I very much want to thank my husband, Yoshihiro, his family and our children, Youki and Miki, from the bottom of my heart, for the tremendous support and compassion that they have afforded me during this long Journey. I really couldn't have done it without them.

TABLE OF CONTENTS

LIST OF TABLES

LIST OF FIGURES

LIST OF SYMBOLS AND ABBREVIATIONS

ABC	Avidin-biotin complex
ACA	Adenocarcinoma
AgNORs	The silver-stained nucleolar organizer regions
AnCA	Anaplastic carcinoma
ATP	Adenosine triphosphate
ANOVA	Analysis of variance
bFGF	Basic fibroblast growth factor
Bx	Biopsy
BrdU/BrdUrd	Bromodeoxyuridine
CA	Carcinoma
CA9	Carbonic anhydrase-9
CCI-103F	Hexafluorinated 2-nitroimidazole, F6, 1-(2-hydroxy-3-hexafluoroisopropoxy-propyl)-2-nitroimidazole
cm	Centimeter-0.01 meters
CO	Carbon monoxide
CO_2	Carbon dioxide
CT	Computerized axial tomography (scan)
CSA	Chondorosarcoma
DNA	Deoxyribonucleic acid
Dx	Diagnosis
ELISA	Enzyme-linked immunosorbent assay
ER	Endoplasmic reticulum
FMISO	[18F]fluoromisonidazole
FNA	Fine needle aspiration - a type of biopsy using a thin needle (or FNAB)
DiOC7(3)	Carbocyanine dye
EPO	Erythropoietin
FSA	Fibrosarcoma
Gy	Grays (units of radiation)
H&E	Hematoxylin and Eosin (stain)
HAS	Hemangiosarcoma

Hb	Hemoglobin
HbO_2	Oxyhemoglobin
HIF-1	Hypoxia inducible factor - 1
HPC	Hemangiopericytoma
HPF	High power field
HPLC	High performance liquid chromatography
hsp70	Heat shock protein, protective proteins
^{3}H-TdR	Tritiated thymidine
I-131	Radioactive Iodine
ICF	Intercellular fluid
IFP	Interstitial fluid pressure
IdUrd	Iododeoxy uridine
IgG	Immunoglobulin
IHC	Immunohistochemistry
IMISO	[(131)I] iodomisonidazole
IV	Intravenous - into a vein
kD	Kilodalton – unit of mass
kg	Kilogram - a thousand grams
l	Liter - unit of volume
LDH	Lactic dehydrogenase
LET	Linear energy transfer
LI	Labeling index
LN	Lymph Node
LPSA	Liposarcoma
mAb	Monoclonal antibody
MDR	Multi drug resistant
mg	milligram - 0.001 gram
ml	milliliter - 0.001 liter
mM	millimole
MPNST	Malignant Peripheral Nerve Sheath Tumor
MRI	Magnetic resonance imaging (scan)
MSA	Myxosarcoma

NaCl	sodium chloride
NIH	National Institutes of Health
NITP	7-(4'-(2-nitroimidazole-1-yl)-butyl)-theophylline
NMR	Nuclear magnetic resonance (scan)
NF	Neurofibroma
NFSA	Neurofibrosarcoma
O_2	Oxygen
OER	Oxygen enhancement ratio
PAP	Peroxidase-antiperoxidase
PC 10	Mouse anti-human PCNA monoclonal antibody, Dako Corp., Carpinteria, CA
PCNA	Proliferating cellular nuclear antigen
PET	Positron Emission Tomography- a scan after a small radioactive injection
PFCE	Perfluorochemical emulsion
pH	Hydrogen-ion concentration - acid / alkaline
PIMO	pimonidazole, 1-{(2-hydroxy-3-piperidinyl)propyl}-2-nitroimidazole hydrochloride
RBC	Red blood cell / red blood count
RNA	Ribonucleic acid
RT	Radiotherapy
SA	Sarcoma
SC	Subcutaneous
SCC	Squamous cell carcinoma
SCSA	Synovial cell sarcoma
SPECT	Single positron emission computed tomography
TCD50	50% tumor control dose
Tpot	Potential doubling time
TUNEL	Terminal d-uridine triphosphate[UTP] nick-end-labeling
VEGF	Vascular endothelial growth factor

GENERAL INTRODUCTION

The significance of the tumor microenvironment has been well documented in cancer treatment. Hypoxia is a well-known environmental factor that promotes malignant progression of cancers and leads to treatment failures. Two types of tumor hypoxia, acute and chronic hypoxia, are different in terms of their development and effects on radiation therapy.

Approaches for eliminating hypoxia have been developed and tested in clinical settings with some success although the overall impact on cancer therapy is not significant at this point. One of the key points for successful therapy will be selection of patients for tumor hypoxia targeted therapy. Detection and estimation of tumor hypoxia is likely to be important for selection of patients for appropriate treatment and formulating a prognosis. A wide variety of methods for evaluating hypoxia and proliferation are available. Nitroimidazole markers of hypoxia have been used in canine and rodent tumors and this method is feasible in human patients. PCNA is useful for evaluation of proliferation based on its differential expression throughout the cell cycle. In theory, tumor proliferation and hypoxia may be related based on oxygen consumption by rapidly proliferating cells.

Spontaneously occurring canine and feline tumors are valuable models of human malignancy. Many canine and feline tumors are similar to their human counterpart in histology, natural history, biological behavior and response to therapy. One difference between humans and dogs is their life span. Dogs may live 8-14 years and the shorter life span of animals makes them a suitable subject to identify endpoints of disease earlier. Thus, this project will provide fundamental information regarding cell populations and the relationship between two important biological factors, hypoxia and cell proliferation.

Biological and environmental factors may affect the behavior of cancer. Studying those factors will be potentially useful as prognostic factors and predicting treatment response. There have been several attempts to demonstrate the relationship between hypoxia and proliferation although a clear relationship has not been shown.

Hypotheses of this study are 1) hypoxia may be more pronounced in rapidly proliferating tumors because of increased O_2 consumption, 2) hypoxia and proliferation are potential prognostic factors in reference to response to radiation therapy, and 3) evaluating proliferation and hypoxia will enhance the ability to formulate an accurate prognosis.

LITERATURE REVIEW

This review is divided into eight major sections:

1. Physiology of Normal Tissues
2. Physiology of Tumors
3. The Effects of Hypoxia on Mammalian Cells *In Vitro* and *In Vivo*
4. Measurement of Proliferation
5. Measurement of Hypoxia in Tumors
6. Approaches to Overcome Tumor Hypoxia
7. Relationship Between Tumor Hypoxia and Tumor Proliferation
8. Canine Model of Spontaneous Tumors

1. PHYSIOLOGY OF NORMAL TISSUES

Homeostasis

The normal tissue environment is highly regulated in responses to stimuli by a process called homeostasis. Homeostasis results in maintenance of a stable internal environment. The ultimate control of homeostasis is locally and by the nervous system. Changes in tissue O_2 and CO_2 content, pH, nutrients and waste products, salt and electrolytes, and volume and pressure of extracellular fluid are regulated within physiologic values according to metabolic demand.

The vascular network in normal tissues is highly organized to transport and export O_2, CO_2, nutrients, and waste products through vessels. The vascular network consists of arteries, arterioles, capillaries, venues, and veins. The main exchange of O_2 and other nutrients occurs at the capillary level where the active exchange area is the largest.

Cell regulation

Normal stem cells display a number of characteristic properties. Cellular proliferation is tightly controlled thereby supporting normal tissue growth and maintenance of function. Stem cells constitute a small subpopulation of cells, capable of self-maintenance and at the same time providing for normal cell turnover and tissue integrity by a steady input of

amplifying cells with limited proliferative capability. They are also capable of regenerating and rescuing tissue after insult, and to do so they must be able to up- and down-regulate the balance between self-replication and cell input into the amplification compartment.

Respiration

Mammalian cells use molecular O_2 as the final electron acceptor in the respiratory electron transfer pathway. Normally tissues use glucose as the main source of energy. Glucose metabolism consists of three parts: glycolysis, the citric acid cycle, and oxidative respiration.

1. *Glycolysis*

Glycolysis takes place in the cytoplasm, does not require O_2 and produces two ATP molecules per molecule of glucose. The final product is pyruvate.

2. *In the presence of O_2*: Acetyl CoA is produced and used as a substrate in the citric acid cycle. It continues to oxidative respiration.

   In the absence of O_2: Lactic acid is created as a final product of glucose metabolism.

3. *Oxidative respiration*

Oxidative respiration is the primary energy production mechanism in normal tissues. O_2 is required for this process. It takes place in the mitochondria and produces 38 molecules of ATP per molecule of glucose.

Cell cycle

In normal tissues that undergo cell renewal, there is a balance between cell proliferation, differentiation and loss of mature cells. There are mainly four phases of the cell cycle, Gap1 (G1), Synthesis (S), Gap2 (G2), and Mitosis (M) (Hirst and Denekamp, 1979). The principle task of the cell division cycle is to replicate DNA (without errors during S phase) and segregate the duplicated chromosomal DNA equally to two daughter cells. Cell cycle time varies from as little as 10 hours up to several hundreds of hours. Non-proliferating cells that retain the capacity to divide following a stimulus are usually arrested between the M and S phases and are referred to as G0 cells. Most normal cells are in a quiescent or G0 state. Genetic lesions that disable key regulators of G1 phase progression in mammalian cells are present in most human cancers (Sherr, 2001).

1. G1 phase

Gene expression, acquisition of ATP and protein synthesis occurs to prepare for DNA replication. It can be regulated by extracellular stimuli. Variation in cell cycle time between different tumor types is mainly due to a change in the duration of G1.

2. S phase

Cell replicates its DNA. DNA content is doubled at the end of S phase.

3. G2 phase

Gene expression, acquisition of ATP and protein synthesis occurs to prepare for cell division. DNA content is still doubled.

4. M phase

Cell splits (cytokinesis) into two daughter cells. DNA content returns to original size.

Cell cycle checkpoints

The cell cycle is an irreversible, one-way process. Two checkpoints to detect DNA damage are well known (Shackelford et al., 1999). Checkpoints present before and after DNA synthesis are called the G1 and G2 checkpoint, respectively. Detected DNA damage is either repaired or eliminated through apoptosis under control of genes such as p53. The cell cycle checkpoints are controlled by cyclin dependent kinase (CDK) complexes, which are composed of two proteins, a cyclin (structural protein) and a kinase (enzyme). Different CDKs are responsible at each G1 or G2 checkpoint.

1. G1 checkpoint

In normal tissue, DNA damage is detected and either repaired or terminated. The G1 checkpoint is important to maintain genetic stability in normal cells. This is a highly regulated process and necessary to prevent a mutated gene from being transmitted to the next generation of cells. *p*53 is the key transcriptional factor to control the G1 checkpoint although other gene products are implicated as well. In tumor cells, the G1 checkpoint is mostly absent, which leads to genetic instability.

2. G2 checkpoint

When cells are damaged by external stimuli such as radiation or drugs, cells are arrested in G2 to be repaired. Failure of repair leads cells to apoptosis or gene mutation. The G2 checkpoint is mediated through the cyclins A and B/cdc2 checkpoint pathway.

Cell death

There are three documented cell death pathways: apoptosis, oncosis, and necrosis (Trump et al., 1997). The end result of each pathway is cell death; however, the path by which death is achieved and the morphological and physiological traits of each may be strikingly distinct (Koester and Bolton, 1999).

1. Apoptosis

Apoptosis is the process by which multicellular organisms eliminate cells produced in excess during embryonic and adult development or cells that are functionally or genetically abnormal. Apoptosis requires energy and often gene activation. Apoptosis involves single cells and proceeds via a series of discrete steps that are characteristic. During apoptosis, the plasma membrane remains largely intact and no inflammatory response is elicited. Initially, apoptotic cells have membrane blebbing and condensation of the cytoplasm. The cytoplasm becomes convoluted and separates into pieces containing fragments of the broken nucleus (apoptotic bodies). These are then phagocytized by macrophages. TUNEL (terminal d-uridine triphosphate [UTP] nick-end-labeling) is the one of the useful methods to detect apoptosis in histologic sections.

2. Oncosis

Oncosis is an early stage of primary necrosis. Oncosis is a form of cell death induced by energy depletion and initially characterized by cell swelling. Oncosis, derived from the Greek word "swelling," is the common pattern of change in infarcts and in zonal killing following chemical toxicity. In this common reaction, the earliest changes involve cytoplasmic blebbing, dilatation of the endoplasmic reticulum (ER), swelling of the cytosol, normal or condensed mitochondria, and chromatin clumping in the nucleus.

3. Necrosis

Necrosis is a passive response to injury. The morphologic expression of necrosis is nonspecific and generally affects groups of cells. Breakdown of the plasma membrane is an early feature, thereby promoting the leakage of intercellular contents that elicit an inflammatory response. Necrosis is a common feature of aggressive tumors (Leek et al., 1999). Highly angiogenic tumors often are characterized by blood vessel shunting from one tumor area to another, which further exacerbates ischemia and the formation of tumor necrosis.

Summary

Normal tissue physiology is highly regulated and there are complex defense mechanisms against any physiological insults. Understanding normal physiology is essential to identify the abnormal physiological state, which might lead to cancer development. Transition from a normal physiological status to an abnormal status is smooth and quiet, and it is not rare to detect malignancy at the end stage of disease. Prevention and early detection are the keys to control cancer progression. Studying tumor physiology is important to identify the difference between normal and abnormal, and it provides an opportunity to control progression or to restore to the normal status through introduction of a normal gene to the area of disease.

2. PHYSIOLOGY OF TUMORS

Tumors are characterized by uncontrolled cellular proliferation of clonogenic cells and abnormal cellular behavior including local invasion and metastasis. Tumor tissues are characterized by many physiological differences compared to normal tissues.

Tumor development

Initiation, promotion and progression are three important steps of carcinogenesis. Genetic mutation is required for tumor development. Tumors may originate from a single cell. A single cell going through 30 doublings will reach 10^9 cells at which time it can be grossly detected. During the growth stage, tumor cells go through a series of genetic mutations and may acquire different properties depending on the mutation of genes or the tumor microenvironment (Lowe, 1999).

Proliferation

Tumor proliferation may lead to treatment failure. Uncontrolled cancer may continue to grow, destroy normal tissue and form cancer nests in distant areas from the primary disease. Progressive growth of malignant tumors, metastatic spread and local recurrence after treatment can only be explained by the presence of clonogenic cells which have unlimited proliferative potential through mutation of protooncogenes and/or tumor suppressor genes (Smith et al., 1998). The fraction of cells in the cell cycle and the cell cycle time is different between various tumors, and between tumors and normal tissues (Shackney and Shankey, 1999; Wilson, 2001). Energy is required for proliferation and proliferation is active near tumor vessels (Hirst and Denekamp, 1979). Actively proliferating cells near the vessel persistently displace their precursors away from nutrients and O_2, and progressively into quiescent compartments which may be hypoxic and ultimately there is cell death via hypoxia induced apoptosis or necrosis. Cell proliferation is dependent not only on proximity to a blood vessel, but also on temporal changes in blood flow and nutrient delivery (Durand and Aquino-Parsons, 2001a). Many cytokines and growth factors are involved in regulation of cell proliferation, differentiation and death (Teicher, 2001). Blocking several major pathways of tumor growth and survival in combination with other cancer therapies may have an important role in controlling cancer progression.

Energy metabolism

Mitochondria in tumor cells have long been known to be abnormal in their structure and size, which may interfere with efficient energy production (Carafoli, 1986). Increased capacity for glycolytic metabolism is a well-known characteristic of neoplastic cells (Terpstra et al., 1996). Tumor cells preferentially use glucose as an energy source by anaerobic glycolysis and produce lactate and pyruvate, the end products even in the presence of oxygen. In one study it was reported that lactate and pyruvate are capable regulating hypoxia-inducible gene expression independently of hypoxia by stimulating the accumulation of hypoxia-inducible Factor 1α (HIF-1α) (Lu et al., 2002).

Energy charge

The reduction of energy charge is another characteristic of malignant tumors. Energy charge reduction results in overall nutrient deprivation. This can be detectable by magnetic resonance spectroscopy (MRS), as reduction of high-energy phosphates (ATP and ADP), and a resultant increase in low-energy phosphate (AMP) and inorganic phosphate (Gerweck et al., 1995; Gerweck et al., 1992; Rofstad et al., 1989).

pH

Extracellular pH is substantially and consistently lower in tumors than in normal tissues and this results in accumulation of lactate due to alterations either in acidic export from tumor cells or in clearance of extracellular acid (Stubbs et al., 2000). Low pH inhibits cell proliferation, DNA synthesis, glycolysis and immune response, alters drug diffusion capacity, and promotes invasiveness and metastasis (Fischer et al., 2000; Park et al., 2000; Walenta et al., 2000; Webb et al., 1999). In contrast, intracellular pH estimated by the ^{31}P-magnetic resonance spectroscopy is essentially identical or slightly more basic in tumors compared to normal tissues (Gerweck, 1998). Tumor cells are capable of maintaining relatively normal intracellular pH even with an acidic extracellular interstitial tumor pH (Prescott et al., 2000).

Interstitial fluid pressure (IFP)

IFP is elevated in tumors due to lack of a functional lymphatic system, blood vessel permeability, microvascular pressure, and tissue hydraulic conductivity (Boucher et al., 1990; Jain, 1994; Rutz, 1999; Schmid-Schonbein, 1990). High IFP may interfere with drug

delivery to tumor cells (Milosevic et al., 1999) and it may be also related hypoxia development in tumors.

Intrinsic radiosensitivity

Many studies have been performed in tissue culture to study intrinsic cellular radiosensitivity (Arlett and Harcourt, 1980; Bjork-Eriksson et al., 1998; Fertil and Malaise, 1981; Lambin et al., 1996; West, 1995). Established cell lines have been used extensively, and more recently freshly explanted tumor cells from human patients have been used for clonogenic analysis. Various features of radiation response have been described, including the variation in sensitivity during the cell cycle, the effect of exponential versus confluent growth, the protective effect of contact between cells, genetic composition, and the environmental effect of media. Survival ranges from 0.1 to 0.9 after exposure to 2 Gy. There has been no correlation between radiosensitivity of tumor cells and their normal tissue counterpart.

Vascular network and oxygen supply

The tumor vasculature is abnormal and complex (Bernsen et al., 1999). In most solid tumors, oxygenation is poorer than in normal tissues at the site of tumor growth. This is due to larger intercapillary distances and to variable blood flow. Tumor vessels are formed by angiogenesis and the vascular network is not well organized leading to development of hypoxia (Secomb et al., 1993; Secomb et al., 1998; Siemann, 1998). It has been suggested that high vascularization predicts locally aggressiveness and high metastatic potential. The parameter “microvascular density” (MVD) has been proposed to be a prognostic factor for treatment failure and survival although study results conflict (Aebersold et al., 2000; Jenssen et al., 1996; Koukourakis et al., 2000; Sundfor et al., 1998). For example, an intermediate MVD was associated with a better prognosis than both low and high MVD, which might suggest that low MVD is related to poor oxygenation and drug delivery, and high MVD is related to an increased metastatic potential (Koukourakis et al., 2000).

1. Structure of tumor vessels (Dewhirst, 1998; Konerding et al., 1995; Konerding et al., 1999; Shubik, 1982)
    - Maximally dilated, tortuous, and leaky vessels
    - Low and heterogeneous vascular density

- An incomplete endothelial cell layer
- Lack of vascular smooth muscle
- An absent or interrupted basement membrane
- Arterial-venous shunts in up to 30 % of vessels
- No or slow vascular response to the physiological or pharmacological stimulation because of lack of innervation
- No lymphatic vessels

2. Tumor perfusion (Braun et al., 1999; Ding et al., 2002; Jain, 1988)
   - Highly variable including fluctuation and reverse flow
   - Variable flow rate depending on the region, typically high velocity
   - Vascular occlusion due to tumor cell or leukocytes emboli

3. O_2 tension of blood (Clavo et al., 2003; Dewhirst, 1998; Dewhirst et al., 1999; Walenta et al., 2001)
   - Reduced arterial blood O_2 carrying capacity due to low number of vessels
   - Longitudinal gradient
   - Limited O_2 availability due to arterio-venous shunt
   - Transient change of O_2 supply to the cells due to fluctuation or occlusion of the flow and plasma channels
   - Rheological effects
   - Variation in O_2 consumption rate of tumor cells
   - Shift of hemoglobin and O_2 association curve
   - Anemia influences oxygenation

O_2 requirement in tumor

O_2 consumption depends upon the energy requirement of the cells. It has been noted that tumors can live temporarily in the absence of glucose or O_2 (Warburg, 1930). Tumor cells require more energy than normal cells (Vaupel et al., 1989). There is a correlation between growth fraction and O_2 consumption rate; rapidly dividing cells have almost a five fold increase in O_2 consumption compared to slower dividing cells (Freyer, 1994). In tumors, O_2

supply may not meet demand resulting in the tumor cells becoming hypoxic (Gulledge and Dewhirst, 1996; Thomlinson and Gray, 1955; Vaupel et al., 1998b).

Tumor hypoxia

Rapid tumor cell growth creates regions of chronic and transient hypoxia in many solid tumors. Hypoxia produces cell death if severe or prolonged. These two characteristics, hypoxia and necrosis, represent clear differences between tumors and normal tissues. Hypoxia has long been recognized as one of the most characteristic features of advanced solid tumors resulting from an imbalance between the supply and consumption of O_2. There is a large body of evidence that tumor hypoxia exists in experimental and spontaneous tumors in human and animals (Brizel et al., 1995a; Cline et al., 1990; Durand and Aquino-Parsons, 2001a; Durand and Aquino-Parsons, 2001b; Movsas et al., 1999; Rasey et al., 1996). Tumor oxygenation is independent of tumor size, stage of disease, and histopathologic type and grade of tumor (Vaupel et al., 2001). Clinically PO_2 < 10 mmHg defines radiobiological hypoxia. Cells that exist at O_2 levels above 20 mmHg are referred to as aerobic. The cells at acute intermediate O_2 levels (0.5-20 mmHg) have been categorized as transiently hypoxic. Some hypoxic tumor cells (< 5.0 mmHg) maintain clonogenic potential in experimental tumor systems (Kim et al., 1993).

Hypoxia formation is a dynamic process: an interplay of nutrient and O_2 supply and demand, modulated by a differential ability of tumor cells to survive in substandard conditions (Coleman, 1988; Gulledge and Dewhirst, 1996). Two distinct forms of hypoxia are recognized, chronic and acute hypoxia (Denekamp and Dasu, 1999; Horsman, 1998). Major pathogenetic mechanisms for the development of hypoxia are (1) increased diffusion distances for development of chronic hypoxia, and (2) structural and functional abnormalities of the tumor microvasculature for acute hypoxia (Brown, 1979; Thomlinson and Gray, 1955). It has been suggested that acute hypoxia can account for at least 25% of the total hypoxic fraction in some tumors (Iyer et al., 1998b). Although there is no clear distinction between acute and chronic hypoxia, there seems to be fundamental differences between these two types of hypoxia (Denekamp and Dasu, 1999). Some of the chronically hypoxic cells never become reoxygenated and have a limited life expectancy (Durand and Sham, 1998), but acutely hypoxic cells are likely to retain their viability and growth potential as a result of intermittent perfusion with O_2 and nutrients (Durand and Aquino-Parsons, 2001b).

1. Chronic hypoxia

Chronic, diffusion-limited hypoxia occurs at the nadir of the nutrient and O_2 gradient around each feeding vessel (Evans et al., 1996; Haustermans et al., 2000; Hodgkiss et al., 1995a; Hodgkiss et al., 1991b; Raleigh et al., 1987; Thomlinson and Gray, 1955). Chronic hypoxia was recognized before acute hypoxia. The more rapid growth of tumor cells than of the supporting vasculature results in areas of the tumor being largely inaccessible to O_2. Chronic hypoxia develops slowly and progressively worsens, ultimately leading to starvation-induced cell death (Durand and Sham, 1998). Thomlinson and Gray provided the first indirect evidence for the existence of hypoxic regions within human tumors (Thomlinson and Gray, 1955). Based on their histopathologic observations, the size of the rim of viable cells that surrounds tumor blood vessels doesn't exceed the calculated O_2 diffusion distance. Diffusion distance is dependent on the arrangement of microvessels within the tumor, blood flow rate, O_2 content of blood, and the rate of O_2 consumption by tissue. At arteriolar sites, red blood cells carry higher O_2 than at venous sites. When traveling through vessels, red blood cells release O_2. The diffusion distance from vessels is estimated to be around 50 *u*m – 300 *u*m, and beyond these distances, tumor cells become chronically hypoxic (Haustermans et al., 2000; Olive et al., 1992; Rijken et al., 2002; Rijken et al., 2000). The clinical importance of chronic hypoxia is not clear if cells are going to survive, or live long enough to be therapeutically relevant during or after therapy. It has been predicted from hypoxia labelling studies that the survival of the hypoxic cells next to necrotic areas is only 5-11 hours (Hirst and Denekamp, 1979; Hirst et al., 1982). Recently, it has shown that human tumor cells remained viable in the hypoxic regions of xenografts for 4-10 days (Durand and Sham, 1998). Cells in a naturally occurring tumor may withstand hypoxia better *in vivo* than cells in experimental tumors (Azuma et al., 1997).

2. Acute hypoxia

Another form of hypoxia is acute, perfusion-limited or intermittent hypoxia. Development of acute hypoxia is highly influenced by loco-regional O_2 supply due to the closure of individual vessels or blood flow ceasing for seconds, minutes or hours. Tumor blood flow fluctuates, and vessels collapse and open irregularly leading to regional hypoxia around the collapsed vessels (Dewhirst et al., 1996a; Kimura et al., 1996). In experimental tumors, blood flow changes can easily be detected with sequential injections of blood-borne dyes (Brown,

1979; Chaplin et al., 1986; Chaplin et al., 1987; Durand and LePard, 1995; Trotter et al., 1989b). In human tumors, it is very difficult to assess perfusion changes though some measurements with O_2 and blood flow probes have suggested that at least regional perfusion changes can be observed (Pigott et al., 1996). Acute hypoxia has a lower probability of leading to cell death during fractionated radiation therapy because hypoxia is transient and cells should recover more rapidly from damage and should repopulate the tumor more efficiently (Dasu and Denekamp, 1998). Although radiosensitivity of cells may not vary significantly between acute versus chronic hypoxia, acutely hypoxic cells are expected to have a higher clonogenicity than chronically hypoxic cells. The cells at acute intermediate oxygen levels may be more significant in terms of being a limiting factor to treatment (Durand and Aquino-Parsons, 2001a; Durand and Aquino-Parsons, 2001b; Wouters and Brown, 1997).

Angiogenesis

The formation of new blood vessels is a crucial step for survival, growth and progression of primary and metastatic tumors. Angiogenesis is the development of new blood vessels from the existing vascular bed (Koukourakis, 2001; Malonne et al., 1999). Solid tumors up to about 2 mm in diameter can acquire oxygen and nutrients by passive diffusion from blood vessels in surrounding normal tissue. Tumor hypoxia is the one of the primary stimuli to induce angiogenesis (Dunst et al., 2001). Among many angiogenic factors, basic fibroblast growth factor (bFGF) and vascular endothelial growth factor (VEGF) are the most potent and well-studied angiogenic factors induced by hypoxia. Neovascularization requires the coordinated activities of multiple factors and cell types. For tumors to develop a neovascular blood supply, tumor cells and host cells must secrete proangiogenic factors that offset the activities of inhibitory angiogenic factors. In addition, the newly derived tumor endothelium must respond to signals in the microenvironment to survive under conditions such as hypoxia and acidity. The basic steps of angiogenesis are:

1. Activation of the endothelial cell of a mature vessel
2. Degradation of the surrounding basement membrane
3. Migration into the surrounding connective tissue stroma
4. Proliferation of migrated cells and tubular structure formation
5. Forming tumor vascular network

Anti-angiogenesis is one of the promising strategies for cancer control (Folkman, 2002). Combining anti-angiogenesis with conventional treatment may be effective in stabilizing the existing tumor, inhibiting metastasis development and/or prolonging survival without the significant toxicity which may be often associated with standard chemotherapy (Ellis et al., 2001). Clinical trials are in progress to evaluate this strategy for treatment of human cancer (Fenton et al., 2001).

Tumor heterogeneity

Tumors are heterogeneous in cellularity, oxygenation, nutrition, proliferation and vascularity. Some heterogeneity can be attributed to physiological factors such as blood supply, while other aspects of heterogeneity must be due to genetic mutations affecting normal cell cycle control, differentiation and death. Both intra-tumor and inter-tumor heterogeneity of hypoxia has been observed in spontaneous tumors (Adam et al., 1999b; De Jaeger et al., 1998; Evans et al., 1997a; Evans et al., 2001; Nordsmark et al., 1994; Olive et al., 1998; Rasey et al., 1996). Tumor heterogeneity is often a major limitation factor to the study of tumor physiology in the tumor as a whole. Intra-tumoral heterogeneity is usually smaller than inter-tumoral heterogeneity (Begg et al., 2001; Brizel et al., 1995a; Brizel et al., 1994; Kavanagh et al., 1999a). The intra- and inter-tumoral heterogeneity necessitates sampling from multiple sites and within multiple tumors. Acceptable estimates of the hypoxic fraction in a tumor may be obtained from a clinically feasible number of biopsies in as little as four despite intra-tumor variation (Cline et al., 1997).

Summary

Tumor physiology has been studied extensively in experimental tumor systems although there is still a great deal to learn. Tumor hypoxia is a well-known abnormal condition in solid tumors. Acute and chronic hypoxia seem to have different effects for therapeutic intervention. Spontaneous tumors in human and animals often have different characteristics from experimental tumors. Accurate evaluation of microenvironmental conditions including hypoxia and proliferation need to be established to understand tumor physiology and develop effective cancer therapy strategy.

3. THE EFFECTS OF HYPOXIA ON MAMMALIAN CELLS *in vitro* AND *in vivo*

Prolonged and extreme hypoxia results in cell death. Tumor necrosis is often observed in the region beyond O_2 diffusion. Cells undergo a variety of biological responses when placed in hypoxic conditions including activation of signaling pathways that regulate proliferation, glycolysis, erythropoiesis, angiogenesis and cell death (Harris, 2002; Smith et al., 2001). Hypoxia is a powerful trigger for specific gene inductions. Normal cells are able to sense hypoxia and modulate the expression of specific genes to adapt to hypoxic conditions (Dachs and Chaplin, 1998; Sutherland, 1998; Wang and Semenza, 1996). Cancer cells also have adapted these pathways, allowing tumors to survive and even grow under hypoxic conditions. The hypoxia inducible transcription factor -1 (HIF-1) is considered to be a master regulator of response to hypoxia insults (Gleadle and Ratcliffe, 1998; Semenza, 2000b). This hypoxia induced gene expression also promotes malignant progression, and results in more aggressive loco-regional and distant disease (Sutherland, 1998). The genomic and phenotypic changes might be induced by HIF-1 under hypoxic conditions including induction of point mutations, deletions and gene amplifications, which lead increased genomic instability and selective pressure for metastatic development (Rofstad, 2000). HIF-1 is described in more detail in a later section.

Metabolic Alterations

Hypoxia results in a significantly higher reducing environment in the tumor compared to normal tissue (Ilangovan et al., 2002). Metabolic responses include the transition from aerobic respiration to anaerobic glycolysis, and a decrease in overall protein synthesis (Dang and Semenza, 1999; Esumi et al., 2002; Minn et al., 1996). Stimulation of glycolysis has been regarded as the main response that increases energy production during hypoxia. Hypoxic cancer cells use glycolysis as a primary mechanism of ATP production. Glycolysis provides only two ATP molecules for each glucose molecule, in contrast to the TCA cycle, which provides 38 ATP molecules. HIF-1 is able to induce the expression of glycolytic genes and hence ATP production (Minet et al., 2000).

Cell cycle response

Hypoxia decreases cellular uptake of thymidine (Clavo and Wahl, 1996). Cycling mammalian cells that are rendered extremely hypoxic (less than 4 ppm O_2) tend to accumulate in the G1 phase. There is O_2 dependent arrest in late G1 and S, and there is inhibition of cell proliferation through S phase under extremely hypoxic conditions (Amellem and Pettersen, 1991; Amellem et al., 1994; Green and Giaccia, 1998). Although the rate of cell cycle progression of hypoxic cells was slower than that of well oxygenated cells, hypoxic cells could progress through the cell cycle (Webster et al., 1998).

Apoptosis induced by hypoxia

Hypoxia induces apoptosis by a number of HIF-1 mediated and independent pathways. Apoptosis in areas distal to blood vessels was co-localized with hypoxic regions detected by hypoxia markers (Koch et al., 1998). This apoptotic sensitivity tends to be lost during malignant progression. There is evidence for the existence of both p53 dependent and independent pathways. Initiation of apoptosis occurred in all phases of the cell cycle although predominantly for cells in S phase. It has been shown that hypoxic cervical cancers with a low apoptotic index are highly aggressive (Hockel et al., 1999).

Metastasis development

In experimental tumor cells, increased metastatic efficiency, transplantability and angiogenic potential following exposure to hypoxia has been shown (Rofstad and Danielsen, 1999). In that study, tumors that are more hypoxic are more likely to metastasize. Induction of acute but not chronic hypoxia in the primary tumor significantly increased the number of spontaneous microscopic lung metastases in mice (Cairns et al., 2001).

Oxygen effect on the radiosensitivity

O_2 is a powerful radiosensitizer. In the early 1900's Schwarz (1909) and Holthusen (1921) observed the influence of O_2 on the radiosensitivity of tissues and cells.

In the region of the survival curve representing exponential cell killing, mammalian cells under severely hypoxic conditions required up to three times the dose of ionizing radiation for survival to be reduced by the same fraction (Elkind and Whitmore, 1965; Gray et al.,

1953). Decreased efficient cell killing occurs at O_2 tensions below 30 mmHg (2%) *in vitro*, and is half-maximal at approximately 3 mmHg (0.5%).

The relationship between hypoxia and resistance to treatment has been observed for a long time although understanding of the biological basis has not been clearly shown (Molls et al., 1998). The hypothesis of O_2 effects is that DNA damage, which is produced by radiation via free radicals, becomes fixed in the presence of O_2. Radicals also interact with macromolecules and membranes. The DNA lesion can be repaired without O_2 or result in cell death with O_2.

Approximately 70-80% of low LET radiation induced cell damage occurs through the "indirect effect". The indirect effect involves ionization of the most abundant molecule in tissue, water, to form a reactive hydroxyl radical as follows:

$$\text{Ionizing radiation} + H_2O \rightarrow [H_2O^+], e^- \rightarrow {}^*OH + H^+ + e^-$$

Next the hydroxyl free radical interacts with a critical cellular macromolecule such as DNA results in the formation of a macromolecular radical such as a DNA and hydroxyl radical.

$$^*OH + DNA \rightarrow DNA^* \text{ or } DNAOH^*$$

In the presence of oxygen, the DNA hydroxyl radical is converted to a DNA peroxyl radical, which leads to products, which are irreparable and have the potential to cause cell death.

$$DNA^* + O_2 \rightarrow DNAOO^*$$

In the absence of O_2, radical scavengers bearing thiol groups such as glutathione, can effect conversion of the radical back to its original form and a non-damaging thiol radical is formed.

$$DNA^* + RSH \rightarrow DNA + RS^*$$

The term O_2 enhancement ratio (OER) is the ratio of radiation doses under hypoxic versus oxygenated conditions, required to produce the same biological effect.

OER = Dose under hypoxia / Dose under oxygenated conditions

The OER at doses of radiation commonly used in conventional fractionated radiation therapy regimes (2 Gy) is lower than the OER at higher doses of radiation. Densely ionizing radiations such as neutrons and heavy ions act directly on target molecules do not require O_2 for cell killing. Thus, the OER decreases as a function of increasing linear energy transfer (LET), becoming essentially equal to 1 at LET values $\geq$100 keV/*u*m.

Genetic alterations and gene expressions

Gene products that are induced by hypoxia include transcription factors (AP-1, HF-kB, p53, and HIF-1), metabolic enzymes (glycolytic enzymes and tyrosine hydroxylase), cellular redox regulators (Ref-1 and NADPH), and protective proteins (hsp70), cytokines and growth factors (erythropoietin and vascular endothelial growth factor) (Harris, 2002; Lal et al., 2001; Rofstad et al., 2002).

1. p53

p53 is a transcription factor, a key regulator of the cell cycle as a tumor suppressor gene. Under normal conditions, the p53 gene is inactive. Expression of p53 is increased in damaged cells leading to arrest of the cell cycle in G1 to allow for damaged cells to be repaired. p53 induction occurs within hours after exposure to hypoxia (Royds et al., 1998). The stable p53 protein is activated by phosphorylation, dephosphorylation and acetylation yielding a potent sequence-specific DNA-binding transcription factor. Cells with repaired DNA resume cycling and undergo normal cell proliferation. If DNA repair is not successful, the cell undergoes apoptosis. Mutation of the p53 gene is one of the most common genetic changes in human tumors (el-Deiry, 1998). Mutation of the p53 gene inactivates its functional protein. Without normal function of p53, DNA damaged cells are not arrested in G1 and advance through the cell cycle with damaged DNA. Failure of DNA repair permits mutations to be accumulated in the DNA and this may lead to carcinogenesis. A wide range of biologic effects can be expressed when p53 is dysfunctional because of the large number of downstream genes of p53 including p21, GADD45, 14-3-3 sigma, bax, Fas/APO1, KILLER/DR5, PIG3, Tsp1, IGF-BP3 and others.

2. Hypoxia-inducible factor 1 (HIF-1)

HIF-1 is the only known mammalian transcription factor expressed uniquely in response to physiologically relevant levels of hypoxia (Iyer et al., 1998a; Semenza, 1998; Semenza, 1999; Wang et al., 1995). HIF-1 is a protein necessary for the development of normal embryonic and cardiovascular systems, and evidence indicates that HIF-1 also contributes to tumor progression (Semenza, 2002). HIF-1 is composed of an O_2- and growth factor-regulated HIF- 1 alpha subunit and a constitutively expressed HIF-1 beta subunit. HIF-1 transcriptional activity is determined by regulated expression of the HIF-1 alpha subunit. The alpha-subunit of HIF-1 is rapidly degraded by the proteasome under normoxic conditions, but it is stabilized in conditions of hypoxia. HIF-1 activates the transcription of genes encoding erythropoietin, glucose transporters, glycolytic enzymes, vascular endothelial growth factor (VEGF), and other genes whose protein products increase O_2 delivery or facilitate metabolic adaptation to hypoxia (Alfranca et al., 2002; Blancher and Harris, 1998; Chilov et al., 1999; Minet et al., 2000; Richard et al., 1999). The level of HIF-1 alpha expression is often correlated with tumor grade, angiogenesis, and survival, and overexpression of HIF-1 alpha in the majority of common human cancers and their metastases, including colon, breast, gastric, lung, skin, ovarian, pancreatic, prostate, and renal carcinomas, and bladder cancer cancers has been reported (Beasley et al., 2002; Koukourakis et al., 2002; Semenza, 2000a; Xia et al., 2002; Zhong et al., 1999).

3. von Hippel-Lindau (VHL) tumor suppressor protein

O_2 dependent binding of the VHL tumor suppressor protein targets the HIF-1 alpha subunit for ubiquitination and proteasomal degradation (Mahon et al., 2001; Maxwell et al., 1999). Essentially, VHL controls HIF-1 levels by proteolysis. In addition, HIF-1 binds to VHL and VHL also functions as a transcriptional factor that inhibits HIF-1 alpha transactivation function.

4. Vascular endothelial growth factor (VEGF)

Hypoxia is the most important stimulus for upregulation of VEGF, one of the key cytokines for angiogenesis as well as permeabilization of blood vessels (Neufeld et al., 1999). Transcriptional activation of the VEGF gene is by HIF-1 in hypoxic cells. VEGF induces endothelial cell proliferation, promotes cell migration, and inhibits apoptosis (Harmey and

Bouchier-Hayes, 2002). VEGF is often expressed in tumors at substantially increased levels (Rosen, 2002).

5. Erythropoietin (EPO)

Hypoxia stimulates up-regulation of EPO, which improves the peripheral O_2 supply (Semenza et al., 1994). Endogenous EPO and recombinant EPO (rHu-EPO) are similar except for minor differences in the pattern of their 4 carbohydrate chains. The administration of rHu-EPO to tumor patients could improve tumor oxygenation prior to chemotherapy and radiotherapy (Jelkmann and Hellwig-Burgel, 2001). Although the EPO is effective to improve anemia, EPO has been associated with thromboembolism and is being withdrawn from clinical trials (Vreugdenhil et al., 1993; Wun et al., 2003).

6. Insulin-like growth factor binding protein-3 (IGFBP-3)

IGFBP-3 is a pro-apoptotic gene that is transcriptionally upregulated in response to hypoxia (Koong et al., 2000).

7. Plasminogen activator inhibitor-1 (PAI-1)

PAI-1, an essential component of homeostasis, which is induced by hypoxia. Elevation of PAI-1 level in tumor has been associated with invasiveness and metastasis and correlated with poor prognosis in a variety of solid tumors (Bajou et al., 1998). PAI-1 serum levels also elevated in cancer patient compare to normal controls (Koong et al., 2000).

8. *Multidrug Resistance (MDR)*

MDR1, the gene product, P-glycoprotein, is an approximately 170kd transmembrane protein and is associated with tumor resistance to chemotherapeutics. P-glycoprotein is also induced by hypoxia. MDR1 gene induction seems to be controlled by HIF-1 (Comerford et al., 2002).

9. Carbonic anhydrase-9 (CA9)

CA is transmembranic enzymes involved in the catalytic hydration of CO_2 to carbonic acid. CA9 is upregulated by hypoxia and upstream genes such as HIF-1alpha and HIF-2 alpha (Hui et al., 2002; Koukourakis et al., 2001). Under hypoxic conditions, CA9 levels steeply

increased from 4 to 24 hours and pO_2 levels of approximately less than 20 mmHg is required for induction (Wykoff et al., 2000). A high level of CA9 expression has been found in cancer cell lines and fresh and archived tumor tissues (Ivanov et al., 2001). Upon comparison of CA9 expression and the hypoxia marker pimonidazole binding, there was a similar, although more tightly circumscribed, pattern of expression of CA9 around regions of necrosis and substantial although incomplete overlap. CA9 seems to be promising as an endogenous marker for detection of tumor hypoxia.

10. Metallothionein

The 7 kDa, heavily thiolated polypeptide, metallothionein, is an endogenous chemo- and radioprotectant. Metallothionein is strongly induced by tumor hypoxia and is expressed in both chronically and acutely hypoxic cells in rodent tumors (Murphy et al., 1994; Raleigh et al., 1998a), but not expressed in the majority of hypoxic cells in human squamous cell carcinaomas (Azuma et al., 2003; Raleigh et al., 2000).

Summary

Cells undergo a variety of biological responses when placed in hypoxic conditions, including activation of signaling pathways that regulate proliferation, angiogenesis and cell death. Cancer cells adapt these pathways, allowing tumors to survive and even grow under hypoxic conditions. Tumor hypoxia is documented to be associated with poor prognosis. Identifying the genes that are transcriptionally activated within hypoxic malignant cells is very important in understanding the complex interactions driving the hypoxia response in modulating the gene for therapeutic interventions.

4. MEASUREMENT OF PROLIFERATION

The proliferative rate of tumor cells varies widely between tumors. Non-proliferating cells are common and there is often a high rate of cell loss. Cell kinetic parameters such as the fraction of the proliferating cells and cell cycle doubling time are indicators of the rate of tumor growth (Madewell, 2001). Proliferation dictates the rate of tumor progression, and it is also useful as a prognostic factor or a diagnostic tool. Cell kinetic parameters have been shown to be important as potential prognostic factors in several human and animal tumors (Bostock et al., 1989; Bratulic et al., 1996; Hazan et al., 2002; Hsu et al., 1998; Pena et al., 1998; Puglisi et al., 2002; Sarac et al., 1998; Schouten van Meeteren et al., 2002; Simoes et al., 1994) although assessment of proliferation failed to make an impact in overall clinical practice (Wilson, 2001). In a recent review article only 50% of reports on the prognostic relevance of markers for cell cycle acceleration and proliferation found a significant association with prognosis (Schliephake, 2003). A variety of markers and techniques have been used to determine cell cycle status.

Tritiated thymidine incorporation followed by autoradiography

Initially cell proliferation was measured by autoradiographic detection of tritiated thymidine (^{3}H-TdR) incorporation into the DNA of cells during S phase in experimental tumors (Meyer et al., 1983). Cells that were synthesizing DNA at the time of exposure to tritiated thymidine create exposure of the photographic emulsion due to emitted β particles. It requires a significant amount of time (10-20 days) to produce autoradiographs. It cannot be used in clinical application because of its toxicity.

Detection of incorporated 5-Bromo-2'-deoxyuridine (BrdUrd) incorporation

BrdUrd, a nonisotopic thymidine analogue, has largely replaced ^{3}H-TdR (Dolbeare et al., 1983). The rate of tumor growth can be estimated through *in vivo* labelling of tumor tissue with BrdUrd or iododeoxy uridine (IdUrd) several hours before biopsy. Cells in S-phase actively incorporate BrdUrd into their DNA. Anti-BrdUrd immunotechniques (IHC and flow cytometry) can be used to detect cells that have incorporated BrdUrd (Eldridge et al., 1990). The labeling index (LI, the fraction of cells in S-phase), the time spent in S phase (Ts), and

the potential doubling time of the tumor population (Tpot) can be estimated with measured values.

Detection of the endogenous cell-cycle specific proteins by produced antibody

Detection of the endogenous cell cycle specific proteins to assess proliferative fractions in histological and cytological preparations has great advantage over the ^{3}H-TdR or BrdUrd labelling methods because prior *in vivo* application of an S-phase marker is not required and the detection system is nonisotopic (Schipper et al., 1998). Many of these antibodies can be used on formalin-fixed paraffin embedded samples, thus allowing the use of archival material with preserved structure of the tissue (Greenwell et al., 1991). Antibodies detecting these antigens can be used for a wide range of applications including western blotting, immunoprecipitation, flow cytometry and IHC analysis. One major disadvantage is that the endogenous markers are not really specific to any particular phase of the cell cycle (Eldridge and Goldsworthy, 1996).

1. The proliferating cell nuclear antigen (PCNA)

PCNA, an endogenous cell proliferation marker is one of the most widely used antigens to assess proliferation (Hall et al., 1990). PCNA was originally detected using auto-antibodies from human patients with systemic lupus erythematosus (Miyachi et al., 1978). PCNA has been identified as a cyclin or DNA-polymerase delta accessory protein and highly conserved 36 kD endogenous nuclear proteins associated with the cell cycle (Mathews et al., 1984). PCNA is required for the DNA synthesis and DNA repair (Shivji et al., 1992). Commercially produced monoclonal antibodies that recognize not only human PCNA, but also PCNA in other species are available (Mathews et al., 1984). PCNA reactivity has been found in canine and feline tumors (Preziosi et al., 1995a; Sarli et al., 1995). PCNA is detectable during G1, S, G2, and M phases with a striking accumulation in the nucleolus late in G1 and early in S (Celis and Celis, 1985; Kurki et al., 1986; Sasaki et al., 1994). PCNA has a relatively long half-life (20 hours) and might remain in cells that have already exited the cell cycle such as cells in G0 and G1. Correlation between BrdUrd and PCNA indices has been studied extensively and relatively good correlation supports the use of PCNA for detection of proliferating cells (Eldridge and Goldsworthy, 1996; Wijsman et al., 1992). The assessment

of the cell proliferation by PCNA has been shown to be of prognostic values in limited human cancers (Sarac et al., 1998).

2. Ki-67

Ki-67 antigen in the granular components of the nucleolus is detectable during late G1, S, G2 and M phases, while cells in G0 phase consistently lack the antigen detected by commercially available antibody (Hazan et al., 2002). The half-life of Ki-67 is 1-2 hours or less and it is synthesized continuously in cycling cells. The assessment of cell proliferation by Ki-67 has been shown to be of prognostic value in canine mammary tumors (Pena et al., 1998). In comparative studies, the fraction of PCNA positive cells has been found to be greater than Ki-67 positive cells (Barrett et al., 1997). The superiority of Ki-67 probably reflects the rapidity of catabolism of the Ki-67 antigen at the end of M phase (McCormick et al., 1993). There was good correlation between BrdUrd and Ki-67 indices (Sakai et al., 2002). Problems associated with using Ki-67 include the staining technique since the half-life is short, and the interpretation of positive staining because it has unknown functions.

3. Fen1

Fen1, a nuclear antigen, is another cell cycle specific protein that is expressed by cycling cells. It co-localizes with PCNA during S phase (Warbrick et al., 1998). Fen1 is not induced in cells during DNA repair. A polyclonal antibody has been raised which recognizes the structure-specific endonuclease Fen1.

4. Cyclins

A number of antibodies, which recognize specific cyclins are available. The measurement of specific cyclin expressions could be used to identify sub classifications of cycling cells in the cell cycle (Darzynkiewicz et al., 1996).

The silver-stained nucleolar organizer regions (AgNORs)

The quantitative evaluation of the nucleolar organizing regions associated with argyrophil proteins (AgNORs) can be used to study tumor proliferation. This method seems to be technically demanding and somewhat subjective. These regions can be stained with a specific silver stain and quantified directly by light microscopy and by computerized image

analysis (Bratulic et al., 1996; Hung et al., 2000; Preziosi et al., 1995b). An association has been found between cell proliferation and AgNOR score in human oral squamous cell carcinoma (Costa et al., 1999). In one study PCNA, Ki-67 indices and AgNOR scores correlated with each other and with tumor grade, stage and prognosis (Bozlu et al., 2002).

Mitotic index

Mitotic index has been used to evaluate mitotic activity in canine and feline solid tumor (Bostock and Dye, 1980; Sarli et al., 1999). This is a very simple light microscopic technique to evaluate proliferation. Mitotic index is one of the most important factors in the grading system to indicate aggressiveness of canine soft tissue sarcomas (Bostock and Dye, 1980). PCNA, Ki-67 and mitotic indices had highly significant positive correlations with each other in spontaneous canine lung cancer (Griffey et al., 1999).

Potential doubling time (Tpot)

Tpot is a hypothetical doubling time derived from two cell kinetics parameters, labeling index (LI) and the duration of S phase (Ts). The cell production rate, described by Tpot, is remarkably rapid in most tumors, a median value on the order of 5 days, and much faster than the clinical volume doubling times for most cancers because Tpot does not take into account cell loss as a factor. Tpot values of a few days have been measured in many human and animal tumors (Begg et al., 1990; Begg et al., 1999; Schwyn et al., 1998; Wilson, 1991; Wilson et al., 1995). Although Tpot failed as a universal prognostic factor of outcome in radiotherapy (Begg et al., 1999), it may still be useful as a diagnostic tool to evaluate growth rate for individualized treatment.

DNA ploidy

DNA ploidy is one of the simpler measurements and in most instances is easily measured by flow cytometry. Fluorescent stains with affinity for nucleic acids can be evaluated depending on intensity of staining from which cell cycle distributions of populations of cells can be determined. This method cannot distinguish G2 from M, and there is overlap in cell cycle phases. Evaluation of DNA ploidy is particularly useful when combined with detection of other markers.

Summary

The accurate determination of the proliferative status of tumors would provide useful tools to diagnose, predict treatment response, and monitor treatment response. Detection of BrdUrd incorporation provides detailed information of the proliferation patterns especially in an experimental setting although it is generally impractical to use routinely in the clinical setting. Alternatively, endogenous proliferating markers are excellent alternatives to use in the clinical setting since antigens can be detectable by a variety of monoclonal antibodies in formalin-fixed paraffin embedded samples. These antibodies can be used on sectioned tissue as well as single cell suspensions by flow cytometry techniques, which is particularly useful to determine the phases of cell cycle. More investigation is necessary to establish endogenous proliferation markers as standard practice.

5. MEASUREMENT OF HYPOXIA IN TUMORS

Measuring tumor oxygenation has been studied extensively in experimental and spontaneous tumors (Brown and Le, 2002; Horsman, 1998; Raleigh et al., 1996). Measurement of oxygenation and identification of hypoxic cells in naturally occurring tumors is more difficult than experimental tumors, primarily because most of the direct measurement procedures used in animals are not applicable to humans due to invasiveness and extensive sampling procedures. Invasive and non-invasive techniques to evaluate tumor oxygenation are rapidly improving, making it possible to use the distribution of pO_2 as a predictive assay for cancer treatment. Assessing oxygenation will be important to select patients for appropriate treatment modalities such as for hypoxia-targeted therapies. Many hypoxia-targeted therapies have been investigated with variable results, which may be due to inappropriate patient selection whether the tumor had no or a minimum fraction of hypoxic tumor cells. Direct and indirect methods for assessing oxygenation are becoming widely accepted in the clinical setting. To date, only one method, the Eppendorf polarographic oxygen electrode, has provided measurement of tumor oxygenation that bears a relationship to prognosis. Tumor hypoxia is an important independent poor prognostic factor in cancer treatment. The first clinical evidence that tumor oxygenation was predictive of survival was published in 1993 (Hockel et al., 1993). There is increasing evidence that there is a positive relationship between the presence of hypoxia and poor treatment outcome after radiation therapy alone, surgery alone, or radiation combined with other therapies because hypoxic tumors are more locally aggressive and more likely to metastasize (Brizel et al., 1999; Brizel et al., 1997a; Brizel et al., 1996; Dachs and Tozer, 2000; Fyles et al., 1998; Gatenby et al., 1988; Hockel et al., 1999; Hockel et al., 1996; Hockel et al., 1998; Knocke et al., 1999; Nordsmark and Overgaard, 2000; Nordsmark et al., 1996a; Rofstad et al., 2000; Schindl et al., 2002; Stadler et al., 1999; Sundfor et al., 1998; Vaupel et al., 2001).

Other promising methods involve use of nitroimidazoles as hypoxia markers (Kaanders et al., 2002c). This method could be a suitable alternative to the Eppendorf electrode method in the clinic. The O_2-dependent bioreductive metabolism of 2-nitroimidazoles provides a way of labeling hypoxic cells *in vivo* and a variety of isotopic labels have been proposed for non-invasive detection of bound metabolites of exogenous markers as well as non-radiolabeled

conventional immunochemical assays. Recently non-invasive methods of hypoxia measurement have been actively studied using high technical imaging systems. These noninvasive means will likely be the mainstay of evaluation of tumor oxygenation in the future.

Radiobiological method

The radiobiologically viable fraction of hypoxic tumor cells can be measured indirectly by comparing the response of tumors to large single doses of radiation given under normal aeration and artificial hypoxia (Moulder and Rockwell, 1984). The site of tumor implantation, the use of anesthesia, and certain host characteristics may influence the hypoxic fraction. This method has been established in experimental models, but is not feasible in human tumors. These three major hypoxic fraction assay techniques for measuring hypoxic fractions share common biological assumptions. Each technique uses additional special assumptions and each may measure a different population of hypoxic cells.

Assumptions are:

1. The survival curves for naturally and artificially hypoxic cells have the same slope and intercept
2. Hypoxic condition is artificially made. The model assumes either complete oxygenation or hypoxia. There is no intermediate range of hypoxia
3. The artificial production of hypoxia does not produce tumor cell killing

There are three major methods:

1. Paired Survival Curve Assay

The comparison of survival curves for tumor cells irradiated under normal aeration and acute hypoxia. The animal is asphyxiated several minutes before irradiation by breathing nitrogen. Under these conditions, all tumor cells are hypoxic. In another experiment, the animal is alive and breathing air, so that the proportion of hypoxic cells in the tumor is at its normal level where the tumor contains mixed population of hypoxic and oxygenated cells. The vertical separation of those two survival curves gives the proportion of hypoxic cells in the tumor.

2. Clamped Tumor Control Dose Assay

Radiation doses necessary to control tumors irradiated under normal aeration and acute hypoxia by clamping the blood supply to the tumor are determined. Typically, a range of single doses of radiation is administered to the tumor. Then, the tumor is observed at regular intervals following irradiation until some end-point in time to give sufficient chance to recur. The number of recurrences per dose group is compiled. Then, the 50% response level (the TCD50) can be estimated. The hypoxic faction can be calculated from comparison of the TCD50 values for tumors irradiated under clamped or unclamped conditions. While the clamped TCD50 technique lacks the precision of the paired survival curve assay, it can detect and measure much smaller hypoxia fractions.

3. Clamped Tumor Growth Delay Assay:

Comparison of growth of tumors irradiated under normal aeration and acute hypoxia involves daily measurement of tumor volume or size as a function of time after irradiation. The hypoxic fraction is determined by comparing the post-irradiation growth of normally-aerated and clamped tumors and analyzing the time required for irradiated tumors to reach a specified size minus the time for untreated tumors to reach the same size, the “growth delay”.

The comet assay, single-cell gel electrophoresis

The alkaline and neutral comet assay is a sensitive, simple and rapid method for detecting DNA single-strand and double-strand breaks, respectively and the individual cell's DNA repair profile (Olive et al., 1994; Reinhardt-Poulin et al., 2000). The alkaline comet assay can be used as an indirect measure of hypoxia because the amount of DNA damage is proportional to the number of DNA single-strand breaks after irradiation depending on the O_2 concentration in each cell (Olive and Durand, 1992; Olive et al., 1994; Romanet et al., 1999; Ward and Marples, 2000). The comet assay got its name from the distinct 'tail' of stretched and broken DNA observed when irradiated DNA is placed in a voltage difference. During single-cell electrophoresis, DNA is drawn out of cells and, the more damaged the DNA, the further it moves toward the positive pole. This method applies fluorescence microscopy and image analysis to measure the amount of migration of DNA from individual cells embedded in agarose. Relatively large doses of radiation (> 5 Gy) must be given and samples collected

immediately after irradiation because of rapid repair of DNA damage (estimated repair half-life of 4.2 minutes) (Terris et al., 2002). Sampling can be done by fine-needle aspiration (McLaren et al., 1997). The comet assay has been used in patients undergoing palliative irradiation where dose ranges were 5 - 10 Gy (Olive et al., 1993; Olive et al., 1999; Terris et al., 2002). For routine clinical use, the sensitivity of the comet assay needs to be improved to allow detection of hypoxic cells after a dose approximating 2.0 Gy, the typical fraction size used in conventional radiation therapy.

Histomorphometry

Thomlinson and Gray observed indirect evidence of chronic hypoxia between active tumor cells and necrotic tumor cells (Thomlinson and Gray, 1955). They reported a histological study of fresh specimens of bronchial carcinoma where they used endogenous landmarks such as vessels and necrosis to estimate hypoxia. The procedure was relatively unperturbed by the assay procedure. Tumors grow in solid cords that appear to be circular areas surrounded by stroma from which O_2 and nutrients diffuse. The centers of large tumor areas are necrotic and are surrounded by intact tumor cells, which appear as rings. They observed large areas of necrosis separated by bands of tumor cells about 100 to 150 *u*m wide, beyond which hypoxia and necrosis were present. They estimated that the thickness of the viable tumor cells remained essentially constant at 100 to 180 *u*m. They concluded that tumor cells could proliferate and grow actively only if they were close to a supply of O_2 or nutrients. This was the first observation to develop the concept of the diffusion limited, chronic hypoxia.

The measurement of tumor vascularity may provide a histological assessment of hypoxia as a surrogate assessment (West et al., 2001). Intercapillary distance and microvessel density have been studied in cervical cancer. Intercapillary distance may reflect tumor oxygenation where a long intercapillary distance indicates vascularization to be poor and microvessel density may provide an assessment of angiogenesis particularly using the hotspot method. Both intercapillary distance and microvessel density were significant independent prognostic factors for local control. Tumors with long intercapillary distance had poor local control and tumors with high microvessel density had poor local control.

Cryospectrophotometry

The extent of intracapillary oxyhemoglobin (HbO_2) saturation evaluated by the cryospectrophotometric method can be used to study tissue oxygenation on frozen tissue sections (Mueller-Klieser et al., 1990). Cryospectrophotometric measurements of HbO_2 saturations in tumor microvessels allow for estimates of the proportion of well-oxygenated tissues (Mueller-Klieser et al., 1991). This method is mainly used for studies of experimental tumors since it requires large amount of tissue for assay (Fenton et al., 1988).

Bioluminescent imaging

Bioluminescent imaging of tumor cell metabolites can be performed on frozen sections of biopsy samples. This indirect technique can be used to measure the spatial distribution of metabolites, such as ATP, glucose, and lactate. There is good correlation between the distribution of ATP and of cellular viability at a microregional level (Mueller-Klieser and Walenta, 1993).

Perfusion assays

1. Fluorescent markers of perfusion

Hoechst 33342

Hoechst 33342 is a fluorescent perfusion marker and has potential to be used as an agent for quantifying tissue perfusion via fluorescence microscopy of frozen tissue sections (Olive et al., 1985). The dye exits rapidly from the blood, with a half-life of 110 seconds but remains bound within target cells, redistributing with a half-life longer than 2 hours. Hoechst 33342 can be quantified by flow cytometry with single cell suspensions, and cell populations can be selected on the basis of their fluorescence (distance from the vasculature) using a fluorescence-activated cell sorter (Durand et al., 1990; Olive et al., 1985). A computerized digital image analysis system provides a fast and accurate technique for simultaneous quantitative analysis of tumor perfusion and vasculature (Rijken et al., 1995). However, Hoechst dyes are not applicable in patients for toxicity reasons.

Carbocyanine dye, DiOC7 (3)

Carbocyanine dye, DiOC7 (3) is also a fluorescent perfusion marker. DiOC7 (3) stains cells immediately adjacent to blood vessels and thus, like Hoechst 33342, outlines perfused tumor vasculature. The dye has a distribution half-life in blood of 180s and staining of

perivascular tumor cells is sufficiently stable to allow visualization of vasculature for up to 30 min after DiOC7 (3) injection.

The different fluorescence excitation and emission properties of DiOC7 (3) and Hoechst 33342 permit discrimination of the stains in the same tissue section (Trotter et al., 1989a).

2. Laser Doppler flowmetry

Laser Doppler flowmetry is a simple, direct, real time method to determine red blood cell perfusion in tissue (Acker et al., 1990). The method is potentially non-invasive and can measure the normal physiological state of the microcirculation. Laser Doppler flowmetry works by illuminating the tissue under observation with low power laser light from a probe containing optical fibre light guides. Laser light from one fibre is scattered within the tissue and some is scattered back to the probe. A multi-channel laser Doppler system can be used to monitor microregional changes in flow in human tumors (Pigott et al., 1996).

Measuring tissue PO_2

1. O_2 electrode measurement

Polarographic electrodes were initially used in the 1960s to measure O_2 tension in human tumors based upon generation of electrical current which occurs when O_2 is reduced. Advances in polarographic electrode technology have facilitated the in situ measurement of human tumor pO_2 directly (Brizel et al., 1994; Movsas et al., 2001). A real-time, direct measurement, Eppendorf pO_2 histogram system (Kimoc-pO_2 histograph, Eppendorf-Netheler-Hinz GmbH, Hamburg, Germany) has been used widely in the human clinic and has been called as the "Gold standard" to assess tumor hypoxia (Hockel et al., 1993). Hypoxia measured with the Eppendorf system has been correlated with prognosis including loco-regional control, metastasis and survival in human head and neck, cervical, breast, lung and bladder cancers, and lymphomas.

Newer systems provide improvements in microelectrodes including miniaturization and the addition of a recessed tip, which greatly reduced both O_2 consumption rate and tissue volumes sampled (about 12 um in diameter). Disadvantages include the invasiveness of the procedure, accessibility of tumor insertion, sampling area error (in necrosis or normal tissue), a damaged sampling area from needle insertion and *in vitro* calibration. This method is only applicable to easily accessible tumors, it is invasive, and is time consuming both for the

patient and the person performing the measurements. Three dimensional image systems such as CT or MRI might be useful to identify the areas of tumor, necrosis and normal tissue and to minimize the error associated with areas of sampling. Ultrasound with color doppler imaging guided technique of pO_2 measurement using Eppendorf oxygen electrodes might be a convenient way to improve the accuracy of needle placement and to monitor needle movement during the measurement (Vujaskovic et al., 2003).

2. Optical Sensor-Based O_2 tension measurement

A time-resolved luminescence-based fibre-optical sensor (OxyLite™) can be used to measure tissue oxygenation in human tumors. This sensor has a high signal-to-noise ratio at low PO_2, in contrast to the Eppendorf electrode which has a low signal-to-noise ratio at low PO_2. Another important strength is that oxygen consumption with this probe is minimal, so continuous measurements can be made at the same position during therapy or physiological manipulations, providing dynamic information on the oxygenation status of tumors. It can also be used to measure multiple sites (20+) in the same tumor using pull-back methods. A limitation of this method is mainly short life-time of the fluorescent probe (Bussink et al., 2000a; Griffiths and Robinson, 1999).

3. Phosphorescence lifetime imaging

Water-soluble phosphorescence probes such as Green 2W (Vinogradov et al., 1996) and Oxyphor R2 (Wilson et al., 1998) suitable for measuring O_2 pressure in the blood have used for noninvasive, *in vivo* imaging of O_2 distribution in the vascular systems of experimental animals (Wilson et al., 2002). This O_2-dependent quenching of phosphorescence has been used to obtain digital maps of the O_2 distribution in the tissue vasculature and to detect volumes of tissue with below normal O_2 pressure in the presence of much larger volumes of tissue with normal O_2 pressures. In addition, tissue O_2 pressures can be monitored in real time, even through centimeter thicknesses of tissue. In one study it was found that the superficial layers of tumors were hypoxic whereas the host tissue was well oxygenated (Wilson et al., 1998).

4. *Oxymetric spectral imaging*

Oxymetric spectral imaging can be used to measure the quantitative O_2 concentration in the body water of tumors by using low frequency electron paramagnetic spectroscopy (Halpern et al., 1994).

Hypoxia imaging

Present therapy for cancer patients is based primarily on tumor histology and anatomic location. Tumor imaging is a valuable tool to evaluate tumor physiology and metabolism, with and without various markers (Chapman et al., 2003). Physiologic and metabolic imaging may yield valuable data regarding tumor aggressiveness and stage, and allow assessment of tumor response during and after treatment before morphological changes are detectable.

1. Magnetic resonance imaging (MRI)

MRI gives us a picture of anatomical and physiological conditions. MRI techniques have the unique ability to investigate *in vivo* tumor physiology in a dynamic, non-invasive and non-destructive manner. Functional MRI techniques can be used to measure tissue oxygenation and tumor perfusion (Robinson et al., 1998; Stubbs, 1999).

2. Nuclear magnetic resonance spectroscopy (MRS)

In vivo MRS obtains spectra from single volumes of tissue. These single volume techniques are used for ^{1}H, ^{31}P, ^{13}C, ^{19}F and other nuclei. MRS generates a frequency domain spectrum that provides information about biochemical and metabolic processes occurring within tissues. Metabolic imaging is possible using Magnetic Resonance Spectroscopic Imaging (MRSI), that uses phase encoding to obtain spectra from multiple regions across a field of view. MRSI is largely used for ^{1}H and ^{31}P. ^{31}P MRS can be used to investigate the energy status in tissue following ATP metabolism (Mueller-Klieser et al., 1990). Also, ^{31}P MRS is a potentially useful method for monitoring tumor oxygenation following radiation treatment (Olsen and Rofstad, 1999).

3. Nuclear magnetic resonance (NMR)

The NMR signal is a natural physical property of the certain atomic nuclei but it can only be detected with an external magnetic field. The most commonly observed nucleus is hydrogen (1H) as found in water (H_2O), although the NMR signal from many other nuclei can be observed with the appropriate hardware. ^{19}F NMR spin lattice echo planar imaging relaxometry of hexafluorobenzene can be used to measure regional tumor oxygenation (Mason et al., 1994; Mason et al., 1998; Maxwell et al., 1989).

4. Positron emission tomography: PET

Metabolic imaging by PET is a promising technology to evaluate glucose metabolism, hemodynamics, tumor hypoxia, estrogen receptor density, O_2 utilization, protein synthesis and thymidine incorporation (Koh et al., 1994; Veronesi et al., 2002). The distribution is most accurately determined through use of a PET scanner, to localize and quantify the tracer molecules, in which have been incorporated positron-emitting isotopes. These tracers include hypoxia markers, receptor ligands, substrates for enzymatic modification by the products of expression of specific genes, and precursors of protein anabolism and carbohydrate catabolism (Clavo and Wahl, 1996; Silverman et al., 1998). Cancer cells have increased metabolism of both glucose and amino acids, which can be monitored with ^{18}F-2-deoxy-2-fluoro-D-glucose (FDG), a glucose analogue, and ^{11}C-L-methionine (Met), respectively. FDG uptake is higher in fast-growing than in slow-growing tumors. FDG uptake has potential to be a good marker of the grade of malignancy (Kubota, 2001). Metabolic imaging is useful for the detection of recurrence and for monitoring the therapeutic response in various cancers.

Endogenous markers of hypoxia

Endogenous hypoxia markers are genes or gene products that are specifically up-regulated under hypoxic conditions. Identification of endogenous hypoxic markers will be a great alternative to use of exogenous markers to perform study on archival tissues or fresh tissue without a marker injection. As with other hypoxia markers, establishing basic information such as the actual level of the hypoxia for binding is difficult for endogenous hypoxia marker. Many endogenous hypoxia markers were compared with nitroimidazole hypoxia markers because of the extensive data. An overall correlation between nitroimidazole markers and

endogenous markers is often suggested, but this is difficult to interpret. More research will be needed for endogenous hypoxia markers to become the standard practice.

1. Lactate dehydrogenase (LDH)

LDH is expressed at high levels in many human tumors and has been shown to be an effective serum marker for cancer. The major hypoxic-stress protein p34 has been shown to be a specific LDH isozyme. Under well-oxygenated conditions LDH is synthesized as a soluble form, while hypoxia induces synthesis of an isozyme that binds to membranes. Histochemical methods for accessing lactate dehydrogenase activity, endogenous lactate and accumulation of neutral fat can be used to estimate tissue hypoxia indirectly.

2. Endogenous Carbonic anhydrase 9 (CA9)

CA9 is a transmembrane protein induced by hypoxia and overexpressed in a wide variety of tumor types (Koukourakis et al., 2001). This enzyme catalyzes the reversible hydration of carbon dioxide to carbonic acid. High levels of expression were found in many cancer cell lines and tumor tissues (Ivanov et al., 2001). Under hypoxic conditions, CA9 protein levels steeply increased from 4 to 24 hours. Induction of CA9 protein is estimated to occur at pO_2 levels of less than 20 mmHg, which is higher than with nitroimidazole hypoxic marker binding levels (Wykoff et al., 2000). The staining pattern is similar to 2-nitroimidazole, PIMO, which is mainly considered to correlate with diffusion-limited hypoxia. High CA9 expression was associated poor survival in cervical carcinomas (Loncaster et al., 2001).

3. Endogenous hypoxia-inducible factors 1alpha and 2alpha (HIF-1α & 2α)

Overexpression of HIF-1α and HIF-2α have been demonstrated in tumor cell lines and human tumors under hypoxic conditions. HIF-1α is specially upregulated under hypoxic conditions and rapidly degraded under ambient O_2 conditions. On IHC, HIF-1α and HIF-2α expressions were localized to tumor nuclei and HIF-2α expression was also seen in tumor-associated macrophages. Localization of HIF-1α expression is typically consistent with diffusion limited hypoxia, but localization is also seen closer to the vessels than other hypoxia markers which may suggest that induction of genes occurs at higher pO_2. Although results of human tumor studies are controversial (Beasley et al., 2002; Haugland et al., 2002), in the majority of studies overexpression of HIF-1α indicated a poor prognosis

(Aebersold et al., 2001; Birner et al., 2001; Giatromanolaki et al., 2001; Sivridis et al., 2002). In the recent study HIF-α expression was O_2 dependent although the level of staining wasn't always consistent with PIMO staining in different hypoxia conditions (Vordermark and Brown, 2003).

4. Endogenous Glut-1 and Glut-3

Glucose transporters Glut-1 and Glut-3 are regulated by the VHL and HIF-1 pathway, and these transporters could be useful markers of hypoxia. They mediate cellular glucose uptake and facilitate anaerobic glycolysis. Staining patterns indicated that they seem to be related to diffusion limited hypoxia (Hoskin et al., 2003). Glut-1 overexpression was associated with poor prognosis in several carcinomas (Airley et al., 2001).

Use of 2-nitroimidazole hypoxia marker

Nitroimidazole markers are exogenous hypoxia markers, are bio-reducible under hypoxic conditions (Hodgkiss, 1998). Clinically relevant exogenous markers are the 2-nitroimidazoles, pimonidazole (PIMO) and EF5 (Evans et al., 2000b; Raleigh et al., 1998b). 2-nitroimidazole markers provide hypoxia measurements with a high spatial resolution. Histological evaluation can be achievable on the same section of tissues to define tumor cells, necrotic tissue and other than tumor cells. Necrosis is free of labeling due to loss of metabolic ability. Multiple color fluorescent immunochemical staining allows hypoxia to be correlated with other markers on histologic samples.

1. <u>History of nitroimidazole hypoxia marker development</u>

- 2-nitroimidazole initially developed as a radiosensitizer such as misonidazole, forms adducts in hypoxic cells *in vitro* and *in vivo* (Varghese et al., 1976).
- Adduct formation was restricted to cells in which misonidazole was reductively activated under hypoxic conditions (Chapman et al., 1983; Franko and Koch, 1984).
- ^{14}C- or ^{3}H-misonidazole binding in experimental and clinical studies showed feasibility of using these agents as hypoxia markers (Chapman et al., 1981; Urtasun et al., 1986).

- Non-radioactive, immunochemical assays were developed (Evans et al., 2000b; Franko, 1986; Hodgkiss, 1998; Raleigh et al., 1996; Raleigh et al., 1987). Hypoxia marker was first to apply to spontaneous tumors in dogs (Cline et al., 1990).
- Non-invasive assays were developed (Cook et al., 1998; Groshar et al., 1993; Honess et al., 1998; Raleigh et al., 1991).

2. *Advantages of nitroimidazole hypoxia markers*
    - With histological examination, detection and discrimination of hypoxia in non-tumor tissue is possible at the cellular level
    - Diffusion of drug is high to reach necrotic tumor areas
    - Labeling is established *in vivo* without physical disruption of the tissue
    - Non-invasive detection is possible with suitably labeled hypoxia markers
    - Microregional distributions of hypoxia can be related to other markers such as markers for proliferation, differentiation, apoptosis, vascularity and hypoxia related gene expressions

3. *Disadvantage of nitroimidazole hypoxia markers*
    - Marker administration is required prior to detection
    - Indirect detection system may be influenced by intensity of labeling

4. *Metabolism of the 2-nitroimidazoles in mammals*

2-nitroimidazoles are reduced by nitroreductase enzymes under hypoxic conditions. Reductive metabolism is carried out by widely distributed constitutive flavo-enzymes that are able to use nitro-aromatic compounds as alterative electron acceptors (Clarke et al., 1982). Different kinds of nitroreductases are present in the cytoplasm, microsomes, and mitochondria.

- Cytoplasm: aldehyde oxidase, DT-diaphorase and xanthine oxidase,
- Microsomes: NADPH cytochrome reductase and cytochrome P-450
- Mitochondria: dihydrolipoamide dehydrogenase, cytochrome b5 reductase, NADH-dehydrogenase and succinate dehydrogenase

The O_2 dependent bioreductive metabolism of 2-nitroimidazoles proceeds in cells as a series of one-electron reductions. However, the nitro-radical anion, produced by the first one-electron reduction step, is very reactive towards O_2 and is oxidized back to the parent nitroimidazole so efficiently, that in well-oxygenated conditions there is effectively no substrate for the second step. Under hypoxic conditions, metabolism proceeds further stepwise by reduction of the one-electron reduction product to the nitroso (2 e^-) hydroxylamine (4 e^-) and amine (6 e^-) derivatives.

5. Adduct formation

Adduct formation between reductive activated nitroimidazole and thiol containing compounds such as glutathione involved sulfide bounds to the imidazole ring of the reduced 2-nitroimidazole. The chemically confirmed structures of glutathione adducts are most readily understood in terms of a four electron reduction, hydroxylamine binding intermediate (Berube et al., 1992). The binding of bioreductively activated 2-nitroimidazoles is confined primarily to the cells in which activation occurs but in some cases up to 3 % of the binding can be detected in extracellular proteins (Chapman et al., 1983). The chemical structures of macromolecular adducts of reductively activated 2-nitroimidazoles *in vivo* are not known in detail but indirect evidence indicates that they are analogous to the glutathione adducts.

6. Adduct detection by antibody

Macromolecular adducts of 2-nitroimidazole can be used as immunogens for the preparation of monoclonal and polyclonal antibodies or for the production of solid phase antigens for immunochemical detection systems (Arteel et al., 1995; Lord et al., 1993; Olive, 1995; Thrall et al., 1994).

7. Methods used for analysis

<u>Immunochemical assays</u>

Several 2-nitroimidazoles with immunologically identifiable side-chains have been described as hypoxia markers and conventional IHC procedures or flow cytometric analysis can be used to detect their metabolites, bound to hypoxic cells in frozen or paraffin-embedded histological sections, or fresh single cell suspensions of biopsy material (Arteel et al., 1995; Cline et al., 1994; Cline et al., 1990; Evans et al., 1996; Olive et al., 2000; Hodgkiss et al.,

1994; Hodgkiss et al., 1991a; Hodgkiss et al., 1991b; Koch et al., 1995; Lord et al., 1993; Raleigh et al., 1987).

An enzyme-linked immunosorbent assay (ELISA)

ELISA is a rapid, sensitive, quantitative, and non-radioactive technique to measure the binding of a hypoxia marker in biopsy samples of tumors (Raleigh et al., 1994; Raleigh et al., 1992; Thrall et al., 1994). The ELISA is based on reagents prepared from synthetic antigens formed by the reductive activation and binding of 2-nitroimidazole to proteins in novel test tube experiments. Calibration of the ELISA involves comparing the ELISA with the radioactivity contained either in protein- nitroimidazole adducts formed *in vitro* with tritiated 2-nitroimidazole or in tissues isolated from a tumor-bearing dog which had been injected with tritium- labeled 2-nitroimidazole.

8. Nitroimidazole markers (figure 0.1)

- CCI-103F: a hexafluorinated 2-nitroimidazole, F6 (Cline et al., 1994; Cline et al., 1990; Hodgkiss et al., 1994; Hodgkiss et al., 1991b; Raleigh et al., 1987).
- Pimonidazole: 1-{(2-hydroxy-3-piperidinyl)propyl}-2-nitroimidazole hydrochloride (Arteel et al., 1995; Kennedy et al., 1997; Raleigh et al., 1999; Raleigh et al., 2001; Rijken et al., 2000; Rofstad and Halsor, 2002; Varia et al., 1998).
- EF5: a pentafluorinated derivative of etanidazole, 2-(2-nitro-1H-imidazol-1-yl)-N-(2,2,3,3,3 pentafluoropropyl)-acetamide (Evans et al., 1996; Evans et al., 2000b; Koch et al., 2001; Lee et al., 1996; Lord et al., 1993).
- NITP: 7(-)[4'-(2-nitroimidazol-l-yl)-butyl]-theophylline. Oral administration could be done for clinical studies with NITP (Hodgkiss et al., 1995b; Webster et al., 1998).
- IAZA: 1-(5-iodo-5-deoxy-bata-D-arabinofuranosyl)-2-nitroimidazole (Groshar et al., 1993).

9. Non-invasive hypoxia marker detection system

Noninvasive imaging with a hypoxia-directed radiopharmaceutical could be of great clinical utility (Cook et al., 1998; Groshar et al., 1993; Honess et al., 1998). Various isotopically labeled 2-nitroimidazoles have been proposed as hypoxia markers. For evaluation of hypoxia, severe perfusion deficit is usually associated with an increased uptake of the

hypoxic marker and this trend was observed in several human tumors (Groshar et al., 1993; Tatsumi et al., 1999; Yutani et al., 1999).

Nuclear medicine

Isotopically labelled 2-nitoimidazoles can be detected by planer nuclear scintigraphy, single photon emission tomography (SPECT), position emission tomography (PET), and magnetic resonance spectroscopy (MRS). Non-nitro-containing bioreductive complexes have also been evaluated (Ballinger, 2001). Isotopes include ^{3}H (Kim et al., 1993; Raleigh et al., 1985), ^{14}C (Chapman et al., 1981), ^{75}Br, ^{76}Br, ^{77}Br (Rasey et al., 1985a; Rasey et al., 1985b), ^{18}F, ^{123}I, ^{131}I and ^{99m}Tc.

Planer nuclear scintigraphy

Planar scintigraphy is relatively easy, inexpensive and widely available. ^{99m}Tc, ^{131}I and ^{125}I labeled hypoxia markers have been evaluated for measurement of tumor oxygenation (Ballinger et al., 1996; Cherif et al., 1996; Iyer et al., 1998b; Iyer et al., 1998c; Melo et al., 2000; Yang et al., 1999; Zhang et al., 1998). Comparison of several markers labeled with ^{99m}Tc, ^{131}I and ^{18}F showed that it is feasible and convenient to use a ^{99m}Tc labeled marker to image tumor hypoxia (Yang et al., 1999). Biodistribution studies showed high tumor-to-blood ratios (T/B: i.e. the contrast between the target and the background activity). The T/B of marker radioactivity in mice had been shown to be proportional to radiobiological hypoxic fraction. These results suggest planar scintigraphy will be a potentially useful technique to investigate the status of hypoxia in solid tumors in the clinic (Hoebers et al., 2002).

Single photon emission computed tomography (SPECT)

SPECT images are generated using gamma cameras or ring-type imaging systems that record photons emitted by tracers trapped in the tissues. Three dimensional surface and volume rendered images add perspective and facilitate the localization and sizing of lesions. SPECT results in better image quality than planar (2-D) imaging because focal sources of activity are not superimposed upon each other; hence the T/B becomes greatly increased. The volume imaging capacity of SPECT systems permits reconstruction at any angle, including transverse, dorsal and sagittal planes, or at the same angle of imaging obtained with CT or MRI to facilitate image comparisons. SPECT images can be merged with MRI

and CT, creating a single image that combines anatomy and physiology (morphological and functional correlation). SPECT can be used for studying tumor tissue perfusion and oxygenation in patients with ^{123}I, ^{131}I, ^{99m}Tc or ^{67}Cu labeled 2-nitroimidazole (Cook et al., 1998; Engelhardt et al., 2002; Groshar et al., 1993; Hulshof et al., 1998; Urtasun et al., 1996).

Positron emission tomography (PET)

The particular advantages of PET are that it has higher sensitivity, higher resolution, and a higher quality of image than conventional nuclear medicine. The possibility of quantification and the wide range of useful isotopes have raised expectations of this method. 2-nitroimidazoles can be labeled with the short-lived isotope ^{18}F and ^{64}Cu (Casciari et al., 1995; Engelhardt et al., 2002; Evans et al., 2000a; Koh et al., 1994; Koh et al., 1992; Lehtio et al., 2001; Leskinen-Kallio, 1994; Rasey et al., 1999; Rasey et al., 2000; Rasey et al., 1996; Yang et al., 1999).

Nuclear Magnetic Resonance Spectroscopy (NMR or MRS)

MRS can be used to detect ^{19}F, a fluorinated 2-nitroimidazole (Aboagye et al., 1998a; Aboagye et al., 1997; Kwock et al., 1992; Maxwell et al., 1989; Raleigh et al., 1991). ^{19}F is a single naturally occurring paramagnetic isotope of fluorine. Most current NMR detection sensitivities are still low, requiring long signal averaging times and this limitation needs to be refined for routine clinical use.

Comparison of methods for measurement of hypoxia

Comparison of methods for detecting hypoxia in the clinic is more complicated for several reasons. It is impossible to perform the “clamped tumor control” type assay to measure clonogenic hypoxic cells. O_2 electrode and 2-nitroimidazole hypoxia markers have been used extensively clinically. Only electrode measurement has shown that hypoxia is a negative prognostic factor in human tumors. Several techniques have been evaluated for their compatibility, which is inconclusive in many circumstances (Aboagye et al., 1998b; Aquino-Parsons et al., 1999; Begg et al., 2001; Collingridge et al., 1997; Evans et al., 1997b; Fenton et al., 1999; Haugland et al., 2002; Honess et al., 1998; Jenkins et al., 2000; Kavanagh et al., 1999a; Kavanagh et al., 1996; Kavanagh et al., 1999b; Kim et al., 1993;

Lee et al., 1996; Lyng et al., 1997; Mahy et al., 2003; Nordsmark et al., 1995; Nordsmark et al., 1997; Nordsmark et al., 2003; Nozue et al., 1997; Olive et al., 2000; Olive et al., 2001b; Raleigh et al., 1999; Rijken et al., 2002; Siemann et al., 1998; Stern et al., 1996).

Although the good correlation between the Eppendorf O_2 microelectrode measurement and PIMO labeled area fraction has been reported in experimental tumors (Raleigh et al., 1999), no significant correlations were found between two methods in human tumors (Evans et al., 2000b; Nordsmark et al., 2001; Nordsmark et al., 2003; Olive et al., 2001a). The two methods seem different as the Eppendorf microelectrode measures tissue pO_2 in a quantitative manner while 2-nitroimidazole labeling is based on a non-linear system. Necrosis seems to be a major confounding factor in the two measurements. Microelectrode readings characterize necrosis as low O_2 tension, whereas absence of nitroimidazole binding in necrotic areas would identify them as necrosis with manual evaluation or oxic with computer based automatic counting. The Eppendorf needle electrode technique could overestimate the presence of hypoxia in tumors with high necrosis. There are also distinct differences in spatial and time resolution between these two methods. The 2-nitroimidazole, EF5 measurements had greater spatial heterogeneity than did the electrode measurements (Jenkins et al., 2000).

Hypoxic fraction measured using the comet assay correlated with the percentage of pO_2 values <10 mmHg (Aquino-Parsons et al., 1999; Partridge et al., 2001). Tumors defined as hypoxic based on a median pO_2 <10 mmHg appear to contain more than 20% radiobiologically hypoxic cells as estimated by the comet assay.

Hypoxic fraction estimated by a nitroimidazole marker correlated well with the hypoxic fraction measured using the comet assay (Olive et al., 2001a; Olive et al., 2000; Raleigh et al., 1999).

CA9 and PIMO IHC were compared in formalin-fixed sections from tumors of patients undergoing treatment for cancer of the cervix (Olive et al., 2001b), head and neck (Kaanders et al., 2002c), and bladder (Hoskin et al., 2003). Excellent co-localization was observed between CA9 and PIMO IHC in cancers although the area of the tumor section that bound anti-CA9 antibodies represented the larger number of cells that bound anti-PIMO antibodies (Kaanders et al., 2002c; Olive et al., 2001b). Occasional regions staining with PIMO but not CA9 could be indicative of transient changes in tumor perfusion. Results

support the hypothesis that CA9 is a useful endogenous marker of tumor hypoxia (Olive et al., 2001b).

The relationships between hypoxia using an Eppendorf needle electrode and histological landmarks such as intercapillary distance and microvessel density were investigated in cervical cancer (West et al., 2001). Both intercapillary distance and microvessel density were significant independent prognostic factors for local control. There was a significant correlation between tumor hypoxia and intercapillary distance but not microvessel density.

Table 0.1 Comparison of measurement method to assess hypoxia in selected references

Author, Year	Reference	pO_2 vs 2-nito.	pO_2 vs RB	2-nitro. vs RB	pO_2 vs comet	2-nitro. vs comet
Kim, 1993	(Kim et al., 1993)	Yes				
Lee, 1996	(Lee et al., 1996)			Yes		
Stern, 1996	(Stern et al., 1996)			Yes		
Kavanagh, 1996	(Kavanagh et al., 1996)	No	No	Yes		
Lyng, 1997	(Lyng et al., 1997)	Yes				
Nozue, 1997	(Nozue et al., 1997)	Yes				
Siemann, 1998	(Siemann et al., 1998)		Yes			
Raleigh, 1999	(Raleigh et al., 1999)	Yes		Yes		
Kavanagh, 1999	(Kavanagh et al., 1999b)	No	No	Yes		
Aquino-Parsons, 1999	(Aquino-Parsons et al., 1999)				Yes	
Jenkins, 2000	(Jenkins et al., 2000)	No				
Olive, 2000	(Olive et al., 2000)					Yes
Olive, 2001	(Olive et al., 2001b)					
Haugland, 2002	(Haugland et al., 2002)					
Mahy, 2003	(Mahy et al., 2003)	Yes				
Nordsmark, 2003	(Nordsmark et al., 2003)	No				
Le, 2003	(Le et al., 2003)				No	

pO_2: by needle electrode, 2-nito: 2-nitroimidazole hypoxia marker, RB: radiobiological method, comet: comet assay
Yes: there was correlation, no: there was no correlation

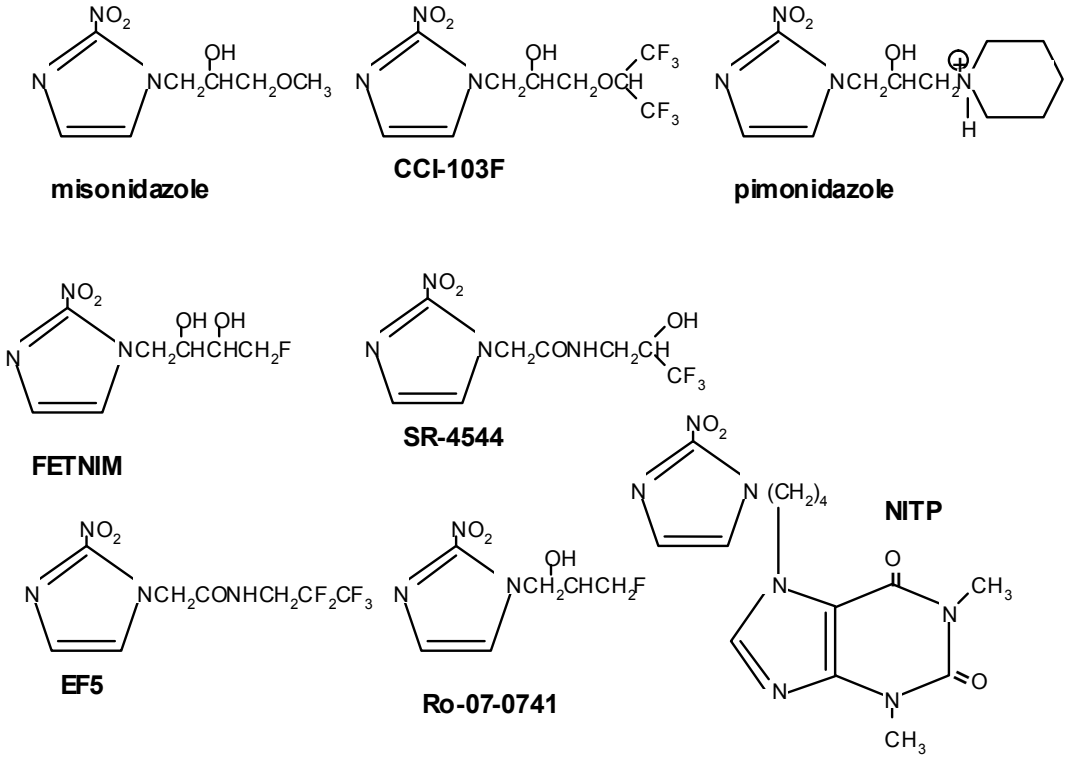

Figure 0.1 Structures of some 2-nitroimidazole hypoxia markers

6. APPROACHES TO OVERCOME TUMOR HYPOXIA

There is only limited support for the theory that radiation resistance due to tumor hypoxia can be effectively eliminated. Hypoxia-targeted therapy can be an excellent strategy to improve treatment outcome without excessive normal tissue toxicity (Brown, 2002). It is advantageous to base the selection of patients for hypoxia-targeted approaches on oxygenation or microenvironmental characteristics of individual tumors (Bussink et al., 1999a). Clinical trials aim to improve the therapeutic ratio and thus the study of morbidity is as important as local tumor control. Many of these treatments are associated with toxicities or high cost of treatment. The success of randomized controlled trials would be improved greatly if methods were available to measure tumor hypoxia to identify the best candidates for hypoxia-targeted approaches. When tumor oxygenation is evaluated, the differential detection of acute versus chronic hypoxia is likely to be important since there seems to be different effects on therapeutic response (Stern and Guichard, 1996). Acutely hypoxia cells may have a more significant role than chronically hypoxic cells because acutely hypoxic cells may be metabolically active right after the hypoxic insult and actively proliferating. Appropriate combinations should be aimed at eradicating the two different kinds of tumor hypoxia (Masunaga et al., 2000).

There are mainly five categories of ways to overcome the presence of tumor hypoxia in cancer therapy that include:

- ***Improving tumor oxygenation***
- ***Radiosensitization of hypoxic tumor cells***
- ***Killing of hypoxic tumor cells***
- ***Protection of normal tissues, and***
- ***Others***

Improving tumor oxygenation

The degree of tumor hypoxia depends on the balance between O_2 supply and O_2 consumption of the tissues (Vaupel et al., 1998a). Simulation of effects of blood flow rate, O_2 content and O_2 consumption on the hypoxic fraction suggested that the most effective way to eliminate tumor hypoxia would be to suppress O_2 consumption (Secomb et al., 1995).

Theoretically, if a tumor contains 30% hypoxic cells, hypoxia is abolished by a reduction in consumption rate of at least 30%, an increase in flow rate by a factor of 4 or more, or an increase in arterial pO_2 by a factor of 11 or more. According to the theory, reduction of O_2 consumption may be the only practical way to eliminate tumor hypoxia.

Improving blood supply to the tumor

To increase blood supply specifically to the tumor is difficult. Moreover, increasing blood flow by a factor of 4 times to eliminate 30% hypoxia won't be achievable. Tumor vessels formed by angiogenesis do not have systematic control of vessel tone. Also blood flow in the tumor is largely influenced by systemic perfusion. For example, blood flow is maintained in vital organs during hypotensive episodes and blood flow in tumor is decreased (steal phenomena) thereby resulting in more hypoxia in the tumor. Hyperthermia, carbogen and nicotinamide have been evaluated to improve tumor perfusion in clinical trials and almost always they are used in combination with radiation therapy or other therapeutic agents.

1. Mild local hyperthermia

Dilation of blood vessels is a normal response to excessive heat exposure. Dilation of tumor vessels is also seen in many tumors following hyperthermia and results in increased blood flow and oxygenation in the tumor (Griffin et al., 1996a; Masunaga et al., 1997b; Shakil et al., 1999). Hyperthermic increase in perfusion is likely to preferentially oxygenate the chronically hypoxic fraction (Masunaga et al., 1997a). To maximize the effect of hyperthermia on radiation, concurrent administration of the hyperthermia with radiation is ideal (Horsman and Overgaard, 1997).

2. Rheologically active drugs

Rheologically active drugs might be able to decrease blood viscosity and improve tumor perfusion. Calcium channel blockers and methylxanthine derivatives have successfully been used in experimental tumor models (Honess et al., 1995). Substantial improvements in tumor oxygenation and perfusion were observed after administration of methylxanthine derivatives (Kelleher et al., 1998a).

3. Systemic hemodilution

Systemic hemodilution will decrease blood viscosity and improve blood perfusion and O_2 availability in the experimental tumor model. To achieve maximum improvement of the O_2 supply, hematocrit values have to be minimally 30% (Jung et al., 1984).

4. Vasoactive drugs

Angiotensin is a potent vasoconstrictive drug. Such a drug might be useful to increase tumor perfusion and lead to an increased O_2 supply. Systemic administration of angiotensin led to vasoconstriction of tumor vessels followed by a decrease in tumor oxygenation in small tumors whereas the increased systemic perfusion pressure resulted in increased of oxygenation in large tumors (Thews et al., 1995).

Nitric oxide (NO) is a potent vessel-dilating agent. The effect of NO on radiosensitization showed that it markedly radiosensitized the hypoxic cells *in vitro* (Griffin et al., 1996b; Janssens et al., 1999).

5. Nicotinamide, the amide derivative of B3

Nicotinamide increases blood flow and mean pO_2, and enhances the radiation damage of tumors selectively in preference to normal tissue (Horsman et al., 1989). Improving and increasing the uniformity of microcirculatory flow rate will possibly enhance perfusion limited O_2 delivery (acute hypoxia) although the mechanism of action is still under investigation (Kelleher and Vaupel, 1994). One of the proposed mechanisms is that nicotinamide reduces tumor interstitial fluid pressure; thereby the fraction of previously non-perfused vessels became perfused after nicotinamide administration (Peters et al., 1997). Transient plugging of microcapillaries by leukocytes is another possible mechanism for the development of acute hypoxia in tumors and nicotinamide might modify acute hypoxia by increasing leukocyte filterability (Honess et al., 1996). In a human clinical trial, toxicities included upper gastro-intestinal toxicity (Bernier et al., 1998; Bernier et al., 1999; Denekamp and Fowler, 1997; Hoskin et al., 1995) and renal dysfunction (Kaanders et al., 1995). For the best anti-tumor effect, radiation should be given at the time of peak plasma drug concentrations (Horsman et al., 1997). Microvascular response and changing oxygenation might vary depending on tumor type, or other factors and there were controversial findings for vascular

response and tumor oxygenation with nicotinamide (Fenton et al., 2000; McLaren et al., 1997; van der Maazen et al., 1995).

Increasing oxygen content

1. 100% oxygen

Increased O_2 solubility in plasma improves O_2 carrying capacity to tissues. The maximum enhancement ratio using 100% normobaric O_2 in a mouse tumor with fractionated radiation was 1.45 which was more than found with the O_2-mimetic compound 2-nitroinidazole (Rojas et al., 1990). Potential disadvantages to using 100% O_2 are that the radiosensitization is transient (Hill et al., 1998) and there are vasoconstrictive effects of O_2.

2. Carbogen (95% O2/5% CO2)

Carbogen predominantly affects O_2 diffusion distance by increasing the O_2 carrying capacity of blood and radiosensitizes the chronically hypoxic tumor cells (Powell et al., 1996; Robinson et al., 1999) although the true mechanism is unknown (Dewhirst et al., 1996b). Breathing CO_2 blocks the vasoconstrictive effects of O_2, thereby maintaining tumor blood flow with a high partial pressure of O_2 (Honess and Bleehen, 1995). Carbogen may also increase O_2 delivery to the tumor by shifting the hemoglobin O_2 dissociation curve to the right (Rojas, 1991). The effects of carbogen are often unpredictable and also dependent on tumor type (Bussink et al., 1999b; Dunn et al., 1999; Lanzen et al., 1998). In one study carbogen produced a substantial closing of vessels (Fenton et al., 2000). In humans, heart rate was significantly reduced and O_2 saturation was significantly increased by carbogen breathing while systemic arterial blood pressure remained stable (Kergoat and Faucher, 1999). Systemic effects of longer exposure of carbogen include hypertension, which limits the duration of exposure time to 20 minutes in clinic (Laurence et al., 1995). The maximal effect was obtained in the majority of patients after 1 to 6 minutes of carbogen exposure (Guichard et al., 1994) and effects were transient.

3. Hyperbaric oxygen (HBO)

HBO at 3-4 atmospheres pressure has been proposed to reduce tumor hypoxia by increasing the amount of dissolved O_2 in the plasma to carry O_2 to tissues. HBO can improve tumor oxygenation significantly and was more effective than carbogen/nicotinamide

treatment in an experimental system (Brizel et al., 1995b; Brizel et al., 1997b). The effects of HBO in muscles decreased rapidly and returned to the control level within 40 min after decompression, whereas in tumors the effect decreased gradually and remained at a high level 60 minutes after HBO exposure (Kinoshita et al., 2000). In human trials, results are still contradictory (Becker et al., 2002; Cade et al., 1978; Haffty et al., 1999a; Haffty et al., 1999b; Watson et al., 1978). In one study, there was evidence for an increase in late radiation morbidity with HBO (Dische et al., 1999).

4. Correction of Anemia

Anemia in cancer patients is multifactorial and may occur as an either a direct effect of the cancer, an indirect effect of cancer, or a result of the cancer treatment itself. A hemoglobin concentration above 12 g/l in patients was associated with better response to therapy (Harrison et al., 2002; Littlewood, 2001). There is accumulating clinical evidence of significantly reduced local-regional tumor control and overall survival in anemic patients receiving radiotherapy for a variety of cancers (Becker et al., 2000; Bush, 1986; Dische, 1991; Fein et al., 1995; Fyles et al., 2000; Kumar, 2000; Lee et al., 1998b). Although blood transfusion is relatively inexpensive and effective to correct anemia (Grogan et al., 1999), it is associated with certain risks such as transmission of diseases and is subject to limitations in blood supply. Erythropoietin (EPO) treatment has been found to be effective in preventing anemia and in reducing the need for blood transfusions, although it is expensive (Dunphy et al., 1999; Mercadante et al., 2000). Epoetin alfa is a recombinant human erythropoietin (Cella and Bron, 1999) which is effective and well-tolerated in maintaining hemoglobin level and reducing transfusion requirement in patients (Thatcher et al., 1999; Wolchok et al., 1999). EPO has been associated with thromboembolism and is being withdrawn from clinical trials (Vreugdenhil et al., 1993; Wun et al., 2003).

5. Modified hemoglobin

Administration of hemoglobin or a modified hemoglobin decreased the level of hypoxia and increased tumor response to radiation therapy in experimental tumors (Nozue et al., 1996; Robinson et al., 1995; Rowinsky, 1999; Teicher et al., 1995b; Teicher et al., 1997). Tissue oxygenation might be enhanced by O_2 carrying capacity of modified hemoglobin as well as

hemodynamic factors, and it seemed to improve both perfusion-limited and diffusion-limited hypoxia.

6. Perfluorochemical Emulsions (PFCE)

PFCEs have been investigated to increase the O_2 carrying capacity of blood (Teicher, 1992; Teicher et al., 1995a). Increased oxygenation in previously hypoxic tumor regions was observed after administration of PFCE and carbogen breathing (Koch et al., 2002). The preclinical studies have shown positive effects with irradiation in several rodent tumor models.

7. Eliminate respiratory compromise-cigarette smoking

Chronic non-neoplastic lung conditions, such as due to smoking, that impair blood oxygenation have negative impact for radiation therapy. Carboxyhemoglobin (HbCO) is formed when CO is bound to hemoglobin. Heavy smokers have high levels of HbCO in their circulation that are known to reduce the amount of oxygen transport to tissues. Chronic exposure to CO significantly decreases tumor blood flow and response to radiation treatment in an experimental system (Grau et al., 1992).

8. Combination of nicotinamide and carbogen

The combination of nicotinamide and carbogen breathing is designed to improve the radiation response of tumors by reducing both acute and chronic hypoxia (Fenton, 1995; Honess and Bleehen, 1995). The greater radiosensitization occurred when nicotinamide and carbogen were combined (Fenton et al., 2000; Horsman et al., 1994; Laurence et al., 1995; Stuben et al., 1998). There have been few trials in human tumors (Hoskin et al., 1999).

9. Accelerated Radiotherapy combined with Carbogen and Nicotinamide (ARCON)

ARCON was designed to overcome repopulation of clonogenic tumor cells during radiotherapy and to minimize the effect of the chronic and acute tumor hypoxia. Experimental studies have shown a significant radiosensitization (Rojas et al., 1996). The plasma concentrations considered necessary to radiosensitize could be achievable with nicotinamide in ARCON without unacceptable toxicity (Bernier et al., 1998; Kaanders et al., 2002b). Several results of clinical testing have been reported with mostly favorable results

particularly for carcinomas of the larynx, oropharynx and bladder (Bernier et al., 2000; Bernier et al., 1999; Hoskin et al., 1999; Kaanders et al., 2002a; Kaanders et al., 1998; Miralbell et al., 1999).

10. Combination of nicotinamide, carbogen, and perflubron emulsion

The combination of nicotinamide, carbogen and perflubron emulsion has been studied with the result being enhancement of radiation response in rodent tumors (Thomas et al., 1996).

11. Continuous hyperfractionated accelerated radiation therapy (CHART)

CHART was also designed to overcome repopulation of clonogenic tumor cells during radiotherapy. Conventional radiotherapy was delivered in 30 fractions of 2 Gy to a total dose of 60 Gy in 6 weeks. CHART was delivered in 36 fractions of 1.5 Gy 3 times per day to give 54 Gy in 12 consecutive days. This study showed that CHART is superior to conventional radiotherapy in achieving local tumor control and survival (Saunders et al., 1999).

12. CHART and nimorazole

One of the limitations of CHART is the limited time interval between fractionation for reoxygenation, so that hypoxia becomes a more potent cause of failure. Combination of CHART and nimorazole was designed to overcome repopulation of clonogenic tumor cells during radiotherapy and to minimize the effect of the chronic and acute tumor hypoxia (Henk et al., 2003). A phase II study has shown promising results in advanced squamous cell carcinoma of the head and neck (Cottrill et al., 1998). Side effects of this combination therapy included a possible slight increase in acute skin reaction and slightly greater nimorazole toxicity. Local control rates are higher than those previously seen with CHART, suggesting a positive effect of nimorazole.

Decreasing oxygen consumption

Reduction in the O_2 consumption rate would permit further diffusion of O_2 from feeding vessels into distant tissue layers of tumors results in improvement of tissue oxygenation.

1. Local hypothermia

A 60% reduction in the O_2 consumption rate was achieved when local tumor temperature is lowered to 25°C. Despite of the significant reduction of O_2 consumption, no significant change in oxygenation was seen (Kelleher et al., 1998b).

2. Mitochondrial inhibitors

Mitochondrial inhibitors including Ca^{2++} channel blockers and the respiratory inhibitor meta-iodo-benzylguanidine, MIBG can be used to reduced O_2 consumption (Biaglow et al., 1986; Vaupel and Mueller-Klieser, 1986). MIBG in its ^{131}I-labeled form is clinically used as a tumor-targeted radiopharmaceutical in the diagnosis and treatment of adrenergic tumors. MIBG reportedly inhibits mitochondrial respiration *in vitro* (Kuin et al., 1994; Loesberg et al., 1990). The mechanism for MIBG inhibition of cellular O_2 consumption is uncertain and further investigation is needed (Biaglow et al., 1998).

3. Inhibiting DNA synthesis

Fludarabine and lovastatin can inhibit tumor cell proliferation because both drugs lowered DNA synthesis significantly. The cellular O_2 consumption rate following lovastatin application was significantly impaired, whereas fludarabine had practically no effect on the respiration rate of tumor cells. From these data, it was concluded that a reduction in DNA synthesis does not necessarily result in a decrease in the O_2 consumption rate of tumor cells *in vivo* (Thews et al., 1996).

4. Acute hyperglycemia, Crabtree effect

Exposure of tumor cells to glucose decreases O_2 consumption (Crabtree effect) *in vitro*. Acute hyperglycemia is also known to transiently reduce the O_2 consumption rate of tumor cells because glucose inhibits O_2 uptake (Vaupel and Thews, 1976). However, some cell lines are not susceptible to the Crabtree effect, and the magnitude is dependent on baseline pO_2. Additional or alternative manipulations may be necessary to achieve more uniform improvement in pO_2 (Snyder et al., 2001).

5. Hyperglycemia plus MIBG

Administration of glucose plus MIBG increases tumor O_2 tension and also increases the magnitude and duration of acidification. Hyperglycemia plus MIBG has the potential to improve response to radiation therapy as well as to hyperthermia and some chemotherapies (Burd et al., 2001; Burd et al., 2003).

6. Inhibiting RAS

Farnesyltransferase inhibitors can alter the oxygenation of certain tumors. Experimental tumor cell lines with mutations in H-ras had markedly improved oxygenation after farnesyltransferase treatment. In contrast, xenografts from two tumors without ras mutations had equivalent hypoxia regardless of treatment. Inhibitors of RAS might be useful to reduce O_2 consumption of tumors (Cohen-Jonathan et al., 2001).

7. Irradiation

In experimental tumors, improvement of tumor oxygenation was found several hours after irradiation. That was most likely due to a decrease in O_2 consumption (Bussink et al., 2000b; Olive, 1994).

Radiosensitization of hypoxic cells

In the early 1960s there was extensive research for O_2 substitutes that diffuse into poorly vascularized areas of tumors and produce radiosensitization. Nitroimidazoles, hypoxic cell sensitizers, enhance the tissue response to conventional radiation generally by mimicking the effects of O_2, which induces the formation and stabilization of toxic DNA radicals (Allen et al., 1984). The two most commonly used in clinical trials were misonidazole and etanidazole (Overgaard, 1994)**.** Today, nimorazole is the most successful radiosensitizer among nitroimidazoles. Sensitizing efficiency is directly related to the electron affinity of the compounds. Nitroimidazoles are true sensitizers, as their effects are synergistic rather than additive, and they usually don't have much of an effect against the tumor themselves. Five essential properties for a clinically useful hypoxic cell sensitizer include:

1. Selectivity to sensitize hypoxic cells at a concentration without unacceptable toxicity to normal tissues
2. High chemical stability without rapid metabolic breakdown in tissues

3. The octanol:water partition coefficient must be in a clinically useful range. High water solubility is beneficial because this facilitates formulation of the injectate and also beause of rapid equilibration in the extracellular fluid volume. However, some degree of lipid solubility is necessary for diffusion through lipid-containing cellular components.
4. Effective throughout most of the cell cycle
5. Effective at the relatively low daily irradiation doses of a few Gy used in conventional fractionated radiotherapy

Drugs are required to be present in tumor cells at the time of irradiation to be effective. In addition to radiosensitizing hypoxic cells, several of the nitroimidazoles have also shown to be preferentially cytotoxic to hypoxic cells. In an experimental model, the enhancement ratio of 1.8 was achieved with misonidazole (Sheldon et al., 1974). Although many hypoxic cell sensitizers have been evaluated in combination with radiation, these agents had no or only a minimal therapeutic impact due to either their limited potency or toxicity at biologically relevant concentrations (Dische, 1985; Eschwege et al., 1997; Overgaard and Horsman, 1996). Common dose limiting side effects are gastro-intestinal syndromes and peripheral neuropathy. In general, 2-nitroimidazoles have a higher electron affinity than 5-nitroimidazoles and are more efficient radiosensitizers of hypoxic cells, although 5-nitroimidazoles are associated with fewer and less severe side effects and better therapeutic response.

Possible explanations for the fair to poor therapeutic benefits seen with 2-nitroimidazoles include:

1. Therapeutic dose was not achievable due to toxicity
2. Hypoxia evaluation has never been done prior to trial. Assumption was that all tumors contain radiobiological hypoxia, which may not be true
3. Sensitizer may not work well when used with multifractionated irradiation

<u>Dose limiting toxicity and drug</u>

Peripheral neuropathy (Etanidazole, Benznidazole, Desmisonidazole, Misonidazole)
Central nervous symptom (Pimonidazole, Metronidazole, Nimorazole, Ornidazole)
Gastro-intestinal signs (RSU-1069)

Misonidazole, a 2- nitroimidazole

Misonidazole was the first radiosensitizing drug in clinical trials and intensive testing was done without benefit (Urtasun et al., 1984). In the oral form, the dose-limiting toxicity is manifested in gastrointestinal effects (nausea and vomiting) and peripheral neuropathy that progressed to central nervous system toxicity if drug administration was not discontinued. The inability to deliver a sufficient dose to radiosensitize tumors may be one of the main reasons that a majority of the clinical trials failed to show benefit from this drug. Interestingly, however, selected patients with tumors in head and neck population did benefit from the drug (Overgaard et al., 1989).

Etanidazole, a 2- nitroimidazole

Etanidazole was developed with the aim of reducing the neurotoxicity seen with misonidazole since etanidazole is less lipophilic (Wouters et al., 1996). There are two reasons for the superiority of etanidazole over misonidazole. First, etanidazole has a shorter half-life *in vivo*. Second, it has a smaller partition coefficient that results in less neurotoxicity than misonidazole. The dose-limiting toxicity is also a peripheral neuropathy, but at a much higher drug concentration. Etanidazole was also used in multidrug chemotherapy regimens, but effective modulatory doses of etanidazole could not be given with acceptable toxicity (Elias et al., 1998). Overall results were also disappointing.

Pimonidazole, a 2- nitroimidazole

Pimonidazole gave no benefit in the radiotherapy of advanced cervical cancer (1993) (Allen et al., 1984).

Nimorazole, 5-nitroinidazole

5-nitroimidazoles are less toxic and the most tolerable probably due to less lipophilicity and neurotoxicity. The significant therapeutic benefit has been shown in locoregional control for patients with head and neck tumors (Overgaard et al., 1998).

Other nitroimidazole radiosensitizer

Several newer drugs have been developed to hope making potent and safe radiosensitizers. Several Japanese groups are active in developing a hypoxia nitroimidazole radiosensitizer.

Doranidazole, 1-(1',3',4'-Trihydroxy-2'-Butoxy) Methyl-2-Nitroimidazol (PR-350) was tested in experimental models (Aoki et al., 2002; Mizumoto et al., 2002; Suzuki et al., 1999) and a human trial (Nemoto et al., 2001). 2-Nitroimidazole acetamide TX-1877 and its derivatives (TX- 1877 analogs) (Kasai et al., 1998) were also tested with promise.

Phenothiazines

Phenothiazines are known to radiosensitize hypoxic cancer cells while offering protection to the normal surrounding tissues (Kale, 1996). It is hypothesized that the differential radiosensitization of tumor cells and radioprotection of normal cells by phenothiazines is related to the presence of Fe^{2+} and Fe^{3+} ion concentration respectively.

Killing of the hypoxic tumor cells with bioreductive drugs

Bioreductive drugs are compounds that are bioreductively activated intracellularly to form active cytotoxic agents killing nearby tumor cells under hypoxic conditions. Such compounds include benzoquinone antibiotics, nitroimidazole compounds, which are primarily used as hypoxia radiosensitizers (detailed in previous section) and organic nitroxides (Rauth et al., 1998). Activation of these prodrugs is catalysed by various families of reductases, the most important to be considered being the cytochrome P450 reductase and cytochrome P450 family. Bioreductive drugs especially tirapazamine has demonstrated significant success clinically in combination with radiation and chemotherapeutic agents, in particular platinum compounds (Diab-Assef et al., 2002; Gandara et al., 2002).

Benzoquinone antibiotics

Benzoquinone antibiotics include mitomycin C and porfiromycin. Mitomycin C is a natural product, which requires metabolic reduction of its benzoquinone ring to produce the cytotoxic agent toward cells (Holden et al., 1990). The cytotoxicity is greater under hypoxic than aerated conditions by only a small factor and these are not clinically attractive drugs.

Organic nitroxides

Tirapazamine (TPZ, SR 4233, WIN 59075, 3-amino-1,2,4-benzotriazine 1,4- dioxide, Tirazone) is a benzotriazine compound and a promising anti-cancer drug activated to a toxic free radical under hypoxic conditions exhibiting selective cytotoxicity for hypoxic cells

(Gandara et al., 2002). The activation of the TPZ involves a hypoxia-dependent one-electron reduction of the parent molecule to a free radical species that interacts with DNA to produce single- and double-strand breaks and lethal chromosome aberrations (Brown and Wang, 1998). Under aerobic conditions, the radical is back oxidized to the parent compound. *In vitro* and *in vivo* studies demonstrated that TPZ was 50 to 300 times more toxic to cells under hypoxic conditions as compared to oxygenated conditions (Zeman et al., 1986).

TPZ has undergone extensive preclinical and clinical testing with promising results (Minchinton et al., 2002; Shulman et al., 1999). A drug half-life is about 20 to 60 minutes. Dose limiting toxicities were muscle cramping, emesis, and acute reversible hearing loss. The maximum tolerated dose was 390 mg/m^2 when given as a 2-hour intravenous infusion every 3 weeks. TPZ has produced tumor selective potentiation of cisplatin and carboplatin in both pre-clinical and clinical studies (von Pawel et al., 2000; Wouters et al., 1999). The observed potentiation effect was schedule dependent, with maximum tumor cell killing seen when tirapazamine was administered approximately 2.5 hours before cisplatin. CATAPULT I (Cisplatin and Tirapazamine in Subjects with Advanced Previously Untreated Non-Small-Cell Lung Tumors) was a phase III trial comparing the combination of tirapazamine and cisplatin with cisplatin alone (von Pawel et al., 2000). The trial provided proof of principle with improved survival in patients receiving combination therapy. However, in the CATAPULT II which was the subsequent study comparing combination of tirapazamine and cisplatin with etoposide and cisplatin, the tirapazamine containing arm proved to be more toxic and less effective in the trial**.**

Several combination approaches have been proposed with TPZ to enhance the other primary modality including radiotherapy and radioimmunotherapy (Blumenthal et al., 2001; Lee et al., 1998a). The administration of a bioreductive drug immediately after irradiation reduces the number of hypoxic cells and improves tumor response. Fractionated radiotherapy in conjunction with bioreductive drugs is also effective, as it allows rehypoxiation, which provides the conditions necessary for bioactivation of the drug.

Quinoxaline 1,4-dioxides (QdNOs)

QdNOs are heterocyclic aromatic N-oxides that have been found to possess potent antibacterial activities (inhibit microbial DNA synthesis) especially under hypoxic conditions. QdNOs are hypoxia-cytotoxic drugs whose activity varies according to the substituents on

the quinoxaline 1,4-dioxide heterocycle. Because of their selective toxicity to hypoxic cells, these drugs may provide useful therapeutic agents against solid tumors (Diab-Assef et al., 2002; Gali-Muhtasib et al., 2001).

Protecting normal tissues

Radioprotectors, which depend upon poor uptake of the drugs in tumors but high uptake in normal tissues, can be used to protect normal tissues against radiation or chemotherapy (Hahn et al., 1998). Enhancing the radioprotection of normal tissues would allow higher radiation doses to be administered to the tumor cells without increased normal tissue complications. The natural radioprotector, glutathione, is an oxygen free radical scavenger. Many non-thiol protectors, particularly the biological response modifiers and antioxidants were discovered in the 1980s (Uma Devi, 1998).

Amifostine (Ethyol)

Amifostine, an inorganic thiophosphate, is a selective broad- spectrum cytoprotector of normal tissues that provides cytoprotection against ionizing radiation and some chemotherapeutic agents (Mehta, 1999; Wasserman, 1999). Amifostine has been approved for clinical radiotherapy as a protector against radiation-induced xerostomia. Amifostine, an inactive pro-drug, is transformed to an active thiol after dephosphorylation by alkaline phosphatase in the normal endothelium. The absence of alkaline phosphatase in the tumoral endothelium and stromal components, and the hypovascularity and acidity of the tumor environment, may explain its cytoprotective selectivity. However, preclinical investigations concerning the selectivity of amifostine are controversial and the clinical studies are inconclusive and do not have the power to evaluate the influence of amifostine on the therapeutic index. The cytoprotective mechanism of amifostine is complicated, involving free radical scavenging, DNA protection, repair acceleration, and induction of cellular hypoxia. The degree of protection is therefore highly dependent on oxygen tension, with protection factors ranging from 1 to 3. Maximal protection is observed at physiological levels of oxygenation. A great variability in protection has also been observed between different normal tissues. Some tissue, such as brain, is not protected while salivary glands and bone marrow may exhibit a three-fold increase in radiation tolerance. The feasibility of accelerated hypofractionation (3.5-4Gy, 5 fractions/week) supported by high dose daily

amifostine was shown that the regimen was well-tolerated and effective and has minimal acute and late toxicity to normal tissues (Koukourakis and Yannakakis, 2001). Further investigation is needed for acceptance in routine practice (Koukourakis, 2002; Lindegaard and Grau, 2000).

Others

1. High LET radiations

Fast neutrons, heavier ions and pions have been used in the clinical radiation therapy of tumors because of experimental evidence that their cytotoxic effects are much less dependent on O_2 levels than those of low-LET photons (Auberger et al., 1999; Warenius et al., 2000). The use of high-energy neutrons may provide a potential therapeutic gain for tumor types that can be identified as very resistant to photons.

2. Hyperthermia (HT)

The nature of HT-induced cell lethality is different from that of radiation-induced killing. The G1-phase of the cell cycle is the most resistant to HT while S-phase cells are quite sensitive. With higher temperature (> 43 °C degree), there is a direct cytotoxic effect of heat to cells and supportive structures. The mechanism of heat cytotoxicity is distinct from that of ionizing radiation. Unlike the response to ionizing radiation, heat cytotoxicity is influenced by thermotolerance, acute reductions in intracellular pH and nutritional deprivation, but is independent of acute hypoxia. In addition to heat-induced cytotoxicity, HT sensitizes cells to low-LET ionizing radiation. Acute reductions in intracellular pH also enhance thermoradiosensitization. HT chemo- or radio-sensitization may occur by an increased reaction rate, increased permeability, or decreased repair. The most promising chemosensitization by HT would seem to be with alkylating agents and cis-platinum since they are enhanced at all elevated temperatures (Engin, 1994).

3. Hypoxia inducible gene therapy

Hypoxic environment can be used to activate gene expression driven by a hypoxia-responsive element (HRE), which interacts with the transcriptional complex hypoxia-inducible factor-1 (HIF-1) (Dachs et al., 1997; Shibata et al., 2002). There is exciting

potential for expoitation of tumor-specific conditions for the targeted expression of diagnostic or therapeutic genes in cancer therapy.

Summary

This area of research is still active and some of the approaches seem promising. Targeting tumor cells, or more specifically, hypoxic tumor cells, is an excellent approach to improve therapeutic outcome while sparing normal tissue. Hypoxia manipulations can be expensive and still carry potentially significant normal tissue toxicity. Identifying tumors with high hypoxic fraction will be the key to conduct successful hypoxia manipulating therapy for hypoxic tumors.

7. RELATIONSHIP BETWEEN TUMOR HYPOXIA AND PROLIFERATION

The outcome of cancer therapy is affected by many physical and biological factors. Both hypoxia and proliferation are important prognostic factors in human tumors. It is natural to investigate the relationship between hypoxia and proliferation. In experimental tumors, it was shown that proliferation of tumor cells was the highest immediately adjacent to blood vessels and decreased with distance form the vessels (Bussink et al., 1998; Hirst and Denekamp, 1979). On the other hand, the highest hypoxia was detected beyond 100 *u*m from the blood vessels (Bussink et al., 1999b; Rijken et al., 2000). A cancer cell begins to grow after several steps of carcinogenesis. Proliferation is obviously necessary to grow. O_2 and nutrients are required to support cancer activity. At a certain point, angiogenesis is required for continuous progression. A tumor may only grow about 2 mm without supporting vessels. Deficient O_2 means that tissue becomes hypoxic. Tumor hypoxia stimulates important hypoxia responsive genes to increase tissue oxygenation. Cells become hypoxic when, for a variety of reasons, O_2 demand exceeds O_2 supply. Proliferating cells require more O_2 and energy than quiescent cells (Freyer, 1994). Increased O_2 consumption may result in decreased tissue oxygenation. There are methods to evaluate fractions of hypoxia and proliferation markers simultaneously using flow cytometry, which showed that there was evidence that hypoxic cells could progress in the cell cycle (Webster et al., 1995). The highest proportion of hypoxia occurred in the G2/M phase (Webster et al., 1998). Combination of flow cytometric analysis with histologic study will enhance the accuracy of the evaluation in the tumor.

There have been several attempts to correlate the relationship between proliferation and oxygenation using different techniques in different kinds of canine and human tumors. The points that we could make from these studies were:

1. There was little or no overlap of markers in histological sections in canine and human tumors (Kennedy et al., 1997; Raleigh et al., 1995), proliferation and hypoxia were mutually exclusive except in areas of a tumor subjected to transient changes in perfusion (Durand and Raleigh, 1998)
2. There have been no clear relationships between the two factors (Evans et al., 2001; Tsang et al., 2000; Varia et al., 1998; Zeman et al., 1993).

3. There was a significant correlation between the median pO_2 and the tumor cell potential doubling time, as the fastest proliferating tumor cells were found in the poorest oxygenated soft tissue sarcomas (Nordsmark et al., 1996b)
4. Tumor hypoxia and proliferation measurements were independent and potentially complementary predictive assays (Tsang et al., 2000)

By measuring both factors, we will likely get different biological information to understand cancer biology better between the two factors. The information will be also important for cancer therapy. Selection of the patient for appropriate treatment including targeting cancer cells and prediction of the prognosis and response to therapy may be better predicted with combination of the two markers. Monitoring during therapy might be another application and if there were a relationship between hypoxia and proliferation, just monitoring proliferation during and after therapy would also provide information on tumor oxygenation. Targeting specific tumor subsets with drugs or radiation will be the main approach to increase therapeutic benefit without increasing toxicity. When elimination of one of the subsets of cancer cells could be achieved, then the next step might be elimination of the other subsets, which survive the particular targeted approach. Establishing biological markers is critical to assess response and administer appropriate cancer therapy to individual patients such as targeting either hypoxia, proliferation or both. Hypoxia and/or proliferation marker methods based on IHC are already accepted well in the clinic. If we could identify the appropriate usage of markers, then it might be possible to have a significant impact on cancer care.

8. CANINE MODEL OF SPONTANEOUS TUMORS

Spontaneous tumors in dogs and cats, large animal tumor models for human cancers are a valuable model system for studying tumor biology or testing cancer therapeutic agents (Grossniklaus et al., 2000; MacEwen, 1990; Page and Thrall, 1994; Vail and MacEwen, 2000; Veldhoen and Milner, 1998). The canine lifespan is getting longer with development of preventive medicine and daily supporting care for older animals. Dogs develop spontaneous tumors and incidence increases with aging of the animals. Typically spontaneous tumors are very invasive, and difficult to cure by conventional treatment modalities with/without metastatic potential. Their biologic behavior, histological morphology and response to therapeutic agents are often similar to tumors occurring in humans (Rainov et al., 2000). Experimental rodent models are useful for carrying out preclinical studies, but the natural history, environmental factors and anatomic structure of rodent tumors is sometimes very different from spontaneous tumors in dogs and humans (Adam et al., 1999a). Often human clinical trials fail to show the same magnitude of results seen in experimental animal studies based on rodent models (Wood et al., 1992). The pet population is a vastly underutilized resource of animals available for cancer research as a model for humans. Using canine patients as a model for human cancers has great advantages.

1. The natural history of canine tumors is similar to that of human tumors.
2. There are molecular parallels between tumors in dogs and humans in some cancers.
3. Humans and dogs share a similar living environment.
4. The food and digestive tracts are more similar than in small laboratory animals.
5. The life span of a dog is shorter than a human, so the endpoint occurs earlier.
6. Extensive sampling such as tumor biopsies, complete follow-up and necropsy to search for systemic dissemination is possible.
7. Observation of the host response is possible.
8. Study of canine cancer may provide valuable information regarding design and conduct of human clinical trials.
9. Entering a clinical trial is also beneficial for canine patents to receive advanced treatment because there is no gold standard treatment for many spontaneous canine tumors.

10. Conducting canine clinical trials is expensive but are still cost effective compared to conducting human clinical trials.

Conclusion

This is an exciting opportunity to study tumor hypoxia and proliferation, which are important factors affecting therapeutic response and survival in cancer. Cancer biology is complex, but hypoxia and proliferation are major factors that may have a relationship in cancer progression. Canine patients with spontaneous tumors are an excellent model to study tumor biology and identifying biological factors, which may be related to malignant progression or treatment response. The main advantages to conducting a canine study are the feasibility of extensive sampling and follow up as well as their earlier disease endpoint than humans. The hypoxia marker, PIMO is an excellent marker to investigate tumor hypoxia. PCNA is well-established endogenous proliferation marker and can be detected easily with IHC. Differential accumulation of PCNA can be used to estimate the fraction of cells in S-phase. There seems to be a relationship between hypoxia and proliferation in microscopic regions. Generally hypoxic cells are not actively proliferating, but active proliferation in the adjacent tissue may have an important influence in the development of hypoxia due to reduction of overall tumor oxygenation.

Although a histologic study does not provide any information on activation of genes other than what the marker is detecting, a histological study is the first step toward learning tumor biology and designing a more comprehensive investigation.

To conduct this research, I

1. Organized clinical patients to enter the study. I prepared paper work and documented each procedure.
2. Prepared for PIMO administration
3. Sampled blood for pharmacokinetics
4. Biopsied the tumor and processed the samples
5. Performed IHC for PIMO and PCNA
6. Counted for PIMO and PCNA fraction
7. Organized data
8. Analyzed data
9. Completed publication and the dissertation

References

1993. A trial of Ro 03-8799 (pimonidazole) in carcinoma of the uterine cervix: an interim report from the Medical Research Council Working Party on advanced carcinoma of the cervix. Radiother Oncol 26:93-103.

Aboagye, E.O., A.B. Kelson, M. Tracy, and P. Workman. 1998a. Preclinical development and current status of the fluorinated 2- nitroimidazole hypoxia probe N-(2-hydroxy-3,3,3-trifluoropropyl)-2-(2- nitro-1-imidazolyl) acetamide (SR 4554, CRC 94/17): a non-invasive diagnostic probe for the measurement of tumor hypoxia by magnetic resonance spectroscopy and imaging, and by positron emission tomography [published erratum appears in Anticancer Drug Des 1998 Dec;13(8):1009- 10]. Anticancer Drug Des 13:703-30.

Aboagye, E.O., R.J. Maxwell, M.R. Horsman, A.D. Lewis, P. Workman, M. Tracy, and J.R. Griffiths. 1998b. The relationship between tumour oxygenation determined by oxygen electrode measurements and magnetic resonance spectroscopy of the fluorinated 2-nitroimidazole SR-4554. Br J Cancer 77:65-70.

Aboagye, E.O., R.J. Maxwell, A.B. Kelson, M. Tracy, A.D. Lewis, M.A. Graham, M.R. Horsman, J.R. Griffiths, and P. Workman. 1997. Preclinical evaluation of the fluorinated 2-nitroimidazole N-(2-hydroxy-3,3,3-trifluoropropyl)-2-(2-nitro-1-imidazolyl) acetamide (SR-4554) as a probe for the measurement of tumor hypoxia. Cancer Res 57:3314-8.

Acker, J.C., M.W. Dewhirst, G.M. Honore, T.V. Samulski, J.A. Tucker, and J.R. Oleson. 1990. Blood perfusion measurements in human tumours: evaluation of laser Doppler methods. Int J Hyperthermia 6:287-304.

Adam, M.F., M.J. Dorie, and J.M. Brown. 1999a. Oxygen tension measurements of tumors growing in mice. Int J Radiat Oncol Biol Phys 45:171-80.

Adam, M.F., E.C. Gabalski, D.A. Bloch, J.W. Oehlert, J.M. Brown, A.A. Elsaid, H.A. Pinto, and D.J. Terris. 1999b. Tissue oxygen distribution in head and neck cancer patients. Head Neck 21:146-53.

Aebersold, D.M., K.T. Beer, J. Laissue, S. Hug, A. Kollar, R.H. Greiner, and V. Djonov. 2000. Intratumoral microvessel density predicts local treatment failure of radically irradiated squamous cell cancer of the oropharynx. Int J Radiat Oncol Biol Phys 48:17-25.

Aebersold, D.M., P. Burri, K.T. Beer, J. Laissue, V. Djonov, R.H. Greiner, and G.L. Semenza. 2001. Expression of hypoxia-inducible factor-1alpha: a novel predictive and prognostic parameter in the radiotherapy of oropharyngeal cancer. Cancer Res 61:2911-6.

Airley, R., J. Loncaster, S. Davidson, M. Bromley, S. Roberts, A. Patterson, R. Hunter, I. Stratford, and C. West. 2001. Glucose transporter glut-1 expression correlates with tumor hypoxia and predicts metastasis-free survival in advanced carcinoma of the cervix. Clin Cancer Res 7:928-34.

Alfranca, A., M.D. Gutierrez, A. Vara, J. Aragones, F. Vidal, and M.O. Landazuri. 2002. c-Jun and hypoxia-inducible factor 1 functionally cooperate in hypoxia-induced gene transcription. Mol Cell Biol 22:12-22.

Allen, J.G., S. Dische, I. Lenox-Smith, S.L. Malcolm, and M.I. Saunders. 1984. The pharmacokinetics of a new radiosensitiser, Ro 03-8799 in humans. Eur J Clin Pharmacol 27:483-9.

Amellem, O., and E.O. Pettersen. 1991. Cell inactivation and cell cycle inhibition as induced by extreme hypoxia: the possible role of cell cycle arrest as a protection against hypoxia-induced lethal damage. Cell Prolif 24:127-41.

Amellem, O., M. Loffler, and E.O. Pettersen. 1994. Regulation of cell proliferation under extreme and moderate hypoxia: the role of pyrimidine (deoxy)nucleotides. Br J Cancer 70:857-66.

Aoki, M., Y. Furusawa, Y. Shibamoto, A. Kobayashi, and M. Tsujitani. 2002. Effect of a hypoxic cell sensitizer doranidazole on the radiation-induced apoptosis of mouse L5178Y lymphoma cells. J Radiat Res (Tokyo) 43:161-6.

Aquino-Parsons, C., C. Luo, C.M. Vikse, and P.L. Olive. 1999. Comparison between the comet assay and the oxygen microelectrode for measurement of tumor hypoxia. Radiother Oncol 51:179-85.

Arlett, C.F., and S.A. Harcourt. 1980. Survey of radiosensitivity in a variety of human cell strains. Cancer Res 40:926-32.

Arteel, G.E., R.G. Thurman, J.M. Yates, and J.A. Raleigh. 1995. Evidence that hypoxia markers detect oxygen gradients in liver: pimonidazole and retrograde perfusion of rat liver. Br J Cancer 72:889-95.

Auberger, T., B. Thurriegl, T. Freude, L. Weissfloch, R. Senekowitsch-Schmidke, P. Kneschaurek, F.M. Wagner, and M. Molls. 1999. Oxygen tension in transplanted mouse osteosarcomas during fractionated high-LET- and low-LET radiotherapy--predictive aspects for choosing beam quality? Strahlenther Onkol 175 Suppl 2:52-6.

Azuma, C., J.A. Raleigh, and D.E. Thrall. 1997. Longevity of pimonidazole adducts in spontaneous canine tumors as an estimate of hypoxic cell lifetime. Radiat Res 148:35-42.

Azuma, Y., S.C. Chou, R.A. Lininger, B.J. Murphy, M.A. Varia, and J.A. Raleigh. 2003. Hypoxia and differentiation in squamous cell carcinomas of the uterine cervix: pimonidazole and involucrin. Clin Cancer Res 9:4944-52.

Bajou, K., A. Noel, R.D. Gerard, V. Masson, N. Brunner, C. Holst-Hansen, M. Skobe, N.E. Fusenig, P. Carmeliet, D. Collen, and J.M. Foidart. 1998. Absence of host plasminogen activator inhibitor 1 prevents cancer invasion and vascularization. Nat Med 4:923-8.

Ballinger, J.R. 2001. Imaging hypoxia in tumors. Semin Nucl Med 31:321-9.

Ballinger, J.R., J.W. Kee, and A.M. Rauth. 1996. In vitro and in vivo evaluation of a technetium-99m-labeled 2-nitroimidazole (BMS181321) as a marker of tumor hypoxia. J Nucl Med 37:1023-31.

Barrett, T.L., K.J. Smith, J.J. Hodge, R. Butler, F.W. Hall, and H.G. Skelton. 1997. Immunohistochemical nuclear staining for p53, PCNA, and Ki-67 in different histologic variants of basal cell carcinoma. J Am Acad Dermatol 37:430-7.

Beasley, N.J., R. Leek, M. Alam, H. Turley, G.J. Cox, K. Gatter, P. Millard, S. Fuggle, and A.L. Harris. 2002. Hypoxia-inducible factors HIF-1alpha and HIF-2alpha in head and neck cancer: relationship to tumor biology and treatment outcome in surgically resected patients. Cancer Res 62:2493-7.

Becker, A., T. Kuhnt, H. Liedtke, A. Krivokuca, M. Bloching, and J. Dunst. 2002. Oxygenation measurements in head and neck cancers during hyperbaric oxygenation. Strahlenther Onkol 178:105-8.

Becker, A., P. Stadler, R.S. Lavey, G. Hansgen, T. Kuhnt, C. Lautenschlager, H.J. Feldmann, M. Molls, and J. Dunst. 2000. Severe anemia is associated with poor tumor oxygenation in head and neck squamous cell carcinomas. Int J Radiat Oncol Biol Phys 46:459-66.

Begg, A.C., I. Hofland, L. Moonen, H. Bartelink, S. Schraub, P. Bontemps, R. Le Fur, W. Van Den Bogaert, R. Caspers, M. Van Glabbeke, and et al. 1990. The predictive value of cell kinetic measurements in a European trial of accelerated fractionation in advanced head and neck tumors: an interim report. Int J Radiat Oncol Biol Phys 19:1449-53.

Begg, A.C., H. Janssen, D. Sprong, I. Hofland, G. Blommestijn, J.A. Raleigh, M. Varia, A. Balm, L. Van Velthuyzen, P. Delaere, R. Sciot, and K.M.G. Haustermans. 2001. Hypoxia and perfusion measurements in human tumors--initial experience with pimonidazole and IUdR. Acta Oncol 40:924-8.

Begg, A.C., K. Haustermans, A.A. Hart, S. Dische, M. Saunders, B. Zackrisson, H. Gustaffson, P. Coucke, N. Paschoud, M. Hoyer, J. Overgaard, P. Antognoni, A. Richetti, J. Bourhis, H. Bartelink, J.C. Horiot, R. Corvo, W. Giaretti, H. Awwad, T. Shouman, T. Jouffroy, Z. Maciorowski, W. Dobrowsky, H. Struikmans, G.D. Wilson, and et al. 1999. The value of pretreatment cell kinetic parameters as predictors for radiotherapy outcome in head and neck cancer: a multicenter analysis. Radiother Oncol 50:13-23.

Bernier, J., M.R. Stratford, J. Denekamp, M.F. Dennis, S. Bieri, F. Hagen, O. Kocagoncu, M. Bolla, and A. Rojas. 1998. Pharmacokinetics of nicotinamide in cancer patients treated with accelerated radiotherapy: the experience of the Co-operative Group of Radiotherapy of the European Organization for Research and Treatment of Cancer. Radiother Oncol 48:123-33.

Bernier, J., J. Denekamp, A. Rojas, E. Minatel, J. Horiot, H. Hamers, P. Antognoni, O. Dahl, P. Richaud, M. van Glabbeke, and M. Pierart. 2000. ARCON: accelerated radiotherapy with carbogen and nicotinamide in head and neck squamous cell carcinomas. The experience of the Co-operative group of radiotherapy of the european organization for research and treatment of cancer (EORTC). Radiother Oncol 55:111-9.

Bernier, J., J. Denekamp, A. Rojas, M. Trovo, J.C. Horiot, H. Hamers, P. Antognoni, O. Dahl, P. Richaud, J. Kaanders, M. van Glabbeke, and M. Pierart. 1999. ARCON: accelerated radiotherapy with carbogen and nicotinamide in non small cell lung cancer: a phase I/II study by the EORTC. Radiother Oncol 52:149-56.

Bernsen, H.J., P.F. Rijken, N.E. Hagemeier, and A.J. van der Kogel. 1999. A quantitative analysis of vascularization and perfusion of human glioma xenografts at different implantation sites [In Process Citation]. Microvasc Res 57:244-57.

Berube, L.R., S. Farah, R.A. McClelland, and A.M. Rauth. 1992. Depletion of intracellular glutathione by 1-methyl-2-nitrosoimidazole. Int J Radiat Oncol Biol Phys 22:817-20.

Biaglow, J.E., M.E. Varnes, B. Jacobson, and H.D. Suit. 1986. Effect of calcium channel blocking drugs on tumor cell oxygen utilization. Adv Exp Med Biol 200:583-9.

Biaglow, J.E., Y. Manevich, D. Leeper, B. Chance, M.W. Dewhirst, W.T. Jenkins, S.W. Tuttle, K. Wroblewski, J.D. Glickson, C. Stevens, and S.M. Evans. 1998. MIBG inhibits respiration: potential for radio- and hyperthermic sensitization. Int J Radiat Oncol Biol Phys 42:871-6.

Birner, P., B. Gatterbauer, G. Oberhuber, M. Schindl, K. Rossler, A. Prodinger, H. Budka, and J.A. Hainfellner. 2001. Expression of hypoxia-inducible factor-1 alpha in oligodendrogliomas: its impact on prognosis and on neoangiogenesis. Cancer 92:165-71.

Bjork-Eriksson, T., C.M. West, E. Karlsson, N.J. Slevin, S.E. Davidson, R.D. James, and C. Mercke. 1998. The in vitro radiosensitivity of human head and neck cancers. Br J Cancer 77:2371-5.

Blancher, C., and A.L. Harris. 1998. The molecular basis of the hypoxia response pathway: tumour hypoxia as a therapy target. Cancer Metastasis Rev 17:187-94.

Blumenthal, R.D., A. Taylor, L. Osorio, R. Ochakovskaya, J.A. Raleigh, M. Papadopoulou, W.D. Bloomer, and D.M. Goldenberg. 2001. Optimizing the use of combined radioimmunotherapy and hypoxic cytotoxin therapy as a function of tumor hypoxia. Int J Cancer 94:564-71.

Bostock, D.E., and M.T. Dye. 1980. Prognosis after surgical excision of canine fibrous connective tissue sarcomas. Vet Pathol 17:581-8.

Bostock, D.E., J. Crocker, K. Harris, and P. Smith. 1989. Nucleolar organiser regions as indicators of post-surgical prognosis in canine spontaneous mast cell tumours. Br J Cancer 59:915-8.

Boucher, Y., L.T. Baxter, and R.K. Jain. 1990. Interstitial pressure gradients in tissue-isolated and subcutaneous tumors: implications for therapy. Cancer Res 50:4478-84.

Bozlu, M., D. Orhan, S. Baltaci, O. Yaman, A.H. Elhan, O. Tulunay, and Y.Z. Muftuoglu. 2002. The prognostic value of proliferating cell nuclear antigen, Ki-67 and nucleolar organizer region in transitional cell carcinoma of the bladder. Int Urol Nephrol 33:59-66.

Bratulic, M., Z. Grabarevic, B. Artukovic, and D. Capak. 1996. Number of nucleoli and nucleolar organizer regions per nucleus and nucleolus--prognostic value in canine mammary tumors. Vet Pathol 33:527-32.

Braun, R.D., J.L. Lanzen, and M.W. Dewhirst. 1999. Fourier analysis of fluctuations of oxygen tension and blood flow in R3230Ac tumors and muscle in rats. Am J Physiol 277:H551-68.

Brizel, D.M., G.L. Rosner, L.R. Prosnitz, and M.W. Dewhirst. 1995a. Patterns and variability of tumor oxygenation in human soft tissue sarcomas, cervical carcinomas, and lymph node metastases. Int J Radiat Oncol Biol Phys 32:1121-5.

Brizel, D.M., R.K. Dodge, R.W. Clough, and M.W. Dewhirst. 1999. Oxygenation of head and neck cancer: changes during radiotherapy and impact on treatment outcome. Radiother Oncol 53:113-7.

Brizel, D.M., G.L. Rosner, J. Harrelson, L.R. Prosnitz, and M.W. Dewhirst. 1994. Pretreatment oxygenation profiles of human soft tissue sarcomas. Int J Radiat Oncol Biol Phys 30:635-42.

Brizel, D.M., G.S. Sibley, L.R. Prosnitz, R.L. Scher, and M.W. Dewhirst. 1997a. Tumor hypoxia adversely affects the prognosis of carcinoma of the head and neck. Int J Radiat Oncol Biol Phys 38:285-9.

Brizel, D.M., S. Lin, J.L. Johnson, J. Brooks, M.W. Dewhirst, and C.A. Piantadosi. 1995b. The mechanisms by which hyperbaric oxygen and carbogen improve tumour oxygenation. Br J Cancer 72:1120-4.

Brizel, D.M., W.D. Hage, R.K. Dodge, M.T. Munley, C.A. Piantadosi, and M.W. Dewhirst. 1997b. Hyperbaric oxygen improves tumor radiation response significantly more than carbogen/nicotinamide [see comments]. Radiat Res 147:715-20.

Brizel, D.M., S.P. Scully, J.M. Harrelson, L.J. Layfield, J.M. Bean, L.R. Prosnitz, and M.W. Dewhirst. 1996. Tumor oxygenation predicts for the likelihood of distant metastases in human soft tissue sarcoma. Cancer Res 56:941-3.

Brown, J.M. 1979. Evidence for acutely hypoxic cells in mouse tumours, and a possible mechanism of reoxygenation. Br J Radiol 52:650-6.

Brown, J.M. 2002. Tumor microenvironment and the response to anticancer therapy. Cancer Biol Ther 1:453-8.

Brown, J.M., and L.H. Wang. 1998. Tirapazamine: laboratory data relevant to clinical activity. Anticancer Drug Des 13:529-39.

Brown, J.M., and Q.T. Le. 2002. Tumor hypoxia is important in radiotherapy, but how should we measure it? Int J Radiat Oncol Biol Phys 54:1299-301.

Burd, R., P.R. Wachsberger, J.E. Biaglow, M.L. Wahl, I. Lee, and D.B. Leeper. 2001. Absence of Crabtree effect in human melanoma cells adapted to growth at low pH: reversal by respiratory inhibitors. Cancer Res 61:5630-5.

Burd, R., S.N. Lavorgna, C. Daskalakis, P.R. Wachsberger, M.L. Wahl, J.E. Biaglow, C.W. Stevens, and D.B. Leeper. 2003. Tumor Oxygenation and Acidification are Increased in Melanoma Xenografts after Exposure to Hyperglycemia and meta-Iodo-benzylguanidine. Radiat Res 159:328-35.

Bush, R.S. 1986. The significance of anemia in clinical radiation therapy. Int J Radiat Oncol Biol Phys 12:2047-50.

Bussink, J., J.H. Kaanders, and A.J. Van der Kogel. 1999a. Clinical outcome and tumour microenvironmental effects of accelerated radiotherapy with carbogen and nicotinamide. Acta Oncol 38:875-82.

Bussink, J., J.H. Kaanders, P.F. Rijken, C.A. Martindale, and A.J. van der Kogel. 1998. Multiparameter analysis of vasculature, perfusion and proliferation in human tumour xenografts. Br J Cancer 77:57-64.

Bussink, J., J.H. Kaanders, A.M. Strik, B. Vojnovic, and A.J. van Der Kogel. 2000a. Optical sensor-based oxygen tension measurements correspond with hypoxia marker binding in three human tumor xenograft lines [In Process Citation]. Radiat Res 154:547-55.

Bussink, J., J.H. Kaanders, P.F. Rijken, J.A. Raleigh, and A.J. Van der Kogel. 2000b. Changes in blood perfusion and hypoxia after irradiation of a human squamous cell carcinoma xenograft tumor line. Radiat Res 153:398-404.

Bussink, J., J.H. Kaanders, P.F. Rijken, J.P. Peters, R.J. Hodgkiss, H.A. Marres, and A.J. van der Kogel. 1999b. Vascular architecture and microenvironmental parameters in human squamous cell carcinoma xenografts: effects of carbogen and nicotinamide. Radiother Oncol 50:173-84.

Cade, I.S., J.B. McEwen, S. Dische, M.I. Saunders, E.R. Watson, K.E. Halnan, G. Wiernik, D.J. Perrins, and I. Sutherland. 1978. Hyperbaric oxygen and radiotherapy: a Medical Research Council trial in carcinoma of the bladder. Br J Radiol 51:876-8.

Cairns, R.A., T. Kalliomaki, and R.P. Hill. 2001. Acute (cyclic) hypoxia enhances spontaneous metastasis of KHT murine tumors. Cancer Res 61:8903-8.

Carafoli, E. 1986. Mitochondrial pathology: an overview. Ann N Y Acad Sci 488:1-18.

Casciari, J.J., M.M. Graham, and J.S. Rasey. 1995. A modeling approach for quantifying tumor hypoxia with [F- 18]fluoromisonidazole PET time-activity data. Med Phys 22:1127-39.

Celis, J.E., and A. Celis. 1985. Cell cycle-dependent variations in the distribution of the nuclear protein cyclin proliferating cell nuclear antigen in cultured cells: subdivision of S phase. Proc Natl Acad Sci U S A 82:3262-6.

Cella, D., and D. Bron. 1999. The effect of Epoetin alfa on quality of life in anemic cancer patients. Cancer Pract 7:177-82.

Chaplin, D.J., R.E. Durand, and P.L. Olive. 1986. Acute hypoxia in tumors: implications for modifiers of radiation effects. Int J Radiat Oncol Biol Phys 12:1279-82.

Chaplin, D.J., P.L. Olive, and R.E. Durand. 1987. Intermittent blood flow in a murine tumor: radiobiological effects. Cancer Res 47:597-601.

Chapman, J.D., A.J. Franko, and J. Sharplin. 1981. A marker for hypoxic cells in tumours with potential clinical applicability. Br J Cancer 43:546-50.

Chapman, J.D., K. Baer, and J. Lee. 1983. Characteristics of the metabolism-induced binding of misonidazole to hypoxic mammalian cells. Cancer Res 43:1523-8.

Chapman, J.D., J.D. Bradley, J.F. Eary, R. Haubner, S.M. Larson, J.M. Michalski, P.G. Okunieff, H.W. Strauss, Y.C. Ung, and M.J. Welch. 2003. Molecular (functional) imaging for radiotherapy applications: an RTOG symposium*1. International Journal of Radiation Oncology*Biology*Physics 55:294-301.

Cherif, A., S. Wallace, D.J. Yang, R.A. Newman, V.L. Harrod, A. Nornoo, T. Inoue, C.G. Kim, L.R. Kuang, E.E. Kim, and D.A. Podoloff. 1996. Development of new markers for hypoxic cells: [131I]Iodomisonidazole and [131I]Iodoerythronitroimidazole. J Drug Target 4:31-9.

Chilov, D., G. Camenisch, I. Kvietikova, U. Ziegler, M. Gassmann, and R.H. Wenger. 1999. Induction and nuclear translocation of hypoxia-inducible factor-1 (HIF- 1): heterodimerization with ARNT is not necessary for nuclear accumulation of HIF-1alpha. J Cell Sci 112:1203-12.

Clarke, E.D., K.H. Goulding, and P. Wardman. 1982. Nitroimidazoles as anaerobic electron acceptors for xanthine oxidase. Biochem Pharmacol 31:3237-42.

Clavo, A.C., and R.L. Wahl. 1996. Effects of hypoxia on the uptake of tritiated thymidine, L-leucine, L-methionine and FDG in cultured cancer cells. J Nucl Med 37:502-6.

Clavo, B., J.L. Perez, L. Lopez, G. Suarez, M. Lloret, J. Morera, D. Macias, J.C. Martinez, M. Santana, M.A. Hernandez, F. Robaina, and M. Gunderoth. 2003. Influence of haemoglobin concentration and peripheral muscle pO2 on tumour oxygenation in advanced head and neck tumours. Radiother Oncol 66:71-4.

Cline, J.M., D.E. Thrall, G.L. Rosner, and J.A. Raleigh. 1994. Distribution of the hypoxia marker CCI-103F in canine tumors. Int J Radiat Oncol Biol Phys 28:921-33.

Cline, J.M., G.L. Rosner, J.A. Raleigh, and D.E. Thrall. 1997. Quantification of CCI-103F labeling heterogeneity in canine solid tumors. Int J Radiat Oncol Biol Phys 37:655-62.

Cline, J.M., D.E. Thrall, R.L. Page, A.J. Franko, and J.A. Raleigh. 1990. Immunohistochemical detection of a hypoxia marker in spontaneous canine tumours. Br J Cancer 62:925-31.

Cohen-Jonathan, E., S.M. Evans, C.J. Koch, R.J. Muschel, W.G. McKenna, J. Wu, and E.J. Bernhard. 2001. The farnesyltransferase inhibitor L744,832 reduces hypoxia in tumors expressing activated H-ras. Cancer Res 61:2289-93.

Coleman, C.N. 1988. Hypoxia in tumors: a paradigm for the approach to biochemical and physiologic heterogeneity. J Natl Cancer Inst 80:310-7.

Collingridge, D.R., W.K. Young, B. Vojnovic, P. Wardman, E.M. Lynch, S.A. Hill, and D.J. Chaplin. 1997. Measurement of tumor oxygenation: a comparison between polarographic needle electrodes and a time-resolved luminescence-based optical sensor. Radiat Res 147:329-34.

Comerford, K.M., T.J. Wallace, J. Karhausen, N.A. Louis, M.C. Montalto, and S.P. Colgan. 2002. Hypoxia-inducible Factor-1-dependent Regulation of the Multidrug Resistance (MDR1) Gene. Cancer Res 62:3387-94.

Cook, G.J., S. Houston, S.F. Barrington, and I. Fogelman. 1998. Technetium-99m-labeled HL91 to identify tumor hypoxia: correlation with fluorine-18-FDG. J Nucl Med 39:99-103.

Costa, A.d.L., N.S. de Araujo, D.d.S. Pinto, Jr., and V.C. de Araujo. 1999. PCNA/AgNOR and Ki-67/AgNOR double staining in oral squamous cell carcinoma. J Oral Pathol Med 28:438-41.

Cottrill, C.P., K. Bishop, M.I. Walton, and J.M. Henk. 1998. Pilot study of nimorazole as a hypoxic-cell sensitizer with the "chart" regimen in head and neck cancer. Int J Radiat Oncol Biol Phys 42:807-10.

Dachs, G.U., and D.J. Chaplin. 1998. Microenvironmental control of gene expression: implications for tumor angiogenesis, progression, and metastasis. Semin Radiat Oncol 8:208-16.

Dachs, G.U., and G.M. Tozer. 2000. Hypoxia modulated gene expression: angiogenesis, metastasis and therapeutic exploitation. Eur J Cancer 36:1649-60.

Dachs, G.U., A.V. Patterson, J.D. Firth, P.J. Ratcliffe, K.M. Townsend, I.J. Stratford, and A.L. Harris. 1997. Targeting gene expression to hypoxic tumor cells. Nat Med 3:515-20.

Dang, C.V., and G.L. Semenza. 1999. Oncogenic alterations of metabolism. Trends Biochem Sci 24:68-72.

Darzynkiewicz, Z., J. Gong, G. Juan, B. Ardelt, and F. Traganos. 1996. Cytometry of cyclin proteins. Cytometry 25:1-13.

Dasu, A., and J. Denekamp. 1998. New insights into factors influencing the clinically relevant oxygen enhancement ratio. Radiother Oncol 46:269-77.

De Jaeger, K., F.M. Merlo, M.C. Kavanagh, A.W. Fyles, D. Hedley, and R.P. Hill. 1998. Heterogeneity of tumor oxygenation: relationship to tumor necrosis, tumor size, and metastasis. Int J Radiat Oncol Biol Phys 42:717-21.

Denekamp, J., and J.F. Fowler. 1997. ARCON--current status: summary of a workshop on preclinical and clinical studies. Acta Oncol 36:517-25.

Denekamp, J., and A. Dasu. 1999. Inducible repair and the two forms of tumour hypoxia--time for a paradigm shift. Acta Oncol 38:903-18.

Dewhirst, M.W. 1998. Concepts of oxygen transport at the microcirculatory level. Semin Radiat Oncol 8:143-50.

Dewhirst, M.W., H. Kimura, S.W. Rehmus, R.D. Braun, D. Papahadjopoulos, K. Hong, and T.W. Secomb. 1996a. Microvascular studies on the origins of perfusion-limited hypoxia. Br J Cancer Suppl 27:S247-51.

Dewhirst, M.W., E.T. Ong, R.D. Braun, B. Smith, B. Klitzman, S.M. Evans, and D. Wilson. 1999. Quantification of longitudinal tissue pO2 gradients in window chamber tumours: impact on tumour hypoxia. Br J Cancer 79:1717-22.

Dewhirst, M.W., E.T. Ong, G.L. Rosner, S.W. Rehmus, S. Shan, R.D. Braun, D.M. Brizel, and T.W. Secomb. 1996b. Arteriolar oxygenation in tumour and subcutaneous arterioles: effects of inspired air oxygen content. Br J Cancer Suppl 27:S241-6.

Diab-Assef, M., M.J. Haddadin, P. Yared, C. Assaad, and H.U. Gali-Muhtasib. 2002. Quinoxaline 1,4-dioxides: hypoxia-selective therapeutic agents. Mol Carcinog 33:198-205.

Ding, I., W. Liu, J. Sun, B. Fenton, and P. Okunieff. 2002. Comparison and modulation of angiogenic responses by FGFs, VEGF and SCF in murine and human fibrosarcomas. Comp Biochem Physiol A Mol Integr Physiol 132:17-25.

Dische, S. 1985. Chemical sensitizers for hypoxic cells: a decade of experience in clinical radiotherapy. Radiother Oncol 3:97-115.

Dische, S. 1991. Radiotherapy and anaemia--the clinical experience. Radiother Oncol 20:35-40.

Dische, S., M.I. Saunders, R. Sealy, I.D. Werner, N. Verma, C. Foy, and S.M. Bentzen. 1999. Carcinoma of the cervix and the use of hyperbaric oxygen with radiotherapy: a report of a randomised controlled trial. Radiother Oncol 53:93-8.

Dolbeare, F., H. Gratzner, M.G. Pallavicini, and J.W. Gray. 1983. Flow cytometric measurement of total DNA content and incorporated bromodeoxyuridine. Proc Natl Acad Sci U S A 80:5573-7.

Dunn, T.J., R.D. Braun, W.E. Rhemus, G.L. Rosner, T.W. Secomb, G.M. Tozer, D.J. Chaplin, and M.W. Dewhirst. 1999. The effects of hyperoxic and hypercarbic gases on tumour blood flow. Br J Cancer 80:117-26.

Dunphy, F.R., B.R. Harrison, T.L. Dunleavy, J.J. Rodriguez, J.G. Hilton, and J.H. Boyd. 1999. Erythropoietin reduces anemia and transfusions: A randomized trial with or without erythropoietin during chemotherapy. Cancer 86:1362-7.

Dunst, J., P. Stadler, A. Becker, T. Kuhnt, C. Lautenschlager, M. Molls, and G. Haensgen. 2001. Tumor hypoxia and systemic levels of vascular endothelial growth factor (VEGF) in head and neck cancers. Strahlenther Onkol 177:469-73.

Durand, R.E., and N.E. LePard. 1995. Contribution of transient blood flow to tumour hypoxia in mice. Acta Oncol 34:317-23.

Durand, R.E., and E. Sham. 1998. The lifetime of hypoxic human tumor cells. Int J Radiat Oncol Biol Phys 42:711-5.

Durand, R.E., and J.A. Raleigh. 1998. Identification of nonproliferating but viable hypoxic tumor cells in vivo. Cancer Res 58:3547-50.

Durand, R.E., and C. Aquino-Parsons. 2001a. Non-constant tumour blood flow--implications for therapy. Acta Oncol 40:862-9.

Durand, R.E., and C. Aquino-Parsons. 2001b. Clinical relevance of intermittent tumour blood flow. Acta Oncol 40:929-36.

Durand, R.E., D.J. Chaplin, and P.L. Olive. 1990. Cell sorting with Hoechst or carbocyanine dyes as perfusion probes in spheroids and tumors. Methods Cell Biol 33:509-18.

el-Deiry, W.S. 1998. Regulation of p53 downstream genes. Semin Cancer Biol 8:345-57.

Eldridge, S.R., and S.M. Goldsworthy. 1996. Cell proliferation rates in common cancer target tissues of B6C3F1 mice and F344 rats: effects of age, gender, and choice of marker. Fundam Appl Toxicol 32:159-67.

Eldridge, S.R., L.F. Tilbury, T.L. Goldsworthy, and B.E. Butterworth. 1990. Measurement of chemically induced cell proliferation in rodent liver and kidney: a comparison of 5-bromo-2'-deoxyuridine and [3H]thymidine administered by injection or osmotic pump. Carcinogenesis 11:2245-51.

Elias, A.D., C. Wheeler, L.J. Ayash, G. Schwartz, J. Ibrahim, L. Mills, M. McCauley, N. Coleman, D. Warren, L. Schnipper, K.H. Antman, B.A. Teicher, and E. Frei, 3rd. 1998. Dose escalation of the hypoxic cell sensitizer etanidazole combined with ifosfamide, carboplatin, etoposide, and autologous hematopoietic stem cell support. Clin Cancer Res 4:1443-9.

Elkind, M., and G. Whitmore. 1965. Oxygen, nitrogen, recovery, and radiation therapy. Cellular Radiation Biology:442-461.

Ellis, L.M., W. Liu, S.A. Ahmad, F. Fan, Y.D. Jung, R.M. Shaheen, and N. Reinmuth. 2001. Overview of angiogenesis: Biologic implications for antiangiogenic therapy. Semin Oncol 28:94-104.

Engelhardt, E.L., R.F. Schneider, S.H. Seeholzer, C.C. Stobbe, and J.D. Chapman. 2002. The synthesis and radiolabeling of 2-nitroimidazole derivatives of cyclam and their preclinical evaluation as positive markers of tumor hypoxia. J Nucl Med 43:837-50.

Engin, K. 1994. Biological rationale for hyperthermia in cancer treatment (II). Neoplasma 41:277-83.

Eschwege, F., H. Sancho-Garnier, D. Chassagne, D. Brisgand, M. Guerra, E.P. Malaise, P. Bey, L. Busutti, L. Cionini, T. N'Guyen, A. Romanini, J. Chavaudra, and C. Hill. 1997. Results of a European randomized trial of Etanidazole combined with radiotherapy in head and neck carcinomas [see comments]. Int J Radiat Oncol Biol Phys 39:275-81.

Esumi, H., K. Izuishi, K. Kato, K. Hashimoto, Y. Kurashima, A. Kishimoto, T. Ogura, and T. Ozawa. 2002. Hypoxia and nitric oxide treatment confer tolerance to glucose starvation in a 5?f-AMP-activated protein kinase-dependent manner. J Biol Chem 28:28.

Evans, S.M., W.T. Jenkins, M. Shapiro, and C.J. Koch. 1997a. Evaluation of the concept of "hypoxic fraction" as a descriptor of tumor oxygenation status. Adv Exp Med Biol 411:215-25.

Evans, S.M., S.M. Hahn, D.P. Magarelli, and C.J. Koch. 2001. Hypoxic heterogeneity in human tumors: EF5 binding, vasculature, necrosis, and proliferation. Am J Clin Oncol 24:467-72.

Evans, S.M., W.T. Jenkins, B. Joiner, E.M. Lord, and C.J. Koch. 1996. 2-Nitroimidazole (EF5) binding predicts radiation resistance in individual 9L s.c. tumors. Cancer Res 56:405-11.

Evans, S.M., K.M. Laughlin, C.R. Pugh, C.M. Sehgal, and H.M. Saunders. 1997b. Use of power Doppler ultrasound-guided biopsies to locate regions of tumour hypoxia. Br J Cancer 76:1308-14.

Evans, S.M., A.V. Kachur, C.Y. Shiue, R. Hustinx, W.T. Jenkins, G.G. Shive, J.S. Karp, A. Alavi, E.M. Lord, W.R. Dolbier, Jr., and C.J. Koch. 2000a. Noninvasive detection of tumor hypoxia using the 2-nitroimidazole [18F]EF1 [In Process Citation]. J Nucl Med 41:327-36.

Evans, S.M., S. Hahn, D.R. Pook, W.T. Jenkins, A.A. Chalian, P. Zhang, C. Stevens, R. Weber, G. Weinstein, I. Benjamin, N. Mirza, M. Morgan, S. Rubin, W.G. McKenna, E.M. Lord, and C.J. Koch. 2000b. Detection of hypoxia in human squamous cell carcinoma by EF5 binding. Cancer Res 60:2018-24.

Fein, D.A., W.R. Lee, A.L. Hanlon, J.A. Ridge, C.J. Langer, W.J. Curran, Jr., and L.R. Coia. 1995. Pretreatment hemoglobin level influences local control and survival of T1-T2 squamous cell carcinomas of the glottic larynx. J Clin Oncol 13:2077-83.

Fenton, B.M. 1995. The effects of carbogen and nicotinamide on intravascular oxyhaemoglobin saturations in SCCVII and KHT murine tumours. Br J Cancer 71:945-9.

Fenton, B.M., E.M. Lord, and S.F. Paoni. 2000. Enhancement of tumor perfusion and oxygenation by carbogen and nicotinamide during single- and multifraction irradiation. Radiat Res 153:75-83.

Fenton, B.M., E.K. Rofstad, F.L. Degner, and R.M. Sutherland. 1988. Cryospectrophotometric determination of tumor intravascular oxyhemoglobin saturations: dependence on vascular geometry and tumor growth. J Natl Cancer Inst 80:1612-9.

Fenton, B.M., S.F. Paoni, J. Lee, C.J. Koch, and E.M. Lord. 1999. Quantification of tumour vasculature and hypoxia by immunohistochemical staining and HbO2 saturation measurements. Br J Cancer 79:464-71.

Fenton, B.M., B.K. Beauchamp, S.F. Paoni, P. Okunieff, and I. Ding. 2001. Characterization of the effects of antiangiogenic agents on tumor pathophysiology. Am J Clin Oncol 24:453-7.

Fertil, B., and E.P. Malaise. 1981. Inherent cellular radiosensitivity as a basic concept for human tumor radiotherapy. Int J Radiat Oncol Biol Phys 7:621-9.

Fischer, B., B. Muller, P. Fisch, and W. Kreutz. 2000. An acidic microenvironment inhibits antitumoral non-major histocompatibility complex-restricted cytotoxicity: implications for cancer immunotherapy. J Immunother 23:196-207.

Folkman, J. 2002. Role of angiogenesis in tumor growth and metastasis. Semin Oncol 29:15-8.

Franko, A.J. 1986. Misonidazole and other hypoxia markers: metabolism and applications. Int J Radiat Oncol Biol Phys 12:1195-202.

Franko, A.J., and C.J. Koch. 1984. Binding of misonidazole to V79 spheroids and fragments of Dunning rat prostatic and human colon carcinomas in vitro: diffusion of oxygen and reactive metabolites. Int J Radiat Oncol Biol Phys 10:1333-6.

Freyer, J.P. 1994. Rates of oxygen consumption for proliferating and quiescent cells isolated from multicellular tumor spheroids. Adv Exp Med Biol 345:335-42.

Fyles, A.W., M. Milosevic, M. Pintilie, A. Syed, and R.P. Hill. 2000. Anemia, hypoxia and transfusion in patients with cervix cancer: a review [In Process Citation]. Radiother Oncol 57:13-9.

Fyles, A.W., M. Milosevic, R. Wong, M.C. Kavanagh, M. Pintilie, A. Sun, W. Chapman, W. Levin, L. Manchul, T.J. Keane, and R.P. Hill. 1998. Oxygenation predicts radiation response and survival in patients with cervix cancer [published erratum appears in Radiother Oncol 1999 Mar;50(3):371]. Radiother Oncol 48:149-56.

Gali-Muhtasib, H.U., M.J. Haddadin, D.N. Rahhal, and I.H. Younes. 2001. Quinoxaline 1,4-dioxides as anticancer and hypoxia-selective drugs. Oncol Rep 8:679-84.

Gandara, D.R., P.N. Lara, Jr., Z. Goldberg, Q.T. Le, P.C. Mack, D.H. Lau, and P.H. Gumerlock. 2002. Tirapazamine: prototype for a novel class of therapeutic agents targeting tumor hypoxia. Semin Oncol 29:102-9.

Gatenby, R.A., H.B. Kessler, J.S. Rosenblum, L.R. Coia, P.J. Moldofsky, W.H. Hartz, and G.J. Broder. 1988. Oxygen distribution in squamous cell carcinoma metastases and its relationship to outcome of radiation therapy. Int J Radiat Oncol Biol Phys 14:831-8.

Gerweck, L.E. 1998. Tumor pH: implications for treatment and novel drug design. Semin Radiat Oncol 8:176-82.

Gerweck, L.E., J. Koutcher, and S.T. Zaidi. 1995. Energy status parameters, hypoxia fraction and radiocurability across tumor types. Acta Oncol 34:335-8.

Gerweck, L.E., J.A. Koutcher, S.T. Zaidi, and T. Seneviratne. 1992. Energy status in the murine FSaII and MCaIV tumors under aerobic and hypoxic conditions: an in-vivo and in-vitro analysis. Int J Radiat Oncol Biol Phys 23:557-61.

Giatromanolaki, A., M.I. Koukourakis, E. Sivridis, H. Turley, K. Talks, F. Pezzella, K.C. Gatter, and A.L. Harris. 2001. Relation of hypoxia inducible factor 1 alpha and 2 alpha in operable non-small cell lung cancer to angiogenic/molecular profile of tumours and survival. Br J Cancer 85:881-90.

Gleadle, J.M., and P.J. Ratcliffe. 1998. Hypoxia and the regulation of gene expression. Mol Med Today 4:122-9.

Grau, C., M.R. Horsman, and J. Overgaard. 1992. Influence of carboxyhemoglobin level on tumor growth, blood flow, and radiation response in an experimental model. Int J Radiat Oncol Biol Phys 22:421-4.

Gray, L.H., A. Conger, M. Ebert, S. Hornsey, and O. Scott. 1953. Concentration of oxygen dissolved in tissue at time of irradiation as a factor in radiotherapy. Br J Radiol 26:638-648.

Green, S.L., and A.J. Giaccia. 1998. Tumor hypoxia and the cell cycle: implications for malignant progression and response to therapy. Cancer J Sci Am 4:218-23.

Greenwell, A., J.F. Foley, and R.R. Maronpot. 1991. An enhancement method for immunohistochemical staining of proliferating cell nuclear antigen in archival rodent tissues. Cancer Lett 59:251-6.

Griffey, S.M., S.A. Kraegel, and B.R. Madewell. 1999. Proliferation indices in spontaneous canine lung cancer: proliferating cell nuclear antigen (PCNA), Ki-67 (MIB1) and mitotic counts. J Comp Pathol 120:321-32.

Griffin, R.J., K. Okajima, B. Barrios, and C.W. Song. 1996a. Mild temperature hyperthermia combined with carbogen breathing increases tumor partial pressure of oxygen (pO2) and radiosensitivity. Cancer Res 56:5590-3.

Griffin, R.J., C.M. Makepeace, W.J. Hur, and C.W. Song. 1996b. Radiosensitization of hypoxic tumor cells in vitro by nitric oxide. Int J Radiat Oncol Biol Phys 36:377-83.

Griffiths, J.R., and S.P. Robinson. 1999. The OxyLite: a fibre-optic oxygen sensor. Br J Radiol 72:627-30.

Grogan, M., G.M. Thomas, I. Melamed, F.L. Wong, R.G. Pearcey, P.K. Joseph, L. Portelance, J. Crook, and K.D. Jones. 1999. The importance of hemoglobin levels during radiotherapy for carcinoma of the cervix. Cancer 86:1528-36.

Groshar, D., A.J. McEwan, M.B. Parliament, R.C. Urtasun, L.E. Golberg, M. Hoskinson, J.R. Mercer, R.H. Mannan, L.I. Wiebe, and J.D. Chapman. 1993. Imaging tumor hypoxia and tumor perfusion. J Nucl Med 34:885-8.

Grossniklaus, H.E., S. Dithmar, and D.M. Albert. 2000. Animal models of uveal melanoma [In Process Citation]. Melanoma Res 10:195-211.

Guichard, M., E. Lartigau, L. Martin, C. Thomas, P. Weeger, P. Lambin, A.M. Le Ridant, A. Lusinchi, P. Wibault, B. Luboinski, and et al. 1994. Tumor oxygenation after 1) carbogen and/or perflubron emulsion administration in tumor xenografts 2) carbogen administration in patients. Artif Cells Blood Substit Immobil Biotechnol 22:1355-60.

Gulledge, C.J., and M.W. Dewhirst. 1996. Tumor oxygenation: a matter of supply and demand. Anticancer Res 16:741-9.

Haffty, B.G., R.A. Hurley, and L.G. Peters. 1999a. Carcinoma of the larynx treated with hypofractionated radiation and hyperbaric oxygen: long-term tumor control and complications. Int J Radiat Oncol Biol Phys 45:13-20.

Haffty, B.G., R. Hurley, and L.J. Peters. 1999b. Radiation therapy with hyperbaric oxygen at 4 atmospheres pressure in the management of squamous cell carcinoma of the head and neck: results of a randomized clinical trial [see comments]. Cancer J Sci Am 5:341-7.

Hahn, S.M., A.M. DeLuca, D. Coffin, C.M. Krishna, and J.B. Mitchell. 1998. In vivo radioprotection and effects on blood pressure of the stable free radical nitroxides. Int J Radiat Oncol Biol Phys 42:839-42.

Hall, P.A., D.A. Levison, A.L. Woods, C.C. Yu, D.B. Kellock, J.A. Watkins, D.M. Barnes, C.E. Gillett, R. Camplejohn, R. Dover, and et al. 1990. Proliferating cell nuclear antigen (PCNA) immunolocalization in paraffin sections: an index of cell proliferation with evidence of deregulated expression in some neoplasms [see comments]. J Pathol 162:285-94.

Halpern, H.J., C. Yu, M. Peric, E. Barth, D.J. Grdina, and B.A. Teicher. 1994. Oxymetry deep in tissues with low-frequency electron paramagnetic resonance. Proc Natl Acad Sci U S A 91:13047-51.

Harmey, J.H., and D. Bouchier-Hayes. 2002. Vascular endothelial growth factor (VEGF), a survival factor for tumour cells: implications for anti-angiogenic therapy. Bioessays 24:280-3.

Harris, A.L. 2002. Hypoxia--a key regulatory factor in tumour growth. Nature Rev Cancer 2:38-47.

Harrison, L.B., M. Chadha, R.J. Hill, K. Hu, and D. Shasha. 2002. Impact of tumor hypoxia and anemia on radiation therapy outcomes. Oncologist 7:492-508.

Haugland, H.K., V. Vukovic, M. Pintilie, A.W. Fyles, M. Milosevic, R.P. Hill, and D.W. Hedley. 2002. Expression of hypoxia-inducible factor-1alpha in cervical carcinomas: correlation with tumor oxygenation. Int J Radiat Oncol Biol Phys 53:854-861.

Haustermans, K., I. Hofland, I. Van de Pavert, K. Geboes, M. Varia, J. Raleigh, and A.C. Begg. 2000. Diffusion limited hypoxia estimated by vascular image analysis: comparison with pimonidazole staining in human tumors. Radiother Oncol 55:325-33.

Hazan, C., K. Melzer, K.S. Panageas, E. Li, H. Kamino, A. Kopf, C. Cordon-Cardo, I. Osman, and D. Polsky. 2002. Evaluation of the proliferation marker MIB-1 in the prognosis of cutaneous malignant melanoma. Cancer 95:634-40.

Henk, J.M., K. Bishop, and S.F. Shepherd. 2003. Treatment of head and neck cancer with CHART and nimorazole: phase II study. Radiother Oncol 66:65-70.

Hill, S.A., D.R. Collingridge, B. Vojnovic, and D.J. Chaplin. 1998. Tumour radiosensitization by high-oxygen-content gases: influence of the carbon dioxide content of the inspired gas on PO2, microcirculatory function and radiosensitivity. Int J Radiat Oncol Biol Phys 40:943-51.

Hirst, D.G., and J. Denekamp. 1979. Tumour cell proliferation in relation to the vasculature. Cell Tissue Kinet 12:31-42.

Hirst, D.G., J. Denekamp, and B. Hobson. 1982. Proliferation kinetics of endothelial and tumour cells in three mouse mammary carcinomas. Cell Tissue Kinet 15:251-61.

Hockel, M., K. Schlenger, S. Hockel, and P. Vaupel. 1999. Hypoxic cervical cancers with low apoptotic index are highly aggressive. Cancer Res 59:4525-8.

Hockel, M., K. Schlenger, B. Aral, M. Mitze, U. Schaffer, and P. Vaupel. 1996. Association between tumor hypoxia and malignant progression in advanced cancer of the uterine cervix. Cancer Res 56:4509-15.

Hockel, M., K. Schlenger, S. Hockel, B. Aral, U. Schaffer, and P. Vaupel. 1998. Tumor hypoxia in pelvic recurrences of cervical cancer. Int J Cancer 79:365-9.

Hockel, M., C. Knoop, K. Schlenger, B. Vorndran, E. Baussmann, M. Mitze, P.G. Knapstein, and P. Vaupel. 1993. Intratumoral pO2 predicts survival in advanced cancer of the uterine cervix. Radiother Oncol 26:45-50.

Hodgkiss, R.J. 1998. Use of 2-nitroimidazoles as bioreductive markers for tumour hypoxia. Anticancer Drug Des 13:687-702.

Hodgkiss, R.J., L. Webster, and G.D. Wilson. 1995a. Development of bioreductive markers for tumour hypoxia. Acta Oncol 34:351-5.

Hodgkiss, R.J., J. Parrick, M. Porssa, and M.R. Stratford. 1994. Bioreductive markers for hypoxic cells: 2-nitroimidazoles with biotinylated 1-substituents. J Med Chem 37:4352-6.

Hodgkiss, R.J., M.R. Stratford, M.F. Dennis, and S.A. Hill. 1995b. Pharmacokinetics and binding of the bioreductive probe for hypoxia, NITP: effect of route of administration. Br J Cancer 72:1462-8.

Hodgkiss, R.J., G. Jones, A. Long, J. Parrick, K.A. Smith, M.R. Stratford, and G.D. Wilson. 1991a. Flow cytometric evaluation of hypoxic cells in solid experimental tumours using fluorescence immunodetection. Br J Cancer 63:119-25.

Hodgkiss, R.J., A.C. Begg, R.W. Middleton, J. Parrick, M.R. Stratford, P. Wardman, and G.D. Wilson. 1991b. Fluorescent markers for hypoxic cells. A study of novel heterocyclic compounds that undergo bio-reductive binding. Biochem Pharmacol 41:533-41.

Hoebers, F.J., H.L. Janssen, A.V. Olmos, D. Sprong, A.D. Nunn, A.J. Balm, C.A. Hoefnagel, A.C. Begg, and K.M. Haustermans. 2002. Phase 1 study to identify tumour hypoxia in patients with head and neck cancer using technetium-99m BRU 59-21. Eur J Nucl Med Mol Imaging 29:1206-11.

Holden, S.A., T.S. Herman, and B.A. Teicher. 1990. Addition of a hypoxic cell selective cytotoxic agent (mitomycin C or porfiromycin) to Fluosol-DA/carbogen/radiation. Radiother Oncol 18:59-70.

Honess, D.J., and N.M. Bleehen. 1995. Perfusion changes in the RIF-1 tumour and normal tissues after carbogen and nicotinamide, individually and combined. Br J Cancer 71:1175-80.

Honess, D.J., M.S. Andrews, R. Ward, and N.M. Bleehen. 1995. Pentoxifylline increases RIF-1 tumour pO2 in a manner compatible with its ability to increase relative tumour perfusion. Acta Oncol 34:385-9.

Honess, D.J., Y. Kitamoto, M.R. Rampling, and N.M. Bleehen. 1996. Nicotinamide and pentoxifylline increase human leucocyte filterability: a possible mechanism for reduction of acute hypoxia. Br J Cancer Suppl 27:S236-40.

Honess, D.J., S.A. Hill, D.R. Collingridge, B. Edwards, G. Brauers, N.A. Powell, and D.J. Chaplin. 1998. Preclinical evaluation of the novel hypoxic marker 99mTc-HL91 (Prognox) in murine and xenograft systems in vivo. Int J Radiat Oncol Biol Phys 42:731-5.

Horsman, M.R. 1998. Measurement of tumor oxygenation. Int J Radiat Oncol Biol Phys 42:701-4.

Horsman, M.R., and J. Overgaard. 1997. Can mild hyperthermia improve tumour oxygenation? Int J Hyperthermia 13:141-7.

Horsman, M.R., D.J. Chaplin, and J.M. Brown. 1989. Tumor radiosensitization by nicotinamide: a result of improved perfusion and oxygenation. Radiat Res 118:139-50.

Horsman, M.R., D.W. Siemann, D.J. Chaplin, and J. Overgaard. 1997. Nicotinamide as a radiosensitizer in tumours and normal tissues: the importance of drug dose and timing. Radiother Oncol 45:167-74.

Horsman, M.R., M. Nordsmark, A.A. Khalil, S.A. Hill, D.J. Chaplin, D.W. Siemann, and J. Overgaard. 1994. Reducing acute and chronic hypoxia in tumours by combining nicotinamide with carbogen breathing. Acta Oncol 33:371-6.

Hoskin, P.J., M.I. Saunders, and S. Dische. 1999. Hypoxic radiosensitizers in radical radiotherapy for patients with bladder carcinoma: hyperbaric oxygen, misonidazole, and accelerated radiotherapy, carbogen, and nicotinamide [In Process Citation]. Cancer 86:1322-8.

Hoskin, P.J., A. Sibtain, F.M. Daley, and G.D. Wilson. 2003. GLUT1 and CAIX as intrinsic markers of hypoxia in bladder cancer: relationship with vascularity and proliferation as predictors of outcome of ARCON. Br J Cancer 89:1290-7.

Hoskin, P.J., M.R. Stratford, M.I. Saunders, D.W. Hall, M.F. Dennis, and A. Rojas. 1995. Administration of nicotinamide during chart: pharmacokinetics, dose escalation, and clinical toxicity. Int J Radiat Oncol Biol Phys 32:1111-9.

Hsu, D.W., J.T. Efird, and E.T. Hedley-Whyte. 1998. MIB-1 (Ki-67) index and transforming growth factor-alpha (TGF alpha) immunoreactivity are significant prognostic predictors for meningiomas. Neuropathol Appl Neurobiol 24:441-52.

Hui, E.P., A.T. Chan, F. Pezzella, H. Turley, K.F. To, T.C. Poon, B. Zee, F. Mo, P.M. Teo, D.P. Huang, K.C. Gatter, P.J. Johnson, and A.L. Harris. 2002. Coexpression of hypoxia-inducible factors 1alpha and 2alpha, carbonic anhydrase IX, and vascular endothelial growth factor in nasopharyngeal carcinoma and relationship to survival. Clin Cancer Res 8:2595-604.

Hulshof, M.C., C.J. Rehmann, J. Booij, E.A. van Royen, D.A. Bosch, and D. Gonzalez Gonzalez. 1998. Lack of perfusion enhancement after administration of nicotinamide and carbogen in patients with glioblastoma: a 99mTc-HMPAO SPECT study. Radiother Oncol 48:135-42.

Hung, L.C., V.F. Pong, C.R. Cheng, F.I. Wong, and R.M. Chu. 2000. An improved system for quantifying AgNOR and PCNA in canine tumors. Anticancer Res 20:3273-80.

Ilangovan, G., H. Li, J.L. Zweier, and P. Kuppusamy. 2002. In vivo measurement of tumor redox environment using EPR spectroscopy. Mol Cell Biochem 234-235:393-8.

Ivanov, S., S.Y. Liao, A. Ivanova, A. Danilkovitch-Miagkova, N. Tarasova, G. Weirich, M.J. Merrill, M.A. Proescholdt, E.H. Oldfield, J. Lee, J. Zavada, A. Waheed, W. Sly, M.I. Lerman, and E.J. Stanbridge. 2001. Expression of hypoxia-inducible cell-surface transmembrane carbonic anhydrases in human cancer. Am J Pathol 158:905-19.

Iyer, N.V., L.E. Kotch, F. Agani, S.W. Leung, E. Laughner, R.H. Wenger, M. Gassmann, J.D. Gearhart, A.M. Lawler, A.Y. Yu, and G.L. Semenza. 1998a. Cellular and developmental control of O2 homeostasis by hypoxia- inducible factor 1 alpha. Genes Dev 12:149-62.

Iyer, R.V., E. Kim, R.F. Schneider, and J.D. Chapman. 1998b. A dual hypoxic marker technique for measuring oxygenation change within individual tumors. Br J Cancer 78:163-9.

Iyer, R.V., E.L. Engelhardt, C.C. Stobbe, R.F. Schneider, and J.D. Chapman. 1998c. Preclinical assessment of hypoxic marker specificity and sensitivity. Int J Radiat Oncol Biol Phys 42:741-5.

Jain, R.K. 1988. Determinants of tumor blood flow: a review. Cancer Res 48:2641-58.

Jain, R.K. 1994. Barriers to drug delivery in solid tumors. Sci Am 271:58-65.

Janssens, M.Y., V.N. Verovski, D.L. Van den Berge, C. Monsaert, and G.A. Storme. 1999. Radiosensitization of hypoxic tumour cells by S-nitroso-N- acetylpenicillamine implicates a bioreductive mechanism of nitric oxide generation. Br J Cancer 79:1085-9.

Jelkmann, W., and T. Hellwig-Burgel. 2001. Biology of erythropoietin. Adv Exp Med Biol 502:169-87.

Jenkins, W.T., S.M. Evans, and C.J. Koch. 2000. Hypoxia and necrosis in rat 9L glioma and Morris 7777 hepatoma tumors: comparative measurements using EF5 binding and the Eppendorf needle electrode. Int J Radiat Oncol Biol Phys 46:1005-17.

Jenssen, N., M. Boysen, A. Kjaerheim, and M. Bryne. 1996. Low vascular density indicates poor response to radiotherapy in small glottic carcinomas. Pathol Res Pract 192:1090-4.

Jung, C., W. Muller-Klieser, and P. Vaupel. 1984. Tumor blood flow and O2 availability during hemodilution. Adv Exp Med Biol 180:281-91.

Kaanders, J.H., J. Bussink, and A.J. van der Kogel. 2002a. ARCON: a novel biology-based approach in radiotherapy. Lancet Oncol 3:728-37.

Kaanders, J.H., L.A. Pop, H.A. Marres, R.W. van der Maazen, A.J. van der Kogel, and W.A. van Daal. 1995. Radiotherapy with carbogen breathing and nicotinamide in head and neck cancer: feasibility and toxicity. Radiother Oncol 37:190-8.

Kaanders, J.H., L.A. Pop, H.A. Marres, J. Liefers, F.J. van den Hoogen, W.A. van Daal, and A.J. van der Kogel. 1998. Accelerated radiotherapy with carbogen and nicotinamide (ARCON) for laryngeal cancer. Radiother Oncol 48:115-22.

Kaanders, J.H., L.A. Pop, H.A. Marres, I. Bruaset, F.J. van den Hoogen, M.A. Merkx, and A.J. van der Kogel. 2002b. ARCON: experience in 215 patients with advanced head-and-neck cancer. Int J Radiat Oncol Biol Phys 52:769-78.

Kaanders, J.H., K.I. Wijffels, H.A. Marres, A.S. Ljungkvist, L.A. Pop, F.J. van den Hoogen, P.C. de Wilde, J. Bussink, J.A. Raleigh, and A.J. van der Kogel. 2002c. Pimonidazole binding and tumor vascularity predict for treatment outcome in head and neck cancer. Cancer Res 62:7066-74.

Kale, R.K. 1996. Exploitation of hypoxia for radiation therapy: a lesson from phenothiazines. Med Hypotheses 47:107-10.

Kasai, S., H. Nagasawa, H. Kuwasaka, T. Oshodani, A. Nishioka, Y. Ogawa, S. Yoshida, S. Inayama, T. Inomata, and H. Hori. 1998. TX-1877: design, synthesis, and biological activities as a BRM- functional hypoxic cell radiosensitizer. Int J Radiat Oncol Biol Phys 42:799-802.

Kavanagh, M.C., S. Minkin, and R.P. Hill. 1999a. The Use of Needle Biopsies for Radiobiological Assessment of Oxygen Levels in KHT-C Tumors. Radiat Res 152:107-112.

Kavanagh, M.C., A. Sun, Q. Hu, and R.P. Hill. 1996. Comparing techniques of measuring tumor hypoxia in different murine tumors: Eppendorf pO2 Histograph, [3H]misonidazole binding and paired survival assay. Radiat Res 145:491-500.

Kavanagh, M.C., V. Tsang, S. Chow, C. Koch, D. Hedley, S. Minkin, and R.P. Hill. 1999b. A comparison in individual murine tumors of techniques for measuring oxygen levels. Int J Radiat Oncol Biol Phys 44:1137-46.

Kelleher, D.K., and P.W. Vaupel. 1994. Possible mechanisms involved in tumor radiosensitization following nicotinamide administration. Radiother Oncol 32:47-53.

Kelleher, D.K., O. Thews, and P. Vaupel. 1998a. Regional perfusion and oxygenation of tumors upon methylxanthine derivative administration. Int J Radiat Oncol Biol Phys 42:861-4.

Kelleher, D.K., C. Nauth, O. Thews, W. Krueger, and P. Vaupel. 1998b. Localized hypothermia: impact on oxygenation, microregional perfusion, metabolic and bioenergetic status of subcutaneous rat tumours. Br J Cancer 78:56-61.

Kennedy, A.S., J.A. Raleigh, G.M. Perez, D.P. Calkins, D.E. Thrall, D.B. Novotny, and M.A. Varia. 1997. Proliferation and hypoxia in human squamous cell carcinoma of the cervix: first report of combined immunohistochemical assays. Int J Radiat Oncol Biol Phys 37:897-905.

Kergoat, H., and C. Faucher. 1999. Effects of oxygen and carbogen breathing on choroidal hemodynamics in humans. Invest Ophthalmol Vis Sci 40:2906-11.

Kim, I.H., M.J. Lemmon, and J.M. Brown. 1993. The influence of irradiation of the tumor bed on tumor hypoxia: measurements by radiation response, oxygen electrodes, and nitroimidazole binding. Radiat Res 135:411-7.

Kimura, H., R.D. Braun, E.T. Ong, R. Hsu, T.W. Secomb, D. Papahadjopoulos, K. Hong, and M.W. Dewhirst. 1996. Fluctuations in red cell flux in tumor microvessels can lead to transient hypoxia and reoxygenation in tumor parenchyma. Cancer Res 56:5522-8.

Kinoshita, Y., K. Kohshi, N. Kunugita, T. Tosaki, and A. Yokota. 2000. Preservation of tumour oxygen after hyperbaric oxygenation monitored by magnetic resonance imaging. Br J Cancer 82:88-92.

Knocke, T.H., H.D. Weitmann, H.J. Feldmann, E. Selzer, and R. Potter. 1999. Intratumoral pO2-measurements as predictive assay in the treatment of carcinoma of the uterine cervix. Radiother Oncol 53:99-104.

Koch, C.J., S.M. Evans, and E.M. Lord. 1995. Oxygen dependence of cellular uptake of EF5 [2-(2-nitro-1H-imidazol-1-yl)-N-(2,2,3,3,3-pentafluoropropyl)a cet amide] : analysis of drug adducts by fluorescent antibodies vs bound radioactivity. Br J Cancer 72:869-74.

Koch, C.J., J.E. Chasan, W.T. Jenkins, C.Y. Chan, K.M. Laughlin, and S.M. Evans. 1998. Co-localization of hypoxia and apoptosis in irradiated and untreated HCT116 human colon carcinoma xenografts. Adv Exp Med Biol 454:611-8.

Koch, C.J., S.M. Hahn, K. Rockwell, Jr., J.M. Covey, W.G. McKenna, and S.M. Evans. 2001. Pharmacokinetics of EF5 [2-(2-nitro-1-H-imidazol-1-yl)-N-(2,2,3,3,3-pentafluoropropyl) acetamide] in human patients: implications for hypoxia measurements in vivo by 2-nitroimidazoles. Cancer Chemother Pharmacol 48:177-87.

Koch, C.J., P.R. Oprysko, A.L. Shuman, W.T. Jenkins, G. Brandt, and S.M. Evans. 2002. Radiosensitization of hypoxic tumor cells by dodecafluoropentane: a gas- phase perfluorochemical emulsion. Cancer Res 62:3626-9.

Koester, S.K., and W.E. Bolton. 1999. Differentiation and assessment of cell death. Clin Chem Lab Med 37:311-7.

Koh, W.J., T.W. Griffin, J.S. Rasey, and G.E. Laramore. 1994. Positron emission tomography. A new tool for characterization of malignant disease and selection of therapy. Acta Oncol 33:323-7.

Koh, W.J., J.S. Rasey, M.L. Evans, J.R. Grierson, T.K. Lewellen, M.M. Graham, K.A. Krohn, and T.W. Griffin. 1992. Imaging of hypoxia in human tumors with [F-18]fluoromisonidazole. Int J Radiat Oncol Biol Phys 22:199-212.

Konerding, M.A., A.J. Miodonski, and A. Lametschwandtner. 1995. Microvascular corrosion casting in the study of tumor vascularity: a review. Scanning Microsc 9:1233-43; discussion 1243-4.

Konerding, M.A., W. Malkusch, B. Klapthor, C. van Ackern, E. Fait, S.A. Hill, C. Parkins, D.J. Chaplin, M. Presta, and J. Denekamp. 1999. Evidence for characteristic vascular patterns in solid tumours: quantitative studies using corrosion casts. Br J Cancer 80:724-32.

Koong, A.C., N.C. Denko, K.M. Hudson, C. Schindler, L. Swiersz, C. Koch, S. Evans, H. Ibrahim, Q.T. Le, D.J. Terris, and A.J. Giaccia. 2000. Candidate genes for the hypoxic tumor phenotype [In Process Citation]. Cancer Res 60:883-7.

Koukourakis, M. 2002. Amifostine in clinical oncology: current use and future applications. Anticancer Drugs 13:181-209.

Koukourakis, M.I. 2001. Tumour angiogenesis and response to radiotherapy. Anticancer Res 21:4285-300.

Koukourakis, M.I., and D. Yannakakis. 2001. High dose daily amifostine and hypofractionated intensively accelerated radiotherapy for locally advanced breast cancer. A phase I/II study and report on early and late sequellae. Anticancer Res 21:2973-8.

Koukourakis, M.I., A. Giatromanolaki, E. Sivridis, and I. Fezoulidis. 2000. Cancer vascularization: implications in radiotherapy? Int J Radiat Oncol Biol Phys 48:545-53.

Koukourakis, M.I., A. Giatromanolaki, E. Sivridis, K. Simopoulos, J. Pastorek, C.C. Wykoff, K.C. Gatter, and A.L. Harris. 2001. Hypoxia-regulated carbonic anhydrase-9 (CA9) relates to poor vascularization and resistance of squamous cell head and neck cancer to chemoradiotherapy. Clin Cancer Res 7:3399-403.

Koukourakis, M.I., A. Giatromanolaki, E. Sivridis, C. Simopoulos, H. Turley, K. Talks, K.C. Gatter, and A.L. Harris. 2002. Hypoxia-inducible factor (HIF1A and HIF2A), angiogenesis, and chemoradiotherapy outcome of squamous cell head-and-neck cancer. Int J Radiat Oncol Biol Phys 53:1192-202.

Kubota, K. 2001. From tumor biology to clinical Pet: a review of positron emission tomography (PET) in oncology. Ann Nucl Med 15:471-86.

Kuin, A., L. Smets, T. Volk, A. Paans, G. Adams, A. Atema, E. Jahde, A. Maas, M.F. Rajewsky, G. Visser, and et al. 1994. Reduction of intratumoral pH by the mitochondrial inhibitor m-iodobenzylguanidine and moderate hyperglycemia. Cancer Res 54:3785-92.

Kumar, P. 2000. Tumor hypoxia and anemia: impact on the efficacy of radiation therapy [In Process Citation]. Semin Hematol 37:4-8.

Kurki, P., M. Vanderlaan, F. Dolbeare, J. Gray, and E.M. Tan. 1986. Expression of proliferating cell nuclear antigen (PCNA)/cyclin during the cell cycle. Exp Cell Res 166:209-19.

Kwock, L., M. Gill, H.L. McMurry, W. Beckman, J.A. Raleigh, and A.P. Joseph. 1992. Evaluation of a fluorinated 2-nitroimidazole binding to hypoxic cells in tumor-bearing rats by 19F magnetic resonance spectroscopy and immunohistochemistry. Radiat Res 129:71-8.

Lal, A., H. Peters, B. St Croix, Z.A. Haroon, M.W. Dewhirst, R.L. Strausberg, J.H. Kaanders, A.J. van der Kogel, and G.J. Riggins. 2001. Transcriptional response to hypoxia in human tumors. J Natl Cancer Inst 93:1337-43.

Lambin, P., E.P. Malaise, and M.C. Joiner. 1996. Might intrinsic radioresistance of human tumour cells be induced by radiation? Int J Radiat Biol 69:279-90.

Lanzen, J.L., R.D. Braun, A.L. Ong, and M.W. Dewhirst. 1998. Variability in blood flow and pO2 in tumors in response to carbogen breathing. Int J Radiat Oncol Biol Phys 42:855-9.

Laurence, V.M., R. Ward, I.F. Dennis, and N.M. Bleehen. 1995. Carbogen breathing with nicotinamide improves the oxygen status of tumours in patients. Br J Cancer 72:198-205.

Le, Q.T., M.S. Kovacs, M.J. Dorie, A. Koong, D.J. Terris, H.A. Pinto, D.R. Goffinet, K. Nowels, D. Bloch, and J.M. Brown. 2003. Comparison of the comet assay and the oxygen microelectrode for measuring tumor oxygenation in head-and-neck cancer patients. Int J Radiat Oncol Biol Phys 56:375-83.

Lee, D.J., A. Trotti, S. Spencer, R. Rostock, C. Fisher, R. von Roemeling, E. Harvey, and E. Groves. 1998a. Concurrent tirapazamine and radiotherapy for advanced head and neck carcinomas: a Phase II study. Int J Radiat Oncol Biol Phys 42:811-5.

Lee, J., D.W. Siemann, C.J. Koch, and E.M. Lord. 1996. Direct relationship between radiobiological hypoxia in tumors and monoclonal antibody detection of EF5 cellular adducts. Int J Cancer 67:372-8.

Lee, W.R., B. Berkey, V. Marcial, K.K. Fu, J.S. Cooper, B. Vikram, L.R. Coia, M. Rotman, and H. Ortiz. 1998b. Anemia is associated with decreased survival and increased locoregional failure in patients with locally advanced head and neck carcinoma: a secondary analysis of RTOG 85-27. Int J Radiat Oncol Biol Phys 42:1069-75.

Leek, R.D., R.J. Landers, A.L. Harris, and C.E. Lewis. 1999. Necrosis correlates with high vascular density and focal macrophage infiltration in invasive carcinoma of the breast. Br J Cancer 79:991-5.

Lehtio, K., V. Oikonen, T. Gronroos, O. Eskola, K. Kalliokoski, J. Bergman, O. Solin, R. Grenman, P. Nuutila, and H. Minn. 2001. Imaging of blood flow and hypoxia in head and neck cancer: initial evaluation with [(15)O]H(2)O and [(18)F]fluoroerythronitroimidazole PET. J Nucl Med 42:1643-52.

Leskinen-Kallio, S. 1994. Positron emission tomography in oncology. Clin Physiol 14:329-35.

Lindegaard, J.C., and C. Grau. 2000. Has the outlook improved for amifostine as a clinical radioprotector? Radiother Oncol 57:113-118.

Littlewood, T.J. 2001. The impact of hemoglobin levels on treatment outcomes in patients with cancer. Semin Oncol 28:49-53.

Loesberg, C., H. Van Rooij, W.J. Nooijen, A.J. Meijer, and L.A. Smets. 1990. Impaired mitochondrial respiration and stimulated glycolysis by m-iodobenzylguanidine (MIBG). Int J Cancer 46:276-81.

Loncaster, J.A., A.L. Harris, S.E. Davidson, J.P. Logue, R.D. Hunter, C.C. Wycoff, J. Pastorek, P.J. Ratcliffe, I.J. Stratford, and C.M. West. 2001. Carbonic anhydrase (CA IX) expression, a potential new intrinsic marker of hypoxia: correlations with tumor oxygen measurements and prognosis in locally advanced carcinoma of the cervix. Cancer Res 61:6394-9.

Lord, E.M., L. Harwell, and C.J. Koch. 1993. Detection of hypoxic cells by monoclonal antibody recognizing 2-nitroimidazole adducts. Cancer Res 53:5721-6.

Lowe, S.W. 1999. Activation of p53 by oncogenes. Endocr Relat Cancer 6:45-8.

Lu, H., R.A. Forbes, and A. Verma. 2002. Hypoxia-inducible Factor 1 Activation by Aerobic Glycolysis Implicates the Warburg Effect in Carcinogenesis. J. Biol. Chem. 277:23111-23115.

Lyng, H., K. Sundfor, and E.K. Rofstad. 1997. Oxygen tension in human tumours measured with polarographic needle electrodes and its relationship to vascular density, necrosis and hypoxia. Radiother Oncol 44:163-9.

MacEwen, E.G. 1990. Spontaneous tumors in dogs and cats: models for the study of cancer biology and treatment. Cancer Metastasis Rev 9:125-36.

Madewell, B.R. 2001. Cellular proliferation in tumors: a review of methods, interpretation, and clinical applications. J Vet Intern Med 15:334-40.

Mahon, P.C., K. Hirota, and G.L. Semenza. 2001. FIH-1: a novel protein that interacts with HIF-1alpha and VHL to mediate repression of HIF-1 transcriptional activity. Genes Dev 15:2675-86.

Mahy, P., M. De Bast, B. Gallez, J. Gueulette, C.J. Koch, P. Scalliet, and V. Gregoire. 2003. In vivo colocalization of 2-nitroimidazole EF5 fluorescence intensity and electron paramagnetic resonance oximetry in mouse tumors. Radiother Oncol 67:53-61.

Malonne, H., I. Langer, R. Kiss, and G. Atassi. 1999. Mechanisms of tumor angiogenesis and therapeutic implications: angiogenesis inhibitors. Clin Exp Metastasis 17:1-14.

Mason, R.P., P.P. Antich, E.E. Babcock, A. Constantinescu, P. Peschke, and E.W. Hahn. 1994. Non-invasive determination of tumor oxygen tension and local variation with growth. Int J Radiat Oncol Biol Phys 29:95-103.

Mason, R.P., S. Hunjan, D. Le, A. Constantinescu, B.R. Barker, P.S. Wong, P. Peschke, E.W. Hahn, and P.P. Antich. 1998. Regional tumor oxygen tension: fluorine echo planar imaging of hexafluorobenzene reveals heterogeneity of dynamics. Int J Radiat Oncol Biol Phys 42:747-50.

Masunaga, S., K. Ono, M. Suzuki, Y. Kinashi, M. Takagaki, and M. Akaboshi. 1997a. Alteration in the hypoxic fraction of quiescent cell populations by hyperthermia at mild temperatures. Int J Hyperthermia 13:401-11.

Masunaga, S., K. Ono, M. Akaboshi, Y. Nishimura, M. Suzuki, Y. Kinashi, M. Takagaki, M. Hiraoka, and M. Abe. 1997b. Reduction of hypoxic cells in solid tumours induced by mild hyperthermia: special reference to differences in changes in the hypoxic fraction between total and quiescent cell populations. Br J Cancer 76:588-93.

Masunaga, S., K. Ono, Y. Nishimura, S. Kanamori, T. Saga, M. Suzuki, Y. Kinashi, M. Takagaki, S. Kasai, H. Nagasawa, Y. Uto, and H. Hori. 2000. Combined effects of tirapazamine and mild hyperthermia on anti-angiogenic agent (TNP-470) treated tumors-reference to the effect on intratumor quiescent cells [see comments]. Int J Radiat Oncol Biol Phys 47:799-807.

Mathews, M.B., R.M. Bernstein, B.R. Franza, Jr., and J.I. Garrels. 1984. Identity of the proliferating cell nuclear antigen and cyclin. Nature 309:374-6.

Maxwell, P.H., M.S. Wiesener, G.W. Chang, S.C. Clifford, E.C. Vaux, M.E. Cockman, C.C. Wykoff, C.W. Pugh, E.R. Maher, and P.J. Ratcliffe. 1999. The tumour suppressor protein VHL targets hypoxia-inducible factors for oxygen-dependent proteolysis. Nature 399:271-5.

Maxwell, R.J., P. Workman, and J.R. Griffiths. 1989. Demonstration of tumor-selective retention of fluorinated nitroimidazole probes by 19F magnetic resonance spectroscopy in vivo. Int J Radiat Oncol Biol Phys 16:925-9.

McCormick, D., C. Yu, C. Hobbs, and P.A. Hall. 1993. The relevance of antibody concentration to the immunohistological quantification of cell proliferation-associated antigens. Histopathology 22:543-7.

McLaren, D.B., T. Pickles, T. Thomson, and P.L. Olive. 1997. Impact of nicotinamide on human tumour hypoxic fraction measured using the comet assay. Radiother Oncol 45:175-82.

Mehta, M.P. 1999. Amifostine and combined-modality therapeutic approaches. Semin Oncol 26:95-101.

Melo, T., J. Duncan, J.R. Ballinger, and A.M. Rauth. 2000. BRU59-21, a second-generation 99mTc-labeled 2-nitroimidazole for imaging hypoxia in tumors. J Nucl Med 41:169-76.

Mercadante, S., V. Gebbia, A. Marrazzo, and S. Filosto. 2000. Anaemia in cancer: pathophysiology and treatment. Cancer Treat Rev 26:303-11.

Meyer, J.S., E. Friedman, M.M. McCrate, and W.C. Bauer. 1983. Prediction of early course of breast carcinoma by thymidine labeling. Cancer 51:1879-86.

Milosevic, M.F., A.W. Fyles, and R.P. Hill. 1999. The relationship between elevated interstitial fluid pressure and blood flow in tumors: a bioengineering analysis. Int J Radiat Oncol Biol Phys 43:1111-23.

Minchinton, A.I., D.A. Tonn, D.P. Sutherland, and A.H. Kyle. 2002. Carbogen Breathing after Irradiation Enhances the Effectiveness of Tirapazamine in SiHa Tumors but not SCCVII Tumors in Mice. Radiat Res 158:94-100.

Minet, E., G. Michel, J. Remacle, and C. Michiels. 2000. Role of HIF-1 as a transcription factor involved in embryonic development, cancer progression and apoptosis (Review). Int J Mol Med 5:253-259.

Minn, H., A.C. Clavo, and R.L. Wahl. 1996. Influence of hypoxia on tracer accumulation in squamous-cell carcinoma: in vitro evaluation for PET imaging. Nucl Med Biol 23:941-6.

Miralbell, R., F. Mornex, R. Greiner, M. Bolla, G. Storme, M. Hulshof, J. Bernier, J. Denekamp, A.M. Rojas, M. Pierart, M. van Glabbeke, and R.O. Mirimanoff. 1999. Accelerated Radiotherapy, Carbogen, and Nicotinamide in Glioblastoma Multiforme: Report of European Organization for Research and Treatment of Cancer Trial 22933. J Clin Oncol 17:3143-3149.

Miyachi, K., M.J. Fritzler, and E.M. Tan. 1978. Autoantibody to a nuclear antigen in proliferating cells. J Immunol 121:2228-34.

Mizumoto, K., L.W. Qian, L. Zhang, E. Nagai, S. Kura, and M. Tanaka. 2002. A nitroimidazole derivative, PR-350, enhances the killing of pancreatic cancer cells exposed to high-dose irradiation under hypoxia. J Radiat Res (Tokyo) 43:43-51.

Molls, M., P. Stadler, A. Becker, H.J. Feldmann, and J. Dunst. 1998. Relevance of oxygen in radiation oncology. Mechanisms of action, correlation to low hemoglobin levels. Strahlenther Onkol 174 Suppl 4:13-6.

Moulder, J.E., and S. Rockwell. 1984. Hypoxic fractions of solid tumors: experimental techniques, methods of analysis, and a survey of existing data. Int J Radiat Oncol Biol Phys 10:695-712.

Movsas, B., J.D. Chapman, E.M. Horwitz, W.H. Pinover, R.E. Greenberg, A.L. Hanlon, R. Iyer, and G.E. Hanks. 1999. Hypoxic regions exist in human prostate carcinoma. Urology 53:11-8.

Movsas, B., J.D. Chapman, A.L. Hanlon, E.M. Horwitz, W.H. Pinover, R.E. Greenberg, C. Stobbe, and G.E. Hanks. 2001. Hypoxia in human prostate carcinoma: an Eppendorf PO2 study. Am J Clin Oncol 24:458-61.

Mueller-Klieser, W., and S. Walenta. 1993. Geographical mapping of metabolites in biological tissue with quantitative bioluminescence and single photon imaging. Histochem J 25:407-20.

Mueller-Klieser, W., C. Schaefer, S. Walenta, E.K. Rofstad, B.M. Fenton, and R.M. Sutherland. 1990. Assessment of tumor energy and oxygenation status by bioluminescence, nuclear magnetic resonance spectroscopy, and cryospectrophotometry. Cancer Res 50:1681-5.

Mueller-Klieser, W., K.H. Schlenger, S. Walenta, M. Gross, U. Karbach, M. Hoeckel, and P. Vaupel. 1991. Pathophysiological approaches to identifying tumor hypoxia in patients. Radiother Oncol 20:21-8.

Murphy, B.J., K.R. Laderoute, R.J. Chin, and R.M. Sutherland. 1994. Metallothionein IIA is up-regulated by hypoxia in human A431 squamous carcinoma cells. Cancer Res 54:5808-10.

Nemoto, K., Y. Shibamoto, J. Ohmagari, Y. Baba, K. Ebe, H. Ariga, Y. Takai, A. Ouchi, K. Sasai, M. Shinozaki, M. Tsujitani, M. Sakaguchi, S. Yamada, and K. Sakamoto. 2001. Phase Ia study of a hypoxic cell sensitizer doranidazole (PR-350) in combination with conventional radiotherapy. Anticancer Drugs 12:1-6.

Neufeld, G., T. Cohen, S. Gengrinovitch, and Z. Poltorak. 1999. Vascular endothelial growth factor (VEGF) and its receptors. Faseb J 13:9-22.

Nordsmark, M., and J. Overgaard. 2000. A confirmatory prognostic study on oxygenation status and loco-regional control in advanced head and neck squamous cell carcinoma treated by radiation therapy. Radiother Oncol 57:39-43.

Nordsmark, M., S.M. Bentzen, and J. Overgaard. 1994. Measurement of human tumour oxygenation status by a polarographic needle electrode. An analysis of inter- and intratumour heterogeneity. Acta Oncol 33:383-9.

Nordsmark, M., M. Overgaard, and J. Overgaard. 1996a. Pretreatment oxygenation predicts radiation response in advanced squamous cell carcinoma of the head and neck. Radiother Oncol 41:31-9.

Nordsmark, M., C. Grau, M.R. Horsman, H.S. Jorgensen, and J. Overgaard. 1995. Relationship between tumour oxygenation, bioenergetic status and radiobiological hypoxia in an experimental model. Acta Oncol 34:329-34.

Nordsmark, M., J. Keller, O.S. Nielsen, E. Lundorf, and J. Overgaard. 1997. Tumour oxygenation assessed by polarographic needle electrodes and bioenergetic status measured by 31P magnetic resonance spectroscopy in human soft tissue tumours. Acta Oncol 36:565-71.

Nordsmark, M., M. Hoyer, J. Keller, O.S. Nielsen, O.M. Jensen, and J. Overgaard. 1996b. The relationship between tumor oxygenation and cell proliferation in human soft tissue sarcomas. Int J Radiat Oncol Biol Phys 35:701-8.

Nordsmark, M., J. Loncaster, S.C. Chou, H. Havsteen, J.C. Lindegaard, S.E. Davidson, M. Varia, C. West, R. Hunter, J. Overgaard, and J.A. Raleigh. 2001. Invasive oxygen measurements and pimonidazole labeling in human cervix carcinoma. Int J Radiat Oncol Biol Phys 49:581-6.

Nordsmark, M., J. Loncaster, C. Aquino-Parsons, S.C. Chou, M. Ladekarl, H. Havsteen, J.C. Lindegaard, S.E. Davidson, M. Varia, C. West, R. Hunter, J. Overgaard, and J.A. Raleigh. 2003. Measurements of hypoxia using pimonidazole and polarographic oxygen-sensitive electrodes in human cervix carcinomas. Radiother Oncol 67:35-44.

Nozue, M., I. Lee, J.M. Manning, L.R. Manning, and R.K. Jain. 1996. Oxygenation in tumors by modified hemoglobins. J Surg Oncol 62:109-14.

Nozue, M., I. Lee, F. Yuan, B.A. Teicher, D.M. Brizel, M.W. Dewhirst, C.G. Milross, L. Milas, C.W. Song, C.D. Thomas, M. Guichard, S.M. Evans, C.J. Koch, E.M. Lord, R.K. Jain, and H.D. Suit. 1997. Interlaboratory variation in oxygen tension measurement by Eppendorf "Histograph" and comparison with hypoxic marker. J Surg Oncol 66:30-8.

Olive, P.L. 1994. Radiation-induced reoxygenation in the SCCVII murine tumour: evidence for a decrease in oxygen consumption and an increase in tumour perfusion. Radiother Oncol 32:37-46.

Olive, P.L. 1995. Detection of hypoxia by measurement of DNA damage in individual cells from spheroids and murine tumours exposed to bioreductive drugs. II. RSU 1069. Br J Cancer 71:537-42.

Olive, P.L., and R.E. Durand. 1992. Detection of hypoxic cells in a murine tumor with the use of the comet assay. J Natl Cancer Inst 84:707-11.

Olive, P.L., D.J. Chaplin, and R.E. Durand. 1985. Pharmacokinetics, binding and distribution of Hoechst 33342 in spheroids and murine tumours. Br J Cancer 52:739-46.

Olive, P.L., C. Vikse, and M.J. Trotter. 1992. Measurement of oxygen diffusion distance in tumor cubes using a fluorescent hypoxia probe. Int J Radiat Oncol Biol Phys 22:397-402.

Olive, P.L., C.M. Vikse, and R.E. Durand. 1994. Hypoxic fractions measured in murine tumors and normal tissues using the comet assay. Int J Radiat Oncol Biol Phys 29:487-91.

Olive, P.L., J.P. Banath, and C. Aquino-Parsons. 2001a. Measuring hypoxia in solid tumours--is there a gold standard? Acta Oncol 40:917-23.

Olive, P.L., P.J. Johnston, J.P. Banath, and R.E. Durand. 1998. The comet assay: a new method to examine heterogeneity associated with solid tumors. Nat Med 4:103-5.

Olive, P.L., R.E. Durand, J. Le Riche, I.A. Olivotto, and S.M. Jackson. 1993. Gel electrophoresis of individual cells to quantify hypoxic fraction in human breast cancers. Cancer Res 53:733-6.

Olive, P.L., R.E. Durand, J.A. Raleigh, C. Luo, and C. Aquino-Parsons. 2000. Comparison between the comet assay and pimonidazole binding for measuring tumour hypoxia. Br J Cancer 83:1525-31.

Olive, P.L., C. Aquino-Parsons, S.H. MacPhail, S.Y. Liao, J.A. Raleigh, M.I. Lerman, and E.J. Stanbridge. 2001b. Carbonic anhydrase 9 as an endogenous marker for hypoxic cells in cervical cancer. Cancer Res 61:8924-9.

Olive, P.L., R.E. Durand, S.M. Jackson, J.C. Le Riche, C. Luo, R. Ma, D.B. McLaren, C. Aquino-Parsons, T.A. Thomson, and T. Trotter. 1999. The comet assay in clinical practice. Acta Oncol 38:839-44.

Olsen, D.R., and E.K. Rofstad. 1999. Monitoring of tumor reoxygenation following irradiation by 31P magnetic resonance spectroscopy: an experimental study of human melanoma xenografts. Radiother Oncol 52:261-7.

Overgaard, J. 1994. Clinical evaluation of nitroimidazoles as modifiers of hypoxia in solid tumors. Oncol Res 6:509-18.

Overgaard, J., and M.R. Horsman. 1996. Modification of Hypoxia-Induced Radioresistance in Tumors by the Use of Oxygen and Sensitizers. Semin Radiat Oncol 6:10-21.

Overgaard, J., H.S. Hansen, M. Overgaard, L. Bastholt, A. Berthelsen, L. Specht, B. Lindelov, and K. Jorgensen. 1998. A randomized double-blind phase III study of nimorazole as a hypoxic radiosensitizer of primary radiotherapy in supraglottic larynx and pharynx carcinoma. Results of the Danish Head and Neck Cancer Study (DAHANCA) Protocol 5-85. Radiother Oncol 46:135-46.

Overgaard, J., H.S. Hansen, A.P. Andersen, M. Hjelm-Hansen, K. Jorgensen, E. Sandberg, A. Berthelsen, R. Hammer, and M. Pedersen. 1989. Misonidazole combined with split-course radiotherapy in the treatment of invasive carcinoma of larynx and pharynx: report from the DAHANCA 2 study. Int J Radiat Oncol Biol Phys 16:1065-8.

Page, R.L., and D.E. Thrall. 1994. Therapeutic hyperthermia: contribution from clinical studies in dogs with spontaneous neoplasia. In Vivo 8:851-8.

Park, H.J., J.C. Lyons, T. Ohtsubo, and C.W. Song. 2000. Cell cycle progression and apoptosis after irradiation in an acidic environment [In Process Citation]. Cell Death Differ 7:729-38.

Partridge, S.E., C. Aquino-Parsons, C. Luo, A. Green, and P.L. Olive. 2001. A pilot study comparing intratumoral oxygenation using the comet assay following 2.5% and 5% carbogen and 100% oxygen. Int J Radiat Oncol Biol Phys 49:575-80.

Pena, L.L., A.I. Nieto, D. Perez-Alenza, P. Cuesta, and M. Castano. 1998. Immunohistochemical detection of Ki-67 and PCNA in canine mammary tumors: relationship to clinical and pathologic variables. J Vet Diagn Invest 10:237-46.

Peters, C.E., D.J. Chaplin, and D.G. Hirst. 1997. Nicotinamide reduces tumour interstitial fluid pressure in a dose- and time-dependent manner. Br J Radiol 70:160-7.

Pigott, K.H., S.A. Hill, D.J. Chaplin, and M.I. Saunders. 1996. Microregional fluctuations in perfusion within human tumours detected using laser Doppler flowmetry. Radiother Oncol 40:45-50.

Powell, M.E., S.A. Hill, M.I. Saunders, P.J. Hoskin, and D.J. Chaplin. 1996. Effect of carbogen breathing on tumour microregional blood flow in humans. Radiother Oncol 41:225-31.

Prescott, D.M., H.C. Charles, J.M. Poulson, R.L. Page, D.E. Thrall, Z. Vujaskovic, and M.W. Dewhirst. 2000. The relationship between intracellular and extracellular pH in spontaneous canine tumors [In Process Citation]. Clin Cancer Res 6:2501-5.

Preziosi, R., G. Sarli, C. Benazzi, and P.S. Marcato. 1995a. Detection of proliferating cell nuclear antigen (PCNA) in canine and feline mammary tumours. J Comp Pathol 113:301-13.

Preziosi, R., L. Della Salda, A. Ricci, P. Simoni, and P.S. Marcato. 1995b. Quantification of nucleolar organiser regions in canine perianal gland tumours. Res Vet Sci 58:277-81.

Puglisi, F., A.M. Minisini, G. Aprile, F. Barbone, P. Cataldi, D. Artico, G. Damante, C.A. Beltrami, and C. Di Loreto. 2002. Balance between cell division and cell death as predictor of survival in patients with non-small-cell lung cancer. Oncology 63:76-83.

Rainov, N.G., S. Koch, M. Sena-Esteves, and M.E. Berens. 2000. Characterization of a canine glioma cell line as related to established experimental brain tumor models. J Neuropathol Exp Neurol 59:607-13.

Raleigh, J.A., M.W. Dewhirst, and D.E. Thrall. 1996. Measuring Tumor Hypoxia. Semin Radiat Oncol 6:37-45.

Raleigh, J.A., A.J. Franko, C.J. Koch, and J.L. Born. 1985. Binding of misonidazole to hypoxic cells in monolayer and spheroid culture: evidence that a side-chain label is bound as efficiently as a ring label. Br J Cancer 51:229-35.

Raleigh, J.A., J.K. La Dine, J.M. Cline, and D.E. Thrall. 1994. An enzyme-linked immunosorbent assay for hypoxia marker binding in tumours. Br J Cancer 69:66-71.

Raleigh, J.A., S.C. Chou, G.E. Arteel, and M.R. Horsman. 1999. Comparisons among pimonidazole binding, oxygen electrode measurements, and radiation response in C3H mouse tumors. Radiat Res 151:580-9.

Raleigh, J.A., A.J. Franko, D.A. Kelly, L.A. Trimble, and P.S. Allen. 1991. Development of an in vivo 19F magnetic resonance method for measuring oxygen deficiency in tumors. Magn Reson Med 22:451-66.

Raleigh, J.A., E.M. Zeman, D.P. Calkins, M.C. McEntee, and D.E. Thrall. 1995. Distribution of hypoxia and proliferation associated markers in spontaneous canine tumors. Acta Oncol 34:345-9.

Raleigh, J.A., S.C. Chou, E.L. Bono, D.E. Thrall, and M.A. Varia. 2001. Semiquantitative immunohistochemical analysis for hypoxia in human tumors. Int J Radiat Oncol Biol Phys 49:569-74.

Raleigh, J.A., G.G. Miller, A.J. Franko, C.J. Koch, A.F. Fuciarelli, and D.A. Kelly. 1987. Fluorescence immunohistochemical detection of hypoxic cells in spheroids and tumours. Br J Cancer 56:395-400.

Raleigh, J.A., E.M. Zeman, M. Rathman, J.K. LaDine, J.M. Cline, and D.E. Thrall. 1992. Development of an ELISA for the detection of 2-nitroimidazole hypoxia markers bound to tumor tissue. Int J Radiat Oncol Biol Phys 22:403-5.

Raleigh, J.A., S.C. Chou, L. Tables, S. Suchindran, M.A. Varia, and M.R. Horsman. 1998a. Relationship of hypoxia to metallothionein expression in murine tumors. Int J Radiat Oncol Biol Phys 42:727-30.

Raleigh, J.A., S.C. Chou, D.P. Calkins-Adams, C.A. Ballenger, D.B. Novotny, and M.A. Varia. 2000. A clinical study of hypoxia and metallothionein protein expression in squamous cell carcinomas. Clinical Cancer Research 6:855-862.

Raleigh, J.A., D.P. Calkins-Adams, L.H. Rinker, C.A. Ballenger, M.C. Weissler, W.C. Fowler, Jr., D.B. Novotny, and M.A. Varia. 1998b. Hypoxia and vascular endothelial growth factor expression in human squamous cell carcinomas using pimonidazole as a hypoxia marker. Cancer Res 58:3765-8.

Rasey, J.S., P.D. Hofstrand, L.K. Chin, and T.J. Tewson. 1999. Characterization of [18F]fluoroetanidazole, a new radiopharmaceutical for detecting tumor hypoxia. J Nucl Med 40:1072-9.

Rasey, J.S., Z. Grunbaum, K. Krohn, N. Nelson, and L. Chin. 1985a. Comparison of binding of [3H]misonidazole and [14C]misonidazole in multicell spheroids. Radiat Res 101:473-9.

Rasey, J.S., K.A. Krohn, Z. Grunbaum, P.J. Conroy, K. Bauer, and R.M. Sutherland. 1985b. Further characterization of 4-bromomisonidazole as a potential detector of hypoxic cells. Radiat Res 102:76-85.

Rasey, J.S., J.J. Casciari, P.D. Hofstrand, M. Muzi, M.M. Graham, and L.K. Chin. 2000. Determining hypoxic fraction in a rat glioma by uptake of radiolabeled fluoromisonidazole. Radiat Res 153:84-92.

Rasey, J.S., W.J. Koh, M.L. Evans, L.M. Peterson, T.K. Lewellen, M.M. Graham, and K.A. Krohn. 1996. Quantifying regional hypoxia in human tumors with positron emission tomography of [18F]fluoromisonidazole: a pretherapy study of 37 patients. Int J Radiat Oncol Biol Phys 36:417-28.

Rauth, A.M., T. Melo, and V. Misra. 1998. Bioreductive therapies: an overview of drugs and their mechanisms of action. Int J Radiat Oncol Biol Phys 42:755-62.

Reinhardt-Poulin, P., J.R. McLean, Y. Deslauriers, W. Gorman, S. Cabat, and M. Rouabhia. 2000. The use of silver-stained "comets" to visualize DNA damage and repair in normal and Xeroderma pigmentosum fibroblasts after exposure to simulated solar radiation. Photochem Photobiol 71:422-5.

Richard, D.E., E. Berra, and J. Pouyssegur. 1999. Angiogenesis: how a tumor adapts to hypoxia. Biochem Biophys Res Commun 266:718-22.

Rijken, P.F., H.J. Bernsen, and A.J. van der Kogel. 1995. Application of an image analysis system to the quantitation of tumor perfusion and vascularity in human glioma xenografts. Microvasc Res 50:141-53.

Rijken, P.F., J.P. Peters, and A.J. Van der Kogel. 2002. Quantitative analysis of varying profiles of hypoxia in relation to functional vessels in different human glioma xenograft lines. Radiat Res 157:626-32.

Rijken, P.F., H.J. Bernsen, J.P. Peters, R.J. Hodgkiss, J.A. Raleigh, and A.J. van der Kogel. 2000. Spatial relationship between hypoxia and the (perfused) vascular network in a human glioma xenograft: a quantitative multi-parameter analysis. Int J Radiat Oncol Biol Phys 48:571-82.

Robinson, M.F., N.P. Dupuis, T. Kusumoto, F. Liu, K. Menon, and B.A. Teicher. 1995. Increased tumor oxygenation and radiation sensitivity in two rat tumors by a hemoglobin-based, oxygen-carrying preparation. Artif Cells Blood Substit Immobil Biotechnol 23:431-8.

Robinson, S.P., F.A. Howe, L.M. Rodrigues, M. Stubbs, and J.R. Griffiths. 1998. Magnetic resonance imaging techniques for monitoring changes in tumor oxygenation and blood flow. Semin Radiat Oncol 8:197-207.

Robinson, S.P., D.R. Collingridge, F.A. Howe, L.M. Rodrigues, D.J. Chaplin, and J.R. Griffiths. 1999. Tumour response to hypercapnia and hyperoxia monitored by FLOOD magnetic resonance imaging. NMR Biomed 12:98-106.

Rofstad, E.K. 2000. Microenvironment-induced cancer metastasis. Int J Radiat Biol 76:589-605.

Rofstad, E.K., and T. Danielsen. 1999. Hypoxia-induced metastasis of human melanoma cells: involvement of vascular endothelial growth factor-mediated angiogenesis. Br J Cancer 80:1697-707.

Rofstad, E.K., and E.F. Halsor. 2002. Hypoxia-associated spontaneous pulmonary metastasis in human melanoma xenografts: involvement of microvascular hot spots induced in hypoxic foci by interleukin 8. Br J Cancer 86:301-8.

Rofstad, E.K., K. Sundfor, H. Lyng, and C.G. Trope. 2000. Hypoxia-induced treatment failure in advanced squamous cell carcinoma of the uterine cervix is primarily due to hypoxia-induced radiation resistance rather than hypoxia-induced metastasis. Br J Cancer 83:354-9.

Rofstad, E.K., P. DeMuth, B.M. Fenton, T.L. Ceckler, and R.M. Sutherland. 1989. 31P NMR spectroscopy and HbO2 cryospectrophotometry in prediction of tumor radioresistance caused by hypoxia. Int J Radiat Oncol Biol Phys 16:919-23.

Rofstad, E.K., H. Rasmussen, K. Galappathi, B. Mathiesen, K. Nilsen, and B.A. Graff. 2002. Hypoxia promotes lymph node metastasis in human melanoma xenografts by up-regulating the urokinase-type plasminogen activator receptor. Cancer Res 62:1847-53.

Rojas, A. 1991. Radiosensitization with normobaric oxygen and carbogen. Radiother Oncol 20:65-70.

Rojas, A., U. Carl, and K. Reghebi. 1990. Effect of normobaric oxygen on tumor radiosensitivity: fractionated studies. Int J Radiat Oncol Biol Phys 18:547-53.

Rojas, A., V.K. Hirst, A.S. Calvert, and H. Johns. 1996. Carbogen and nicotinamide as radiosensitizers in a murine mammary carcinoma using conventional and accelerated radiotherapy. Int J Radiat Oncol Biol Phys 34:357-65.

Romanet, T., J.L. Re, M. De Meo, F. Serre-Debeauvlais, J.P. Lavieille, E. Reyt, and C. Riva. 1999. Detection of hypoxia by measurement of DNA damage and repair in human lymphocytes (comet assay): a predictive variable for tumor response during chemotherapy in patients with head and neck squamous cell carcinoma. In Vivo 13:343-8.

Rosen, L.S. 2002. Clinical experience with angiogenesis signaling inhibitors: focus on vascular endothelial growth factor (VEGF) blockers. Cancer Control 9:36-44.

Rowinsky, E.K. 1999. Novel radiation sensitizers targeting tissue hypoxia. Oncology (Huntingt) 13:61-70.

Royds, J.A., S.K. Dower, E.E. Qwarnstrom, and C.E. Lewis. 1998. Response of tumour cells to hypoxia: role of p53 and NFkB. Mol Pathol 51:55-61.

Rutz, H.P. 1999. A biophysical basis of enhanced interstitial fluid pressure in tumors. Med Hypotheses 53:526-9.

Sakai, H., A. Noda, N. Shirai, T. Iidaka, T. Yanai, and T. Masegi. 2002. Proliferative activity of canine mast cell tumours evaluated by bromodeoxyuridine incorporation and ki-67 expression. J Comp Pathol 127:233-8.

Sarac, S., A. Ayhan, A.S. Hosal, and S. Kaya. 1998. Prognostic significance of PCNA expression in laryngeal cancer. Arch Otolaryngol Head Neck Surg 124:1321-4.

Sarli, G., C. Benazzi, R. Preziosi, and P.S. Marcato. 1995. Assessment of proliferative activity by anti-PCNA monoclonal antibodies in formalin-fixed, paraffin-embedded samples and correlation with mitotic index. Vet Pathol 32:93-6.

Sarli, G., C. Benazzi, R. Preziosi, L. Della Salda, G. Bettini, and P.S. Marcato. 1999. Evaluating mitotic activity in canine and feline solid tumors: standardizing the parameter. Biotech Histochem 74:64-76.

Sasaki, K., A. Kurose, Y. Ishida, and M. Matsuta. 1994. Estimation of S-phase fraction in tumor tissue sections by immunohistochemical staining of PCNA. J Histochem Cytochem 42:957-60.

Saunders, M., S. Dische, A. Barrett, A. Harvey, G. Griffiths, and M. Palmar. 1999. Continuous, hyperfractionated, accelerated radiotherapy (CHART) versus conventional radiotherapy in non-small cell lung cancer: mature data from the randomised multicentre trial. CHART Steering committee. Radiother Oncol 52:137-48.

Schindl, M., S.F. Schoppmann, H. Samonigg, H. Hausmaninger, W. Kwasny, M. Gnant, R. Jakesz, E. Kubista, P. Birner, and G. Oberhuber. 2002. Overexpression of Hypoxia-inducible Factor 1alpha Is Associated with an Unfavorable Prognosis in Lymph Node-positive Breast Cancer. Clin Cancer Res 8:1831-7.

Schipper, D.L., M.J. Wagenmans, W.H. Peters, and D.J. Wagener. 1998. Significance of cell proliferation measurement in gastric cancer. Eur J Cancer 34:781-90.

Schliephake, H. 2003. Prognostic relevance of molecular markers of oral cancer-A review. Int J Oral Maxillofac Surg 32:233-45.

Schmid-Schonbein, G.W. 1990. Microlymphatics and lymph flow. Physiol Rev 70:987-1028.

Schouten van Meeteren, A.Y., P. van der Valk, H.C. van der Linden, W.J. van Ouwerkerk, A.J. Broekhuizen, D.R. Huismans, A.H. Loonen, and A.J. Veerman. 2002. Features of proliferation and in vitro drug resistance in central primitive neuro-ectodermal tumours. Neuropathol Appl Neurobiol 28:200-9.

Schwyn, U., N.E. Crompton, H. Blattmann, B. Hauser, B. Klink, A. Parvis, D. Ruslander, and B. Kaser-Hotz. 1998. Potential tumour doubling time: determination of Tpot for various canine and feline tumours. Vet Res Commun 22:233-47.

Secomb, T.W., R. Hsu, M.W. Dewhirst, B. Klitzman, and J.F. Gross. 1993. Analysis of oxygen transport to tumor tissue by microvascular networks. Int J Radiat Oncol Biol Phys 25:481-9.

Secomb, T.W., R. Hsu, E.T. Ong, J.F. Gross, and M.W. Dewhirst. 1995. Analysis of the effects of oxygen supply and demand on hypoxic fraction in tumors. Acta Oncol 34:313-6.

Secomb, T.W., R. Hsu, R.D. Braun, J.R. Ross, J.F. Gross, and M.W. Dewhirst. 1998. Theoretical simulation of oxygen transport to tumors by three- dimensional networks of microvessels. Adv Exp Med Biol 454:629-34.

Semenza, G.L. 1998. Hypoxia-inducible factor 1: master regulator of O2 homeostasis. Curr Opin Genet Dev 8:588-94.

Semenza, G.L. 1999. Regulation of mammalian O2 homeostasis by hypoxia-inducible factor 1. Annu Rev Cell Dev Biol 15:551-78.

Semenza, G.L. 2000a. Expression of hypoxia-inducible factor 1: mechanisms and consequences. Biochem Pharmacol 59:47-53.

Semenza, G.L. 2000b. HIF-1: mediator of physiological and pathophysiological responses to hypoxia. J Appl Physiol 88:1474-80.

Semenza, G.L. 2002. HIF-1 and tumor progression: pathophysiology and therapeutics. Trends Mol Med 8:S62-7.

Semenza, G.L., P.H. Roth, H.M. Fang, and G.L. Wang. 1994. Transcriptional regulation of genes encoding glycolytic enzymes by hypoxia-inducible factor 1. J Biol Chem 269:23757-63.

Shackelford, R.E., W.K. Kaufmann, and R.S. Paules. 1999. Cell cycle control, checkpoint mechanisms, and genotoxic stress. Environ Health Perspect 107 Suppl 1:5-24.

Shackney, S.E., and T.V. Shankey. 1999. Cell cycle models for molecular biology and molecular oncology: exploring new dimensions. Cytometry 35:97-116.

Shakil, A., J.L. Osborn, and C.W. Song. 1999. Changes in oxygenation status and blood flow in a rat tumor model by mild temperature hyperthermia. Int J Radiat Oncol Biol Phys 43:859-65.

Sheldon, P.W., J.L. Foster, and J.F. Fowler. 1974. Radiosensitization of C3H mouse mammary tumours by a 2-nitroimidazole drug. Br J Cancer 30:560-5.

Sherr, C.J. 2001. The INK4a/ARF network in tumour suppression. Nat Rev Mol Cell Biol 2:731-7.

Shibata, T., A.J. Giaccia, and J.M. Brown. 2002. Hypoxia-inducible regulation of a prodrug-activating enzyme for tumor-specific gene therapy. Neoplasia 4:40-8.

Shivji, K.K., M.K. Kenny, and R.D. Wood. 1992. Proliferating cell nuclear antigen is required for DNA excision repair. Cell 69:367-74.

Shubik, P. 1982. Vascularization of tumors: a review. J Cancer Res Clin Oncol 103:211-26.

Shulman, L.N., L. Buswell, N. Riese, N. Doherty, J.S. Loeffler, R.W. von Roemeling, and C.N. Coleman. 1999. Phase I trial of the hypoxic cell cytotoxin tirapazamine with concurrent radiation therapy in the treatment of refractory solid tumors. Int J Radiat Oncol Biol Phys 44:349-53.

Siemann, D.W. 1998. The tumor microenvironment: a double-edged sword [editorial]. Int J Radiat Oncol Biol Phys 42:697-9.

Siemann, D.W., I.M. Johansen, and M.R. Horsman. 1998. Radiobiological hypoxia in the KHT sarcoma: predictions using the Eppendorf histograph. Int J Radiat Oncol Biol Phys 40:1171-6.

Silverman, D.H., C.K. Hoh, M.A. Seltzer, C. Schiepers, G.S. Cuan, S.S. Gambhir, L. Zheng, J. Czernin, and M.E. Phelps. 1998. Evaluating tumor biology and oncological disease with positron-emission tomography. Semin Radiat Oncol 8:183-96.

Simoes, J.P., P. Schoning, and M. Butine. 1994. Prognosis of canine mast cell tumors: a comparison of three methods. Vet Pathol 31:637-47.

Sivridis, E., A. Giatromanolaki, K.C. Gatter, A.L. Harris, and M.I. Koukourakis. 2002. Association of hypoxia-inducible factors 1alpha and 2alpha with activated angiogenic pathways and prognosis in patients with endometrial carcinoma. Cancer 95:1055-63.

Smith, I.F., J.P. Boyle, P.F. Vaughan, H.A. Pearson, and C. Peers. 2001. Effects of chronic hypoxia on Ca(2+) stores and capacitative Ca(2+) entry in human neuroblastoma (SH-SY5Y) cells. J Neurochem 79:877-84.

Smith, K.J., T.L. Barrett, W.F. Smith, and H.M. Skelton. 1998. A review of tumor suppressor genes in cutaneous neoplasms with emphasis on cell cycle regulators. Am J Dermatopathol 20:302-13.

Snyder, S.A., J.L. Lanzen, R.D. Braun, G. Rosner, T.W. Secomb, J. Biaglow, D.M. Brizel, and M.W. Dewhirst. 2001. Simultaneous administration of glucose and hyperoxic gas achieves greater improvement in tumor oxygenation than hyperoxic gas alone. Int J Radiat Oncol Biol Phys 51:494-506.

Stadler, P., A. Becker, H.J. Feldmann, G. Hansgen, J. Dunst, F. Wurschmidt, and M. Molls. 1999. Influence of the hypoxic subvolume on the survival of patients with head and neck cancer. Int J Radiat Oncol Biol Phys 44:749-54.

Stern, S., and M. Guichard. 1996. Efficacy of agents counteracting hypoxia in fractionated radiation regimes. Radiother Oncol 41:143-9.

Stern, S., R.J. Hodgkiss, and M. Guichard. 1996. Comparison of two techniques for detecting tumour hypoxia: a fluorescent immunochemical method and an in vitro colony assay. Radiother Oncol 39:129-35.

Stubbs, M. 1999. Application of magnetic resonance techniques for imaging tumour physiology. Acta Oncol 38:845-53.

Stubbs, M., P.M. McSheehy, J.R. Griffiths, and C.L. Bashford. 2000. Causes and consequences of tumour acidity and implications for treatment. Mol Med Today 6:15-9.

Stuben, G., M. Stuschke, K. Knuhmann, M.R. Horsman, and H. Sack. 1998. The effect of combined nicotinamide and carbogen treatments in human tumour xenografts: oxygenation and tumour control studies. Radiother Oncol 48:143-8.

Sundfor, K., H. Lyng, and E.K. Rofstad. 1998. Tumour hypoxia and vascular density as predictors of metastasis in squamous cell carcinoma of the uterine cervix. Br J Cancer 78:822-7.

Sutherland, R.M. 1998. Tumor hypoxia and gene expression--implications for malignant progression and therapy. Acta Oncol 37:567-74.

Suzuki, Y., M. Hasegawa, K. Hayakawa, N. Mitsuhashi, and H. Niibe. 1999. In vivo study of radiosensitizing effect of hypoxic cell radiosensitizer PR-350 on a human small cell lung cancer. Anticancer Res 19:3993-4000.

Tatsumi, M., K. Yutani, H. Kusuoka, and T. Nishimura. 1999. Technetium-99m HL91 uptake as a tumour hypoxia marker: relationship to tumour blood flow. Eur J Nucl Med 26:91-4.

Teicher, B.A. 1992. Use of perfluorochemical emulsions in cancer therapy. Biomater Artif Cells Immobilization Biotechnol 20:875-82.

Teicher, B.A. 2001. Malignant cells, directors of the malignant process: role of transforming growth factor-beta. Cancer Metastasis Rev 20:133-43.

Teicher, B.A., S.A. Holden, G. Ara, N.P. Dupuis, and D. Goff. 1995a. Restoration of Tumor Oxygenation After Cytotoxic Therapy by a Perflubron Emulsion/Carbogen Breathing. Cancer J Sci Am 1:43.

Teicher, B.A., N.P. Dupuis, Y. Emi, M. Ikebe, Y. Kakeji, and K. Menon. 1995b. Increased efficacy of chemo- and radio-therapy by a hemoglobin solution in the 9L gliosarcoma. In Vivo 9:11-8.

Teicher, B.A., G. Ara, R. Herbst, H. Takeuchi, S. Keyes, and D. Northey. 1997. PEG-hemoglobin: effects on tumor oxygenation and response to chemotherapy. In Vivo 11:301-11.

Terpstra, M., W.B. High, Y. Luo, R.A. de Graaf, H. Merkle, and M. Garwood. 1996. Relationships among lactate concentration, blood flow and histopathologic profiles in rat C6 glioma. NMR Biomed 9:185-94.

Terris, D.J., E.Y. Ho, H.Z. Ibrahim, M.J. Dorie, M.S. Kovacs, Q.T. Le, A.C. Koong, H.A. Pinto, and J.M. Brown. 2002. Estimating DNA repair by sequential evaluation of head and neck tumor radiation sensitivity using the comet assay. Arch Otolaryngol Head Neck Surg 128:698-702.

Thatcher, N., E.S. De Campos, D.R. Bell, W.P. Steward, G. Varghese, R. Morant, J.F. Vansteenkiste, R. Rosso, S.B. Ewers, E. Sundal, E. Schatzmann, and H. Stocker. 1999. Epoetin alpha prevents anaemia and reduces transfusion requirements in patients undergoing primarily platinum-based chemotherapy for small cell lung cancer. Br J Cancer 80:396-402.

Thews, O., D.K. Kelleher, and P.W. Vaupel. 1995. Modulation of spatial O2 tension distribution in experimental tumors by increasing arterial O2 supply. Acta Oncol 34:291-5.

Thews, O., D.K. Kelleher, and P. Vaupel. 1996. In vivo oxygen consumption rate of DS sarcoma cells on inhibition of DNA synthesis. Cancer Res 56:2009-12.

Thomas, C.D., S. Stern, D.J. Chaplin, and M. Guichard. 1996. Transient perfusion and radiosensitizing effect after nicotinamide, carbogen, and perflubron emulsion administration. Radiother Oncol 39:235-41.

Thomlinson, R.H., and L.H. Gray. 1955. The histological structure of some human lung cancers and the possible implications for radiotherapy. Br J Cancer 9:539-49.

Thrall, D.E., M.C. McEntee, J.M. Cline, and J.A. Raleigh. 1994. ELISA quantification of CCI-103F binding in canine tumors prior to and during irradiation. Int J Radiat Oncol Biol Phys 28:649-59.

Trotter, M.J., D.J. Chaplin, and P.L. Olive. 1989a. Use of a carbocyanine dye as a marker of functional vasculature in murine tumours. Br J Cancer 59:706-9.

Trotter, M.J., D.J. Chaplin, R.E. Durand, and P.L. Olive. 1989b. The use of fluorescent probes to identify regions of transient perfusion in murine tumors. Int J Radiat Oncol Biol Phys 16:931-4.

Trump, B.F., I.K. Berezesky, S.H. Chang, and P.C. Phelps. 1997. The pathways of cell death: oncosis, apoptosis, and necrosis. Toxicol Pathol 25:82-8.

Tsang, R.W., A.W. Fyles, M. Milosevic, A. Syed, M. Pintilie, W. Levin, and L.A. Manchul. 2000. Interrelationship of proliferation and hypoxia in carcinoma of the cervix. 46 46:95-9.

Uma Devi, P. 1998. Normal tissue protection in cancer therapy--progress and prospects. Acta Oncol 37:247-52.

Urtasun, R.C., C.N. Coleman, T.H. Wasserman, and T.L. Phillips. 1984. Clinical trials with hypoxic cell sensitizers: time to retrench or time to push forward? Int J Radiat Oncol Biol Phys 10:1691-6.

Urtasun, R.C., C.J. Koch, A.J. Franko, J.A. Raleigh, and J.D. Chapman. 1986. A novel technique for measuring human tissue pO2 at the cellular level. Br J Cancer 54:453-7.

Urtasun, R.C., M.B. Parliament, A.J. McEwan, J.R. Mercer, R.H. Mannan, L.I. Wiebe, C. Morin, and J.D. Chapman. 1996. Measurement of hypoxia in human tumours by non-invasive spect imaging of iodoazomycin arabinoside. Br J Cancer Suppl 27:S209-12.

Vail, D.M., and E.G. MacEwen. 2000. Spontaneously occurring tumors of companion animals as models for human cancer [In Process Citation]. Cancer Invest 18:781-92.

van der Maazen, R.W., H.O. Thijssen, J.H. Kaanders, A. de Koster, A. Keyser, M.J. Prick, J.A. Grotenhuis, P. Wesseling, and A.J. van der Kogel. 1995. Conventional radiotherapy combined with carbogen breathing and nicotinamide for malignant gliomas. Radiother Oncol 35:118-22.

Varghese, A.J., S. Gulyas, and J.K. Mohindra. 1976. Hypoxia-dependent reduction of 1-(2-nitro-1-imidazolyl)-3-methoxy-2- propanol by Chinese hamster ovary cells and KHT tumor cells in vitro and in vivo. Cancer Res 36:3761-5.

Varia, M.A., D.P. Calkins-Adams, L.H. Rinker, A.S. Kennedy, D.B. Novotny, W.C. Fowler, Jr., and J.A. Raleigh. 1998. Pimonidazole: a novel hypoxia marker for complementary study of tumor hypoxia and cell proliferation in cervical carcinoma. Gynecol Oncol 71:270-7.

Vaupel, P., and G. Thews. 1976. Pathophysiological aspects of glucose uptake by the tumor tissue under various conditions of oxygen and glucose supply. Adv Exp Med Biol 75:547-53.

Vaupel, P., and W. Mueller-Klieser. 1986. Verapamil inhibits the respiration rate of cancer cells. Adv Exp Med Biol 200:645-8.

Vaupel, P., F. Kallinowski, and P. Okunieff. 1989. Blood flow, oxygen and nutrient supply, and metabolic microenvironment of human tumors: a review. Cancer Res 49:6449-65.

Vaupel, P., D.K. Kelleher, and O. Thews. 1998a. Modulation of tumor oxygenation. Int J Radiat Oncol Biol Phys 42:843-8.

Vaupel, P., D.K. Kelleher, and M. Hockel. 2001. Oxygen status of malignant tumors: pathogenesis of hypoxia and significance for tumor therapy. Semin Oncol 28:29-35.

Vaupel, P., O. Thews, D.K. Kelleher, and M. Hoeckel. 1998b. Oxygenation of human tumors: the Mainz experience. Strahlenther Onkol 174 Suppl 4:6-12.

Veldhoen, N., and J. Milner. 1998. Isolation of canine p53 cDNA and detailed characterization of the full length canine p53 protein. Oncogene 16:1077-84.

Veronesi, G., C. Landoni, G. Pelosi, M. Picchio, A. Sonzogni, M.E. Leon, P.G. Solli, F. Leo, L. Spaggiari, M. Bellomi, F. Fazio, and U. Pastorino. 2002. Fluoro-deoxi-glucose uptake and angiogenesis are independent biological features in lung metastases. Br J Cancer 86:1391-5.

Vinogradov, S.A., L.W. Lo, W.T. Jenkins, S.M. Evans, C. Koch, and D.F. Wilson. 1996. Noninvasive imaging of the distribution in oxygen in tissue in vivo using near-infrared phosphors. Biophys J 70:1609-17.

von Pawel, J., R. von Roemeling, U. Gatzemeier, M. Boyer, L.O. Elisson, P. Clark, D. Talbot, A. Rey, T.W. Butler, V. Hirsh, I. Olver, B. Bergman, J. Ayoub, G. Richardson, D. Dunlop, A. Arcenas, R. Vescio, J. Viallet, and J. Treat. 2000. Tirapazamine plus cisplatin versus cisplatin in advanced non-small-cell lung cancer: A report of the international CATAPULT I study group. Cisplatin and Tirapazamine in Subjects with Advanced Previously Untreated Non-Small-Cell Lung Tumors. J Clin Oncol 18:1351-9.

Vordermark, D., and J.M. Brown. 2003. Endogenous Markers of Tumor HypoxiaPredictors of Clinical Radiation Resistance? Strahlenther Onkol 179:801-11.

Vreugdenhil, G., L.A. Frenken, and R.A. Koene. 1993. Erythropoietin: mechanisms of action and indications for treatment. Neth J Med 42:187-202.

Vujaskovic, Z., E.L. Rosen, K.L. Blackwell, E.L. Jones, D.M. Brizel, L.R. Prosnitz, T.V. Samulski, and M.W. Dewhirst. 2003. Ultrasound guided pO2 measurement of breast cancer reoxygenation after neoadjuvant chemotherapy and hyperthermia treatment. Int J Hyperthermia 19:498-506.

Walenta, S., M. Wetterling, M. Lehrke, G. Schwickert, K. Sundfor, E.K. Rofstad, and W. Mueller-Klieser. 2000. High lactate levels predict likelihood of metastases, tumor recurrence, and restricted patient survival in human cervical cancers [In Process Citation]. Cancer Res 60:916-21.

Walenta, S., S. Snyder, Z.A. Haroon, R.D. Braun, K. Amin, D. Brizel, W. Mueller-Klieser, B. Chance, and M.W. Dewhirst. 2001. Tissue gradients of energy metabolites mirror oxygen tension gradients in a rat mammary carcinoma model. Int J Radiat Oncol Biol Phys 51:840-8.

Wang, G.L., and G.L. Semenza. 1996. Oxgen sensing and response to hypoxia by mammalian cells. Redox Report 2:89-96.

Wang, G.L., B.H. Jiang, E.A. Rue, and G.L. Semenza. 1995. Hypoxia-inducible factor 1 is a basic-helix-loop-helix-PAS heterodimer regulated by cellular O2 tension. Proc Natl Acad Sci U S A 92:5510-4.

Warbrick, E., P.J. Coates, and P.A. Hall. 1998. Fen1 expression: a novel marker for cell proliferation. J Pathol 186:319-24.

Warburg, O. 1930. The Metabolism of Tumors. London, Constable & Co.

Ward, T.H., and B. Marples. 2000. Technical report: SYBR Green I and the improved sensitivity of the single-cell electrophoresis assay. Int J Radiat Biol 76:61-5.

Warenius, H.M., R. White, J.H. Peacock, J. Hanson, R.A. Britten, and D. Murray. 2000. The influence of hypoxia on the relative sensitivity of human tumor cells to 62.5 MeV (p-->Be) fast neutrons and 4 MeV photons. Radiat Res 154:54-63.

Wasserman, T. 1999. Radioprotective effects of amifostine. Semin Oncol 26:89-94.

Watson, E.R., K.E. Halnan, S. Dische, M.I. Saunders, I.S. Cade, J.B. McEwen, G. Wiernik, D.J. Perrins, and I. Sutherland. 1978. Hyperbaric oxygen and radiotherapy: a Medical Research Council trial in carcinoma of the cervix. Br J Radiol 51:879-87.

Webb, S.D., J.A. Sherratt, and R.G. Fish. 1999. Alterations in proteolytic activity at low pH and its association with invasion: a theoretical model. Clin Exp Metastasis 17:397-407.

Webster, L., R.J. Hodgkiss, and G.D. Wilson. 1995. Simultaneous triple staining for hypoxia, proliferation, and DNA content in murine tumours. Cytometry 21:344-51.

Webster, L., R.J. Hodgkiss, and G.D. Wilson. 1998. Cell cycle distribution of hypoxia and progression of hypoxic tumour cells in vivo. Br J Cancer 77:227-34.

West, C.M. 1995. Invited review: intrinsic radiosensitivity as a predictor of patient response to radiotherapy. Br J Radiol 68:827-37.

West, C.M., R.A. Cooper, J.A. Loncaster, D.P. Wilks, and M. Bromley. 2001. Tumor vascularity: a histological measure of angiogenesis and hypoxia. Cancer Res 61:2907-10.

Wijsman, J.H., J.H. Van Dierendonck, R. Keijzer, C.J. van de Velde, and C.J. Cornelisse. 1992. Immunoreactivity of proliferating cell nuclear antigen compared with bromodeoxyuridine incorporation in normal and neoplastic rat tissue [see comments]. J Pathol 168:75-83.

Wilson, D.F., S.M. Evans, W.T. Jenkins, S.A. Vinogradov, E. Ong, and M.W. Dewhirst. 1998. Oxygen distributions within R3230Ac tumors growing in dorsal flap window chambers in rats. Adv Exp Med Biol 454:603-9.

Wilson, D.F., S.A. Vinogradov, B.W. Dugan, D. Biruski, L. Waldron, and S.A. Evans. 2002. Measurement of tumor oxygenation using new frequency domain phosphorometers. Comp Biochem Physiol A Mol Integr Physiol 132:153-9.

Wilson, G.D. 1991. Assessment of human tumour proliferation using bromodeoxyuridine--current status. Acta Oncol 30:903-10.

Wilson, G.D. 2001. A new look at proliferation. Acta Oncol 40:989-94.

Wilson, G.D., S. Dische, and M.I. Saunders. 1995. Studies with bromodeoxyuridine in head and neck cancer and accelerated radiotherapy. Radiother Oncol 36:189-97.

Wolchok, J.D., V.M. Klimek, L. Williams, and P.B. Chapman. 1999. Prophylactic recombinant epoetin alfa markedly reduces the need for blood transfusion in patients with metastatic melanoma treated with biochemotherapy. Cytokines Cell Mol Ther 5:205-6.

Wood, P.J., I.J. Stratford, J.M. Sansom, B.M. Cattanach, R.M. Quinney, and G.E. Adams. 1992. The response of spontaneous and transplantable murine tumors to vasoactive agents measured by 31P magnetic resonance spectroscopy. Int J Radiat Oncol Biol Phys 22:473-6.

Wouters, B.G., and J.M. Brown. 1997. Cells at intermediate oxygen levels can be more important than the "hypoxic fraction" in determining tumor response to fractionated radiotherapy. Radiat Res 147:541-50.

Wouters, B.G., A.M. Sy, and L.D. Skarsgard. 1996. Hypoxic cell sensitization: low-dose intrinsic radiosensitivity is predictive for etanidazole efficacy in a panel of human tumour cell lines. Int J Radiat Biol 70:719-33.

Wouters, B.G., L.H. Wang, and J.M. Brown. 1999. Tirapazamine: a new drug producing tumor specific enhancement of platinum-based chemotherapy in non-small-cell lung cancer. Ann Oncol 10:S29-33.

Wun, T., L. Law, D. Harvey, B. Sieracki, S.A. Scudder, and J.K. Ryu. 2003. Increased incidence of symptomatic venous thrombosis in patients with cervical carcinoma treated with concurrent chemotherapy, radiation, and erythropoietin. Cancer 98:1514-20.

Wykoff, C.C., N.J.P. Beasley, P.H. Watson, K.J. Turner, J. Pastorek, A. Sibtain, G.D. Wilson, H. Turley, K.L. Talks, P.H. Maxwell, C.W. Pugh, P.J. Ratcliffe, and A.L. Harris. 2000. Hypoxia-inducible expression of tumor-associated carbonic anhydrases. Cancer Research 60:7075-7083.

Xia, G., Y. Kageyama, T. Hayashi, N. Hyochi, S. Kawakami, and K. Kihara. 2002. Positive expression of HIF-2alpha/EPAS1 in invasive bladder cancer. Urology 59:774-8.

Yang, D.J., S. Ilgan, T. Higuchi, F. Zareneyrizi, C.S. Oh, C.W. Liu, E.E. Kim, and D.A. Podoloff. 1999. Noninvasive assessment of tumor hypoxia with 99mTc labeled metronidazole. Pharm Res 16:743-50.

Yutani, K., H. Kusuoka, K. Fukuchi, M. Tatsumi, and T. Nishimura. 1999. Applicability of 99mTc-HL91, a putative hypoxic tracer, to detection of tumor hypoxia. J Nucl Med 40:854-61.

Zeman, E.M., J.M. Brown, M.J. Lemmon, V.K. Hirst, and W.W. Lee. 1986. SR-4233: a new bioreductive agent with high selective toxicity for hypoxic mammalian cells. Int J Radiat Oncol Biol Phys 12:1239-42.

Zeman, E.M., D.P. Calkins, J.M. Cline, D.E. Thrall, and J.A. Raleigh. 1993. The relationship between proliferative and oxygenation status in spontaneous canine tumors. Int J Radiat Oncol Biol Phys 27:891-8.

Zhang, X., T. Melo, J.R. Ballinger, and A.M. Rauth. 1998. Studies of 99mTc-BnAO (HL-91): a non-nitroaromatic compound for hypoxic cell detection. Int J Radiat Oncol Biol Phys 42:737-40.

Zhong, H., A.M. De Marzo, E. Laughner, M. Lim, D.A. Hilton, D. Zagzag, P. Buechler, W.B. Isaacs, G.L. Semenza, and J.W. Simons. 1999. Overexpression of hypoxia-inducible factor 1alpha in common human cancers and their metastases. Cancer Res 59:5830-5.

CHAPTER I: Establishing Study Technique

Purpose

I will describe 1) the pharmacokinetics of pimonidazole (PIMO) in dogs, 2) immunohistochemistry (IHC) techniques for detection of PIMO adducts in tissue, 3) IHC techniques for detection of proliferating cell nuclear antigen (PCNA) to estimate the proportion of proliferating cells in canine tumors, 4) analysis of the hypoxic fraction, and 5) analysis of the proliferating fraction.

Introduction

PIMO is a 2-nitroimidazole hypoxia marker, and is a clinically relevant exogenous marker (figure 1.1). Although PIMO was originally used as a radiosensitizer, it was shown to have no therapeutic benefit, but the affinity to hypoxic cells was high enough for PIMO to be developed as a hypoxia marker. This marker can be used to identify and quantify tumor hypoxia, especially diffusion-limited chronic hypoxia. Use of PIMO as a hypoxia maker requires only a single low dose PIMO injection, and this approach is well suited in an outpatient setting for infusion of PIMO in humans.

PCNA is recognized as an endogenous proliferation marker. The expression of PCNA is highest in cells in S-phase. Evaluation of cells heavily stained for PCNA is a useful indicator of tumor cell proliferation.

In this study, we are using IHC to identify these two markers in tumor sections.

The objectives in this chapter are:

1. Characterize the pharmacokinetics of PIMO in dogs,
2. Establish the IHC technique to evaluate hypoxia labeled area fraction by using PIMO as a hypoxia marker, and
3. Establish the IHC technique to evaluate growth fraction by using PCNA as a proliferation marker.

Materials and Methods

Hypoxia Marker

The hypoxia marker, pimonidazole, PIMO, [1-{(2-hydroxy-3-piperidinyl)propyl}-2-nitroimidazole hydrochloride] is a 2-nitroimidazole and its chemical name is pimonidazole hydrochloride. The molecular weight is 290.7. The water solubility is 116 mg/mL, which is equivalent to 400 millimolar. Ultraviolet absorbance maximum is at 324 nm with an extinction coefficient of 7810 in 0.9% saline. The corresponding free base, PIMO, has a pKa of 8.7 and an octanol water partition coefficient of 8.5. At a concentration of 34 millimolar in 0.9% saline, PIMO solutions have a pH of 3.9 +/- 0.1. The plasma half-life of PIMO hydrochloride is 5.6 +/- 0.6 hours in humans and 0.5 hours in C3H/He mice. PIMO is distributed to all tissues in the body but binds only to thiol-containing proteins in cells that have an oxygen concentration less than 10 mmHg at 37°C (http://www.radonc.unc.edu/pimo/).

Hypoxia Marker synthesis

PIMO was synthesized as previously published (Smithen and Hardy, 1982) and characterized by standard chromatographic, spectroscopic and elemental analyses, including analysis for heavy-metal contamination. The name of the commercial product is Hypoxyprobe-1 (Natural Pharmacia International Inc., Belmont, MA).

Solid-phase antigen production

The solid-phase antigen for the ELISA was prepared by reductive activation of PIMO in the presence of thiolated Ficoll produced by an adaptation of published procedures (Inman, 1975) using N-succinimidyl 3-(2-pyridyldithiol) propionate (Pierce Chemical Company, Rockford, IL) as the source of latent thiol groups.

Antibody production

Rabbit polyclonal antibodies to protein-bound PIMO were prepared and characterized as previously published (Cline et al., 1990; Raleigh et al., 1987). IgG monoclonal antibodies (mAbs) were provided as untreated exhausted supernatant from the hybridoma clones (North Carolina State University Hybridoma Facility, Raleigh, NC).

Proliferation marker and antibody

Endogenous proliferating cell nuclear antigen (PCNA) was used as a proliferation marker. Commercially available anti-PCNA monoclonal antibody (PC 10, mouse anti-human, Dako Corp., Carpinteria, CA) was used for IHC analysis.

Canine studies

Dogs with spontaneously arising tumors were selected from oncology patients at the College of Veterinary Medicine, North Carolina State University (Raleigh, NC). All dogs were privately owned and undergoing radiation therapy with or without hyperthermia for their cancer treatment (Thrall et al., 2000). The procedures used for these animals were approved by the North Carolina State University Institutional Animal Care and Use Committee. Owner consent was obtained.

Animals with histologically confirmed malignant solid tumors and no other serious concurrent disease were eligible. The animal's health condition was evaluated according to standard institutional procedures. All tumors were diagnosed according to the classification system of the World Health Organization by the pathology service at College of Veterinary Medicine, North Carolina State University. Tumor volume was calculated using the equation, volume=(a x b x c)$\pi/6$. Soft tissue sarcomas were graded as low-grade (<9 / 10 HPFs) or high-grade ($\geq$ 9 / 10 HPFs) based on their mitotic index (Bostock and Dye, 1980).

Follow-up included periodic oncology rechecks and calls to the owners; status of local disease, development of distant disease, side effects of therapy, development of serious illness, and death were recorded for future study.

Preparation of pimonidazole injectate (Appendix 1)

Pimonidazole hydrochloride was dissolved into 0.9% NaCl at a dose of 0.28 (n=18) or 0.5 (n=46) g/m^2 at a concentration of 0.28 mg/50 ml, filtered through a 0.2-*u*m filter to remove bacteria under a sterile chemical hood. After preparation, the syringe containing the injectate was covered by aluminum foil to avoid light exposure. The dose of the hypoxia marker was given in terms of its hydrochloride salt because this was the form of the chemical that was administered. Otherwise, the marker is referred to as the free base form, PIMO. Each PIMO injectate was analyzed for the PIMO concentration based on ultraviolet absorbance maximum.

Administration of pimonidazole

Dogs were hospitalized for PIMO administration and tumor sampling. Dogs were given PIMO prior to the initiation of cancer therapy. PIMO was administered intravenously via the cephalic vein over 1-2 minutes.

Pharmacokinetic sampling and analysis

Pharmacokinetic monitoring was done in 9 dogs. 4 dogs received one injection and 5 dogs received 2 injections of PIMO. Blood samples were collected from a jugular vein at 2, 4 and 8 hours after PIMO administration. Samples were centrifuged at 3000 rpm for 10 minutes and the plasma was separated for analysis. The plasma was mixed with an equal volume of acetonitrile to precipitate plasma proteins, centrifuged at 5000 rpm for 15 minutes, and the supernatant was analyzed for PIMO by reversed-phase high performance liquid chromatography (HPLC) (Appendix 2).

Tumor sampling and radiation therapy

Tumors were biopsied by an aseptic technique using either a 14-gauge biopsy needle (Tru-Cut Biopsy Needle, Baxter Healthcare Corporation, Pharmaceutical Division, Valencia, CA) or a 4-mm-diameter trephine biopsy punch. At each sampling, 2 to 4 tissue samples from geographically distinct regions of the tumor were obtained but regions of necrotic tissue were avoided. Tissues from each biopsy site were divided in two portions; one portion was frozen at –80°C for analysis of the concentration of PIMO antigen by ELISA and the other was fixed in cold 10% neutral buffered formalin followed by 50-70% ethanol for IHC. Dogs were under general anesthesia (isoflurane and 100% O_2) for tumor biopsy and they received the first radiation fraction with ^{60}Co, γ-ray photons consisting of daily 2.25 or 3.0 Gy fractions immediately after the first biopsy.

Chapter II: 11 dogs

The purpose of the study was to investigate the rate of PIMO adduct decay *in vivo*.

Tumor biopsies were obtained immediately prior to the first three radiation fractions; 24, 48 and 72 hours after administration of PIMO (Azuma et al., 1997).

Chapter III: 9 dogs (all dogs in Canine Soft Tissue Sarcoma Project)
The purpose of the study was to investigate the timing of the PIMO adduct formation *in vivo*. Tumor biopsies were obtained 20 minutes and 24 hours after administration of PIMO. Dogs were received the first radiation fraction after the first sampling (20-minute) and a second biopsy was done prior to the second radiation fraction (24-hour post).

Chapter IV: 50 dogs (10 dogs from chapter II were included and 33 dogs were from the Canine Soft Tissue Sarcoma Project)
The purpose of the study was to investigate the relationship between tumor hypoxia and proliferation.
Tumor biopsies were obtained 24 hours after administration of PIMO. Pretreatment hypoxia and proliferating fractions were compared.

Canine Soft Tissue Sarcoma Project: 44 dogs (Thrall et al., 2000)
Project I: Prospective Thermal Dose Trial in Canine Tumors
This is a multi-institutional prospective phase III thermal dose trial in canine soft tissue sarcomas to investigate the relationship between thermal dose and local tumor control in heatable canine soft tissue sarcomas in combination with radiotherapy. There were two treatment groups, low heat (PIlo, n=10) versus high heat (PIhi, n=15). Dog with unheatable tumors were studied in other projects after the first HT (PIu, n=6 including one lipoma).
Project II: Effects of hyperthermia on tumor physiology (PII, n=9).
Other: PO, n=2

An enzyme-linked immunosorbent assay (ELISA)
The measurement of PIMO binding by ELISA was performed in a manner similar to that developed for another 2-nitroimidazole marker, CCI-103F (Raleigh et al., 1994). Bovine serum albumin adducts of tritium-labeled PIMO of known specific activity were used as a standard for the ELISA (Raleigh and Koch, 1990).

Slide preparation and selection of slide for immunohistochemical analysis
Biopsied tissues were fixed in cold 10% neutral buffered formalin less than 24 hours followed by 50-70% ethanol, then embedded in paraffin, with the two to four biopsy samples

in one block: this was done to reduce the total number of blocks. Paraffin blocks were serially sectioned at 4-*u*m intervals (figure 1.2). Five or six sequential sections from each 150-*u*m increment of the block were mounted on positively charged slides (Probe-on, Fisher Scientific) to ensure adhesion during processing. The median number of the slides made from each dog was 30 (range 20-66). Four randomly selected sets of contiguous sections were immunostained either for PIMO or PCNA. Selection of four slides was based on our previous work using CCI-103F as a hypoxia marker wherein quantifying hypoxia labeled area fraction from four slides from a biopsy was determined to be adequate for estimating labeled area fraction throughout the biopsy (Thrall et al., 1997). One slide per each biopsy tissue was stained with hematoxylin and eosin and reviewed with pathologists to confirm the presence of tumor and the histologic diagnosis.

Immunohistochemical techniques (IHC)

IHC for the hypoxia marker, PIMO and the cell proliferation marker, PCNA was carried out using standard IHC techniques and kits (figure1.3) after deparaffination by xylene (PIMO) or Clear-Rite 3 (Richard-Allen Scientific, Kalamazoo, MI), a non-toxic alternative to xylene (PCNA). Rehydration was done by means of washes with absolute alcohol, 95% alcohol, 80% alcohol, then deionized water with capillary-action slide staining system (MicroProbe Manual Staining System, Fisher Scientific). Peroxidase-antiperoxidase (PAP), avidin-biotin complex (ABC), and indirect peroxidase methods (Wordinger et al., 1987) were used to visualize both PIMO adducts and PCNA. Staining methods are outlined in appendices 3 and 5 using capillary-action slide staining system and commercially available link and label reagents (Vectastain ABC kit elite rabbit IgG PK-6101, Avidin/biotin blocking kit SP-2001 Vector, AEC Substrate kit for horseradish peroxidase SK-4200 Vector, Vector Laboratories, Inc. Burlingame, CA and DAKO ENVISION system K1390 PEROXIDASE, DAB, Dako Corporation). One negative control slide, in which primary antibody was omitted from the protocols for PIMO adducts or PCNA, was selected from each biopsy tissue and stained.

Pimonidazole (Appendices 3 and 4)

Briefly, sections were exposed to 0.3% hydrogen peroxide in phosphate-buffered saline for 5 minutes at 40°C, followed by incubation with pronase (Biomeda Corp., Foster City, CA) for antigen retrieval for 40 minutes at 40°C, then goat non-immune serum with avidin for 30

minutes at 40°C to reduce non-specific staining, then incubated with 1° antibody (a polyclonal, rabbit immunoglobulin to PIMO-bovine serum albumin adducts with biotin) for 1 hour at 40°C. 2° antibody (biotinylated (peroxidase-conjugated) goat anti-rabbit IgG) was applied for 30 minutes at 40°C followed as a linking antibody, followed by the labeling complex (goat peroxidase-anti-peroxidase IgG) for 30 minutes at 40°C. The chromogen used to detect the presence of peroxidase was 1% aminoethyl carbazole (AEC: red) in distilled water. Development of the chromogen was allowed to proceed for 20 minutes. Slides were counterstained with Aqua Hematoxylin (Innovex Biosciences, Richmond, CA) for 45 seconds for visualization of tissue architecture, then mounted with Crystal/Mount (Biomeda). The entire staining procedure required approximately 5 hours.

PCNA (Appendices 5 and 6)

Briefly, sections were exposed to 0.3% hydrogen peroxide in phosphate-buffered saline for 5 minutes at 40°C, and incubated with 1° antibody (a monoclonal mouse immunoglobulin to PCNA, PC10, Dako Corp., Carpinteria, CA) for 15 minutes at 40°C. 2° antibody complex (goat anti-rabbit/mouse IgG coupled to dextran peroxidase) was applied for 10 minutes at 40°C. The chromogen used was 3,3'-diaminobenzidine tetrahydrochloride (DAB: brown) in distilled water. Development of the chromogen was allowed to proceed for 5 minutes. Slides were counterstained in hematoxylin for 45 seconds, and then mounted. The entire staining procedure required approximately 2 hours. The time required for PCNA staining is significantly shorter than for PIMO because of the application of a newer staining system. Using detergent in the washing solution helps wash out soluble-PCNA and facilitates recognition of intense nuclear staining.

Morphometric analysis

Point counting was used to quantify the PIMO labeled area fraction and fraction of tumor cells heavily immunostained for PCNA in individual tumor cells in the tumor sections. Artifacts in the stained sections, including air bubbles in the mounting medium, stain precipitate, and folds or tears, were eliminated from analysis. Adjacent normal tissues in the specimen were included for analysis as other tissues.

PIMO: low-magnification measurements

Cells immunostained for PIMO binding above the visual threshold intensity were scored as labeled, with no distinction being made between light and heavy labeling. It is assumed that all cells labeled with PIMO adducts were at O_2 partial pressure < 10 mm Hg in the tumor tissue (Gross et al., 1995). At low magnification (x100), individual cells were not distinguishable. Labeled area fraction is defined as the fraction of the total geometric area of the histological section labeled with PIMO adducts. For this analysis, the entire available tissue including tumor and normal areas were examined in the section on the slides. A 19-mm-diameter eyepiece micrometer disk 5 was placed into one eyepiece objective of a binocular microscope. The disk contained a 5.0 x 5.0-mm grid, which was subdivided into 25 1.0 x 1.0-mm squares. Each histological section was viewed at a magnification of x100, and the eyepiece grid subsequently positioned over adjacent regions of the histological section until the entire section had been examined. A gap equivalent to the dimension of the one of the 1.0-mm squares was positioned between grid placements to avoid counting the same region more than once. When the grid was superimposed on a region of the histological section, the tissue underlying, i.e. ”hit” by, the orthogonal intersection of any two lines of the grid was recorded as being either PIMO labeled tumor cell, unlabeled tumor cell or other. The “other” designation included vessels, necrosis, connective tissues or any other non-tumor cellular matter. The PIMO labeled area fraction in each tumor section was calculated by:

Labeled area fraction = Labeled tumor area / (Labeled + Unlabeled + Others)

This method provides an estimate of the PIMO labeled area fraction in the tumor section without regard for the composition of the unlabeled area. Also, the corrected PIMO labeled area fraction was calculated by:

Corrected labeled area fraction = Labeled tumor area / (Labeled + Unlabeled)

This method provides an estimate of the PIMO labeled area fraction in the section with only regard for the tumor cell area. The average PIMO labeled area fractions were calculated for each dog.

PCNA: high-magnification measurement

At high magnification (x400), individual cells were distinguishable. Each histological field was viewed at a magnification of x400, and images were captured at x400 magnification by means of an Axioskop 50 microscope and a Fluar x20 objective (Carl Zeiss Inc., Thornwood, NY) linked through a high-resolution three-chip video camera (Carl Zeiss Inc.; model ZVS-3C750E) to a high-resolution Sony Trinitron Color monitor (model PVM 1343 MD) and a 486/33 microprocessor workstation running Image-1 software (NIH *Image* is a public domain image processing and analysis program for the Macintosh, National Institutes of Health (NIH)). Pictures were saved as TIFF files. Fields were subsequently positioned to a next randomly selected field within the section. When the grid was superimposed on a region of the histological field, the tumor cell underlying, i.e. ”hit” by, the orthogonal intersection of any two lines of the grid was recorded as being either PCNA-heavily immunostained tumor cell or other tumor cell. The “other” designation included lightly immunostained tumor cells and non-labeled tumor cells. For the counting purpose, four different staining patterns were assigned for each cell (figure 1.5. and appendix 7).

1. Uniform, dark brown nuclear staining was considered positive for proliferation (may be consistent with cells in S phase).
2. Diffuse, stippled nuclear staining that was lighter than a cell in 1),
3. Distinct, diffuse cytoplasmic stippling with or without nuclear staining, and
4. Unlabeled cells.

Grid spacing was adjusted to have approximately 20 tumor cells “hit” on a single high power field on several tumor sections from different dogs. Subsequently, the 1.5 x 1.5-cm grid was placed on the histological image on the computer using Image1. As a preliminary study, up to 1000 tumor cells were counted with this method. Fields containing artifacts, or not corresponding to tumor tissue, or incompletely filled with tumor tissue, were skipped in favor of the next random field.

Statistical Considerations

The mean and median values were calculated for each section, biopsy tissue, then each dog’s tumor.

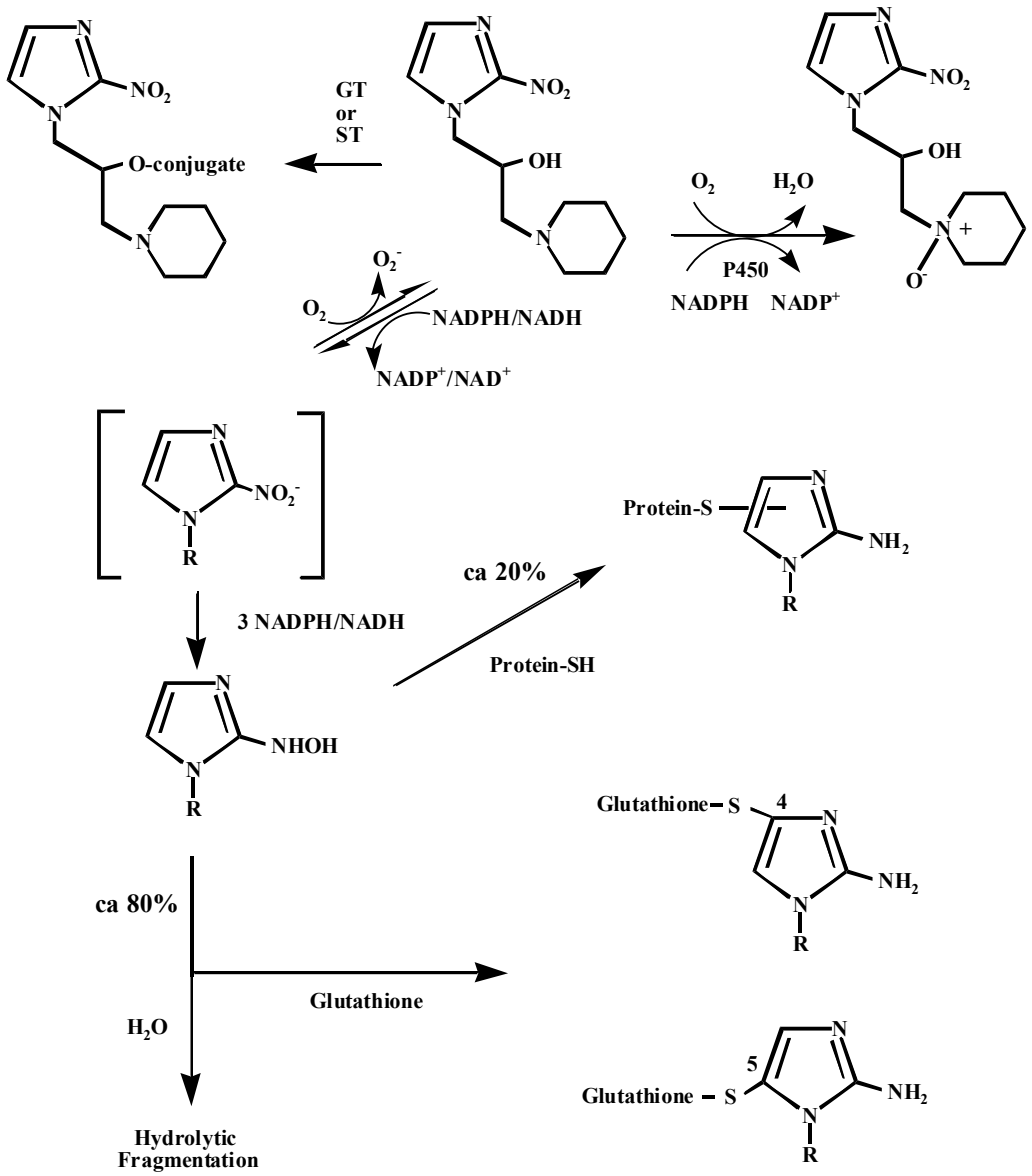

Figure 1.1 Pimonidazole: oxidative and reductive metabolism *in vivo*

Scheme for the reductive activation of pimonidazole under hypoxic conditions. The first step is the addition of an electron to form a nitro radical anion. The activated intermediate that binds to hypoxic cells is believed to be a hydroxylamine derivative resulting from the sequential addition of four electrons to pimonidazole. The hydroxylamine intermediate reacts with thiol-containing peptides and proteins to form stable adducts that can be detected by immunochemical assays (Arteel et al., 1998).

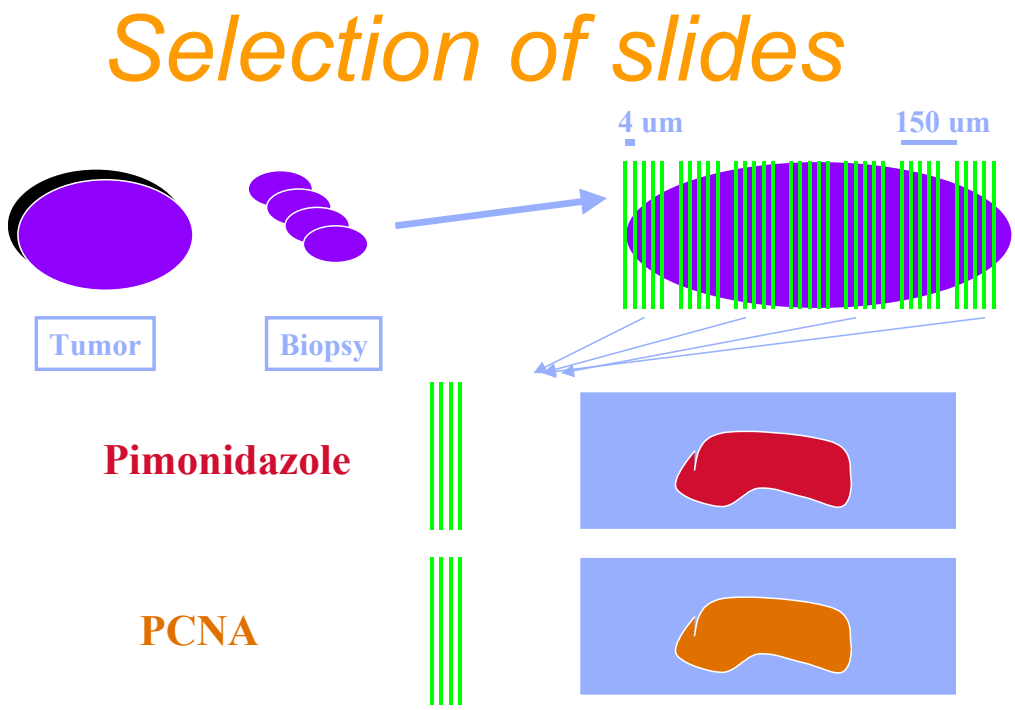

Figure 1.2 Preparation and selection of slides for analysis

At the sampling, 2 to 4 biopsies from each tumor were obtained. After processing, each biopsy tissue was sliced to obtain 5-6 slices of sections every 150 *u*m and 4 slices of section were randomly selected for analysis of hypoxia. Then, each contiguous section was also selected for analysis of proliferation. Two contiguous sections were only 4 *u*m apart and thus had a very similar structure. For each tumor 8 – 16 sections were selected for analysis of hypoxia and proliferation.

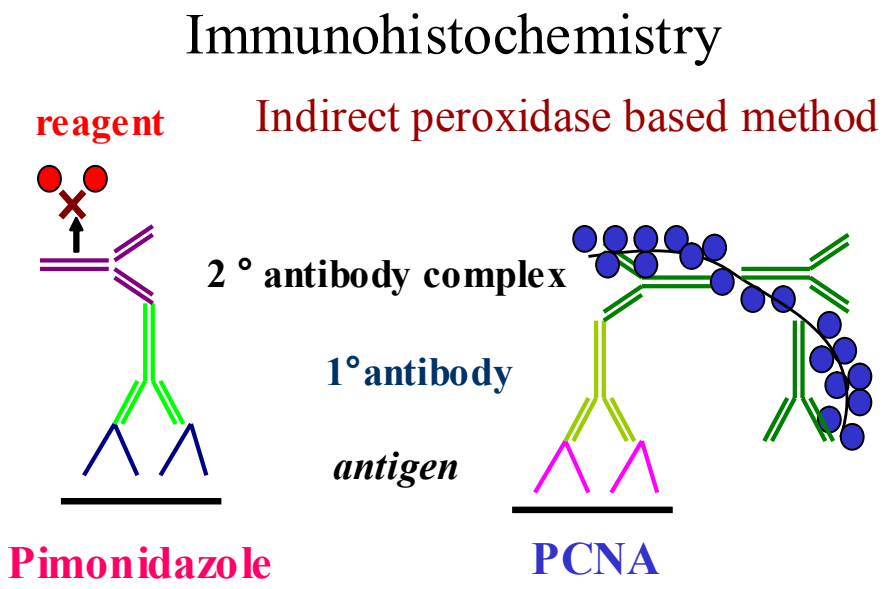

Figure 1.3 Immunohistochemistry: indirect peroxidase based method

IHC for PIMO adducts was achieved with a 1° antibody (a polyclonal, rabbit immunoglobulin to PIMO-bovine serum albumin adducts with biotin), a 2° antibody (biotinylated (peroxidase-conjugated) goat anti-rabbit IgG) and biotin-streptavidin-peroxidase complex. The chromogen used to detect the presence of peroxidase was 1% aminoethyl carbazole (AEC: red) (Vectastain ABC kit elite, AEC, Vector Laboratories,Inc. Burlingame, CA).

IHC for PCNA was achieved with 1° antibody (a monoclonal mouse immunoglobulin to PCNA, PC10, Dako Corp., Carpinteria, CA) and a biotin-conjugated F(ab')2 secondary antibody reagent (goat anti-rabbit/mouse IgG coupled to dextran peroxidase). The chromogen used was 3,3'-diaminobenzidine tetrahydrochloride (DAB: brown). Newer system for PCNA staining provided shorter staining procedure time and higher amplification of signal (DAKO ENVISION system, DAB, Dako Corporation).

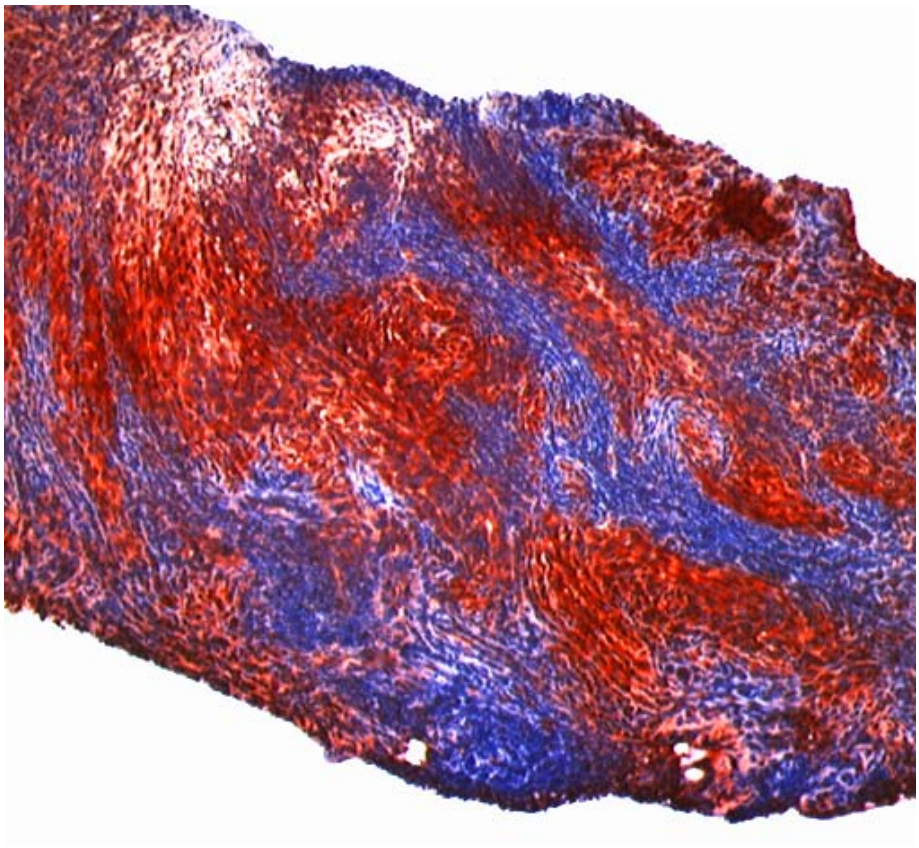

Figure 1.4 Immunohistochemistry: detection of pimonidazole adducts

Pimonidazole adducts were labeled with AEC chromogen: red color and counterstained with hematoxylin: blue color. Variations in intensity can be seen, but only labeled area above threshold was counted as a labeled area. Fibrosarcoma (dog#76969 AM), x 40.

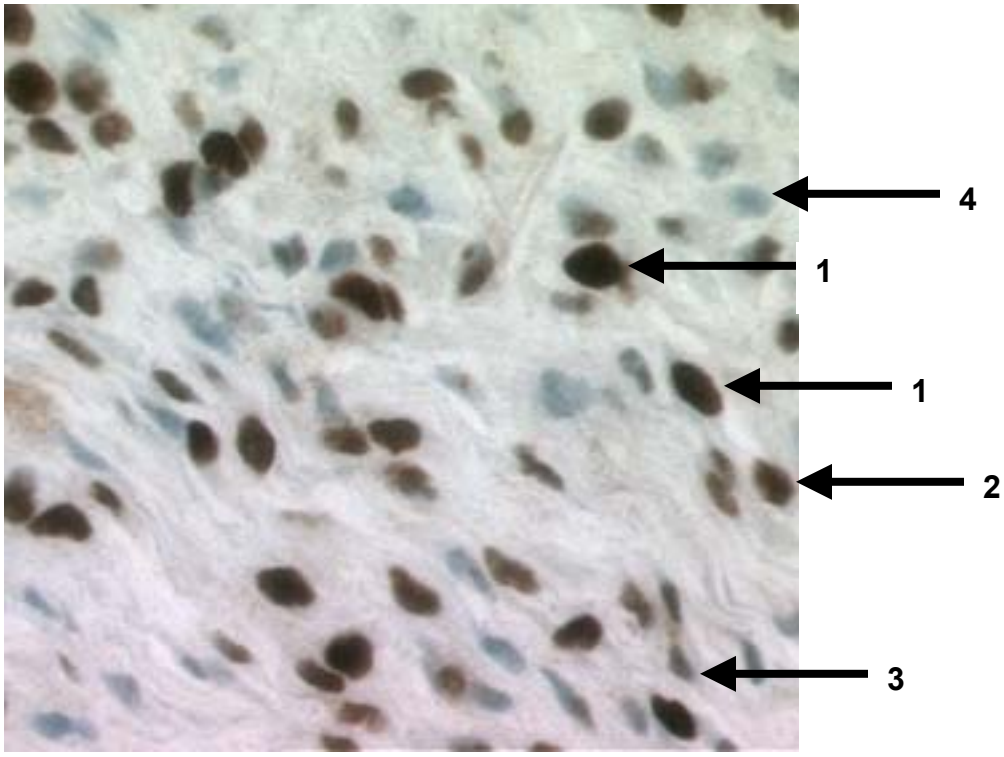

Figure 1.5 Immunohistochemistry: four staining patterns of PCNA

PCNA is a nuclear staining. With high magnification of light microscope, x400, four patterns of PCNA were easily identified. 1. Uniform, dark brown nuclear staining; 2. Diffuse, stippled nuclear staining that was lighter than a cell in 1; 3. Distinct, diffuse cytoplasmic stippling with or without nuclear staining; and 4. Unlabeled cells. Hemangiopericytoma. PCNA labeling is heaviest in cells in S-phase.

Results

Dogs

Sixty four dogs with histologically confirmed malignant solid tumor were entered in this study from September 1993 to March 1999. All dogs received at least one PIMO administration and biopsy procedure. The dogs were of 28 various breeds, 16 mixed breed dogs, 11 Golden retrievers, 4 Labrador retrievers, 4 Shetland sheepdogs and others. There were 31 females and 33 males. The median age of the dogs was 10 years (range: 1 to 15).

Solitary, primary tumors (or recurrent tumors at the primary site) without presence of metastasis were included in this study. The tumors were of various types and varied in grade (low versus high). Soft tissue sarcomas (n=57) were the most common type (figure 1.6). There were 39 low-grade and 16 high-grade soft tissue sarcomas. Two soft tissue sarcomas out of 57 were not graded due to sampling error (not enough tumor tissue). Other tumor types included carcinomas (n=6) and hemangiosarcoma (n=1). The median tumor volume was 58.9 cm^3 (range: 3.4 to 4396 cm^3). Tumor volume was calculated by the equation: a (cm) x b (cm) x c (cm) x $\pi/6$.

Most dogs were receiving therapy with curative intent at the time of PIMO administration. Treatment of these tumors was either ^{60}Co irradiation alone or ^{60}Co irradiation plus local hyperthermia. Twenty-five dogs were included in an ongoing clinical trial (Project I) to assess the combination effects of hyperthermia and irradiation for treatment of canine soft tissue sarcomas. Complete follow up information will be available including local control, side effects of therapy, metastasis, and survival when the trial is closed. Characteristics of dogs were summarized in table 1.1.

All dogs tolerated the PIMO infusion and biopsy procedures with no significant adverse effects. Biopsy of the tumor was attempted in all dogs. In three dogs, sample size and quality of tissues were not adequate for analysis. In one other dog, histology showed only adipose tissue in biopsy samples and the original diagnosis was liposarcoma. However, subsequent surgical biopsy revealed an infiltrating lipoma. The 4 dogs were excluded from analysis and there were adequate samples from 60/64 dogs. The median biopsy number at each sampling was 3 (range: 2 to 4).

Pharmacokinetics of PIMO in dogs

The elimination half-life of PIMO in dogs was 1.5 $\pm$ 1 hours, based on regression analysis of the elimination phase of the concentration versus time curve (n=9)(table 1.2).

Hypoxia labeling: PIMO

The dose of PIMO hydrochloride was initially 0.28 mg/m^2, then increased to 0.5 mg/m^2 because of negative or little reactivity with monoclonal antibody against PIMO adducts. There are little reactivities between 3 different monoclonal antibodies and PIMO adducts in canine tumors even with a higher PIMO dose and several staining working conditions. Subsequently, a polyclonal antibody (#27-10) was used for all PIMO adduct detections. Using negative controls, there was no nonspecific binding of secondary antibody reagents.

In the samples taken 24 hours after administration of PIMO, IHC labeling was seen in 49 out of 50 tumors. Labeling was discrete, intracellular and cytoplasmic. Large variability in labeling was observed within tumors and between tumors. It was noted that the shapes of the cells and intensity of the labeling varied depending on the histological type of the tumor. Examples from several tumors are presented in figure 1.7. Qualitatively, the distribution of labeled areas for PIMO were often adjacent to regions of necrosis, but there was no staining within the necrotic regions, and the cells that were immunostained appeared viable.

Proliferation labeling: PCNA

Using negative controls, there was no nonspecific binding of secondary antibody reagents. In the samples taken 24 hours after administration of PIMO, heavy PCNA labeling was seen in all 50 out of 50 tumors. Labeling was discrete, intracellular, and usually intranuclear (figure 1.8). Heavily stained PCNA positive cells were easily identified in each tumor. The shape of the cells and intensity of the labeling varied depending on the histological type of tumor. For the purpose of the present analysis, cells immunostaining for PCNA were segregated between heavy nuclear staining (may be consistent with S phase cells) and light staining characteristic of cells at other phases of the cell cycle.

As a preliminary study, up to 1000 tumor cells were counted with grid in four dogs. The fraction of heavily labeled cells seemed to be plateau after counting 300 cells (figure 1.9). We concluded that counting 500 cells was adequate to estimate the proliferating fraction of our population of tumor.

Table 1.1 Summary of all dogs (n=64)

No		study	Proj.	Dog	#Patient	vol	#Path.	#bx	Breed	Sex	Age	Grade	Tumor	Location
1	1	II-1, IV-1		BM	49939	33.92	93-3310	2	Labrador Retriever	FS	10	L	FSA	Limb
2	2	II-2, IV-2		TC	52011	483.56	93-3315	2	Golden Retriever	MC	8	L	Fibroma	Head
3	3	II-3, IV-3		OM	20631	272.13	93-3375	2	Golden Retriever	M	10	N/A	HAS	Trunk
4	4	II-4, IV-4		MB	52244	58.88	93-3376	2	Golden Retriever	M	3	L	FSA	Head
5	5	II-5, IV-5		RM	52788	15.83	93-3446	2	Labrador Retriever	M	2	H	FSA	Head
6	6	II-6, IV-6		SA	52986	4396	94-3008	2	Siberian Husky	FS	10	L	HPC	Trunk
7	7	II-7		CL	54263	10.9	94-3098	2	Cocker Spniel	M	11	N/A	FSA->SCC	Head
8	8	II-8, IV-7		CQ	54338	130	94-3105	2	Labrador Retriever	M	12	L	CSA	Limb
9	9	II-9, IV-8		GC	55885	345.9	94-3236	2	mix	FS	10	H	SA	Limb
10	10	II-10, IV-9		CW	57291	16.33	94-3374	2	mix	FS	11	N/A	SCC	Head
12	11	II-11, IV-10		JW	58573	870.8	94-3492	2	Rodesian Ridgeback	M	1	L	NFSA	Trunk
13	12	IV-11		SC	59521	50.2	95-3046	2	Siberian Husky	FS	13	L	HPC	Limb
14	13	IV-12		SD	59117	146.4	95-3047	3	Golden Retriever	FS	11	L	HPC	Limb
15	14	excluded		SJ	59789	NT	95-3167	3	Cairn Terrier	M	11	N/A	SA	Trunk
16	15	IV-13		JB	41349	58.29	95-3204	3	Alaskan Malamute	M	11	L	FSA	Limb
17	16	excluded		SB	60848	NT	95-3229	3	Golden Retriever	M	5	N/A	HPC	Trunk
18	17	IV-14		IL	61200	334.6	95-3278	3	Doberman Pinscher	FS	8	H	FSA	Trunk
19	18	IV-15		BG	62305	6.15	95-3386	3	St Poodle	M	10	L	FSA	Trunk
20	19	IV-16		RR	62376	314	95-3399	3	Great Pyrenees	MC	4	H	FSA	Trunk
21	20	IV-17		BV	63630	98.13	95-3519	3	Golden Retriever	FS	9	N/A	ACA	Trunk
22	21	IV-18		RA	63681	188.4	96-3000	3	Irish Setter	MC	6	N/A	ACA	Trunk
23	22	IV-19		PJ	64653	6	96-3049	3	Shetland Sheepdog	FS	6	N/A	SCC	Head
24	23	IV-20	PII	TS	64950	12.56	96-3133	3	mix	MC	13	L	HPC	Limb
25	24	IV-21	PII	GM	65203	216.5	96-3146	3	mix	MC	11	L	NFSA	Limb
26	25	IV-22	PII	EZ	66885	8.5	96-3268	3	Golden Retriever	FS	6	L	SA	Head
27	26	IV-23	PII	BM	66897	63.1	96-3271	2	mix	FS	10	L	HPC	Limb
28	27	IV-24	PII	JD	66999	40.9	96-3272	2	mix	M	10	L	HPC	Limb
29	28	IV-25	PII	BC	67186	3.8	96-3273	3	Scottish Terrier	MC	10	H	HPC	Limb
30	29	IV-26	PIIo	NF	67298	210.6	96-3274	3	Austlarian Shep.	FS	14	L	HPC	Limb
31	30	IV-27	PIIo	JY	67068	20.2	96-3275	3	St.Poodle	FS	12	L	FSA	Limb
32	31	IV-28	PIhi	TW	67540	80.8	96-3331	3	Golden Retriever	FS	13	H	FSA	Trunk
33	32	IV-29	PIhi	TS	67764	81.9	96-3348	3	Japanese Spitz	FS	13	L	HPC	Limb
34	33	IV-30	PIIo	BW	39492	15.4	96-3368	3	Spaniel.English spr	M	6	L	NF	Limb
35	34	IV-31	PIIo	GS	68298	125.6	96-3381	3	Golden Retriever	MC	5	H	HPC	Limb
37	35	IV-32	PII	BP	68227	1067.5	96-3440	3	Doberman	M	4	L	FSA	Trunk
38	36	IV-33	PIu	SS	69013	182.5	96-3446	3	Labrador Retriever	FS	8	H	NFSA	Trunk
39	37	IV-34	PIhi	MC	69021	7.1	96-3456	3	Beagle	MC	10	H	HPC	Limb
40	38	IV-35	PII	CT	69466	343.3	96-3465	3	mix	MC	9	L	HPC	Limb
41	39	IV-36	PO	LP	69939	302.5	97-3010	3	Cocker Spniel	FS	12	L	HPC	Limb
42	40	IV-37	PIIo	SH	72154	40.4	97-3153	3	Corgi	MC	11	H	FSA	Limb

Table 1.1 Continued

No		study	Proj.	Dog	#Patient	vol	#Path.	#bx	Breed	Sex	Age	Grade	Tumor	Location
54	41	excluded	Plu	RR	75833	NT	98-3016	3	mix	FS	12	L	LPSA	Trunk
43	42	IV-38	PIlo	BL	73113	13.4	97-3232	3	mix	FS	15	L	HPC	Limb
45	43	IV-39	PIhi	RG	70948	12.7	97-3286	3	Irish Setter	MC	10	L	FSA	Limb
47	44	IV-40	PIhi	RH	72960	119.6	97-3298	3	Rottweiler	M	3	L	FSA	Limb
48	45	IV-41	Plu	SO	41480	24.9	97-3321	3	mix	FS	14	L	HPC	Limb
51	46	IV-42	PIhi	ML	74817	19.1	97-3345	3	Fox terrier	FS	13	L	HPC	Limb
52	47	IV-43	PIlo	JV	74947	11	97-3346	3	Great Dane	FS	9	L	SCSA	Limb
53	48	IV-44	PIlo	PC	75456	28.8	97-3368	3	Bichon Frise	MC	10	H	FSA	Head
55	49	IV-45	PO	TG	53444	86.1	98-3043	3	Basset haound	FS	11	N/A	AnCA	Trunk
56	50	III-1	PIhi	PF	76544	45.3	98-3046	4	Golden Retriever	M	9	H	FSA	Limb
59	51	excluded	PIhi	RC	76578	3.75	98-3063	3	English Setter	M	11	L	HPC	Limb
62	52	III-2	Plu	AM	76969	37.7	98-3086	4	Mastiff	FS	8	H	FSA	Trunk
63	53	III-3	PIhi	BG	78108	64.9	98-3138	4	mix	FS	13	H	HPC	Limb
64	54	III-4	PIhi	BK	78229	50.5	98-3139	4	mix	FS	9	L	HPC	Limb
65	55	III-5	PIhi	SB	78261	66.2	98-3140	4	Sheltie	FS	13	H	HPC	Limb
66	56	III-6	PIlo	LR	78604	84.3	98-3203	4	mix	MC	7	L	MSA	Limb
67	57	III-7	PIhi	FM	79341	122.5	98-3271	4	mix	FS	12	L	HPC	Limb
68	58	III-8	PII	LE	79800	47	98-3293	4	Sheltie	FS	8	L	HPC	Trunk
69	59	III-9	Plu	DH	80859	371.2	98-3406	4	Golden Retriever	MC	4	H	HPC	Neck
70	60	IV-46	PIhi	KW	80916	15.7	98-3431	4	Bouvier	MC	10	L	MSA	Limb
71	61	IV-47	PIhi	TK	80976	3.4	98-3450	4	Shetland Sheepdog	FS	7	L	AnSA	Trunk
72	62	IV-48	Plu	AE	81496	116.9	98-3530	4	mix	MC	9	L	HPC	Trunk
73	63	IV-49	PIlo	HS	82360	15.4	99-3104	4	min. schnauzer	FS	10	L	NFSA	Limb
76	64	IV-50	PIhi	VG	83673	66.9	99-3213	4	mix	MC	11	L	HPC	Limb

4 dogs were excluded form analysis due to sampling errors (3dogs) and diagnosis of lipoma (1dog)-shown in blue. No: dog number
Study: II-1-11 in chapter II, III-1-9 in chapter III, IV-1-50 in chapter IV
Proj: Canine soft tissue sarcoma project to study combination effect of hyperthermia (HT) and radiotherapy (RT), PI: thermal dose response study, low dose group (PIlo) vs. high dose group (PIhi), unheatable tumor (Plu), PII: variable heat study group, PO: other study project
Name: initial of dog, #patient: clinical patient number in VTH, NCSU
Vol: tumor volume=(a x b x c)$\pi/6$ (cc), #path: pathology number, NCSU
#bx: number of biopsy, Breed: breed of dog, Sex: M-male, MC-male castrated, FS-female spayed, Grade: L-low grade soft tissue sarcoma, H-high grade soft tissue sarcoma
Tumor type: FSA-fibrosarcoma, HPC-hemangiopericytoma, HAS-hemangiosarcoma, CSA-chrondrosarcoma, SA-sarcoma, SCC- squamous cell carcinoma, NFSA-neurofibrosarcoma, ACA-adenocarcinoma, NF-neurofibroma, LPSA-liposarcoma, SCSA-synovial cell sarcoma, AnCA-anaplastic carcinoma, MSA-myxossarcoma, AnSA-anaplastic sarcoma
Location: trunk, limb, head and neck

Table 1.2 Pharmacokinetics of PIMO in dogs (n=9)

No	Name	Path#	PK1	PK2	slope	T 1/2
1	BM	93-3310	3	N/A	0.73	0.9532
2	TC	93-3315	3	N/A	1.14	0.6063
3	OM	93-3375	3	3	0.65	1.0728
4	MB	93-3376	3	3	0.30	2.31
6	SA	94-3008	3	2	0.18	3.85
7	CL	94-3098	3	N/A	0.50	1.386
9	GC	94-3236	3	N/A	0.46	1.5065
11	NS	94-3383	3	3	0.48	1.4378
13	SC	95-3046	3	1	1.14	0.6063
Average						1.5254
Stdev						1.0166

Pharmacokinetics were measured in 9 dogs. Five dogs received two PIMO injections prior to first and last treatment of radiation therapy. Radiation therapy was delivered daily up to 19 treatments (3Gy x 19=57 Gy).
Half-life of the PIMO was defined 1.5 +/- 1 hours.

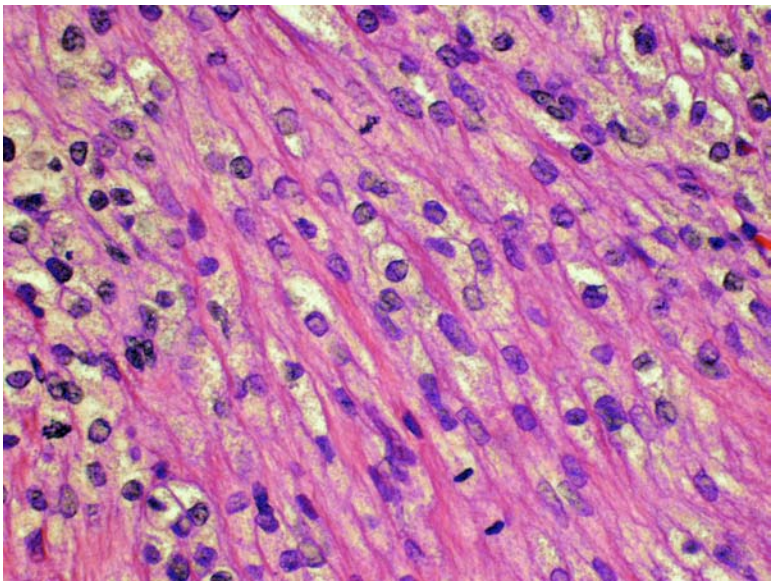

Figure 1.6a: Fibrosarcoma (FSA), H&E, x400

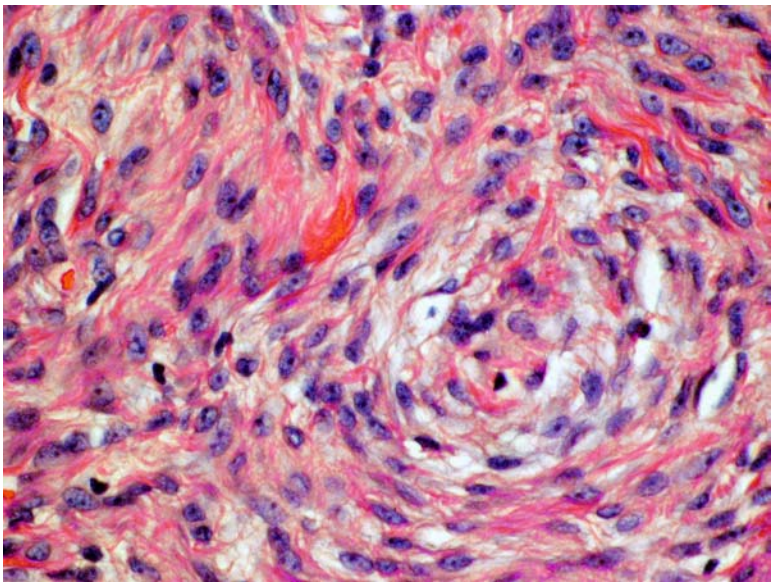

Figure 1.6b: Hemangiopericytoma (HPC), H&E, x400

Figure 1.6 Histology of soft tissue sarcomas

Fibrosarcomas and hemangiopericytomas were the most common soft tissue sarcomas in this study. FSA cells are more spindle shaped and tumors contain abundant fibrous connective tissue (1.6a). HPC cells tended to be round with larger cytoplasm (1.6b) and the amount of connective tissue in HPC was lower than FSA.

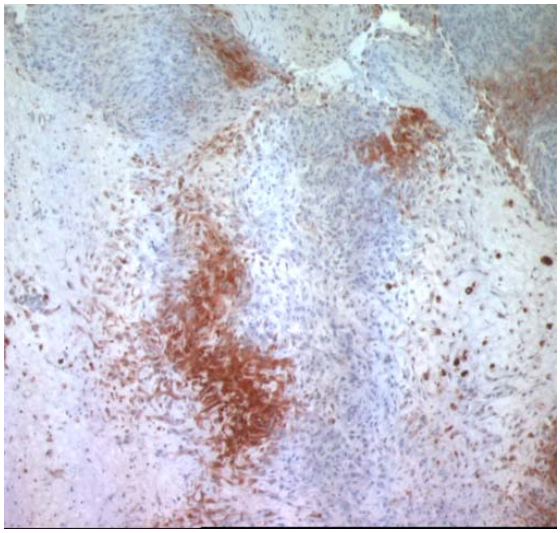

Figure 1.7a

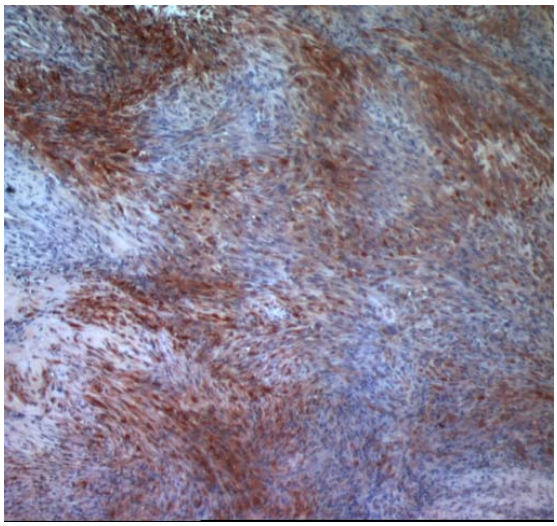

Figure 1.7b

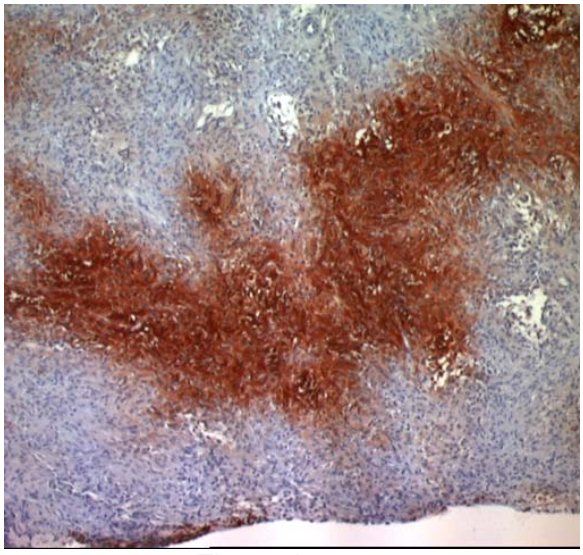

Figure 1.7c

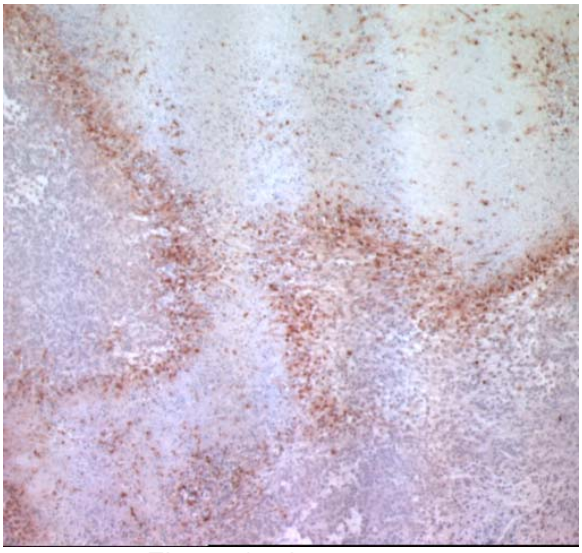

Figure 1.7d

Figure 1.7 Staining patterns of PIMO adducts

1.7a: low-grade hemangiopericytoma: HPC (dog#69939 LP), there is an area of PIMO labeled cells and no labeling of connective tissue or necrosis, 1.7b: high-grade fibrosarcoma: FSA (dog#76544 PF), the labeled area is more diffuse, 1.7c: low-grade hemangiopericytoma: HPC (dog#78229 BK), there is a large area of labeling and 1.7d: high-grade fibrosarcoma: FSA (dog#72154 SH), labeling cell is located at the border of necrosis but there is no labeling within the necrosis, x 100.

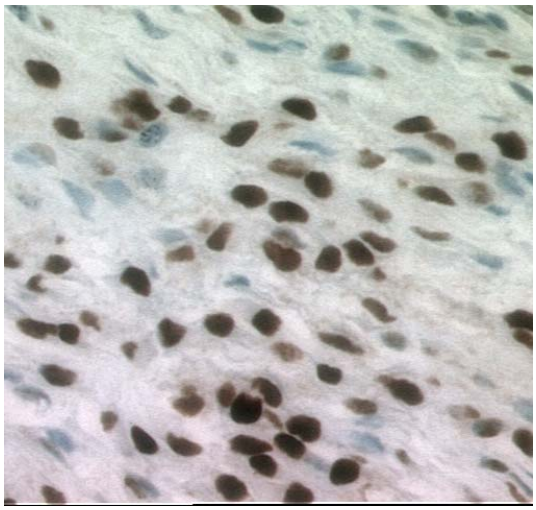

Figure 1.8a

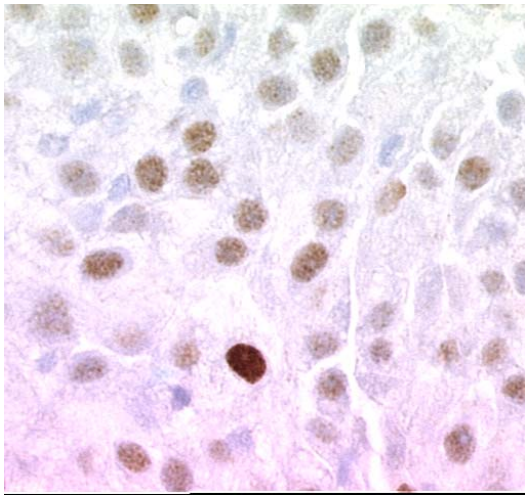

Figure 1.8b

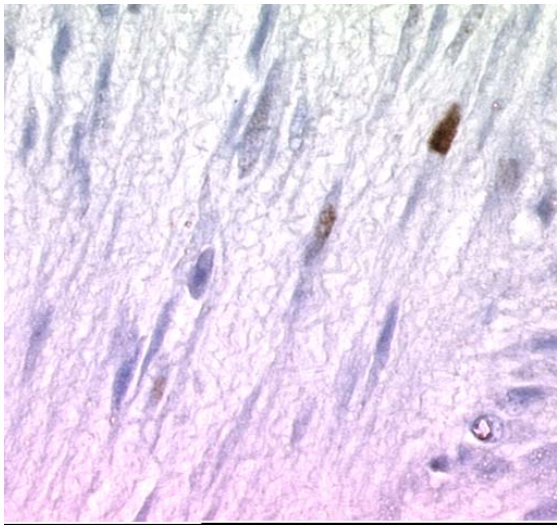

Figure 1.8c

Figure 1.8 Staining patterns of PCNA

Strong nuclear staining can be easily identified in different tumors. There is variation in appearance. 1.8a: low-grade neurofibrosarcoma: NFSA, 1.8b: low-grade hemangiopericytoma: HPC and 1.8c: low-grade neurofibroma: NF (dog#39492 BW), x 400.

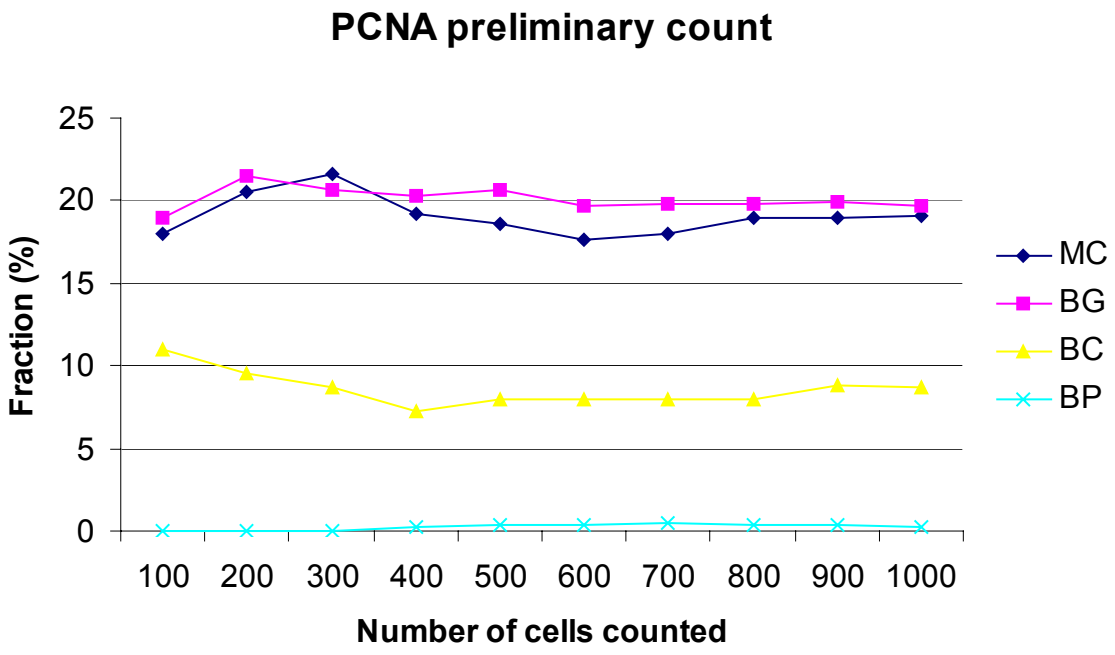

Figure 1.9 PCNA counting

Fraction of cells heavily labeled with PCNA antibodies as a function of the number of cells counted for four different tumors. There is relatively low heterogeneity within a biopsy sample. 1000 tumor cells at the intersection of grid were counted. Counting 500 tumor cells was considered adequate for analysis.

Discussion

PIMO adducts and PCNA were detected by standard IHC. Heavily labeled PCNA cells were easily identified in all tumors. PIMO labeling was quantified as fraction labeled area and PCNA labeling was quantified as fraction of labeled cells. There was little overlap between cells immunostained for PIMO and heavily stained for PCNA in same region on contiguous slides.

The plasma half-life of PIMO in dogs was 1.5 hours so that the time of the biopsy, which was 24 hours post PIMO infusion represents 16 half-lives of circulating marker. At the time of harvesting, circulating PIMO plasma concentration is essentially 0. Combination with rapid transfer of biopsy material to cold fixative seems to be adequate to minimize non-specific PIMO binding in tissue as shown by low background binding.

PCNA provided a useful indication of cell proliferation in tumors examined. PCNA is an endogenous marker of proliferating cells and it gives an indication of the proliferating activity and S phase portion of cells at the particular point in time at which the biopsy is taken (Varia et al., 1998). Positive staining for PCNA was categorized based on cellular distribution and intensity of brown to dark brown pigment over their nuclei that correlated with the different phases of the cell cycle. Only cells exhibiting a distinct nuclear stain for PCNA were scored as an estimation of S-phase cells. However, intensity of binding may be influenced by several factors such as quality of staining and tumor types. Manual point counting is suitable for quantifying hypoxia and proliferation in spontaneous canine tumors although the procedure was time consuming and labor intensive. A semiquantitative IHC image analysis based on the PIMO as a marker showed that the feasibility of the technique (Raleigh et al., 2001). It may be possible to use image analysis to reduce time and subjectivity (Varia et al., 1998), but it was difficult to apply to our dog samples because of the difficulty to standardize the intensity and shape threshold due to variety of shape and size of cells, and level of intensity of binding. For quantitative image analysis of IHC for PIMO adducts, the intent was to adjust color detection thresholds and default settings for the AEC chromogen at x100 magnification in tissue sections. Difficult issues for PIMO adduct detection were related to the composition of the tissue where tumor cells and interstitial connective tissues were mixed and not distinguishable with the imaging analysis system. For PCNA detection, the variation in shape and size of the tumor nuclei made it impossible to standardized the system.

PIMO has some advantages over other clinical useful hypoxia markers. Foremost it has a high solubility in aqueous solution, which allows the marker to be administered to dogs in small volume injections of saline solutions intravenously. Markers such as the hexafluorinated misonidazole, CCI-103F have less aqueous solubility and are usually administered as large volume injection of saline solutions causing hemodilution (Ljungkvist et al., 2000). The piperidine side-chain of PIMO is positively charged, leading to a 3-fold intercellular accumulation of the drug at physiological pH, falling as the extracellular environment becomes more acidic (Dennis et al., 1985).

In conclusion, IHC detection systems for PIMO and PCNA were suitable to study tumor hypoxia and proliferation in canine spontaneous solid tumors.

References

Arteel, G.E., R.G. Thurman, and J.A. Raleigh. 1998. Reductive metabolism of the hypoxia marker pimonidazole is regulated by oxygen tension independent of the pyridine nucleotide redox state. Eur J Biochem 253:743-50.

Azuma, C., J.A. Raleigh, and D.E. Thrall. 1997. Longevity of pimonidazole adducts in spontaneous canine tumors as an estimate of hypoxic cell lifetime. Radiat Res 148:35-42.

Bostock, D.E., and M.T. Dye. 1980. Prognosis after surgical excision of canine fibrous connective tissue sarcomas. Vet Pathol 17:581-8.

Cline, J.M., D.E. Thrall, R.L. Page, A.J. Franko, and J.A. Raleigh. 1990. Immunohistochemical detection of a hypoxia marker in spontaneous canine tumours. Br J Cancer 62:925-31.

Dennis, M.F., M.R. Stratford, P. Wardman, and M.E. Watts. 1985. Cellular uptake of misonidazole and analogues with acidic or basic functions. Int J Radiat Biol Relat Stud Phys Chem Med 47:629-43.

Gross, M.W., U. Karbach, K. Groebe, A.J. Franko, and W. Mueller-Klieser. 1995. Calibration of misonidazole labeling by simultaneous measurement of oxygen tension and labeling density in multicellular spheroids. Int J Cancer 61:567-73.

Inman, J.K. 1975. Thymus-independent antigens: the preparation of covalent, hapten-ficoll conjugates. J Immunol 114:704-9.

Ljungkvist, A.S., J. Bussink, P.F. Rijken, J.A. Raleigh, J. Denekamp, and A.J. Van Der Kogel. 2000. Changes in tumor hypoxia measured with a double hypoxic marker technique. Int J Radiat Oncol Biol Phys 48:1529-38.

Raleigh, J.A., and C.J. Koch. 1990. Importance of thiols in the reductive binding of 2-nitroimidazoles to macromolecules. Biochem Pharmacol 40:2457-64.

Raleigh, J.A., J.K. La Dine, J.M. Cline, and D.E. Thrall. 1994. An enzyme-linked immunosorbent assay for hypoxia marker binding in tumours. Br J Cancer 69:66-71.

Raleigh, J.A., S.C. Chou, E.L. Bono, D.E. Thrall, and M.A. Varia. 2001. Semiquantitative immunohistochemical analysis for hypoxia in human tumors. Int J Radiat Oncol Biol Phys 49:569-74.

Raleigh, J.A., G.G. Miller, A.J. Franko, C.J. Koch, A.F. Fuciarelli, and D.A. Kelly. 1987. Fluorescence immunohistochemical detection of hypoxic cells in spheroids and tumours. Br J Cancer 56:395-400.

Smithen, C., and C. Hardy. 1982. The chemistry of nitroimidazole hypoxic cell radiosensitizers. In Advanced Topics on Radiosensitizers of Hypoxic Cells (A. Breccia, C. Rimondi and G. E. Adams, Eds.):1-47.

Thrall, D.E., G.L. Rosner, C. Azuma, M.C. McEntee, and J.A. Raleigh. 1997. Hypoxia marker labeling in tumor biopsies: quantification of labeling variation and criteria for biopsy sectioning. Radiother Oncol 44:171-6.

Thrall, D.E., G.L. Rosner, C. Azuma, S.M. Larue, B.C. Case, T. Samulski, and M.W. Dewhirst. 2000. Using units of CEM 43 degrees C T90, local hyperthermia thermal dose can be delivered as prescribed. Int J Hyperthermia 16:415-28.

Varia, M.A., D.P. Calkins-Adams, L.H. Rinker, A.S. Kennedy, D.B. Novotny, W.C. Fowler, Jr., and J.A. Raleigh. 1998. Pimonidazole: a novel hypoxia marker for complementary study of tumor hypoxia and cell proliferation in cervical carcinoma. Gynecol Oncol 71:270-7.

Wordinger, R.J., G.W. Miller, and D.S. Nicodemus. 1987. Manual of Immunoperoxidase Techniques. American College of Clinical Pathologists.

CHAPTER II: Longevity of Pimonidazole Adducts in Spontaneous Canine Tumors as an Estimate of Hypoxic Cell Lifetime (Manuscript)

Chieko Azuma, James A. Raleigh and Donald E. Thrall
Radiation Research 148, 35-42 (1997)

This study showed that lifetime of PIMO adducts in tumor *in vivo* was prolonged and stable, which can be detectable at 72 hours post PIMO injection. The stability of PIMO adducts *in vivo* permits considerable latitude in the interval between PIMO injection and tumor biopsy which is very useful to fit busy clinical schedule.

There was important information on tumor biology of labeled cells. The labeled cells were hypoxic at the time of the injection and stable *in vivo* at the 72-hour sampling time, but it is unknown if they were still hypoxic or reoxygenated. There was no difference in the appearance of tumor cells to indicate degeneration. Indeed, labeled tumor cells looked no different at the 72-hour sampling time.

Pimonidazole remains stable in labeled cells as adducts for several days providing information on the lifetime of hypoxic cells which do not die even with 6 Gy of irradiation (daily 3 Gy x 2) and it may indicate radiation resistency of hypoxic cells.

RADIATION RESEARCH 148, 35–42 (1997)
0033-7587/97 $5.00
©1997 by Radiation Research Society.
All rights of reproduction in any form reserved.

Longevity of Pimonidazole Adducts in Spontaneous Canine Tumors as an Estimate of Hypoxic Cell Lifetime

Chieko Azuma,* James A. Raleigh† and Donald E. Thrall*,[1]

*College of Veterinary Medicine, North Carolina State University, Raleigh, North Carolina 27606; and †School of Medicine, University of North Carolina, Chapel Hill, North Carolina 27599-7512

Azuma, C., Raleigh, J. A. and Thrall, D. E. Longevity of Pimonidazole Adducts in Spontaneous Canine Tumors as an Estimate of Hypoxic Cell Lifetime. *Radiat. Res.* **148**, 35–42 (1997).

The longevity of pimonidazole adducts in tumors was quantified as an estimate of the lifetime of hypoxic cells. Pimonidazole was given before irradiation to 12 dogs bearing spontaneous tumors, and tumors were biopsied 24, 48 and 72 h later. Pimonidazole antigen was quantified in the biopsies using ELISA and immunohistochemistry. Pimonidazole antigen was detectable in the initial biopsy in all dogs. In 5 dogs the amount of detectable antigen decreased to less than 50% of the initial amount, in 5 other dogs the amount of detectable antigen decreased to an amount between 50 and 100% of the initial amount, and in 2 dogs the amount of antigen appeared to increase relative to the initial amount. Tumors with high initial adduct concentration were characterized by greater decreases in adduct concentration than tumors with low initial adduct concentration. Immunohistochemically, labeled cells were present in 11 of 12 tumors. The geographic area in tumor biopsies labeled immunohistochemically with pimonidazole adducts (labeled area fraction) tended to decrease over time in 6 dogs, remain stable in 4 dogs and seemingly increase in 1 dog. There was no relationship in individual tumors between the relative change in antigen concentration and the relative change in labeled area fraction. Hypoxic cells which bind pimonidazole may persist for days during fractionated radiation therapy, and the potential exists for them to exert a negative effect on the host.
© 1997 by Radiation Research Society

INTRODUCTION

It is recognized that hypoxic cells exist in rodent (*1*), canine (*2, 3*) and human (*4–10*) tumors. Limitations of oxygen diffusion have been considered a predominant cause of the development of hypoxia (*11*), but limitations of perfusion (*12, 13*) and oxygen consumption (*14*) have also been implicated. Regardless of the inciting cause, hypoxic cells are radioresistant (*15*), and this resistance has stimulated great interest in measuring hypoxia (*16*) as a means of identifying patients at risk for treatment failure. A relationship between tumor hypoxia and the outcome of treatment has been identified in some human tumors (*4, 17–19*). Nevertheless, there are many unanswered questions regarding the specific relationship of hypoxia to the biological behavior of the tumor and how the tumor responds to treatment. For example, little is known about the impact of reoxygenation, or lack thereof, and response to treatment (*20, 21*). It is also becoming increasingly clear that the microenvironmental and metabolic consequences of tumor hypoxia may play an important role in tumor behavior and the outcome of treatment (*22–26*). For example, up-regulation of endothelial growth factor (*24*) or stress proteins (*25*) and the loss of programmed cell death (*23, 26*) could render a tumor more aggressive biologically and decrease the likelihood of tumor control after treatment. The deleterious effects of hypoxia related to these metabolic consequences could influence the outcome of treatment regardless of the clonogenicity of the hypoxic cells. Although the effect of these metabolic factors on the tumor and host may be related to the magnitude of hypoxia throughout the tumor, the longevity of individual hypoxic cells might also influence these events.

In our laboratory, we have been using nitroimidazole markers of hypoxia (*27–31*) as a means to study the manner in which hypoxic tumor cells relate to tumor biology and respond to treatment. Nitroimidazole compounds bind covalently to hypoxic cells *in vitro* (*32*) and *in vivo* (*33*), and the oxygen dependence of marker binding follows kinetics similar to that for radioresistance (*28, 32–34*). Quantification of nitroimidazole binding in tumor biopsies by means of immunohistochemical detection (*2*) or an ELISA (*30*) therefore provides biologically relevant quantitative information regarding tumor hypoxia. The purpose of this study was to estimate the lifetime of tumor cells binding pimonidazole by measuring the longevity of nitroimidazole adducts in canine tumors using immunohistochemical and ELISA methodology.

[1]Author to whom correspondence should be addressed.

TABLE I
Subjects, Tumor Type and Location

Dog number	Tumor type	Tumor location
1	Fibrosarcoma	Limb
2	Fibroma	Head
3	Hemangiosarcoma	Trunk
4	Fibrosarcoma	Head
5	Fibrosarcoma	Head
6	Hemangiopericytoma	Trunk
7	Squamous cell carcinoma	Head
8	Chondrosarcoma	Limb
9	Undifferentiated sarcoma	Limb
10	Squamous cell carcinoma	Head
12	Schwannoma	Trunk
13	Hemangiopericytoma	Limb

MATERIALS AND METHODS

Twelve privately owned dogs bearing a spontaneous solid tumor were studied (Table I). All dogs were undergoing radiation therapy at the College of Veterinary Medicine, North Carolina State University. The procedures used for these animals were approved by the North Carolina State University Institutional Animal Care and Use Committee.

Dogs were given pimonidazole as a hypoxia marker. Pimonidazole hydrochloride [1-[(2-hydroxy-3-piperidinyl)propyl]-2-nitroimidazole hydrochloride] was synthesized according to published procedures (*35*) and characterized by standard chromatographic, spectroscopic and elemental analyses, including analysis for heavy-metal contamination. Pimonidazole was dissolved into 0.9% NaCl, filtered through a 0.2-μm filter to remove bacteria and administered intravenously at a dose of 0.28 g/m^2. Tumors were biopsied using an aseptic technique 24, 48 and 72 h later. At each time, two tissue samples were taken from different geographic regions of the tumor using either a 4-mm-diameter trephine biopsy punch or a 14-gauge biopsy needle.[2] Dogs were under general anesthesia for tumor biopsy, and they were also receiving fractionated irradiation with ^{60}Co γ-ray photons consisting of daily 2.25- or 3.0-Gy fractions. The tumor biopsies were obtained immediately prior to the first three radiation fractions. Tissue from each of the two biopsies was divided; one portion was frozen at –80°C for analysis of the concentration of pimonidazole antigen by ELISA and the other was fixed in formalin followed by ethanol for immunohistochemistry.

The solid-phase antigen for the ELISA was prepared by reductively activating pimonidazole in the presence of thiolated Ficoll produced by an adaptation of published procedures (*36*) using *N*-succinimidyl 3-(2-pyridyldithiol)propionate[3] as the source of latent thiol groups. Bovine serum albumin adducts of tritium-labeled pimonidazole of known specific activity (*37*) were used as a standard for the ELISA. Antibodies were prepared and characterized as described previously (*2, 28*).

The measurement of pimonidazole binding by ELISA was performed in a manner similar to that developed for another 2-nitroimidazole hypoxia marker, CCI-103F (*30*).

For immunohistochemistry, tissues were embedded in paraffin, with the two biopsies from each time placed in one block; this was done to reduce the total number of blocks. Paraffin blocks were serially sectioned at 4-μm intervals; six sequential sections from each 150-μm increment of the block were mounted on slides.[4] Four slides were selected randomly from each biopsy sample for staining. Selection of four slides was based on our previous work wherein quantifying labeled area fraction from four slides from a biopsy was determined to be adequate for estimating labeled area fraction throughout the biopsy (*38*). Slides were stained by a peroxidase-based indirect immunostaining method to visualize pimonidazole antigen. Briefly, sections were exposed to 0.3% hydrogen peroxide in phosphate-buffered saline for 5 min at 40°C, then goat nonimmune serum for 30 min at 40°C, and incubated with a polyclonal rabbit immunoglobulin to pimonidazole-bovine serum albumin adduct for 1 h at 40°C. Biotinylated goat anti-rabbit IgG was applied for 30 min at 40°C followed by incubation with avidin:biotinylated peroxidase complex for 30 min at 40°C. The chromogen used was 1% aminoethyl carbazole in distilled water. Development of the chromogen was allowed to proceed for 20 min. Slides were counterstained in hematoxylin for 1.5 min, then mounted.

Point counting was used to quantify the pimonidazole-labeled area fraction in the slides. Labeled area fraction is defined as the fraction of the total geometric area of the histological section labeled with pimonidazole adducts. A 19-mm-diameter eyepiece micrometer disc[5] was placed into one eyepiece objective of a binocular microscope. The disc contained a 5.0 × 5.0-mm grid, which was subdivided into 25 1.0 × 1.0-mm squares. Each histological section was viewed at a magnification of 100×, and the eyepiece grid subsequently positioned over adjacent regions of the histological section until the entire section had been examined. A gap equivalent to the dimension of one of the 1.0-mm squares was positioned between grid placements to avoid counting the same slide region more than once. When the grid was superimposed on a region of the histological section, the tissue underlying, i.e. "hit" by, the orthogonal intersection of any two lines of the grid was recorded as being either pimonidazole-labeled tumor cell, unlabeled tumor cell or other. The "other" designation included vessels, necrosis, stroma or any other non-tumor cellular matter. The pimonidazole-labeled area fraction in each slide was calculated by:

$$\text{Labeled area fraction} = \frac{\text{Pimonidazole "hits"}}{(\text{Pimonidazole "hits"} + \text{Unlabeled cell "hits"} + \text{Other "hits"})}$$

This method provides an estimate of the pimonidazole-labeled area fraction in the slide without regard for the composition of the unlabeled area. The average pimonidazole-labeled area fraction was calculated for each set of four randomly selected slides. Average pimonidazole-labeled area fraction and antigen concentration (from the ELISA) were then calculated for each biopsy time for each dog.

RESULTS

Pimonidazole adducts were measurable using ELISA in the initial biopsy in all 12 dogs.[6] Adduct concentration ranged from 5.6 to 41.2 μmol antigen/kg tumor. After 72 h the amount of detectable antigen was less than 50% of the initial amount in 5 dogs (dogs 2, 4, 5, 9, 10), the amount decreased to between 50% and 100% of the initial amount in 5 other dogs (dogs 3, 6, 8, 12, 13), and the amount of antigen appeared to increase relative to the initial amount in 2 dogs (dogs 1, 7) (Fig. 1). After 72 h the mean normalized amount of antigen ± SD was 89 ± 87% of the amount present at 24 h. The rate of adduct loss measured by ELISA was greater in tumors characterized by high initial adduct concentration (Fig. 2).

[2]Tru-Cut Biopsy Needle, Baxter Healthcare Corporation, Pharmaceutical Division, Valencia, CA.
[3]Pierce Chemical Company, Rockford, IL.
[4]Probe-on Slides, Fisher Scientific, Pittsburgh, PA.
[5]5 × 5 mm^2 eyepiece micrometer disc, Fisher Scientific, Pittsburgh, PA.
[6]In this paper, dogs are designated as numbers 1 through 10, 12 and 13; there is no dog 11.

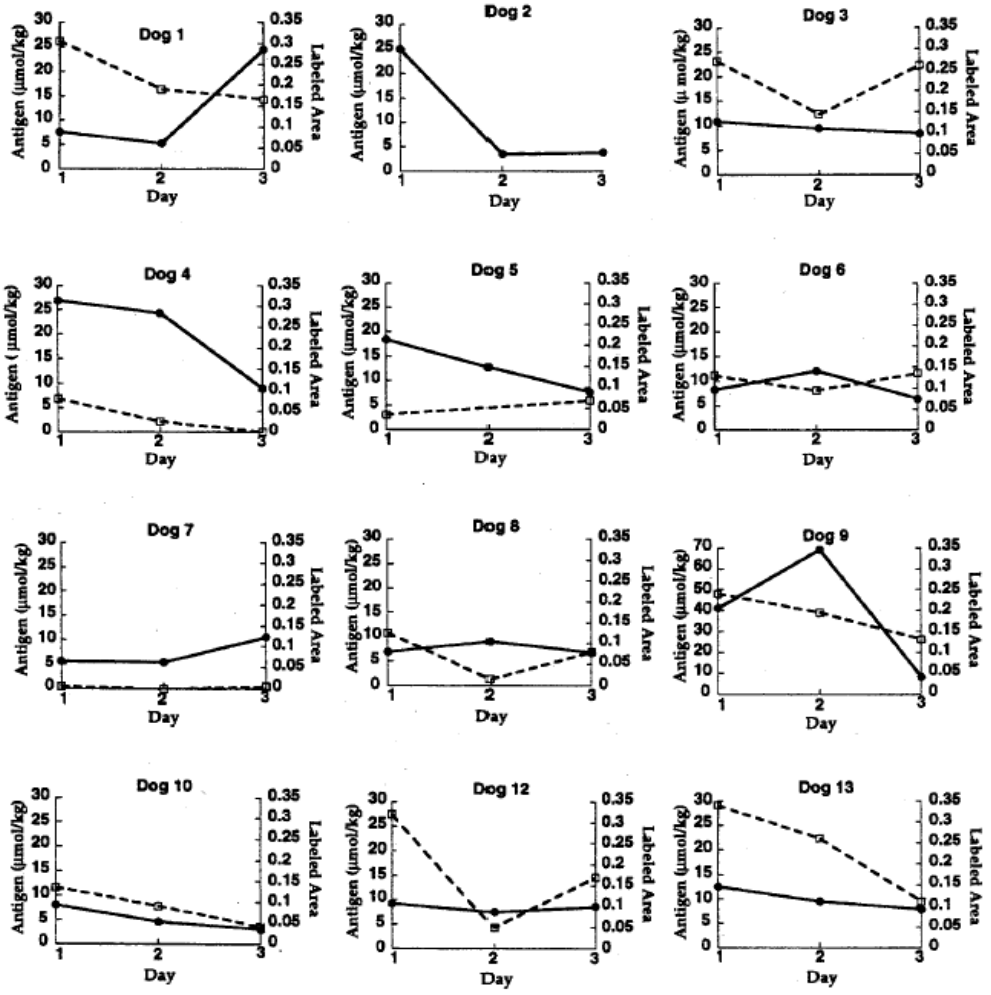

FIG. 1. Average (n = 2 biopsies) pimonidazole antigen concentration (—●—) and labeled area fraction (- -□- -) in biopsies as a function of time after pimonidazole administration.

Immunohistochemically, labeled cells were present in 11 of 12 tumors; in dog 2, tumor cells appeared to be devoid of cytoplasm, and labeling was not detectable in many samples. In the other 11 dogs, labeling was localized primarily in the cytoplasm and labeled cells were typically distant from blood vessels and adjacent to regions of necrosis. Labeled area fraction for each dog in the initial biopsy ranged from 0.005 to 0.34 and tended to decrease over time in 6 dogs (dogs 1, 4, 9, 10, 12, 13) and to remain stable in 4 dogs (dogs 3, 6, 7, 8) and appeared to increase in 1 dog (dog 5) (Fig. 1). Mean labeled area fraction ± SD for all biopsies was 0.18 ± 0.12 in the initial biopsy and 0.11 ± 0.08 after 72 h. After 72 h, the mean normalized labeled area fraction ± SD was 72 ± 53% of the labeled area fraction at 24 h (Fig. 2). There was no relationship in individual tumors between the relative change in antigen concentration and the relative change in labeled area fraction (Fig. 3).

DISCUSSION

The results presented here are interpreted with the assumption that tumor volume did not decrease appreciably during the time when biopsies were being taken. Although tumor volume was not measured, it is our experience that a decrease in the volume of canine tumors during the first 3 days of radiation therapy is highly unusual.

Using ELISA and immunohistochemistry, we identified cells labeled with pimonidazole that persisted for days. These cells did not appear apoptotic or degenerate, and the results can be interpreted to mean that hypoxic cells in

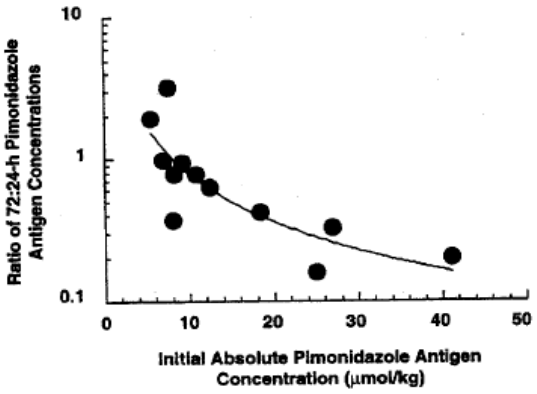

FIG. 2. Pimonidazole antigen concentration at 72 h relative to the concentration at 24 h as a function of the initial absolute pimonidazole antigen concentration. $y = 10.6 \times x^{-1.1}$; $R = 0.65$.

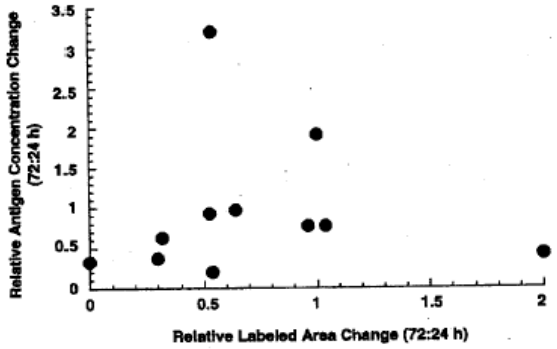

FIG. 3. Relative change in antigen concentration as a function of the relative change in labeled area fraction: 72 h relative to 24 h.

some spontaneous solid tumors persist for days. An alternative explanation for the apparent longevity of hypoxic cells is that apoptosis and reabsorption of pimonidazole-labeled cells by unlabeled aerobic cells migrating into hypoxic zones occurs during the period under consideration. However, the lack of detectable apoptosis in pimonidazole-labeled cells combined with the absence of a band of labeled cells at the interface between aerobic and hypoxic zones which could be expected to develop argues against such a concept.

In contrast to data in this paper suggesting that the lifetime of hypoxic cells may be of the order of days, data on cell kinetics from studies of tumors with a corded architecture are consistent with hypoxic tumor cells having a lifetime of only a few hours (*39–41*). In corded tumors there is an orderly progression of cells from oxygenated to hypoxic to necrotic compartments. However, in studies of ascites tumors (*42–44*) and cells *in vitro* (*45, 46*), it has been shown that hypoxic cells may exist for prolonged periods. This was particularly true for nondividing cells and cells in which metabolism was primarily that of anaerobic glycolysis. In spontaneous tumors the architecture is rarely corded and anaerobic glycolysis is common, so the studies from murine corded tumors are perhaps more relevant to our studies and consistent with our conclusion that hypoxic cell viability can be of the order of days in spontaneous tumors.

It is possible that cells which were hypoxic at the time of the nitroimidazole injection, i.e. labeled cells, subsequently became reoxygenated during the study period. Thus we are not certain that persistently labeled cells are evidence of persistently hypoxic cells. If reoxygenation had occurred, however, it would be expected that metabolism of the nitroimidazole adduct would have occurred; this may explain the more pronounced decrease in intratumoral adduct concentration observed in some tumors. Nevertheless, the existence of persistently nitroimidazole-labeled cells suggests that hypoxic cells are not lost rapidly from spontaneous tumors. We have assessed the kinetics of reoxygenation in canine tumors and found variability in reoxygenation between subjects and little change in pretreatment tumor oxygenation levels in most dogs (*21*). In that study, however, global changes in nitroimidazole binding were assessed rather than individual cells.

We used two methods to quantify tumor hypoxia, ELISA and immunohistochemistry. In a comparison of pimonidazole antigen quantified by ELISA to labeled area fraction quantified by point counting 24 h after administration of pimonidazole, there is poor correlation (Fig. 4). This is expected. When immunohistochemistry is used to quantify pimonidazole binding, cells are classified as labeled or unlabeled, but the degree of labeling is not given. Under hypoxic conditions, pimonidazole is irreversibly reduced by the transfer of two or more electrons and becomes covalently bound to cellular molecules. The immunohistochemical procedure results in visualization of bound drug regardless of its concentration above some very small threshold quantity. On the other hand, the absolute amount of pimonidazole antigen bound to a tumor, or in a biopsy, will be a function of factors other than the number of cells which are hypoxic. First, there are probably gradients in oxygenation throughout the tumor which will result in variation in the amount of pimonidazole bound. These gradients could be present in the setting of diffusion-limited hypoxia (*11*), but perfusion-limited hypoxia occurring on a transient basis (*12, 13*) could also result in oxygenation gradients. The extent of hypoxia marker binding occurring as a result of diffusion-limited compared to perfusion-limited hypoxia is unknown. It is reasonable that the time course of some types of acute hypoxia may allow for detectable hypoxia marker binding. Our analysis of the pattern of binding of CCI-103F in spontaneous canine tumors, however, is most consistent with most labeling being due to diffusion-limited hypoxia, as bound adducts are typically found in regions where mitotic activity is sparse and necrosis is common (*3*). Also, in canine tumors we have assessed

the relationship between hypoxia marker binding and proliferation, measured by detection of PCNA expression, and find little overlap in hypoxic compared to proliferating cells (*47*). Second, although no data are available, it is possible there may be differences in the reductase activity per hypoxic cell in tumors with the same level of overall tumor hypoxia. This could lead to a discrepancy between the amount of nitroimidazole bound and labeled area fraction between tumors with the same distribution of cellular hypoxia. Finally, there is variation in the pharmacokinetics of the distribution and elimination of 2-nitroimidazoles. For example, in two injections of CCI-103F in each of 8 dogs (16 injections), the mean area under the curve for plasma concentration as a function of time was 548 μmol h/l, but the coefficient of variation (CV) was 39% (*21*). Clearance was even more variable, with a mean of 5.6 l/h and a CV of 79.1% (*21*). Variation in pharmacokinetics of the handling of 2-nitroimidazoles has also been documented in humans (*48*). Thus ELISA probably will not be useful for quantifying clinically important hypoxia within an individual tumor, but ELISA will be useful for serially following changes in oxygenation within an individual tumor or with multiple injections of the marker (*21*).

Previously, quantification of tumor hypoxia as a predictor of tumor response to treatment has been criticized because it is not known whether the labeled hypoxic cells were clonogenic. Certainly, if the effect of the hypoxic cells on tumor radiocurability was related only to radioresistance, the clonogenicity of hypoxic cells surviving a course of radiation therapy would be of great importance. However, with recent knowledge regarding the possible adverse effects of hypoxia not related to clonogenicity, such as upregulation of endothelial growth factor (*24*) or stress proteins (*25*) and the absence of programmed cell death (*23, 26*), it is possible that the persistence of cells which were hypoxic at the time of marker injection may be detrimental regardless of their clonogenicity. It is also possible that these chronically labeled hypoxic cells might become reoxygenated at some point during fractionated irradiation and then, if clonogenic, could result in poor treatment response. In other words, the results of this work, which suggest that hypoxic cells may be long-lived, mean that the window of opportunity for reoxygenation might be relatively long. More information in this area is needed before conclusions can be drawn.

In some dogs either the labeled area fraction measured immunohistochemically or adduct concentration measured by ELISA was increased on day 2 or 3 compared to day 1 (Fig. 1). Given the short plasma half-life of pimonidazole in the dog (mean = 1.5 h, SD = 1.0 h, $n = 9$; unpublished data), this apparent increase in marker binding over periods of 24 to 48 h is likely due to sampling error. We evaluated the intratumoral variation in labeling of the hypoxia marker CCI-103F (determined immunohistochemically) and using a computer model have examined the number of biopsies taken with regard to the accuracy of estimating labeled area

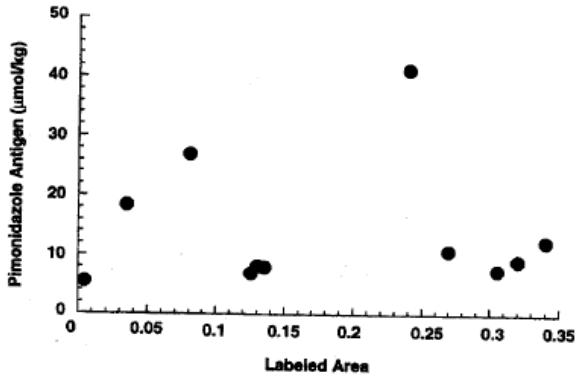

FIG. 4. Day 1 pimonidazole adduct concentration measured by ELISA as a function of day 1 labeled area fraction measured immunohistochemically.

fraction from limited sampling. We found that the accuracy of estimating CCI-103F-labeled area fraction in a tumor increased as the number of biopsies increased from two to four and also as overall intratumoral labeled area fraction decreased. When four random samples (biopsies) were taken, there was essentially a 90% chance that the estimated labeled area fraction would be within an absolute range of ±0.10 of the true labeled area fraction (*49*). When two random samples (biopsies) were taken, there was essentially a 70 to 90% chance that the estimate of overall labeled area fraction would be within 0.10 of the true labeled area fraction, with accuracy being greater when overall labeled area fraction was lower (*49*). We have not examined the intratumoral variation in pimonidazole labeling, but we have no reason to believe there would be a difference between CCI-103F and pimonidazole. Taking four biopsies in this study would have increased the precision of the results, but our data suggest that results obtained from two biopsies can also provide useful information. Nevertheless, results from this study must be tempered with the knowledge that more precise information would have been obtained had more biopsies been taken. Four biopsies were not taken in this study because results from the sampling error study were not yet available.

The finding of more rapid loss of adduct in tumors with higher initial concentration of adduct (Fig. 2) was unexpected. Loss of adduct signal could be due to either cell loss or metabolism of the adduct. In a rapidly proliferating tumor with a high cell loss factor, cells may become hypoxic because of oxygen consumption or because they quickly become positioned beyond the diffusion distance of oxygen. Initial adduct concentration in such cells might be high, but detectable adduct could decline rapidly because of cell loss or, as noted above, reoxygenation. The relationship between hypoxia and proliferation has been assessed in human sarcomas, and the most rapidly proliferating tumor cells were found in the most poorly oxygenated tumors

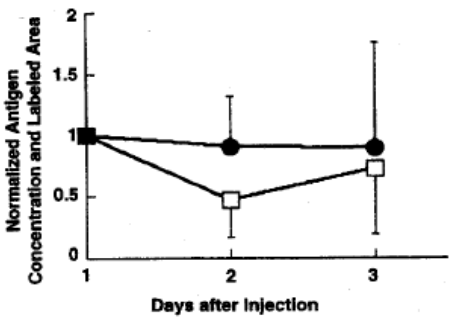

FIG. 5. Normalized antigen concentration (●) and labeled area fraction (□) as a function of time after pimonidazole administration. Bars = standard deviation.

(*50*). However, in our work in human cervix carcinomas, more rapidly proliferating tumors were better oxygenated (*51*). In canine tumors, initial information regarding hypoxic and proliferating populations suggests that there is minimal overlap between the two populations (*47*). More work needs to be done regarding the relationship between proliferation and hypoxia.

Another explanation for the relationship between initial concentration of adduct and the rate of loss of adduct is that tumors with high initial concentrations of adduct are tumors with high redox capabilities and consequently are tumors that are very effective at metabolizing the adduct. At this time the cause for the relationship between the concentration and loss of adduct is unknown, but this relationship could have a bearing on tumor behavior or response to treatment.

We found no relationship between rate of adduct decay and decline in the labeled area fraction in a biopsy in individual tumors (Fig. 3). This is not surprising, as a tumor could metabolize the pimonidazole adduct, resulting in a decline in signal detected with ELISA, but still retain sufficient adduct for detection using immunohistochemical methods. In the histochemical scoring system, cells are graded as labeled or not, and no attempt to quantify the concentration of labeled adduct per cell is made.

Previously, we quantified the rate of decay of another 2-nitroimidazole hypoxia marker, CCI-103F, in canine tumors (*21*). For CCI-103F, a mean initial adduct half-life of 19 h was estimated. The decay of CCI-103F adducts from canine tumors therefore appears to be considerably more rapid than the decay of pimonidazole adducts (Fig. 5), where the mean initial adduct half-life is longer than 3 days. The reason for the apparent difference in the rates of loss of CCI-103F and pimonidazole adduct is uncertain. It seems unlikely that CCI-103F and pimonidazole bind to different sets of proteins that possess differences in inherent stability due to the presence of stabilizing or destabilizing N-terminal amino acids or due to their subcellular location (*52*). It seems more likely that any protein adducted with CCI-103F is more readily recognized and targeted for proteolytic digestion than is a protein adducted with pimonidazole. This difference might lie in the respective side-chain structures that are known to be retained when 2-nitroimidazole hypoxia markers bind to proteins (*53*). For example, hydrophobic peptide sequences in partially denatured proteins are considered to be preferential targets for hydrolysis with possible freeing of end groups that are destabilized with respect to the ubiquitin-dependent pathway to digestion (*54*). CCI-103F, with an octanol/water partition coefficient of 20, is more hydrophobic than pimonidazole, which has a partition coefficient of 8 for the free base and an even lower partition coefficient at physiological pH due to the protonated piperidine side-chain in pimonidazole (pK_a 8.6). It remains to be seen if such differences account for the differences observed for the kinetics of hypoxia marker loss in tumor cells.

In summary, hypoxic cells may exist for days in some solid tumors. These results should be interpreted as defining a lower limit for the lifetime of cells which are hypoxic at the time of administration of markers of hypoxia. Adduct metabolism creates some problems in interpretation of data using an ELISA, but data from point counting are highly supportive of the above conclusion. There appear to be differences in longevity of pimonidazole-binding cells between tumors, and this may be important in a prognostic sense. Relatively long-lived hypoxic cells could have an effect on tumor behavior or response to treatment which is unrelated to their clonogenicity. The lifetime of hypoxic cells may be an important parameter to study in attempting to unravel the complicated effect of tumor hypoxia on treatment response.

ACKNOWLEDGMENTS

This research supported in part by the State of North Carolina and Grant CA 50995 (Raleigh) from the Department of Health and Human Services.

Received: October 3, 1996; accepted: March 4, 1997

REFERENCES

1. J. Moulder and S. Rockwell, Hypoxic fractions of solid tumors: Experimental techniques, methods of analysis, and a survey of existing data. *Int. J. Radiat. Oncol. Biol. Phys.* **10**, 695–712 (1984).
2. J. M. Cline, E. M. Zeman, D. E. Thrall and J. A. Raleigh, Immunohistochemical detection of a hypoxia marker in spontaneous canine tumours. *Br. J. Cancer* **62**, 925–931 (1990).
3. J. M. Cline, D. E. Thrall, G. L. Rosner and J. A. Raleigh, Distribution of the hypoxia marker CCI-103F in canine tumors. *Int. J. Radiat. Oncol. Biol. Phys.* **28**, 921–933 (1994).
4. R. A. Gatenby, H. B. Kessler, J. S. Rosenblum, L. R. Coia, P. J. Moldofsky, W. H. Hartz and G. J. Broder, Oxygen distribution in squamous cell carcinoma metastases and its relationship in outcome of radiation therapy. *Int. J. Radiat. Oncol. Biol. Phys.* **14**, 831–838 (1988).
5. D. M. Brizel, G. L. Rosner, J. Harrelson, L. R. Prosnitz and M. W. Dewhirst, Pretreatment oxygenation profiles of human soft tissue sarcomas. *Int. J. Radiat. Oncol. Biol. Phys.* **30**, 635–642 (1994).

6. D. Brizel, G. Rosner, L. Prosnitz and M. Dewhirst, Patterns and variability of tumor oxygenation in human soft tissue sarcomas, cervical carcinomas and lymph node metastases. *Int. J. Radiat. Oncol. Biol. Phys.* **32**, 1121–1125 (1995).

7. M. Höckel, K. Schlenger, C. Knoop and P. Vaupel, Oxygenation of carcinomas of the uterine cervix: Evaluation by computerized O_2 tension measurements. *Cancer Res.* **51**, 6098–6102 (1991).

8. E. Lartigau, A. Le Ridant, P. Lambin, P. Weeger, L. Martin, R. Sigal, A. Lusinchi, B. Lubonski, F. Eschwege and M. Guichard, Oxygenation of head and neck tumors. *Cancer* **71**, 2319–2325 (1993).

9. M. Nordsmark, S. Bentzen and J. Overgaard, Measurement of human tumour oxygenation status by a polarographic needle electrode. An analysis of inter- and intratumor heterogeneity. *Acta Oncol.* **33**, 383–389 (1994).

10. P. Vaupel, K. Schlenger, C. Knoop and M. Höckel, Oxygenation of human tumors: Evaluation of tissue oxygen distribution in breast cancers by computerized O_2 tension measurements. *Cancer Res.* **51**, 3316–3322 (1991).

11. R. H. Thomlinson and L. H. Gray, The histological structure of some human lung cancers and the possible implications for radiotherapy. *Br. J. Cancer* **9**, 539–549 (1955).

12. J. M. Brown, Evidence for acutely hypoxic cells in mouse tumours and a possible mechanism of reoxygenation. *Br. J. Cancer* **52**, 650–656 (1979).

13. D. Chaplin, P. Olive and R. E. Durand, Intermittent blood flow in a murine tumor: Radiobiological effects. *Cancer Res.* **47**, 597–601 (1987).

14. M. W. Dewhirst, T. W. Secomb, E. T. Ong, R. Hsu and J. F. Gross, Determination of local oxygen consumption rates in tumors. *Cancer Res.* **54**, 3333–3336 (1994).

15. E. J. Hall, *Radiobiology for the Radiologist*, 3rd ed., pp. 137–160. J. B. Lippincott, Philadelphia, 1988.

16. J. A. Raleigh, M. W. Dewhirst and D. E. Thrall, Measuring tumor hypoxia. *Semin. Radiat. Oncol.* **6**, 37–45 (1996).

17. M. Höckel, C. Knoop, K. Schlenger, B. Vorndran, E. Baussmann, M. Mitze, P. Knapstein and P. Vaupel, Intratumoral pO_2 predicts survival in advanced cancer of the uterine cervix. *Radiother. Oncol.* **26**, 45–50 (1993).

18. M. Nordsmark, M. Overgaard and J. Overgaard, Pretreatment oxygenation predicts radiation response in advanced squamous cell carcinoma of the head and neck. *Radiother. Oncol.* **41**, 31–39 (1996).

19. M. Höckel, K. Schlenger, M. Mitze, U. Schäffer and P. Vaupel, Hypoxia and radiation response in human tumors. *Semin. Radiat. Oncol.* **6**, 3–9 (1996).

20. L. van Putten and R. Kallman, Tumour reoxygenation during fractionated radiotherapy: Studies with a transplantable osteosarcoma. *Eur. J. Cancer* **4**, 173–182 (1968).

21. D. E. Thrall, M. C. McEntee, J. M. Cline and J. A. Raleigh, ELISA quantification of CCI-103F in canine tumors prior to and during irradiation. *Int. J. Radiat. Oncol. Biol. Phys.* **28**, 649–659 (1994).

22. R. E. Durand, The influence of microenvironmental factors on the activity of radiation and drugs. *Int. J. Radiat. Oncol. Biol. Phys.* **20**, 253–258 (1991).

23. T. G. Graeber, C. Osmanian, T. Jacks, D. E. Housman, C. J. Koch, S. W. Lowe and A. J. Giaccia, Hypoxia-mediated selection of cells with diminished apoptotic potential in solid tumours. *Nature* **379**, 88–91 (1996).

24. D. Shweiki, A. Itin, D. Soffer and E. Keshet, Vascular endothelial growth factor induced by hypoxia may mediate hypoxia-initiated angiogenesis. *Nature* **359**, 843–845 (1992).

25. R. M. Sutherland, W. A. Ausserer, B. J. Murphy and K. R. Laderoute, Tumor hypoxia and heterogeneity: Challenges and opportunities for the future. *Semin. Radiat. Oncol.* **6**, 59–70 (1996).

26. A. Giaccia, Hypoxic stress proteins: Survival of the fittest. *Semin. Radiat. Oncol.* **6**, 46–58 (1996).

27. J. A. Raleigh, A. J. Franko, E. O. Treiber, J. A. Lunt and P. S. Allen, Covalent binding of fluorinated 2-nitroimidazole to EMT-6 tumors in BALB/C mice. Detection by F-19 nuclear magnetic resonance at 2.35T. *Int. J. Radiat. Oncol. Biol. Phys.* **12**, 1249–1251 (1986).

28. J. A. Raleigh, G. G. Viller, A. J. Franko, C. J. Koch, A. F. Fuciarelli and D. A. Kelly, Fluorescence immunohistochemical detection of hypoxic cells in spheroids and tumours. *Br. J. Cancer* **56**, 395–400 (1987).

29. J. A. Raleigh, A. J. Franko, E. O. Treiber, J. A. Lunt and P. S. Allen, Development of an *in vivo* ^{19}F magnetic resonance method for measuring oxygen deficiency in tumors. *Magn. Reson. Med.* **22**, 451–466 (1991).

30. J. A. Raleigh, J. K. La Dine, J. M. Cline and D. E. Thrall, An enzyme-linked immunosorbent assay for hypoxia marker binding in tumours. *Br. J. Cancer* **69**, 66–71 (1994).

31. J. D. Chapman, A. J. Franko and J. Sharplin, A marker for hypoxic cells in tumours with potential clinical applicability. *Br. J. Cancer* **43**, 546–550 (1981).

32. J. D. Chapman, K. Baer and J. Lee, Characteristics of the metabolism-induced binding of misonidazole to hypoxic mammalian cells. *Cancer Res.* **43**, 1523–1528 (1983).

33. R. C. Urtasun, J. D. Chapman, J. A. Raleigh, A. J. Franko and C. J. Koch, Binding of ^3H-misonidazole to solid human tumors as a measure of tumor hypoxia. *Int. J. Radiat. Oncol. Biol. Phys.* **12**, 1263–1267 (1986).

34. W. Mueller-Kleisser, H. Schlenger, S. Walenta, M. Gross, U. Karbach, U. Hoecker and P. Vaupel, Pathophysiological approaches to identifying tumor hypoxia in patients. *Radiother. Oncol.* **20** (Suppl.), 21–28 (1991).

35. C. E. Smithen and C. R. Hardy, The chemistry of nitroimidazole hypoxic cell radiosensitizers. In *Advanced Topics on Radiosensitizers of Hypoxic Cells* (A. Breccia, C. Rimondi and G. E. Adams, Eds.), pp. 1–47. Plenum Press, New York, 1982.

36. J. K. Inman, Thymus-independent antigens: The preparation of covalent hapten–Ficoll conjugates. *J. Immunol.* **114**, 704–709 (1975).

37. J. A. Raleigh and C. H. Koch, Importance of thiols in the reductive binding of 2-nitroimidazoles to macromolecules. *Biochem. Pharmacol.* **40**, 2457–2464 (1990).

38. D. E. Thrall, G. L. Rosner, C. Azuma, M. C. McEntee and J. A. Raleigh, Hypoxia marker labeling in tumor biopsies: Quantification of labeling variation and criteria for biopsy sectioning. *Radiother. Oncol.*, in press.

39. I. F. Tannock, Oxygen diffusion and the distribution of cellular radiosensitivity in tumours. *Br. J. Radiol.* **45**, 515–524 (1972).

40. D. G. Hirst and J. Denekamp, Tumour cell proliferation in relation to the vasculature. *Cell Tissue Kinet.* **12**, 31–42 (1979).

41. I. Tannock, Oxygen distribution in tumours: Influence on cell proliferation and implications for tumour therapy. *Adv. Exp. Med. Biol.* **75**, 597–603 (1976).

42. I. F. Tannock, A comparison of cell proliferation parameters in solid and ascites Ehrlich tumors. *Cancer Res.* **29**, 1527–1534 (1969).

43. I. F. Tannock and G. G. Steel, Tumor growth and cell kinetics in chronically hypoxic animals. *J. Natl. Cancer Inst.* **45**, 123–133 (1970).

44. U. Del Monte, Changes in oxygen tension in Yoshida ascites hepatoma during growth. *Proc. Exp. Biol. Med.* **125**, 853–856 (1967).

45. R. W. Brosemer and W. J. Rutter, The effect of oxygen tension on the growth and metabolism of a mammalian cell. *Exp. Cell Res.* **25**, 101–113 (1961).

46. G. E. Gifford, Some effects of anaerobiosis on the growth and metabolism of HeLa cells. *Exp. Cell Res.* **31**, 113–118 (1963).

47. J. A. Raleigh, E. M. Zeman, D. P. Calkins, M. C. McEntee and D. E. Thrall, Distribution of hypoxia and proliferation associated markers in spontaneous canine tumors. *Acta Oncol.* **34**, 345–349 (1995).

48. C. N. Coleman, T. H. Wasserman, R. C. Urtasun, J. Halsey, V. K. Hirst, S. Hancock and T. L. Phillips, Phase I trial of the hypoxic cell radiosensitizer SR-2508: The results of the five to six week drug schedule. *Int. J. Radiat. Oncol. Biol. Phys.* **12**, 1105–1108 (1986).

49. J. M. Cline, G. L. Rosner, J. A. Raleigh and D. E. Thrall, Quantification of CCI-103F labeling heterogeneity in canine solid tumors. *Int. J. Radiat. Oncol. Biol. Phys.*, in press.

50. M. Nordsmark, M. Hoyer, J. Keller, O. S. Nielsen, O. M. Jensen and J. Overgaard, The relationship between tumor oxygenation and cell proliferation in human soft tissue sarcomas. *Int. J. Radiat. Oncol. Biol. Phys.* **35**, 701–708 (1996).

51. A. S. Kennedy, J. A. Raleigh, G. M. Perez, D. P. Calkins, D. E. Thrall, D. B. Novotny and M. A. Varia, Proliferation and hypoxia in human squamous cell carcinoma of the cervix: First report of combined immunohistochemical assays. *Int. J. Radiat. Oncol. Biol. Phys.* **37**, 897–905 (1997).

52. A. Hershko and A. Ciechanover, The ubiquitin system for protein degradation. *Annu. Rev. Biochem.* **61**, 761–807 (1992).

53. J. A. Raleigh, A. J. Franko, C. J. Koch and J. L. Born, Binding of misonidazole to hypoxic cells in monolayer and spheroid culture: Evidence that a side-chain label is bound as efficiently as a ring label. *Br. J. Cancer* **51**, 229–235 (1985).

54. B. Alberts, D. Bray, J. Lewis, M. Raff, K. Roberts and J. D. Watson, *Molecular Biology of the Cell*, 2nd ed. Garland Publishing, New York, 1989.

The paper has been cited in twenty two peer-reviewed papers (Bussink et al., 2000a; Bussink et al., 2000b; Bussink et al., 2000c; Danielsson et al., 2003; Durand and Sham, 1998; Haroon et al., 2000; Hayashi et al., 2003; Hockel and Vaupel, 2001; Kaanders et al., 2002c; Koukourakis et al., 2001; Ljungkvist et al., 2000; Nordsmark et al., 2003; Raleigh et al., 1999; Raleigh et al., 2001; Raleigh et al., 1998a; Raleigh et al., 2000; Rijken et al., 2002; Rijken et al., 2000; Rofstad and Maseide, 1999; Seddon et al., 2002; Wyffels et al., 2000; Wykoff et al., 2000).

References

Bussink, J., J.H. Kaanders, A.M. Strik, and A.J. van der Kogel. 2000a. Effects of nicotinamide and carbogen on oxygenation in human tumor xenografts measured with luminescense based fiber-optic probes. Radiother Oncol 57:21-30.

Bussink, J., J.H. Kaanders, A.M. Strik, B. Vojnovic, and A.J. van Der Kogel. 2000b. Optical sensor-based oxygen tension measurements correspond with hypoxia marker binding in three human tumor xenograft lines [In Process Citation]. Radiat Res 154:547-55.

Bussink, J., J.H. Kaanders, P.F. Rijken, J.A. Raleigh, and A.J. Van der Kogel. 2000c. Changes in blood perfusion and hypoxia after irradiation of a human squamous cell carcinoma xenograft tumor line. Radiat Res 153:398-404.

Danielsson, B.R., A.C. Skold, A. Johansson, B. Dillner, and B. Blomgren. 2003. Teratogenicity by the hERG potassium channel blocking drug almokalant: use of hypoxia marker gives evidence for a hypoxia-related mechanism mediated via embryonic arrhythmia. Toxicology and Applied Pharmacology 193:168-176.

Durand, R.E., and E. Sham. 1998. The lifetime of hypoxic human tumor cells. Int J Radiat Oncol Biol Phys 42:711-5.

Haroon, Z.A., J.A. Raleigh, C.S. Greenberg, and M.W. Dewhirst. 2000. Early wound healing exhibits cytokine surge without evidence of hypoxia. Ann Surg 231:137-47.

Hayashi, K., J.D. Frank, Z.L. Hao, G.M. Schamberger, M.D. Markel, P.A. Manley, and P. Muir. 2003. Evaluation of ligament fibroblast viability in ruptured cranial cruciate ligament of dogs. American Journal of Veterinary Research 64:1010-1016.

Hockel, M., and P. Vaupel. 2001. Tumor hypoxia: Definitions and current clinical, biologic, and molecular aspects. Journal of the National Cancer Institute 93:266-276.

Kaanders, J.H., K.I. Wijffels, H.A. Marres, A.S. Ljungkvist, L.A. Pop, F.J. van den Hoogen, P.C. de Wilde, J. Bussink, J.A. Raleigh, and A.J. van der Kogel. 2002. Pimonidazole binding and tumor vascularity predict for treatment outcome in head and neck cancer. Cancer Res 62:7066-74.

Koukourakis, M.I., A. Giatromanolaki, E. Sivridis, K. Simopoulos, J. Pastorek, C.C. Wykoff, K.C. Gatter, and A.L. Harris. 2001. Hypoxia-regulated carbonic anhydrase-9 (CA9) relates to poor vascularization and resistance of squamous cell head and neck cancer to chemoradiotherapy. Clin Cancer Res 7:3399-403.

Ljungkvist, A.S., J. Bussink, P.F. Rijken, J.A. Raleigh, J. Denekamp, and A.J. Van Der Kogel. 2000. Changes in tumor hypoxia measured with a double hypoxic marker technique. Int J Radiat Oncol Biol Phys 48:1529-38.

Nordsmark, M., J. Loncaster, C. Aquino-Parsons, S.C. Chou, M. Ladekarl, H. Havsteen, J.C. Lindegaard, S.E. Davidson, M. Varia, C. West, R. Hunter, J. Overgaard, and J.A. Raleigh. 2003. Measurements of hypoxia using pimonidazole and polarographic oxygen-sensitive electrodes in human cervix carcinomas. Radiother Oncol 67:35-44.

Raleigh, J.A., S.C. Chou, G.E. Arteel, and M.R. Horsman. 1999. Comparisons among pimonidazole binding, oxygen electrode measurements, and radiation response in C3H mouse tumors. Radiat Res 151:580-9.

Raleigh, J.A., S.C. Chou, E.L. Bono, D.E. Thrall, and M.A. Varia. 2001. Semiquantitative immunohistochemical analysis for hypoxia in human tumors. Int J Radiat Oncol Biol Phys 49:569-74.

Raleigh, J.A., S.C. Chou, L. Tables, S. Suchindran, M.A. Varia, and M.R. Horsman. 1998. Relationship of hypoxia to metallothionein expression in murine tumors. Int J Radiat Oncol Biol Phys 42:727-30.

Raleigh, J.A., S.C. Chou, D.P. Calkins-Adams, C.A. Ballenger, D.B. Novotny, and M.A. Varia. 2000. A clinical study of hypoxia and metallothionein protein expression in squamous cell carcinomas. Clinical Cancer Research 6:855-862.

Rijken, P.F., J.P. Peters, and A.J. Van der Kogel. 2002. Quantitative analysis of varying profiles of hypoxia in relation to functional vessels in different human glioma xenograft lines. Radiat Res 157:626-32.

Rijken, P.F., H.J. Bernsen, J.P. Peters, R.J. Hodgkiss, J.A. Raleigh, and A.J. van der Kogel. 2000. Spatial relationship between hypoxia and the (perfused) vascular network in a human glioma xenograft: a quantitative multi-parameter analysis. Int J Radiat Oncol Biol Phys 48:571-82.

Rofstad, E.K., and K. Maseide. 1999. Radiobiological and immunohistochemical assessment of hypoxia in human melanoma xenografts: acute and chronic hypoxia in individual tumours. Int J Radiat Biol 75:1377-93.

Seddon, B.M., R.J. Maxwell, D.J. Honess, R. Grimshaw, F. Raynaud, G.M. Tozer, and P. Workman. 2002. Validation of the fluorinated 2-nitroimidazole SR-4554 as a noninvasive hypoxia marker detected by magnetic resonance spectroscopy. Clinical Cancer Research 8:2323-2335.

Wyffels, K., J. Kaanders, P. Rijken, J. Bussink, F.J.A. van den Hoogen, H.A.M. Marres, P.C.M. de Wilde, J.A. Raleigh, and A.J. van der Kogel. 2000. Vascular architecture and hypoxic profiles in human head and neck squamous cell carcinomas. British Journal of Cancer 83:674-683.

Wykoff, C.C., N.J.P. Beasley, P.H. Watson, K.J. Turner, J. Pastorek, A. Sibtain, G.D. Wilson, H. Turley, K.L. Talks, P.H. Maxwell, C.W. Pugh, P.J. Ratcliffe, and A.L. Harris. 2000. Hypoxia-inducible expression of tumor-associated carbonic anhydrases. Cancer Research 60:7075-7083.

CHAPTER III: Study of the Kinetics of Pimonidazole Adduct Formation in Canine Tumors

Purpose

This section was focused on investigating the timing of PIMO adduct formation. The information will be useful to decide timing of infusion and tissue harvest for studies especially in a clinical setting. Tissue was collected 20-minutes and 24-hours after PIMO intravenous infusion. 24-hour is the conventional sampling time and if results from 20-minute are the same, then there would be considerable flexibility in the timing of tissue sampling after PIMO injection. This timing study is actually comparing to achieve maximum exposure versus partial exposure at 20 minutes exposure from a single intravenous administration of PIMO. Since the half-life of the PIMO is 1.5 hours, there is more than 50 % of the PIMO in the blood circulation at the 20-minute sampling time. This study could also address hypoxia labeling with PIMO between acutely and chronically hypoxic tumor cells. If there is no difference in PIMO labeling between the two time points, we may be able to conclude that PIMO adduct formation occurs rapidly and there is no detectable acute hypoxia adduct formation based on hypoxia marker method.

Hypothesis

There is no difference in PIMO labeled area fractions between 20-minute and 24-hour sample time because labeling is almost complete within 20 minutes to detect chronically hypoxic cells and fraction of acute hypoxia may difficult to detect either due to low acute hypoxia fraction in canine spontaneous tumor or not enough exposure to effectively label acute hypoxic cells with a single PIMO administration.

Materials and Methods

Ten dogs were initially entered in this study. PIMO was administered intravenously 10 minutes after sedation. Anesthesia was induced with intravenous propofol 10 minutes after administration of PIMO; dogs were breathing room air. The tumor was biopsied 20 minutes after administration of PIMO. After biopsy, dogs underwent general anesthesia using inhalant isoflurane in 100% O_2 for the 1^{st} dose of radiation therapy. The biopsy procedure was repeated at 24 hours after administration of PIMO under general anesthesia (isoflurane

and 100% O_2). To minimize intratumor variability in labeling, biopsy samples were obtained from 4 geographically different sites at each sampling time.

Time table of experiment

-10 min: Sedation (0.05 mg/kg of oxymorphone iv)

0 min: PIMO iv infusion

10 min: Induction of anesthesia by propofol (2 mg/kg iv) breathing with room air and preparation for biopsy

20 min: 1st biopsy

24 hours: 2nd biopsy

Sample preparation

Biopsied samples were immediately placed in cold 10 % formalin on ice for fixation followed by standard analysis as described in chapter I.

Statistical analysis

For the tumors examined, the Wilcoxon Signed-Rank Test or one sample Student's t test for the equality of two means were used to test for significant differences in hypoxia labeling between time 20-minute and 24-hour. The 5% significance level was used as the criterion for statistical significance.

Results

Ten dogs received PIMO and underwent tumor biopsy. In one dog, the tumor samples did not contain an adequate number of tumor cells to include the study due to the, fibrotic, and infiltrative nature of the tumor. 9 dogs were included for analysis (tables 3.1 and 3.2). PIMO labeling was observed in all 9 dogs. There was wide variation in PIMO labeled area fraction between the samples (intratumoral variation) at the two times, even though there was considerably less variation within a given time.

There was no significant difference between the 20-minute and 24-hour PIMO labeled area fractions based on the Wilcoxon Signed-Rank Test or the one-sample Student's t test. The uncorrected labeled area fractions had less variability and less difference between 20-minute and 24-hour than the corrected labeled area fractions.

1. Wilcoxon test for uncorrected labeled fraction (24-hour minus 20-minute): p=1 and Student's t test for uncorrected labeled fraction (24-hour minus 20-minute): p=0.868
2. Wilcoxon test for corrected labeled fraction (24-hour minus 20-minute): p=0.301 and Student's t test for corrected labeled fraction (24-hour minus 20-minute): p=0.214

The intensity of the labeling appeared heavier at 24 hours in some dogs although there was no quantification. The level of background staining was very light at the 20 minute sampling time and about the same or little heavier at 24 hours.

Visually the mean uncorrected PIMO labeled area fraction at 24 hours was decreased in 4 dogs, unchanged in 1 dog and increased in 4 dogs compared to the PIMO labeled area fraction at 20 minutes post sampling (figure 3.1, 3.3 and 3.4). The mean corrected labeled area fraction at 24 hours was decreased in 2 dogs, unchanged in 3 dogs and increased in 4 dogs compared to the PIMO labeled area fraction at 20 minutes post sampling (figure 3.2, 3.5 and 3.6). The trend of change was not always consistent with uncorrected and corrected data. Uncorrected PIMO labeled area analysis contains other than tumor cells which suggests structural heterogeneity plus difference of the hypoxia fraction in two time points. The structure of the tissue contains labeled tumor cells, unlabeled tumor cells, other supportive structure and necrosis which are not likely to change dramatically between 20-minutes versus 24-hours. The differences between 20-minutes and 24-hours in uncorrected PIMO labeled area may not be true change in the hypoxia fraction, but could be reflection of natural intratumoral heterogeneity which can be seen by sampling multiple biopsy tissues.

Corrected PIMO labeled area fraction might be better indicator of true tumor hypoxia fraction where evaluation was only done with the ratio of labeled tumor cells to all tumor cells. Corrected PIMO labeled area fraction of hypoxia may be better parameter than uncorrected PIMO labeled area fraction to correlate with other tumor markers. On the other hand, comparing uncorrected PIMO labeled area fraction and pO_2 measurement by O_2 electrode might be reasonable because both methods sample from entire tumor without any discrimination of tissue.

Table 3.1 Summary of PIMO labeled area fraction between 20 minutes and 24 hours sampling time in 9 dogs

	Uncorrected PIMO		Corrected PIMO	
Time	20 min	24 hr	20 min	24 hr
Sample size	9	9	9	9
Average	0.259	0.267	0.313	0.438
St. Dev.	0.193	0.138	0.229	0.223
Minimum	0.036	0.053	0.053	0.205
Median	0.191	0.257	0.216	0.372
Maximum	0.655	0.536	0.704	0.799

Parameters were calculated based on total on 16 sections from 4 biopsy samples (4 section from each biopsy samples). Uncorrected PIMO: Uncorrected PIMO labeled area fraction, Corrected PIMO: Corrected PIMO labeled area fraction.

Table 3.2 Summary of difference (24 hr minus 20 minutes) in PIMO labeled area fraction in 9 dogs

	Uncorrected PIMO	Corrected PIMO
Sample size	9	9
Average	0.008	0.125
St. Dev.	0.147	0.278
Minimum	-0.195	-0.248
Median	-0.02	0.044
Maximum	0.23	0.746

Parameters were calculated based on total on 16 sections from 4 biopsy samples (4 section from each biopsy samples). Average of difference were calculated using equation: mean PIMO labeled fraction (24 hours – 20 minutes). Uncorrected PIMO: Uncorrected PIMO labeled area fraction, Corrected PIMO: Corrected PIMO labeled area fraction.

Captions for Chapter III figures

Figure 3.1 Uncorrected PIMO labeled area fraction (slides within biopsies) between 20-minute and 24-hour after PIMO injection. Each symbol represents uncorrected PIMO labeled area fraction in a section of biopsy. There were four-biopsy tissue from each tumor at each time point, and four sections from each biopsy. Total 16 sections of tissue were analyzed to calculate means of uncorrected PIMO labeled area for each tumor and time point. The bar represents the means for each time point. Each graph shows a single dog, n=9. Symbols at 20-minute xxxx ▵▵▵▵ ○○○○ ++++ and at 24-hour ▽▽▽▽ ▩▩▩▩ ◇◇◇◇ ✳✳✳✳.

Figure 3.2 Corrected PIMO labeled area fraction (slides within biopsies) between 20-minute and 24-hour after PIMO injection. Each symbol represents corrected PIMO labeled area fraction in a section of biopsy. There were four-biopsy tissue from each tumor at each time point, and four sections from each biopsy. Total 16 sections of tissue were analyzed to calculate means of corrected PIMO labeled area for each tumor and time point. The bar represents the means for each time point. Each graph shows a single dog, n=9. Symbols at 20-minute xxxx ▵▵▵▵ ○○○○ ++++ and at 24-hour ▽▽▽▽ ▩▩▩▩ ◇◇◇◇ ✳✳✳✳.

Figure 3.3 and 3.4 Uncorrected PIMO labeled area fraction (biopsy means) between 20-minute and 24-hour after PIMO injection. Each symbol represents a mean of uncorrected PIMO labeled area fraction in a biopsy. There were four-biopsy tissue from each tumor at each time point, and four sections from each biopsy. Total 16 sections of tissue were analyzed to calculate means of uncorrected PIMO labeled area for each tumor and time point. The bar represents the means for each time point. Each graph shows a single dog, n=9. Variable scale (figure 3.3) and same scale (figure 3.4) for all dogs on Y-axis for each dog.

Figure 3.5 and 3.6 Corrected PIMO labeled area fraction (biopsy means) between 20-minute and 24-hour after PIMO injection. Each symbol represents a mean of corrected PIMO labeled area fraction in a biopsy. There were four-biopsy tissue from

each tumor at each time point, and four sections from each biopsy. Total 16 sections of tissue were analyzed to calculate means of corrected PIMO labeled area for each tumor and time point. The bar represents the means for each time point. Each graph shows a single dog, n=9. Variable scale (figure 3.3) and same scale (figure 3.4) for all dogs on Y-axis for each dog.

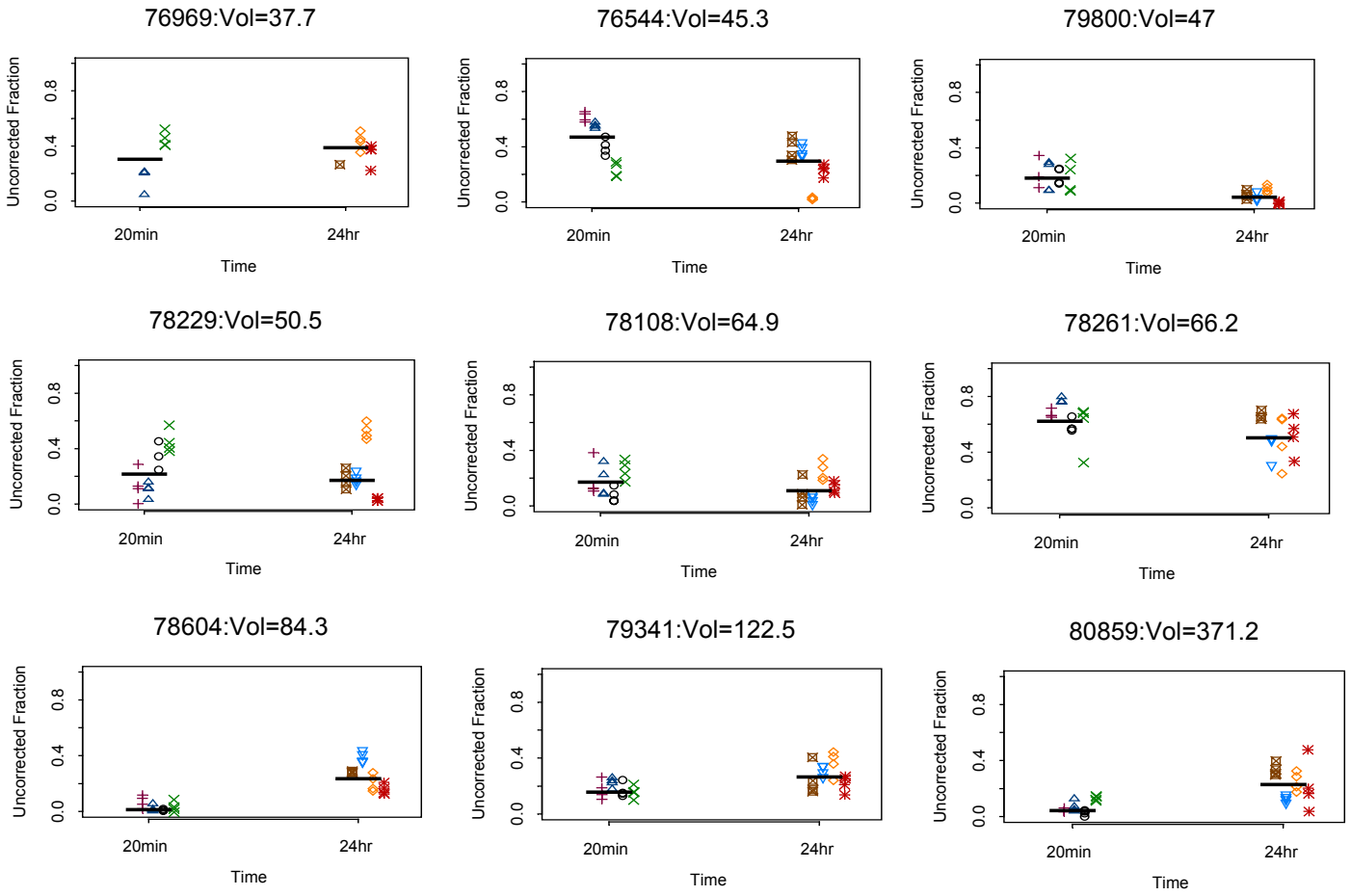

Figure 3.1 Uncorrected PIMO labeled area fraction (slides within biopsies)

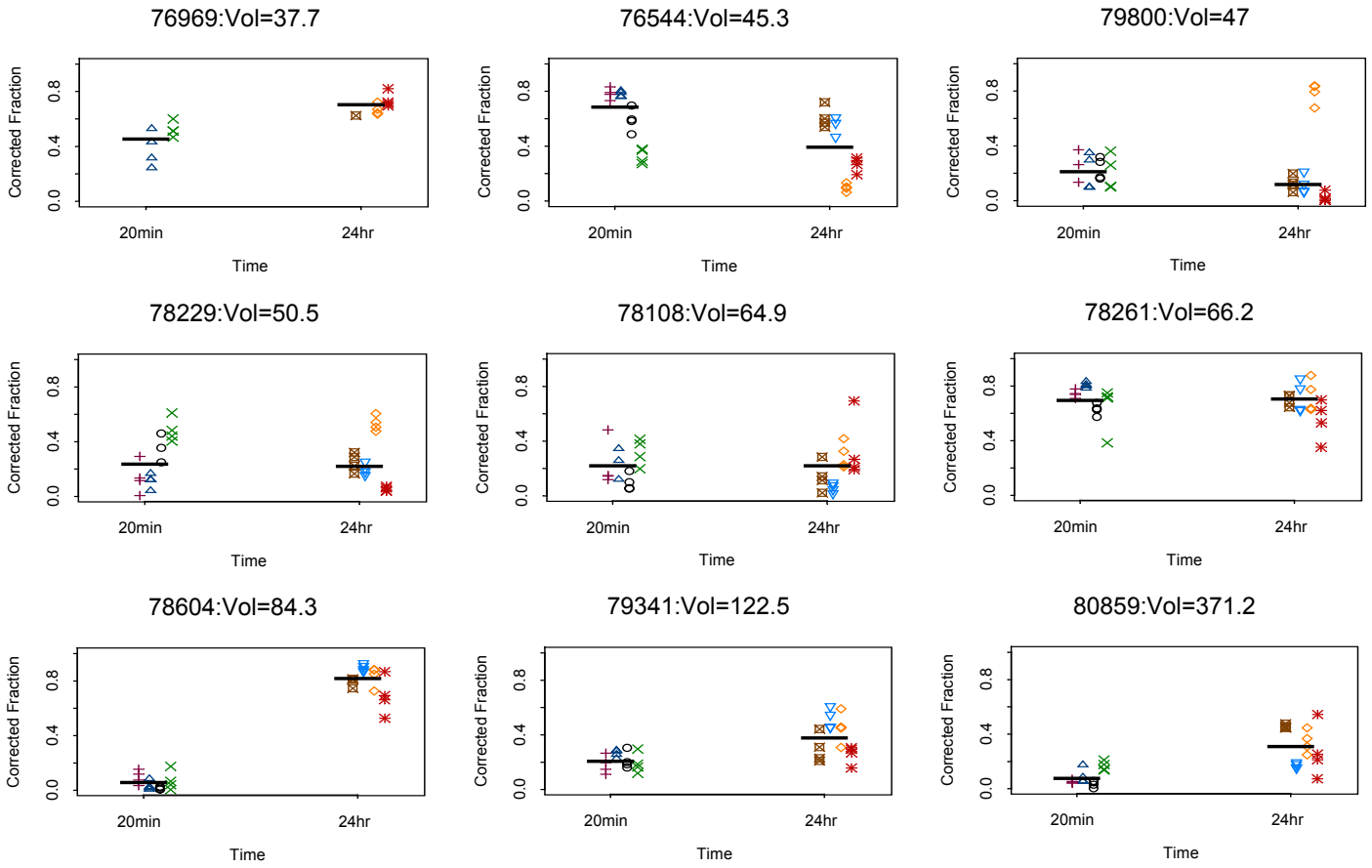

Figure 3.2 Corrected PIMO labeled area fraction (slides within biopsies)

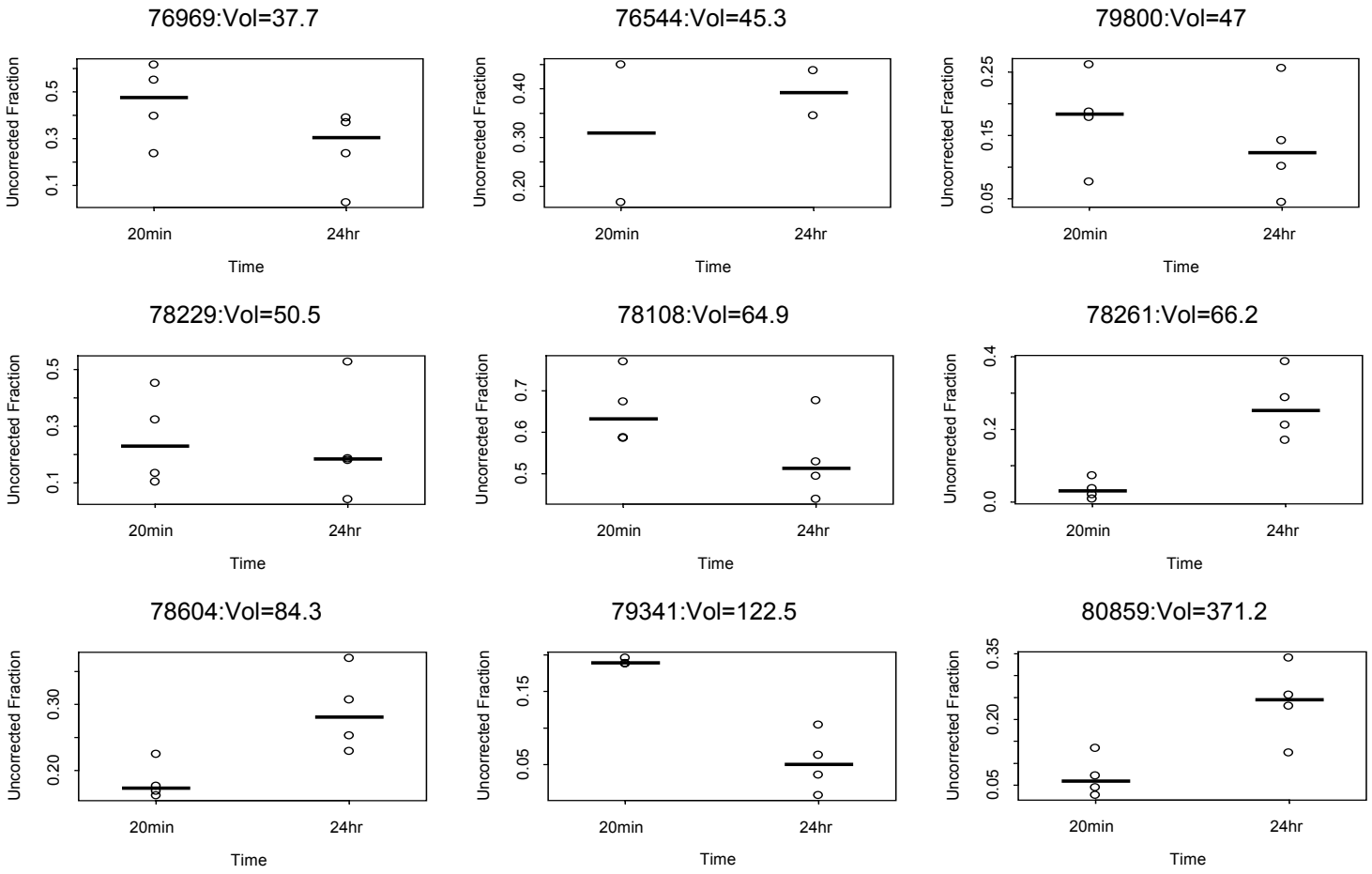

Figure 3.3 Uncorrected PIMO labeled area fraction (biopsy means)

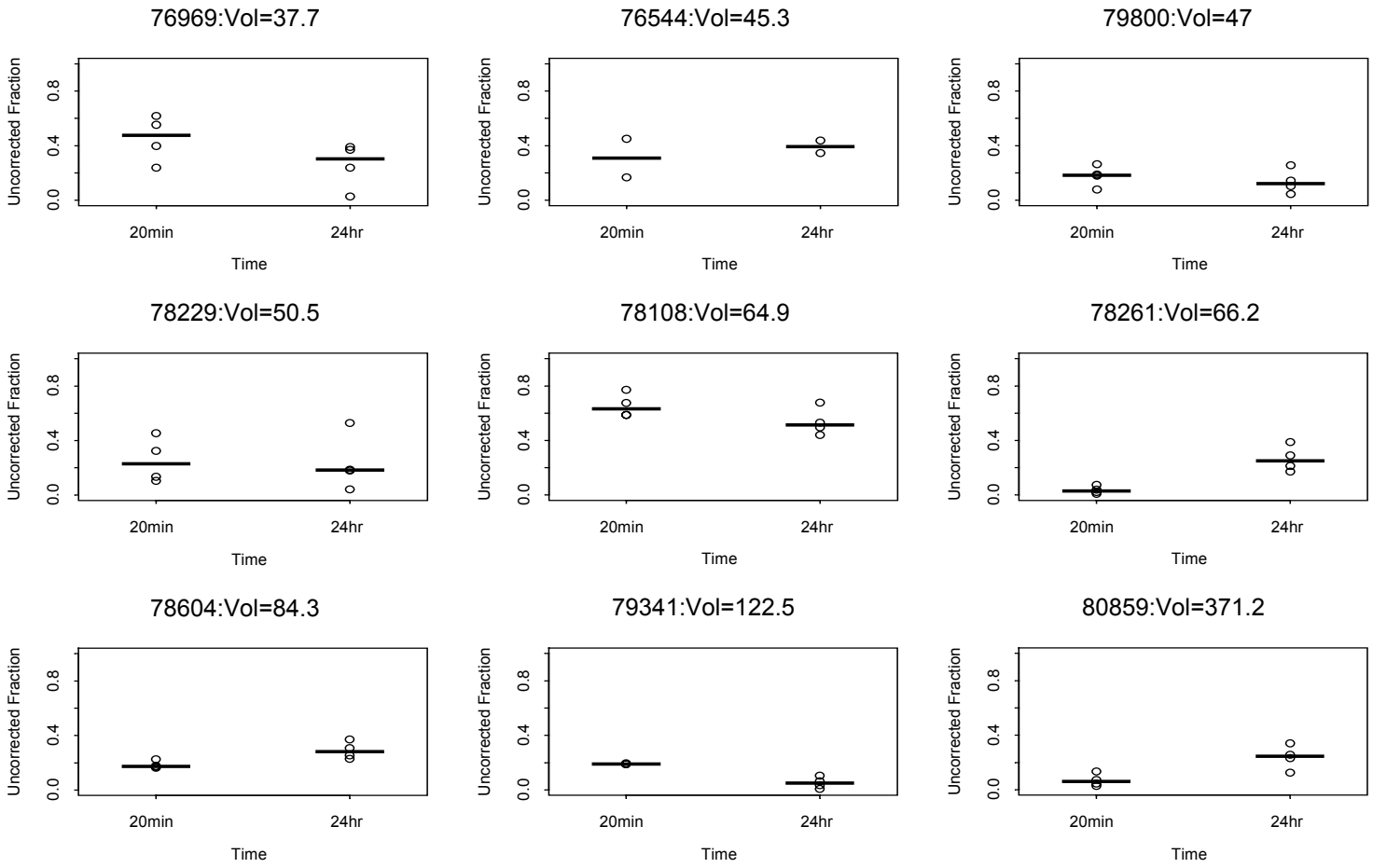

Figure 3.4 Uncorrected PIMO labeled area fraction (biopsy means)

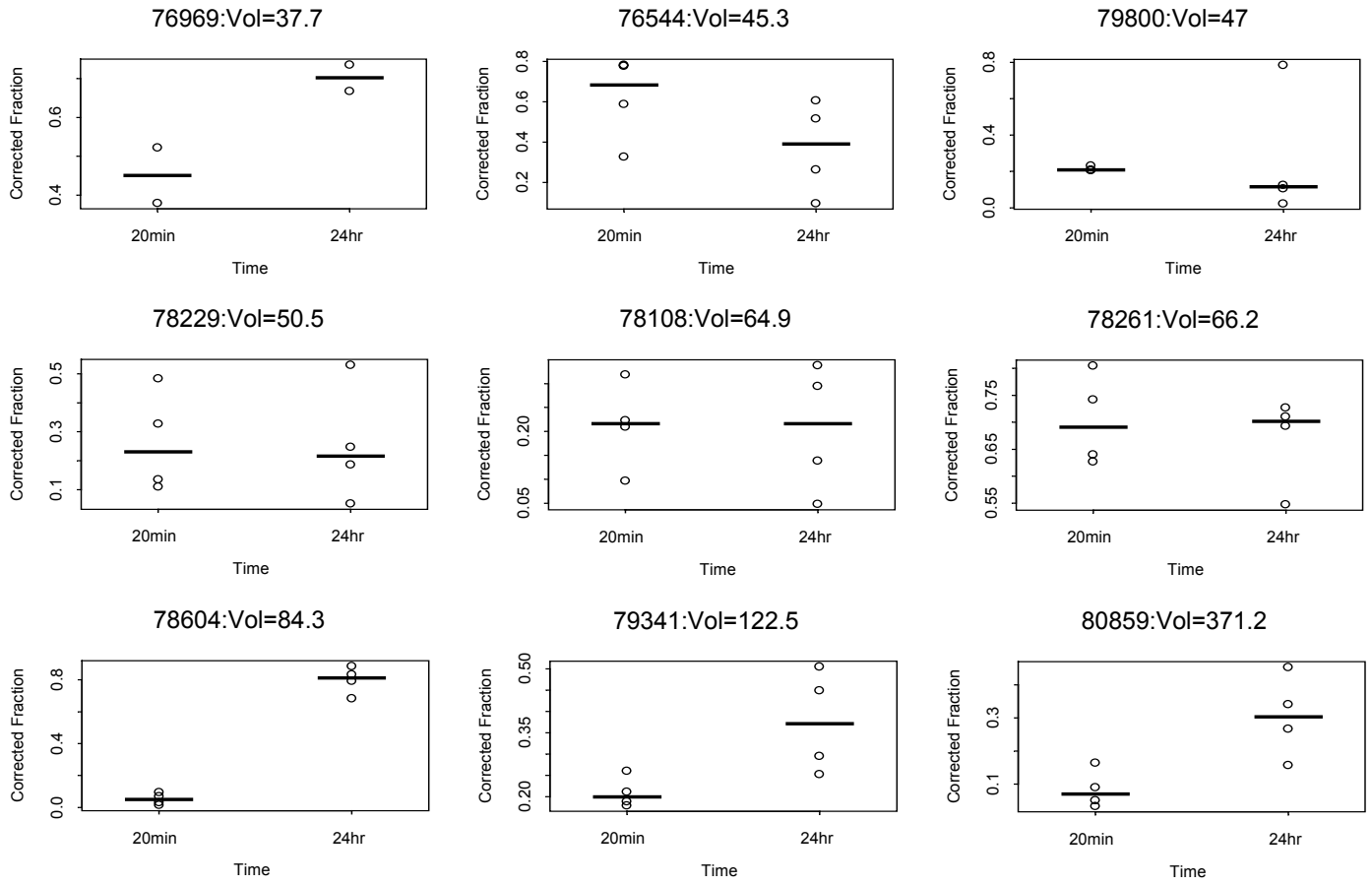

Figure 3.5 Corrected PIMO labeled area fraction (biopsy means)

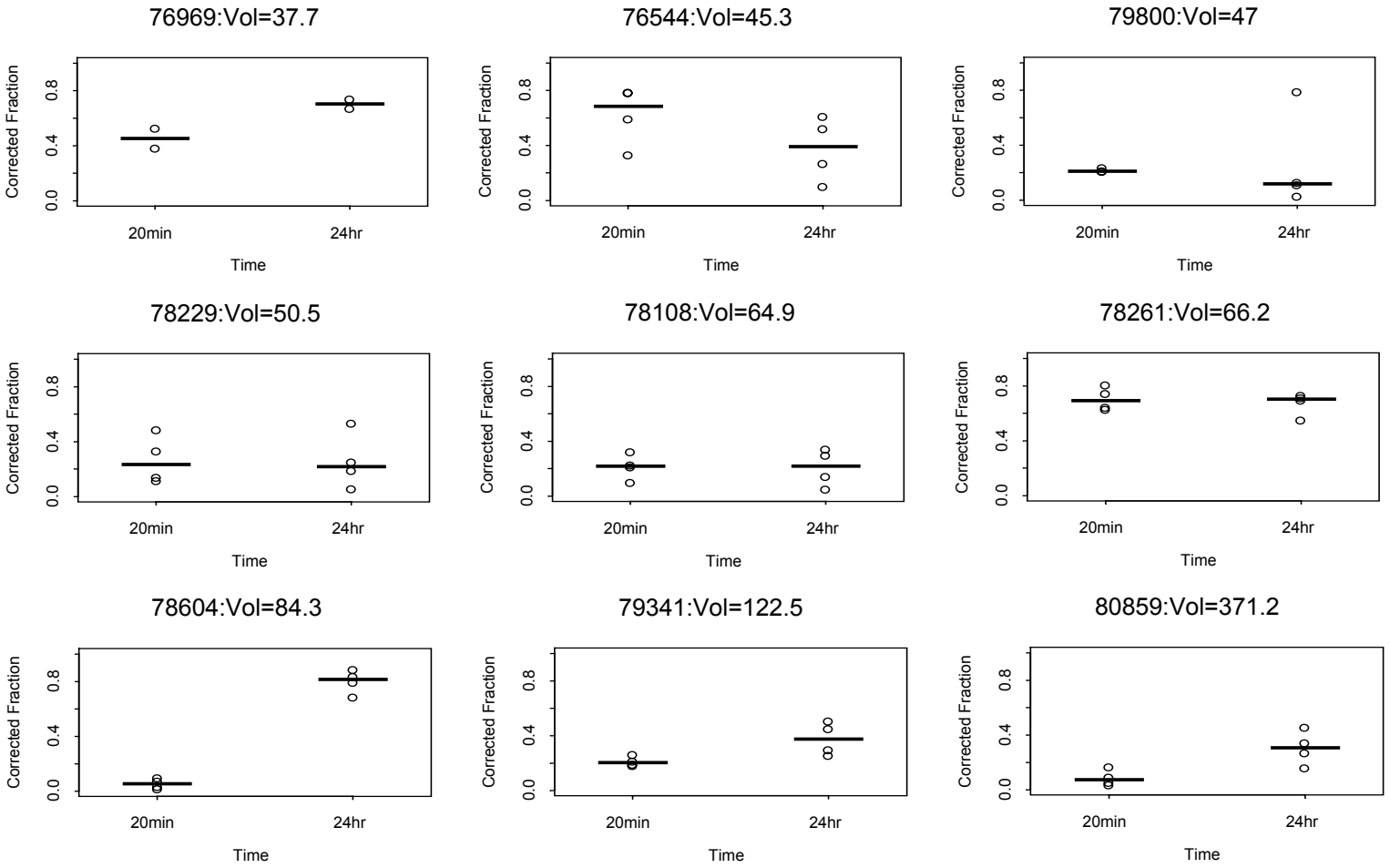

Figure 3.6 Corrected PIMO labeled area fraction (biopsy means)

Discussion

In our study we controlled high level of PIMO concentration in blood and limit exposure time to investigate PIMO adduct formation in canine spontaneous tumors.

Adduct formation was clearly occurring within 20 minutes after injection of PIMO. Importantly, rapid harvest and immediate fixation in cold formalin eliminated measurable levels of non-specific background or artificial binging at the edge of tissues.

These results suggest there is great flexibility of PIMO exposure time, and sampling and preparation methods. Although there seems to have been rapid binding, some tissue samples clearly had less binding at 20 minutes suggesting that more than 20 minutes labeling time might be needed to give maximum exposure and development of adduct formation. On the other hand, the labeling fraction was similar between 20-minutes versus 24-hours suggesting that the majority of adduct formation was completed within 20 minutes and PIMO mainly labeled chronically hypoxic tumor cells. This result is consistent with the observations from using other nitroimidazole markers where 30 minutes was adequate for adduct formation (Busch et al., 2000; Yang et al., 1999).

In recent human tumor studies, biopsies were taken 1.5 to 4 hours after PIMO infusion, which was most likely adequate for maximal labeling. The biopsies were immediately fixed in liquid nitrogen and there was not excessive background binding (Bennewith et al., 2002; Wijffels et al., 2000).

The different trend between uncorrected and corrected PIMO labeled factions suggest that both are important values to examine. Both uncorrected and corrected fractions showed heterogeneity of tumor hypoxia. Uncorrected fractions showed more reflection of structural heterogeneity of the tumor and corrected fractions seems to be useful to examine the true hypoxia fraction in the tumor.

PIMO is known to be excellent hypoxia marker for chronic diffusion limited hypoxia. The question if PIMO can be a good marker for acute hypoxia may be difficult to answer in this study setting where detection of acutely hypoxic fraction might be depending on the occurrence of acute hypoxia, and exposure time of PIMO *in vivo*. The IHC based study will not differentiate hypoxic labeling between acute and chronic hypoxia. It may be possible to estimate acutely hypoxic fraction using two nitroimidazole hypoxia markers.

Application of oral PIMO was investigated in a study in mice bearing tumor (Bennewith et al., 2002). The study showed that the labeling tumor cells by oral administration was gradually

increased with oral PIMO consumption up to 12 to 96 hours and final binding was greater than a single injection of PIMO. They observed that hypoxia fraction identified at 6-hour time point was almost equal to a single i.p or i.v. injection of PIMO in mice. Plasma elimination half-life of PIMO is around 0.5 hour in mice. It may be taken 6 hours to accumulate comparative amount of adduct in tumor by oral administration. They observed that both the number of the PIMO labeled cells and intensity of the labeled cells were increased with time which may suggest chronically hypoxic cells keep accumulating PIMO adducts with continuous exposure, but it is not known if they reach plateau level of PIMO accumulation. Also they suggested that additional labeling seen after 6-hours, which may be related to mainly detection of acute hypoxia in the tumor. Overall labeling at 12-hour oral administration was almost doubled (30% labeling) than previous defined hypoxic fraction in the tumor. It may indicate this tumor contains 15% chronic hypoxic tumor cells and 15% acutely hypoxic cells. Oral administration usually gives a lower level of drug concentration in blood, but it was evident that continuous lower level of prolonged PIMO exposure provided the same or greater degree of PIMO adduct formation in mice.

Hypoxia labeling with PIMO has great flexibility to apply in different circumstances. PIMO can be administered in several routes such as intravenous injection or orally in the near future. PIMO does not require high blood concentration to detect tumor hypoxia although extended exposure rather than single bolus administration may be required maximum detection of acute and chronic hypoxic cells. Pharmacokinetic study of oral PIMO should be done to investigate the dosage, timing and duration of application, and drug formula to control plasma concentration and exposure time in humans and dogs.

Evaluation of acute versus chronic hypoxia might be possible by using two hypoxia markers in canine spontaneous tumors. Oral PIMO can be used for continuous exposure to evaluate “chronic + acute” hypoxia fraction and other markers such as CCI-103F can be injected a single time to evaluate “chronic” hypoxia. The difference should be the “acute hypoxia fraction”. These hypoxia markers were already proven to be effective to label tumor hypoxia in dogs. PIMO and CCI-103F labeling was tested in one dog (dog#61200 IR) in our study and two marker labelings were consistent in the same regions on the contiguous sections without any cross-reaction of the two primary antibodies.

Another application of oral or continuous PIMO administration could be for therapeutic application as a hypoxia-targeting agent. Classic usage of PIMO as a radiosensitizer failed

to improve therapeutic response because it required high drug concentration *in vivo,* results in unacceptable toxicity. Oral PIMO studies in mice showed that continuous administration provided greater labeling over time. There results suggest that a greater therapeutic benefit without major toxicity may be achieved by targeting grater number of hypoxic tumor cells, including chronic and more importantly acute hypoxic cells, with low level prolonged PIMO exposure.

In conclusion there was no significant difference in PIMO labeled area fraction between 20-minutes and 24-hours when analyzed over all dogs. This, suggests a single injection of PIMO detects mainly chronically hypoxic tumor cells at 20-minutes and the chronic hypoxia fraction is no different at 24-hours. However, there were differences in individual dogs between 20 min and 24 hrs. This individual dog difference may be due to differences in acute hypoxia between the two time points or slower formation of PIMO adducts in these dogs. Due to the small sample size (n=9), the results need to be carefully interpreted and larger scale study may add more detailed information on this subject. Multiple hypoxia marker assays may provide important information on tumor hypoxia and the relationship between chronic and acute hypoxia. Further research is warranted to address the importance of acute hypoxia on cancer progression and treatment response.

References

Bennewith, K.L., J.A. Raleigh, and R.E. Durand. 2002. Orally Administered Pimonidazole to Label Hypoxic Tumor Cells. Cancer Res 62:6827-6830.

Busch, T.M., S.M. Hahn, S.M. Evans, and C.J. Koch. 2000. Depletion of tumor oxygenation during photodynamic therapy: detection by the hypoxia marker EF3 [2-(2-nitroimidazol-1[H]-yl)-N-(3,3,3-trifluoropropyl)acetamide]. Cancer Res 60:2636-42.

Wijffels, K.I., J.H. Kaanders, P.F. Rijken, J. Bussink, F.J. van den Hoogen, H.A. Marres, P.C. de Wilde, J.A. Raleigh, and A.J. van der Kogel. 2000. Vascular architecture and hypoxic profiles in human head and neck squamous cell carcinomas. Br J Cancer 83:674-83.

Yang, D.J., S. Ilgan, T. Higuchi, F. Zareneyrizi, C.S. Oh, C.W. Liu, E.E. Kim, and D.A. Podoloff. 1999. Noninvasive assessment of tumor hypoxia with 99mTc labeled metronidazole. Pharm Res 16:743-50.

CHAPTER IV: The Relationship Between Tumor Hypoxia and Proliferation

Purpose

To characterize the relationship between tumor hypoxia and proliferation in spontaneous canine soft tissue tumors.

Introduction

Tumor hypoxia and proliferation are two factors that may have a profound influence on tumor progression. These two factors could provide assessments of different aspects of the tumor. Tumor hypoxia is an environmental factor and proliferation is an intrinsic factor and these two may be or may not be related. By combining the hypoxia and proliferation information it is possible to study more than one aspect of tumor biology and this may enhance the ability to predict treatment response and individualize cancer treatment. Also when targeted therapy is applied to specific tumor characteristics such as hypoxia, it is important to know other aspects of the tumor, such as proliferation behaves. Studying the relationship between hypoxia and proliferation will provide important information which may be useful for selection of appropriate cancer therapy, and monitoring during and after treatment.

Oxygen is required for cells to survive, maintain function and grow. Although tumor proliferation is generally considered to be less active under hypoxic conditions, hypoxia induces expression of genes that are known to promote cell proliferation (Shannon et al., 2003).

Tissue oxygenation depends on the status of the O_2 supply through the vascular network and O_2 consumption in the tissue. O_2 consumption is higher in actively proliferating cells. Rapidly dividing tumor cells have almost five times more O_2 consumption compared to slower dividing cells (Freyer, 1994). Increased O_2 consumption may result in tissue oxygenation becoming lower.

There have been several attempts to examine the relationship between hypoxia and proliferation. In a small study of human patients with soft tissue sarcoma the most rapidly proliferating tumors were found to be the most hypoxic based on needle electrode measurements (Nordsmark et al., 1996b). Although a clear relationship between tumor hypoxia and proliferation within tumors has not been found, we observed in our laboratory a

potential regional relationship between tumor hypoxia and proliferation when small areas of histologic sections were studied using CCI-103F as the hypoxia marker and PCNA as the proliferation marker. This study was done in spontaneous canine tumors.

The observations were:

1. Limited overlap of the two markers
2. Proliferating cells were located close to vessels
3. Hypoxic tumor cells were located away from vessels and at the edge of necrosis
4. There were cells not labeled for either markers
5. There were scattered labeled cells for either markers

Double marker staining for PIMO and PCNA also showed a similar pattern with limited overlap between two markers (figure 4.1).

Tumor heterogeneity is a major obstacle with regard to the use of biological markers in spontaneous tumors. Our sampling and analysis are based on previous data (Cline et al., 1997), where it was determined that the accuracy of hypoxia estimates increased with increasing number of biopsies. With four random biopsies, a good representation of the whole tumor was obtained with the hypoxia marker, CCI-103F.

In this study, we are studying the overall relationship between hypoxia and proliferation in spontaneous canine tumors using immunohistochemistry to identify two markers, a hypoxia marker, PIMO and a proliferation marker, PCNA in contiguous tumor sections.

Hypothesis

Hypoxia may be more pronounced in rapidly proliferating tumors because of increased oxygen consumption.

Materials and Methods

Fifty dogs were included in this study. There has been a parallel study at University of North Carolina, School of Medicine, Chapel Hill, NC in human patients with carcinomas (Kennedy et al., 1997; Varia et al., 1998). Thirty of these dogs were also in a Canine Soft Tissue Sarcoma Project to investigate the effects of hyperthermia dose on radiation response of soft tissue sarcomas (table 1.1). Intensive follow up information will be available on these

dogs when the trial is complete and data generated in this thesis regarding hypoxia and proliferation will be examined for a relationship to outcome.

There were 44 soft tissue sarcomas (33 low-grade (included 1 fibroma) versus 11 high-grade), 1 hemangiosarcoma, and 5 carcinomas. Other parameters tabulated included tumor volume, site of tumor (extremity, frank, and head) and signalment. PIMO was used as a hypoxia marker and PCNA was used as a proliferation marker (figure 4.2). Tumors were biopsied 24 hours after intravenous injection of PIMO to estimate overall pretreatment hypoxia and proliferating fractions. Mean and median uncorrected and corrected hypoxia labeled area fractions (PIMO labeled area fraction), and mean and median PCNA labeled fractions (heavily stained cells only/500 tumor cells) were calculated for each tumor. PCNA labeled cell fraction is defined as fraction of the tumor cells heavily immunostained for PCNA in 500 individual tumor cells at the intersection of a grid in randomly selected fields. Detailed methods were described in chapter I.

Statistical Analysis

Mixed-effects analysis of variance (Searle et al., 1992) was used to examine the relationships between PIMO area labeled fraction, PCNA and tumor volume, accounting for within-tumor and between-tumor variation. Analyses were carried out in S-Plus (1999). Since the data consisted of fractions that are constrained to lie between zero and one, we transformed the data to make the data range over from minus infinity to plus infinity. The transformation was the logarithm of the fraction divided by one minus the fraction, which is similar to a logistic transform (Govindarajulu, 1988). The transformed data were analyzed using a random-effects analysis of variance. The (residual) error variance was decomposed with a nested model: a patient component and a biopsy-within-patient component.

Other study variables were also examined. Associations between overall degree of labeling (PIMO and PCNA) and tumor volume by site, type, and grade were assessed by the Wilcoxon Rank Sum Test. Tests were two-sided, the significance level was 0.05 and SPSS statistical software program was used.

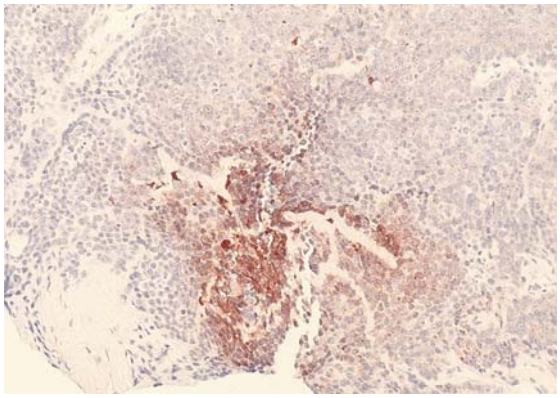

Figure 4.1a PIMO-IHC

Region of PIMO labeled area staining (red labeled areas):
PIMO is area labeling

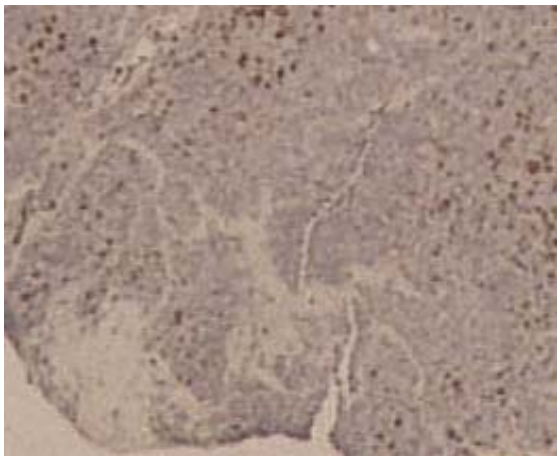

Figure4.1b PCNA-IHC

Intensive nuclear labeling for PCNA (brown dots).
PCNA is nuclear labeling.

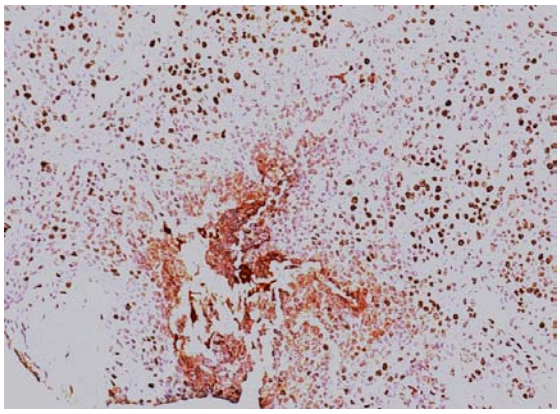

Figure4.1c Double IHC staining-PIMO (red labeled areas) and PCNA (brown dots)

Almost no overlapping between PIMO and PCNA.

Figure 4.1 Loco-regional relationships between PIMO labeled area and PCNA labeled cells

These are three contiguous sections at the same region each stained with PIMO-IHC (4.1a), PCNA-IHC (4.1b) and Double (PIMO+PCNA)-IHC (4.1c). Double staining showed that the two labeling are almost distinct and little overlap in this tumor. Double staining was performed using staining procedure described in chapter I. First, a standard PIMO staining procedure was applied without counterstaining (Aqua hematoxylin). Then, a standard PCNA staining procedure was applied similarly described in chapter I which only difference was using same kit as PIMO staining. Slides were finished with routine counterstaining and mounted (dog#57291: CW) Squamous cell carcinoma.

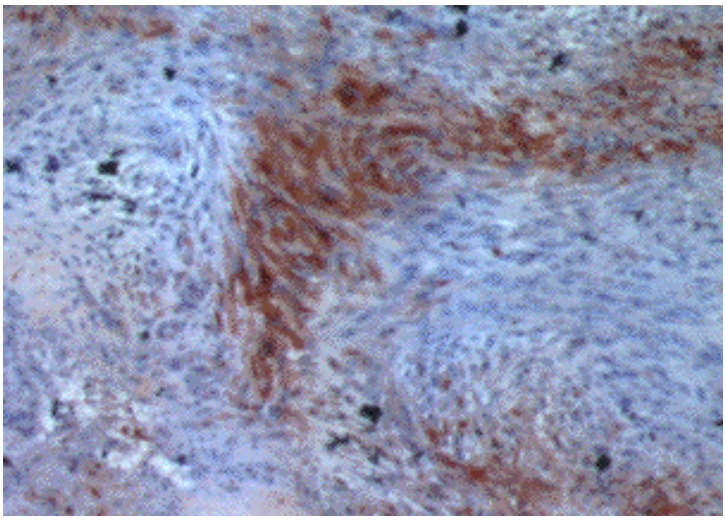

Figure 4.2a PIMO-IHC (x 100 seen without grid)

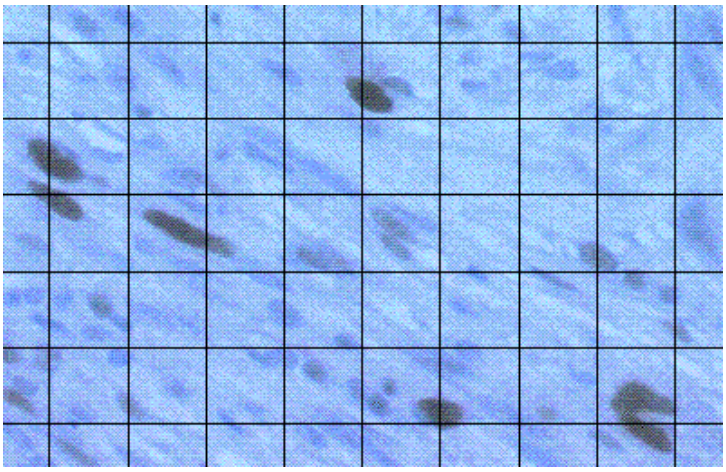

Figure 4.2b PCNA-IHC (x 400 seen with grid). Two heavily labeled cells are at the intersection of grid.

Figure 4.2 Analysis of Immunohistochemistry

Contiguous slides were stained with either for PIMO or PCNA. This tumor was a high-grade fibrosarcoma (dog#76544, PF). Figure 4.2a, PIMO, with lower magnification each cells were not visible and area under intersection of grid (no shown) was counted either labeled tumor area (red), non-labeled tumor area and other. Other may include necrosis, connective tissue, normal tissue and vessels. Figure 4.2b, PCNA, with higher magnification each tumor cell was visible and cells under intersection of grid was counted either heavily labeled tumor cells or other tumor cells. If there was no tumor cell at the intersection, then skip without counting to next intersection.

Results

PIMO adducts and PNCA were detected in 49/50 and 50/50 tumors, respectively. Quantitatively, the mean percentage of uncorrected PIMO labeled area fraction varied from 1.8 to 49.2 % (mean, 19.95 $\pm$ 13 %, table 4.1), when corrected for other than tumor cells, the mean percentage of PIMO labeled area fraction varied from 2.1 to 83.1% (mean, 33.3 $\pm$ 21.71 %, table 4.2). The mean percentage of heavily PCNA stained cells from 0 to 11.7 % (mean, 3.84 $\pm$ 2.74 %, table 4.3). The median tumor volume was 60.99 cm^3 (range, 3.40-4396 cm^3).

Overall, there was no association between either uncorrected PIMO labeled area fraction and PCNA (figure 4.3, p=0.74: a logistic transformation) or corrected PIMO labeled area fraction and PCNA (figure 4.4, p=0.42: a logistic transformation).

There was no significant relationship between the uncorrected PIMO labeled area fraction and tumor volume (figure 4.5, p=0.58 for log(volume) and p=0.73 for volume). There was also no significant relationship between corrected PIMO labeled area fraction and tumor volume (figure 4.6, p=0.46 for log(volume) and p=0.42 for volume).

There was no significant relationship found between PCNA and tumor volume (figure 4.7, p=0.43 for log(volume) and p=0.06 for volume). We noticed that one tumor (#52986) had an extremely large volume (4396 cc). Without this tumor, the p-value for the association between PCNA and log(volume) is p=0.92 and the p-value for the association between PCNA and volume is 0.42.

There was a significant relationship between tumor type and degree of hypoxia. Hemangiopericytomas (HPC: n = 18) had a higher median percentage of PIMO labeled area than fibrosarcomas (FSA: n = 14). The median uncorrected PIMO labeled area fractions in HPC and FSA were 22.4 (range 7.4 to 49.2) % and 7.1 (range 1.8 to 36.7) %, respectively (figure 4.8, Wilcoxon Rank Sum Test, p=0.004). The median corrected PIMO labeled area fractions in HPC and FSA were 35.8 (range 11.4 to 83.1) % and 12.1 (range 2.1 to 72) %, respectively (figure 4.9, Wilcoxon Rank Sum Test, p=0.004).

Based on scatter plots that was no indication of a relationship between hypoxia and proliferation in FSA (figures 4.10 and 4.11) or HPC (figures 4.12 and 4.13). There is a visual trend for a relationship between hypoxia and proliferation in HPC and further study in this tumor may be useful.

There was no relationship between tumor grade and PCNA labeled cells (figure 4.14, Wilcoxon Rank Sum Test, p=0.957), but there was a significant relationship between tumor grade and uncorrected PIMO labeled area fraction (figure 4.15, Wilcoxon Rank Sum Test, p=0.015). The median PCNA fractions in low-grade soft tissue sarcomas (n= 32) and high-grade (n=11) were 3.6 (range 0.3 to 10.2) % and 4.1 (range 0.7 to 11.7) %, respectively.

The median uncorrected PIMO labeled area fractions in low-grade soft tissue sarcomas (n= 32) and high-grade (n=11) were 24.1 (range 1.8 to 49.2) % and 11.1 (range 3.0 to 24.3) %, respectively. The median corrected PIMO labeled area fraction in low- (n= 32) and high-grade (n=11) were 34.4 (range 2.1 to 83.1) % and 17.4 (range 4.7 to 48.8) %, respectively (Wilcoxon Rank Sum Test, p=0.066).

There was no relationship between other study variables and hypoxia or proliferation.

Table 4.1 Summary of uncorrected PIMO labeled area fraction

Clincal #	Total N	N not NA	Mean	StDev	Min	25 %'ile	Median	75 %'ile	Max	Volume
49939	8	8	0.298	0.052	0.216	0.265	0.304	0.339	0.533	33.92
52011	8	0	NA	NA	NA	NA	NA	NA	NA	483.56
20631	8	8	0.255	0.055	0.165	0.220	0.260	0.291	0.325	272.13
52244	8	5	0.075	0.038	0.020	0.058	0.088	0.093	0.118	58.88
52788	8	8	0.030	0.025	0.000	0.018	0.025	0.032	0.081	15.83
52986	8	8	0.172	0.136	0.073	0.089	0.100	0.206	0.409	4396
54338	8	8	0.121	0.063	0.048	0.061	0.119	0.173	0.206	130
55885	8	8	0.243	0.044	0.189	0.207	0.238	0.275	0.305	345.9
57291	8	8	0.141	0.066	0.053	0.098	0.138	0.169	0.239	16.33
58573	8	8	0.317	0.103	0.155	0.247	0.345	0.397	0.432	870.8
59521	8	8	0.345	0.068	0.240	0.313	0.334	0.377	0.440	50.2
59117	12	12	0.355	0.121	0.219	0.263	0.338	0.421	0.597	146.4
41349	12	12	0.067	0.056	0.009	0.029	0.048	0.084	0.177	58.29
61200	12	12	0.082	0.084	0.003	0.013	0.057	0.147	0.228	334.6
62305	12	12	0.018	0.015	0.001	0.008	0.013	0.027	0.045	6.15
62376	12	12	0.111	0.097	0.000	0.032	0.116	0.162	0.326	314
63630	12	12	0.019	0.010	0.009	0.009	0.017	0.026	0.037	98.13
63681	12	12	0.023	0.026	0.002	0.003	0.010	0.037	0.081	188.4
64653	12	12	0.182	0.072	0.043	0.117	0.204	0.228	0.265	6
64950	12	12	0.074	0.038	0.015	0.049	0.079	0.098	0.142	12.56
65203	12	12	0.294	0.084	0.145	0.238	0.302	0.339	0.438	216.5
66885	12	12	0.069	0.078	0.004	0.008	0.059	0.072	0.278	8.5
66897	12	12	0.478	0.080	0.377	0.412	0.477	0.529	0.637	63.1
66999	8	8	0.183	0.084	0.080	0.150	0.174	0.208	0.354	40.9
67186	8	8	0.237	0.047	0.180	0.203	0.229	0.268	0.308	3.8
67298	12	12	0.209	0.081	0.085	0.137	0.231	0.255	0.332	210.6
67068	12	12	0.212	0.121	0.054	0.106	0.186	0.318	0.397	20.2
67540	12	12	0.031	0.019	0.005	0.019	0.025	0.039	0.073	80.8
67764	12	12	0.173	0.078	0.073	0.118	0.174	0.215	0.308	81.9
39492	12	12	0.110	0.075	0.021	0.047	0.093	0.167	0.233	15.4
68298	12	12	0.211	0.210	0.020	0.024	0.127	0.404	0.533	125.6
68227	12	12	0.052	0.046	0.007	0.012	0.042	0.076	0.140	1067.5
69013	12	8	0.207	0.038	0.161	0.179	0.201	0.227	0.267	182.5
69021	12	12	0.143	0.082	0.048	0.076	0.138	0.182	0.315	7.1
69466	12	12	0.251	0.081	0.096	0.208	0.242	0.302	0.384	343.3
69939	12	12	0.142	0.125	0.033	0.041	0.084	0.278	0.360	302.5
72154	12	12	0.057	0.044	0.003	0.023	0.049	0.089	0.129	40.4
73113	12	9	0.297	0.240	0.000	0.196	0.255	0.343	0.866	13.4
70948	12	12	0.369	0.202	0.073	0.196	0.360	0.488	0.675	12.7
72960	12	12	0.247	0.081	0.123	0.176	0.264	0.312	0.382	119.6
41480	12	12	0.411	0.150	0.234	0.264	0.414	0.521	0.642	24.9
74817	12	12	0.110	0.069	0.044	0.074	0.093	0.128	0.305	19.1
74947	12	12	0.234	0.121	0.063	0.128	0.228	0.319	0.438	11
75456	12	12	0.059	0.041	0.008	0.022	0.056	0.091	0.129	28.8
53444	12	8	0.055	0.063	0.005	0.010	0.036	0.069	0.188	86.1
80916	16	16	0.289	0.070	0.153	0.245	0.276	0.352	0.414	15.7
80976	16	16	0.487	0.179	0.185	0.344	0.461	0.630	0.781	3.4
81496	16	16	0.335	0.102	0.192	0.236	0.351	0.419	0.475	116.9
82360	16	16	0.410	0.122	0.118	0.376	0.434	0.480	0.572	15.4
83673	16	16	0.492	0.182	0.092	0.395	0.565	0.621	0.718	66.9
Average	11.4	10.9	0.200	0.085	0.084	0.138	0.193	0.252	0.348	223.6516
St. Dev.	2.3	3.0	0.133	0.052	0.086	0.117	0.141	0.161	0.199	636.7662
Median	12	12	0.183	0.078	0.054	0.117	0.174	0.228	0.325	60.99
Minimum	8	0	0.018	0.010	0.000	0.003	0.010	0.026	0.037	3.4
Maximum	16	16	0.492	0.240	0.377	0.412	0.565	0.630	0.866	4396
Range	8	16	0.474	0.230	0.377	0.408	0.555	0.604	0.829	4392.6

Table 4.2 Summary of corrected PIMO labeled area fraction

Patient	Total N	N not NA	Mean	StDev	Min	25 %'ile	Median	75 %'ile	Max
49939	8	8	0.720	0.085	0.538	0.714	0.722	0.750	0.828
52011	8	0	NA	NA	NA	NA	NA	NA	NA
20631	8	8	0.345	0.059	0.256	0.315	0.346	0.402	0.405
52244	8	5	0.116	0.042	0.057	0.096	0.120	0.138	0.168
52788	8	8	0.090	0.052	0.000	0.071	0.084	0.116	0.172
52986	8	8	0.218	0.171	0.081	0.117	0.142	0.244	0.500
54338	8	8	0.537	0.160	0.276	0.463	0.527	0.641	0.785
55885	8	8	0.341	0.057	0.239	0.306	0.367	0.374	0.402
57291	8	8	0.233	0.099	0.096	0.174	0.231	0.290	0.376
58573	8	8	0.451	0.230	0.166	0.260	0.458	0.644	0.727
59521	8	8	0.555	0.087	0.393	0.536	0.576	0.599	0.664
59117	12	12	0.393	0.135	0.235	0.297	0.363	0.468	0.651
41349	12	12	0.081	0.059	0.012	0.039	0.072	0.097	0.189
61200	12	12	0.126	0.133	0.004	0.020	0.084	0.209	0.352
62305	12	12	0.021	0.015	0.002	0.011	0.019	0.028	0.048
62376	12	12	0.215	0.227	0.000	0.080	0.180	0.235	0.821
63630	12	12	0.153	0.049	0.101	0.118	0.143	0.167	0.271
63681	12	12	0.137	0.098	0.021	0.051	0.133	0.185	0.347
64653	12	12	0.253	0.052	0.154	0.218	0.260	0.291	0.319
64950	12	12	0.345	0.166	0.093	0.236	0.344	0.404	0.738
65203	12	12	0.313	0.082	0.189	0.256	0.326	0.349	0.451
66885	12	12	0.080	0.106	0.004	0.009	0.059	0.076	0.385
66897	12	12	0.647	0.064	0.539	0.616	0.645	0.695	0.749
66999	8	8	0.372	0.220	0.114	0.309	0.333	0.362	0.876
67186	8	8	0.382	0.042	0.332	0.352	0.373	0.414	0.454
67298	12	12	0.263	0.074	0.140	0.211	0.274	0.299	0.399
67068	12	12	0.280	0.164	0.076	0.167	0.235	0.425	0.513
67540	12	12	0.047	0.019	0.012	0.035	0.051	0.060	0.075
67764	12	12	0.202	0.085	0.103	0.131	0.201	0.250	0.363
39492	12	12	0.150	0.095	0.025	0.089	0.121	0.209	0.316
68298	12	12	0.488	0.140	0.226	0.380	0.546	0.592	0.670
68227	12	12	0.090	0.058	0.014	0.030	0.102	0.145	0.163
69013	12	8	0.357	0.076	0.230	0.310	0.357	0.416	0.461
69021	12	12	0.168	0.107	0.050	0.080	0.153	0.225	0.368
69466	12	12	0.343	0.102	0.119	0.266	0.395	0.407	0.458
69939	12	12	0.152	0.138	0.034	0.042	0.088	0.290	0.404
72154	12	12	0.174	0.046	0.063	0.157	0.171	0.206	0.232
73113	12	9	0.340	0.244	0.000	0.196	0.299	0.439	0.866
70948	12	12	0.639	0.121	0.490	0.547	0.633	0.690	0.851
72960	12	12	0.318	0.089	0.145	0.276	0.302	0.368	0.498
41480	12	12	0.831	0.057	0.733	0.787	0.833	0.878	0.913
74817	12	12	0.114	0.069	0.045	0.076	0.104	0.130	0.310
74947	12	12	0.553	0.223	0.230	0.407	0.567	0.704	0.863
75456	12	12	0.092	0.053	0.026	0.058	0.096	0.116	0.210
53444	12	8	0.318	0.107	0.125	0.267	0.342	0.403	0.425
80916	16	16	0.784	0.142	0.475	0.662	0.835	0.883	0.957
80976	16	16	0.591	0.185	0.240	0.475	0.611	0.756	0.836
81496	16	16	0.679	0.109	0.420	0.617	0.700	0.751	0.833
82360	16	16	0.436	0.143	0.121	0.390	0.450	0.514	0.667
83673	16	16	0.789	0.083	0.607	0.735	0.817	0.851	0.894
Average	11.4	10.9	0.333	0.106	0.177	0.266	0.330	0.392	0.515
St. Dev.	2.3	3.0	0.217	0.058	0.182	0.214	0.229	0.237	0.255
Median	12	12	0.318	0.095	0.119	0.236	0.302	0.368	0.454
Minimum	8	0	0.021	0.015	0.000	0.009	0.019	0.028	0.048
Maximum	16	16	0.831	0.244	0.733	0.787	0.835	0.883	0.957
Range	8	16	0.810	0.229	0.733	0.778	0.816	0.855	0.909

Table 4.3 Summary of PCNA fraction

Patient	Total N	N not NA	Mean	StDev	Min	25 %'ile	Median	75 %'ile	Max
49939	8	2	0.051	0.0099	0.044	0.0475	0.051	0.0545	0.058
52011	8	8	0.0002	0.0007	0	0	0	0	0.002
20631	8	8	0.0223	0.0132	0.006	0.008	0.026	0.031	0.04
52244	8	8	0.0398	0.0181	0.016	0.0215	0.047	0.049	0.066
52788	8	8	0.0087	0.0103	0	0	0.007	0.0125	0.03
52986	8	8	0.1005	0.0456	0.036	0.071	0.097	0.1335	0.168
54338	8	8	0.0791	0.0461	0.02	0.0435	0.081	0.0985	0.163
55885	8	8	0.0355	0.0167	0.014	0.027	0.034	0.041	0.066
57291	8	8	0.0555	0.0205	0.03	0.0455	0.051	0.058	0.098
58573	8	8	0.046	0.0175	0.024	0.0295	0.047	0.0591	0.072
59521	8	8	0.0292	0.0126	0.006	0.0235	0.034	0.0365	0.044
59117	12	12	0.0713	0.0309	0.024	0.0435	0.072	0.094	0.114
41349	12	12	0.0535	0.0185	0.024	0.036	0.057	0.0655	0.08
61200	12	11	0.0409	0.0273	0.008	0.024	0.036	0.052	0.098
62305	12	12	0.0566	0.0333	0.006	0.0378	0.048	0.069	0.126
62376	12	12	0.0465	0.0267	0	0.032	0.047	0.066	0.09
63630	12	12	0.0202	0.0132	0.006	0.014	0.018	0.022	0.058
63681	12	12	0.0318	0.0102	0.018	0.0235	0.029	0.039	0.05
64653	12	12	0.0305	0.011	0.014	0.0235	0.031	0.0375	0.05
64950	12	12	0.1017	0.0333	0.02	0.0905	0.1	0.121	0.158
65203	12	12	0.0688	0.0331	0.018	0.0455	0.066	0.0885	0.136
66885	12	12	0.01	0.005	0.002	0.006	0.009	0.0145	0.016
66897	12	12	0.0273	0.0167	0.002	0.0175	0.024	0.0365	0.06
66999	8	8	0.0388	0.0097	0.028	0.0315	0.037	0.0435	0.056
67186	8	8	0.0455	0.0104	0.024	0.042	0.047	0.051	0.058
67298	12	12	0.03	0.0124	0.014	0.024	0.028	0.0335	0.058
67068	12	12	0.0208	0.0151	0.002	0.012	0.018	0.029	0.056
67540	12	12	0.0413	0.0099	0.026	0.0345	0.043	0.048	0.056
67764	12	12	0.0337	0.0136	0.012	0.024	0.031	0.0415	0.06
39492	12	12	0.0085	0.0058	0.002	0.004	0.008	0.0105	0.02
68298	12	11	0.0535	0.0213	0.012	0.038	0.058	0.068	0.0829
68227	12	12	0.008	0.006	0	0.004	0.007	0.0125	0.018
69013	12	8	0.0098	0.0077	0	0.0035	0.01	0.0135	0.022
69021	12	12	0.033	0.0132	0.014	0.0215	0.033	0.041	0.056
69466	12	12	0.0433	0.018	0.016	0.0325	0.043	0.059	0.066
69939	12	12	0.0405	0.0134	0.026	0.03	0.039	0.045	0.072
72154	12	12	0.117	0.0413	0.072	0.0875	0.107	0.1275	0.204
73113	12	6	0.0526	0.0249	0.0238	0.034	0.049	0.0745	0.082
70948	12	12	0.01	0.0064	0.002	0.006	0.007	0.0145	0.024
72960	12	12	0.0025	0.0024	0	0.0015	0.002	0.0025	0.008
41480	12	12	0.0252	0.0121	0.012	0.017	0.023	0.0275	0.05
74817	12	12	0.0187	0.0051	0.012	0.015	0.02	0.022	0.026
74947	12	11	0.0141	0.0094	0	0.0102	0.0125	0.017	0.036
75456	12	12	0.0065	0.0041	0	0.004	0.006	0.01	0.012
53444	12	8	0.0122	0.0092	0.0032	0.0071	0.01	0.0135	0.032
80916	16	16	0.0144	0.0084	0.002	0.0095	0.012	0.0181	0.0375
80976	16	16	0.0186	0.0127	0	0.0095	0.016	0.027	0.05
81496	16	16	0.0255	0.0151	0	0.0145	0.025	0.0376	0.048
82360	16	16	0.0885	0.0311	0.036	0.0655	0.082	0.1105	0.144
83673	16	16	0.078	0.0256	0.038	0.057	0.082	0.1005	0.118
Average	11.4	10.9	0.03835	0.01669	0.01430	0.02701	0.03735	0.04756	0.06791
St. Dev.	2.3	2.8	0.02735	0.01093	0.01457	0.02128	0.02687	0.03336	0.04521
Median	12	12	0.03335	0.01320	0.01200	0.02375	0.03350	0.04100	0.05800
Minimum	8	2	0.00020	0.00070	0.00000	0.00000	0.00000	0.00000	0.00200
Maximum	16	16	0.11700	0.04610	0.07200	0.09050	0.10700	0.13350	0.20400
Range	8	14	0.11680	0.04540	0.07200	0.09050	0.10700	0.13350	0.20200

Captions for Chapter IV figures

Figure 4.3 Uncorrected PIMO labeled area fraction as a function of PCNA fraction, n=49. Each symbol represents a tumor. The median of 12 sections (range 8-16 from 2-4 biopsies) of tissue was analyzed to calculate means of uncorrected PIMO labeled area fraction and PCNA fraction for each tumor. There was no association, p=0.74.

Figure 4.4 Corrected PIMO labeled fraction as a function of PCNA fraction, n=49. Each symbol represents a tumor. The median of 12 sections (range 8-16 from 2-4 biopsies) of tissue was analyzed to calculate means of corrected PIMO labeled area fraction and PCNA fraction for each tumor. There was no association, p=0.42.

Figure 4.5 Uncorrected PIMO labeled fraction as a function of tumor volume, n=49. Each symbol represents a tumor. The median of 12 sections (range 8-16 from 2-4 biopsies) of tissue was analyzed to calculate means of uncorrected PIMO labeled area fraction and tumor volume for each tumor. There was no association, p=0.58 for log(volume) and p=0.73 for volume.

Figure 4.6 Corrected PIMO labeled fraction as a function of tumor volume, n=49. Each symbol represents a tumor. The median of 12 sections (range 8-16 from 2-4 biopsies) of tissue was analyzed to calculate means of uncorrected PIMO labeled area fraction and tumor volume for each tumor. There was no association, p=0.46 for log(volume) and p=0.42 for volume.

Figure 4.7 PCNA fraction as a function of tumor volume, n=50. Each symbol represents a tumor. The median of 12 sections (range 8-16 from 2-4 biopsies) of tissue was analyzed to calculate means of PCNA fraction and tumor volume for each tumor. There was no association, p=0.43 for log(volume) and p=0.06 for volume.

Figure 4.8 Uncorrected PIMO labeled area fraction in FSA (n=14) and HPC (n=18). The median uncorrected PIMO labeled area fraction of HPC (22.4%) was significantly higher than value of FSA (7.1%), p=0.004.

Figure 4.9 Corrected PIMO labeled area fraction in FSA (n=14) and HPC (n=18). The median corrected PIMO labeled area fraction of HPC (35.8%) was significantly higher than value of FSA (12.1%), p=0.004.

Figure 4.10 Uncorrected PIMO labeled area fraction as a function of PCNA fraction in FSA (n=14) showing tumor-specific summary. Each symbol represents the mean of uncorrected PIMO labeled area fraction and PCNA fractions for each tumor.

Figure 4.11 Corrected PIMO labeled area fraction as a function of PCNA fraction in FSA (n=14) showing tumor-specific summary. Each symbol represents the mean of corrected PIMO labeled area fraction and PCNA fraction for each tumor.

Figure 4.12 Uncorrected PIMO labeled area fraction as a function of PCNA fraction in HPC (n=18) showing tumor-specific summary. Each symbol represents the mean of uncorrected PIMO labeled area fraction and PCNA fraction for each tumor.

Figure 4.13 Corrected PIMO labeled area fraction as a function of PCNA fraction in HPC (n=18) showing tumor-specific summary. Each symbol represents the mean of corrected PIMO labeled area fraction and PCNA fraction for each tumor.

Figure 4.14 PCNA Fraction in low (n=32) and high (n=11) grade in soft tissue sarcomas. There was no difference in the median PCNA fraction between low-grade tumors (3.6%) and high-grade tumors (4.1%), p=0.957.

Figure 4.15 Uncorrected PIMO labeled area fraction in low (n=32) and high (n=11) grade in soft tissue sarcomas. The median uncorrected PIMO labeled area fraction in low-grade tumors (24.1%) was higher than in high-grade tumors (11.1%), p=0.015.

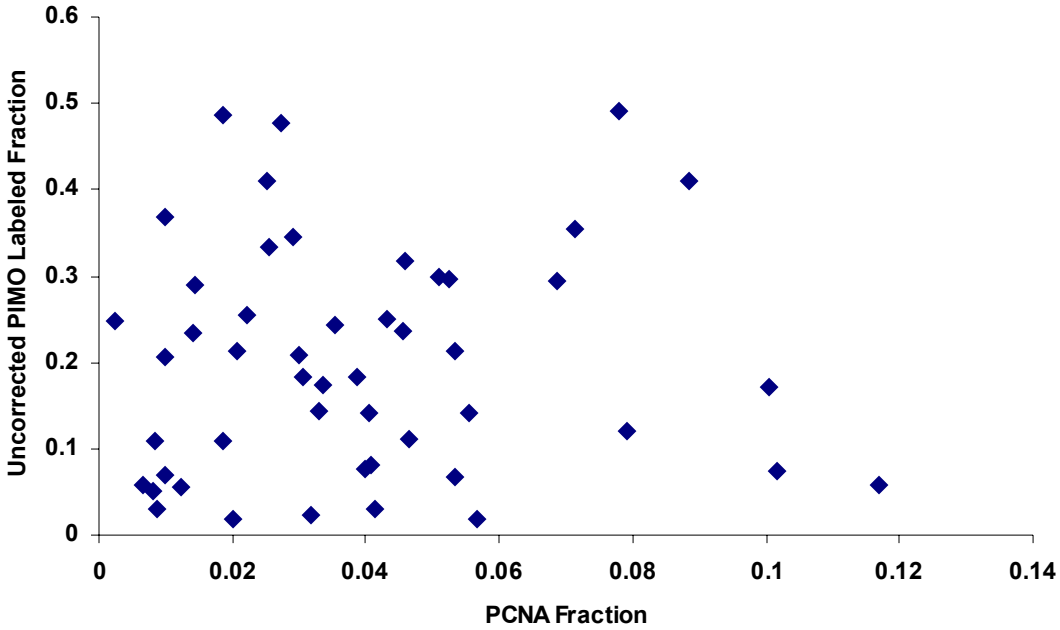

Figure 4.3 Uncorrected PIMO labeled area fraction as a function of PCNA fraction

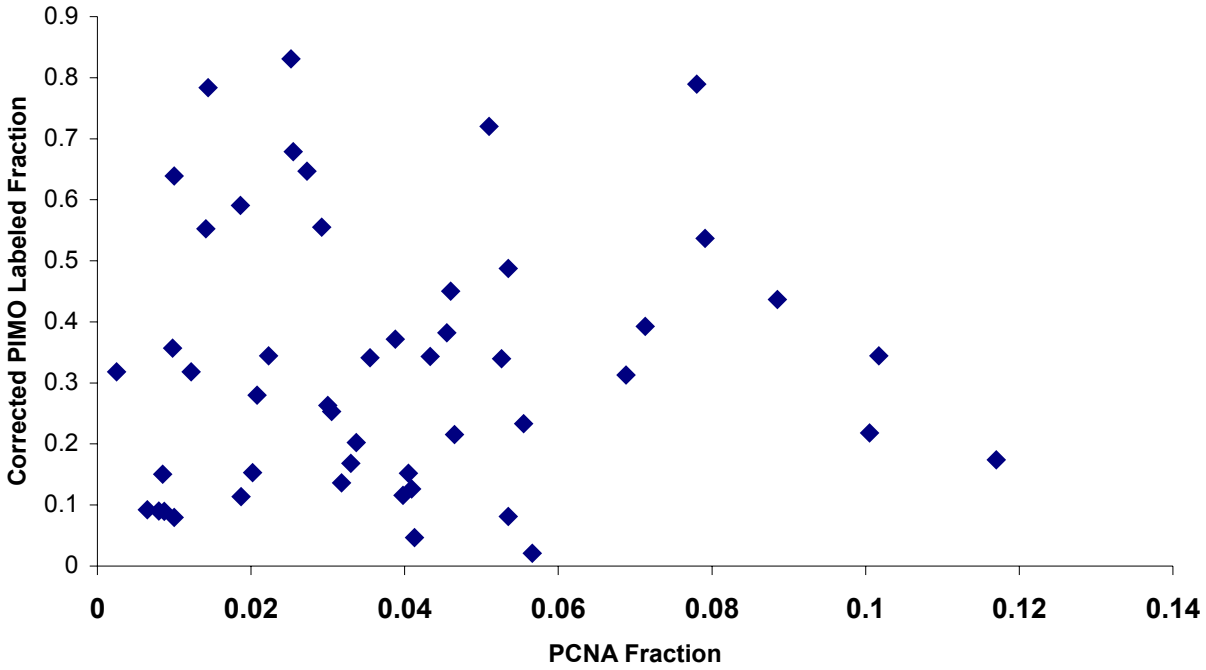

Figure 4.4 Corrected PIMO labeled area fraction as a function of PCNA fraction

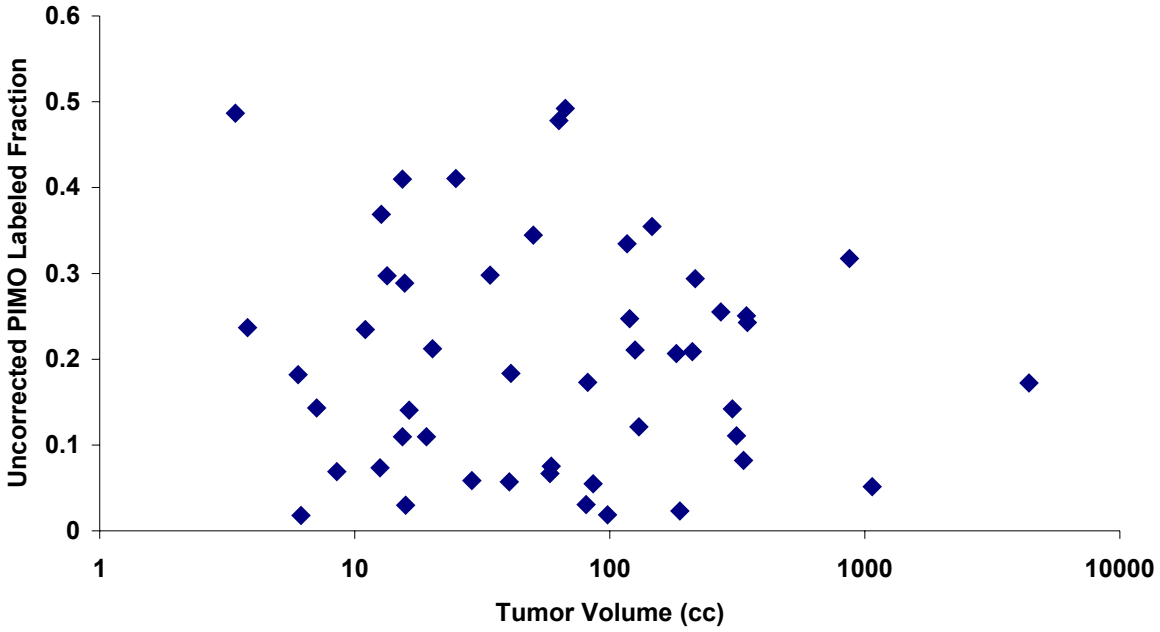

Figure 4.5 Uncorrected PIMO labeled area fraction as a function of tumor volume

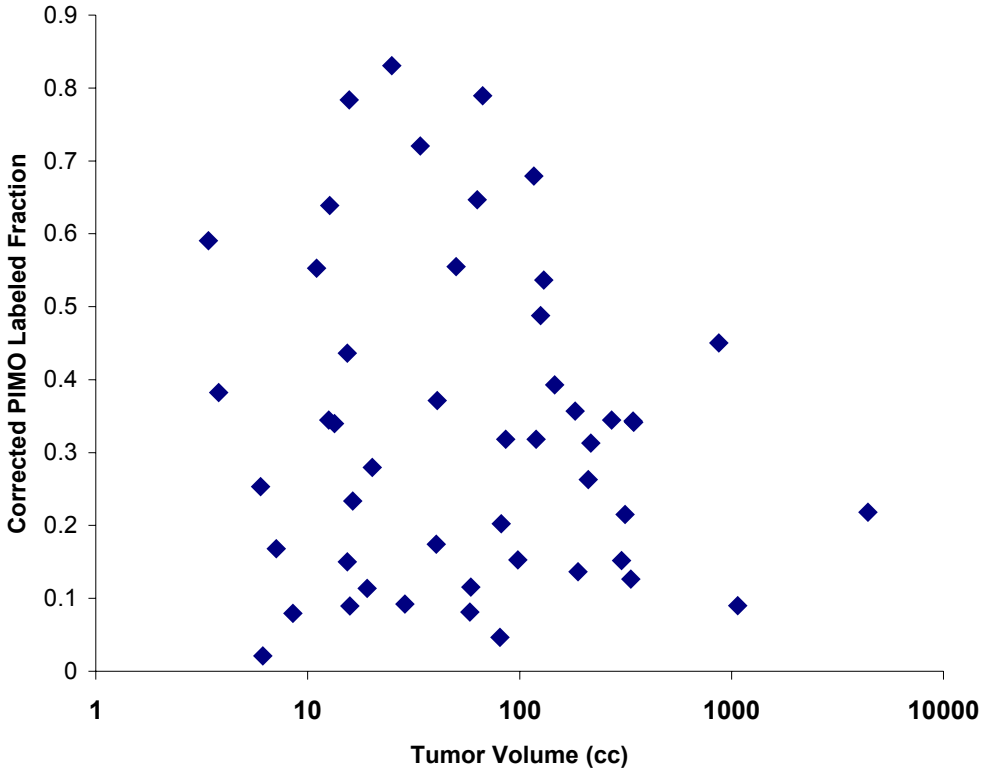

Figure 4.6 Corrected PIMO labeled area fraction as a function of tumor volume

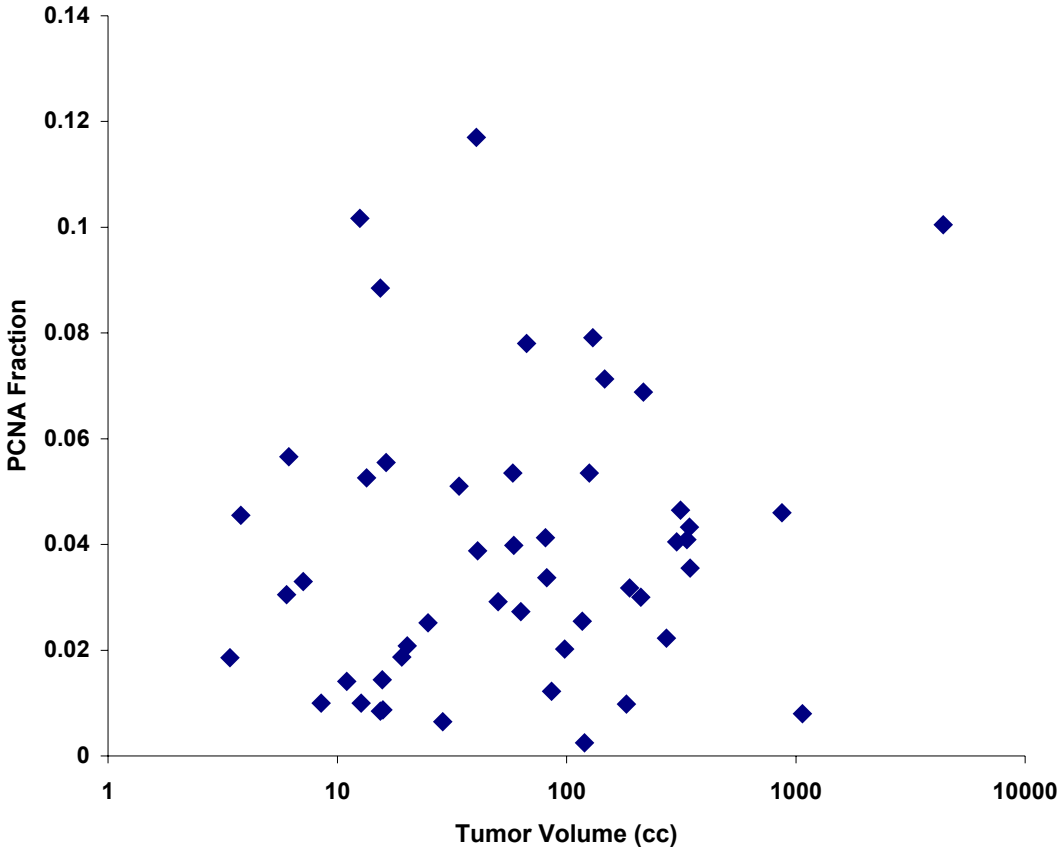

Figure 4.7 PCNA fraction as a function of tumor volume

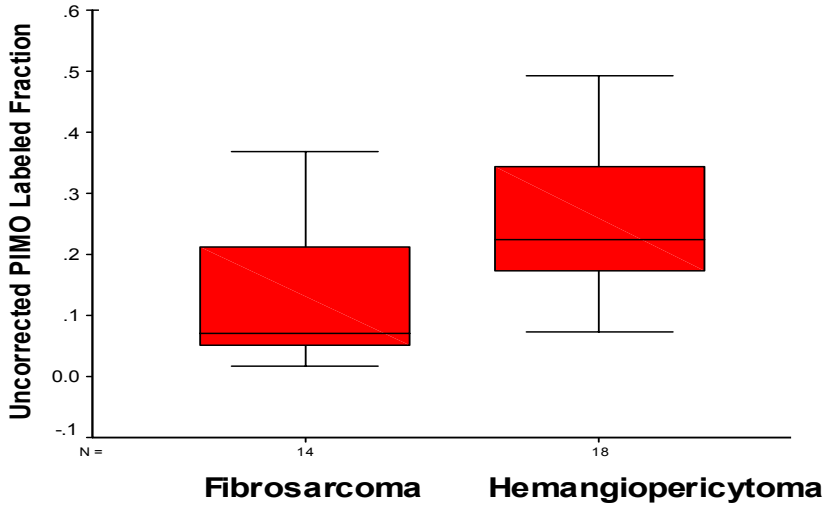

Figure 4.8 Uncorrected PIMO labeled area fraction in FSA and HPC

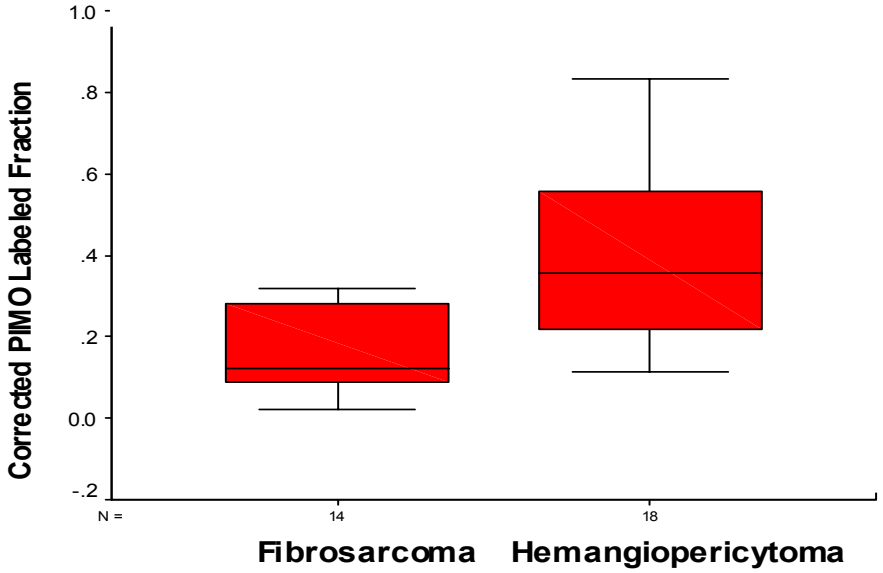

Figure 4.9 Corrected PIMO labeled area fraction in FSA and HPC

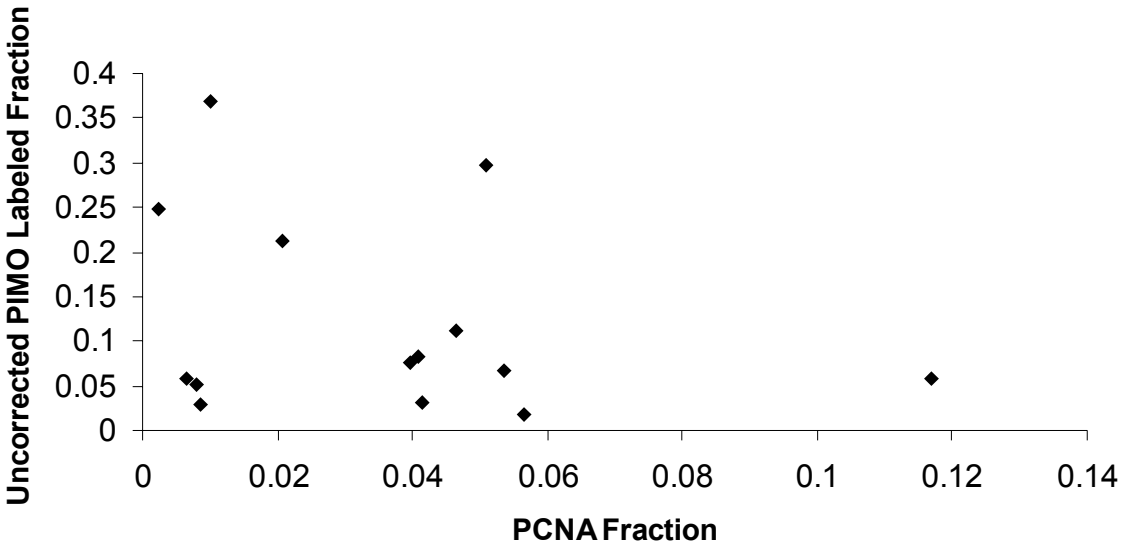

Figure 4.10 Uncorrected PIMO labeled area fraction as a function of PCNA fraction in FSA

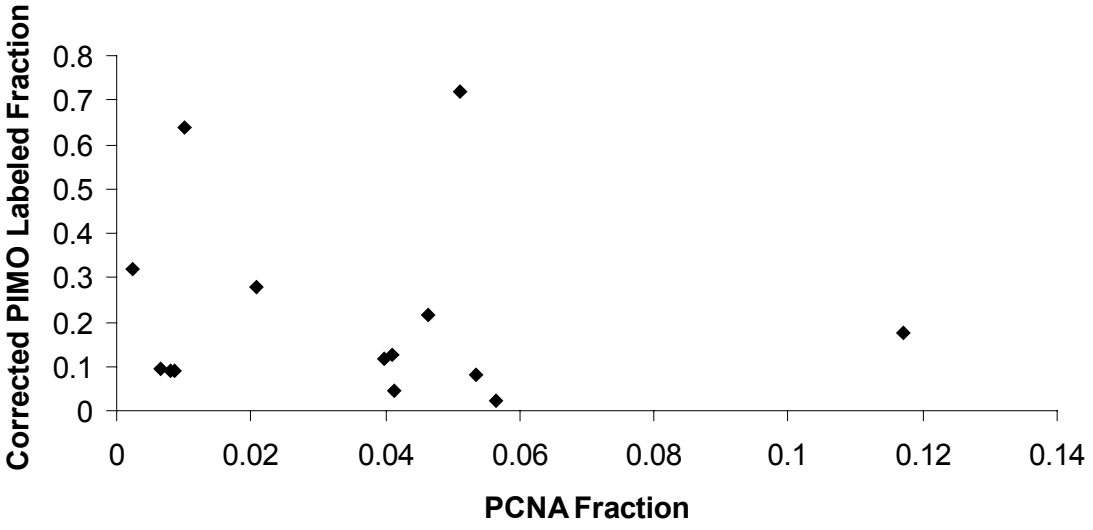

Figure 4.11 Corrected PIMO labeled area fraction as a function of PCNA fraction in FSA

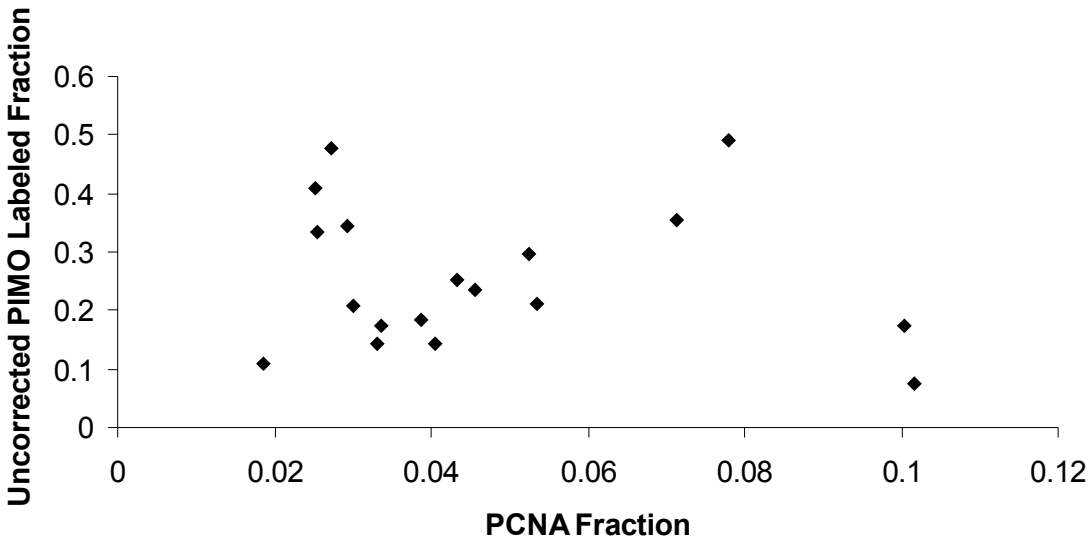

Figure 4.12 Uncorrected PIMO labeled area fraction as a function of PCNA fraction in HPC

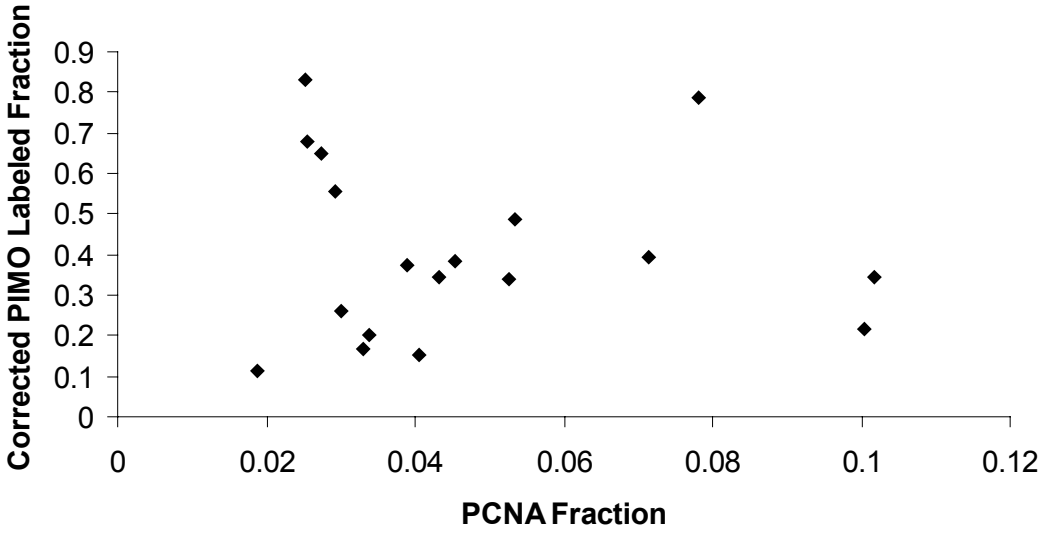

Figure 4.13 Corrected PIMO labeled area fraction as a function of PCNA fraction in HPC

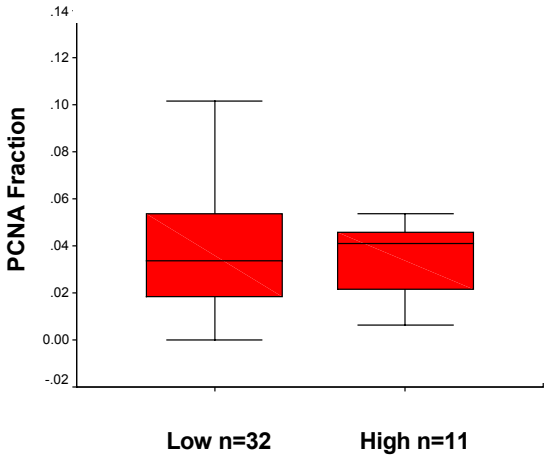

Figure 4.14 PCNA fraction in low and high grade in soft tissue sarcomas

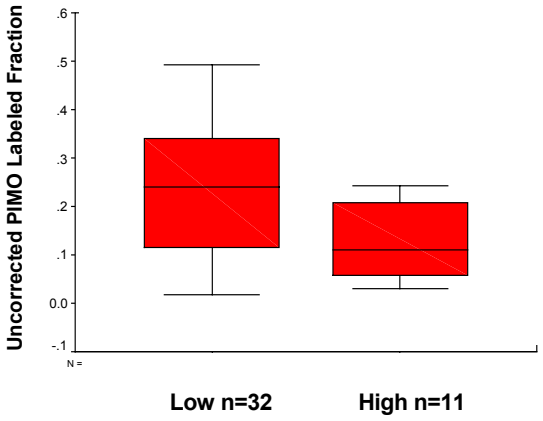

Figure 4.15 Uncorrected PIMO labeled area fraction in low and high grade in soft tissue sarcomas

Discussion

The relationships between hypoxia and other biologic factors are complex. In our IHC based study we did not find an overall relationship between tumor hypoxia and proliferation in canine spontaneous solid tumors using PIMO as a hypoxia marker and PCNA as a proliferation marker. These results are in agreement with our previous study and other's where no relationship was found between hypoxia and proliferation in human and canine tumors (Evans et al., 2001; Tsang et al., 2000; Varia et al., 1998; Zeman et al., 1993).

There was no relationship between tumor volume and either hypoxia or proliferation, which was also consistent with other reports in experimental and human tumors (Evans et al., 2001; Nordsmark et al., 1997; Webster et al., 1998).

Generally, tumor cells under hypoxic conditions are considered to be either slowly proliferating or quiescent and those two tumor populations seemed to be distinct in at least one experimental setting (Durand and Raleigh, 1998). On the other hand, theoretically, increased O_2 consumption due to active proliferation could affect tissue making it more hypoxic (Secomb et al., 1995). Simultaneous measurement of hypoxia and proliferation using flow cytometry could provide information about the relationship between cell phase and hypoxia on an individual cell basis. In one study it was found that hypoxic cells could progress through the cell cycle, although their rate of progression was slower than that of well oxygenated cells (Webster et al., 1998). These cell by cell analyses are powerful, but they may not dictate overall relationships because geographic relationships may be important factor and flow cytometric analysis does not retain this information. Also flow cytometric analysis will not address the importance of necrosis.

There are two possible conclusions to draw from this study. First there may be no detectable association between tumor hypoxia and proliferation. The biology is complex and the existence of hypoxia, proliferation and other tumor factors are just consequences from uncontrolled tumor progression. Those factors including hypoxia and proliferation may still be useful as independent prognostic factors and a means to select patients for targeted therapy for specific tumor subsets. There might be a regional relationship, but one regional relationship does not apply to the whole tumor.

The second is that there was a limitation of our methods to detect an association in this population. Our method was based on a histologic sample and IHC. There are several possible explanations for the lack of association measured by the hypoxia marker approach and PCNA expression in this study. Possible issues may be associated with IHC, markers, methods of analysis, the tumors themselves, and others.

IHC Staining techniques

The advantage of a histologic based study is that the relationship between hypoxia labeled area and histological features such as proliferation, differentiation, size and shape of cells, and necrotic regions of tumor, or other markers can be investigated without a requirement for expensive analytic equipment. Bound adducts of pimonidazole and PCNA are chemically stable during normal histologic processing and histologic analysis can provide rapid quantitative assessment with a light microscope. The disadvantage of a histologic based study is mainly related to tumor heterogeneity, sampling error and staining procedures. It is assumed that randomly selected samples represent the overall tumor, but such is not guaranteed. Staining itself can significantly affect the parameters being estimated. The IHC detection systems are characterized as a non-linearity of signal and antigen concentration. The intensity of the labeling is not linearly correlated with the degree of hypoxia, but the intensity of PCNA labeling is dependent on the cell cycle phase. Fundamental immunohistochemical properties such as antibody concentration as well as antibody affinity, amplification of signals, and sensitivity of the detection system will affect the final estimate. Slight changes in temperature, medium and reagent will introduce variation in quality and intensity of staining even though the conditions of staining are consistent. The labeling signal is highly amplified during the staining process. Selection of the finial chromogen also affects the appearance of the labeling. For example, the brown chromogens (DAB) usually provide a stronger signal than red chromogens (AEC). It is very important to develop a standard IHC procedure and apply it to all study samples. In our study, AEC was used for PIMO detection and DAB was used for PCNA detection. Both are excellent chromogens for IHC, but we noticed higher and heavier labeling when DAB was tested for PIMO adduct detection. There was considerable difference between two staining procedures for PIMO and PCNA. Initially, PIMO staining was performed in a study described chapter II with a conventional IHC kit (Elite ABC, Vectastain). When we were ready for PCNA staining, more

advanced IHC kit (Envision, Dako) was available for the experiment. The basic idea for IHC was the same, but advanced kits will provide more amplification of the signals and less non-specific background, and require a shorter time for procedure. Another source of staining variability relates to the age of some slides, which were cut several years before IHC, this may affect the detection of antigens in the sections.

PIMO as a hypoxia marker

PIMO Adduct formation occurs when drug is available in the tissue. The elimination half-life of PIMO in the dog is 1.5 hours and there was evidence of marker labeling within 20 minutes after intravenous injection. There was no PIMO in the circulation at 24 hours post injection at the time of biopsy. The rate of decay of PIMO adducts in living cells is unknown. In these tumors, where 6 Gy had been given after PIMO injection the oxygenation status of the cells was not known, but these adducts were stable at least for 72 hours. Labeled cells appeared viable in tissues at least 72 hours after injection suggesting that decay of adducts is slow.

Reductive activity of the tissue may also account for some variation in adduct formation. Nitroreductase is required for adduct formation and the amount of nitroreductase in hypoxic cells and SH containing macromolecules may vary in tumors and those would influence estimates of hypoxia based on nitroimidazole markers. It has also been suggested that PIMO metabolism could differ between individuals such as different racial groups in humans. In our study population variation of breeds, shape, size and age could also have affected PIMO binding.

All cells labeled above some threshold intensity are counted as being radiobiologically hypoxic, but it is recognized that the actual O_2 concentration will vary among individual, labeled cells. The basal O_2 requirement in tissue may vary in different tumors and labeled cells do not mean the oxygenation status of the tumor is identical. For example, an oxygen concentration of <10 mmHg may induce hypoxia specific genes in one tumor, but in another tumor the same genes may be upregulated by <5 mmHg.

PIMO is known to label chronically hypoxic cells effectively although it has been suggested that PIMO binding may detect both chronic and acute hypoxia (Olive et al., 2001b). The issue of labeling chronic versus acute hypoxia is complex. Labeling of acutely hypoxic cells should occur if the duration of the hypoxia is long enough to reduce PIMO in tissue (Durand and Aquino-Parsons, 2001b). Hypoxia marker methods alone cannot differentiate acute

versus chronic hypoxia. We are not completely sure that labeled area fraction is representative of chronic hypoxia, acute hypoxia or both. If PIMO labels mainly chronically hypoxic cells, perhaps acute hypoxic is more closely related to proliferation than chronic hypoxia. Chronically hypoxia cells might be programmed for death. On the other hand, transiently hypoxic cells might be more adoptable or aggressive than oxic tumor cells in terms of expression of genes leading to progression and survival after a hypoxic insult. A method to differentiate acute versus chronic hypoxia will be needed.

PIMO is an excellent hypoxia marker in the clinical setting. Although drug administration is required, an oral form of drug may be available making it more convenient. Biopsy of tumors for IHC is well accepted in routine practice at this time. With PIMO, the intensity of labeling does not correlate with the degree of the hypoxia, but areas of intense accumulation may be associated with chronic hypoxia where accumulation of the drug continues until plasma levels decline. A pale background means that there was either a low level of adduct formation, or a background level of staining. In this study, polyclonal antibodies against PIMO were used and the dilution was 1:2000=primary antibody: buffer, this high dilution ratio facilitated the elimination of high background staining.

Identification of endogenous hypoxic marker is an alternative to exogenous markers to perform studies on archival or fresh tissue without a marker injection. PIMO has been used as a standard to assess the ability of endogenous markers to detect hypoxia. IHC associated issues as discussed above will apply to these endogenous markers and hypoxia marker specific issues need to be addressed such as if labeling indicates acute and/or chronic hypoxia in tissues. Promising endogenous hypoxia markers include CA9, GLUT1 (Airley et al., 2001; Hoskin et al., 2003; Hui et al., 2002) and HIF-1 (Aebersold et al., 2001; Beasley et al., 2002; Begg, 2003; Birner et al., 2001; Haugland et al., 2002; Nakayama et al., 2002; Schindl et al., 2002), but exogenous markers are superior at this point to study tumor hypoxia.

Whole tumor imaging will be a valuable alternative to assess overall tumor biology or marker distribution non-invasively. For example, PET imaging allows the whole tumor to be assessed for hypoxia, but the maximum resolution is still poor (>5 mm), implying that averaging of the signal from areas with different levels of oxygenation must occur. Non-invasive imaging will be also useful to monitor tumor hypoxia before, during and after treatment. A general problem with this approach is that a high proportion of tumor cells are

doomed after initiation of therapy and it is impossible to identify the remaining clonogenic cells in the population.

PCNA as a marker

Detection of heavy nuclear PCNA labeling correlated with cells in S-phase (Varia et al., 1998). An attempt was made to estimate the S-phase fraction considering only heavily labeled cells.

Our hypothesis regarding the relationship between tumor hypoxia and proliferation was that the proliferating fraction detected by PCNA is an indication of tumor O2 consumption where a high PCNA fraction and increased O2 consumption have a direct relationship. Our failure to find a relationship between PCNA and PIMO labeling may, at least in part, be due to PCNA labeling having a poor relationship to O2 consumption.

The rate of PCNA production and loss in the tumor is unknown and PCNA is also known to be increased during repair processes. A large number of tumor cells expressed detectable labels of PCNA in different intensities, which may indicate that PCNA was present at low detectable levels in at least some non-cycling cells. Setting the threshold for heavily stained cells can be difficult and counting heavily labeled cells can be subjective. Even though it has been shown that there was a good correlation between the estimation of cells in S-phase by detection of PCNA and by an S-phase specific marker such as BrdUrd, it would have been useful to run test samples to compare those two methods to verify the staining technique and threshold intensity in this study.

The histologic grading of the soft tissue sarcoma was not related to PCNA fraction (indication of S-phase) in this study. Grading was based on mitotic index (M-phase) and PCNA labeling allowed identification of cells in S-phase. The duration of these two phases is different with M-phase lasting up to 20 minutes versus S-phase which lasts 10 hours or more. But, it was assumed a correlation would exist because both are indicators of active proliferation. Only a limited amount of tissue was used for grading which may lead to problems estimating overall tumor grade. In this study, mitotic index was solely used for grading and the cut off value was 9 per 10 high power fields. Nine mitotic figures (Bostock and Dye, 1980) may not be best value for accurate grading, but using this cutoff, dogs with a higher grade of tumor had a median survival time of 49 weeks, compared with 118 weeks for those with lower grade of tumor in their study. Different pathology groups tend to use

slightly different grading schemes for soft tissue sarcomas where other morphologic features and necrosis may be accounted for the grading. It seems that there is a general agreement on the prognostic value of grading soft tissue sarcomas, but a more standardized and objective measurement of grading is needed.

Analyses

Various factors can influence quantification of labeled areas of tissues and cells. The IHC detection systems are characterized by non-linearity of signal and antigen concentration (McCormick et al., 1993). For PIMO staining, intensity of the background might be truly non-specific background or specific labeling in acutely hypoxic cells. For PCNA staining, a large number of the tumor cells expressed detectable labels of PCNA at different intensities, which suggests that PCNA was present in some non-cycling cells. Thus an artificial cut-off had to be employed in assessing the number of proliferating cells and the hypoxia area with IHC, which created some degree of uncertainty.

There was a distinct difference in the spatial resolution to PIMO versus PCNA. PIMO binding provides detailed spatial information on the distribution of hypoxia in the tumor. The assays were different as hypoxia was measured in entire histologic section of the biopsy while proliferation was evaluated in randomly selected high power fields (about 20 fields per section of biopsy). PIMO fractions were evaluated using area of tissue labeled with PIMO (x100) and PCNA fractions were evaluated in individual cells (x400).

There is also a distinct difference in the time resolution between PIMO versus PCNA fractions. Evaluation of hypoxia using PIMO is a reflection of the hypoxic fraction when the drug was metabolized by cells under hypoxic conditions while PIMO binding provides a measure of hypoxia integrated over time (elimination half life: 1.5 hours). For PCNA labeling, the duration of S-phase is important, this is approximately 10 hours and the half-life of the PCNA is about 20 hours. If the time of the biopsy is considered to be time 0, the PCNA fraction was quantified at time 0 and PIMO labeling was occurred when drug was available from the time of injection until elimination of drug, which was up to 24 hours before sampling. Thus, relative to the biopsy, PIMO labeling reflected hypoxia as it was 24 - 20 hours previously and PCNA labeling reflected proliferation 0 -10 hours (S-phase) previously. During this time difference, reoxygenation of acute hypoxia may occur, but as discussed in

chapter III, there was no difference in PIMO labeling between 20-minutes and 24-hours, thus the time difference between PIMO and PCNA is of doubtful significance.

Computerized image analysis could offer a rapid and reliable method for quantitative assessment of tumor hypoxia and proliferation. This technique is particularly useful with identical tumor types because of consistency of threshold setup. In this study, we attempted to use computerized image analysis, but we were not successful. The main reason was due to intratumor heterogeneity making it difficult to set a consistent threshold for all tumors. Individualizing the threshold setting was thought to be a source of bias and it was also more time consuming to use image analysis system than to do point counting.

Another way to investigate information on biological factors is looking for “hotspots” histologically. Basically, a whole section of the tumor is scanned to determine areas containing the defined parameter such as the highest vascular density, highest marker labeled area or highest cell density with a marker. Hotspot analysis is based on the idea that all areas of the tumor do not have the same information regarding the aggressiveness of the cancer. If the hotspot contains the necessary information to dictate prognosis, such hotspot analysis will be a powerful and convenient means to study tumors rapidly. For example, a study of vascular density was based on hotspot analysis to identify the area of high vascular density, which may have maximum or dominant information for the biological behavior of the tumor. Such an analysis has been shown to provide prognostic information in human cancers (West et al., 2001). This hotspot approach is also used to analyze tumor hypoxia using the hypoxia marker, EF5 (Evans et al., 2001) looking for the heaviest labeled region as an indicator of maximal hypoxia. Their hypothesis was that the most hypoxic cells will determine the biology of the tumor. PIMO can detect areas of hypoxia in canine spontaneous tumors. Labeling does not provide the level of tumor hypoxia, but hotspot analysis might be able to find area of most hypoxic area where isolation of cells for a biological study may provide more information.

Tumors have a heterogeneous structure and some of the tumor cells may be programmed for death, some may die after therapeutic intervention and some may survive. It is most useful if we could identify the therapy resistant tumor subsets, which could preserve their clonogenic potential throughout treatment and lead treatment failure. A histology based marker study has the potential to identify makers of tumor aggressiveness.

Tumor population

There were a variety of tumors in this study (table1.1). The mixed tumor types may have interfered with interpretation of the data. The majority of tumors were soft tissue sarcomas. Canine soft tissue sarcomas include several different histologic types, which are grouped because their biological behavior and response to therapy is similar. They are locally invasive and the risk of metastatic potential is dictated by tumor grade. In the canine soft tissue sarcomas (n=44), the two most common histologic types were fibrosarcomas (FSA) and hemangiopericytomas (HPC) (figure 1.6). Although their biologic behavior is similar, their histopathologic appearance is different. Large areas of necrosis were not a common future of soft tissue sarcomas, but there were three highly necrotic tumors (#72154 SH, #41480 SO and #67186 BC). The majority of the canine tumors in this study were low-grade tumors.

Tumor heterogeneity

Histologic studies are potentially limited by heterogeneous intratumoral distribution of hypoxia and proliferation (Jenkins et al., 2000). It was impractical to evaluate the entire tumor histologically. Base on previous studies (Cline et al., 1997; Thrall et al., 1997) a reasonable estimate of intratumoral hypoxic marker binding is possible using a biopsy and tissue sections from the biopsy.

Intratumoral and intertumoral heterogeneity were also evident in this study. Intratumoral heterogeneity was usually smaller than intertumoral heterogeneity (table 4.1, 4.2 and 4.3). Tumors are made up of many different cell types including endothelium, different stromal cells, inflammatory cells, dead cells and cancer cells. Every tumor is unique and this makes analyses complex.

Type and shape of the tumor cells influenced the estimate of hypoxia labeled area because of accumulation of PIMO adducts. Tumor type influenced the average hypoxic fraction, with the HPC having a larger labeled area fraction than FSA. This seemed mainly due to differences in cell size, and the amount of cytoplasm and connective tissue in the tumor. HPC cells tended to be round with larger cytoplasm and the amount of connective tissue in HPC was lower than FSA. FSA cells are more spindle-shaped and tumors contain abundant fibrous connective tissue (figure 1.6).

Connective tissue is usually not labeled with PIMO and small spindle-shaped cytoplasm does not accumulate large amounts of PIMO adducts. On the other hand, HPC contained relatively round tumor cells with little interstitial connective tissue making it easy to identify PIMO labeling for counting. Grouping tumors based on histologic appearance may be more appropriate than an analysis of a variety of tumors with varying microscopic differences. Based on the cytoplasmic nature of PIMO staining, a higher hypoxic fraction with HPC would be expected due to lager cytoplasmic area accumulating more PIMO adducts. Under this circumstance, the number of labeled cells is same, but labeled area fraction can be different between HPC versus FSA (figure 4.13). Figure 4.13 describes the potential issues for PIMO labeling in different histology types. Fifty labeled tumor cells of two different shapes (dark red) and background (contained unlabeled tumor cells and others) are illustrated on the counting grid, which has 25 intersections. On these sections of tumor, fractions of uncorrected PIMO labeled area were 0.28 (7 labeled cells out of 25 leading=7/25) in figure 4.16a representing FSA and 0.56 (14 labeled cells out of 25 leading=14/25) in figure 4.16b representing HPC. Due to the cell size, tumors with larger cells may have a greater chance to lie at the intersection and be counted.

For the tumor hypoxia assessment, it is not known if the total volume of hypoxic tissue is important or the total number of the cells is important. If there is hypoxia induced gene expression the number of cells might be important, but for more environmental effects due to hypoxia then cell number may not be as important as the overall volume of the tumor that is at decreased oxygen tension.

Flow cytometric analysis might be useful to determine the issues on volume of hypoxic tissue versus number of hypoxic tumor cells.

Different accumulation and estimation of PIMO in FSA versus HPC is a serious issue regarding the application of this method to all soft tissue sarcomas. As we have shown, there is significant labeling variation due to cytoplasmic size and shape, and interstitial connective tissues.

Other

There still seems to be a regional relationship between hypoxia and proliferation where two populations are nearly distinct detected by our IHC based marker method. In another IHC study using PIMO and BrdUrd in mice, both hypoxic and proliferating cells were present up

to 250 *u*m from the vessels (Ljungkvist et al., 2002). We don't know that coexistence was a pronounced feature for xenograft tumor growth or common in all tumors including spontaneous tumors. A theoretical tumor model consists of a feeding vessel, supportive structure and tumor cells. Hypoxia may develop chronically or acutely. For example, there might be a vessel surrounded by extensive tumor proliferation while beyond the oxygen diffusion limitation the tumor cells became hypoxic. Marker methods do not address the degree of hypoxia, which was also suggested in our study. A narrow rim of hypoxia at the border of necrosis might be significantly hypoxic (figure 1.6d) but a wide hypoxic area could exist without histologic evidence of necrosis (figure 1.6c). Development of chronic hypoxia was observed in the classic experiment by Thomlinson and Gray. This regional relationship may have a strong influence on the entire tumor, or effects may only influence the local area (feeding vessels plus supported structures and cells). Beyond the local region the effects may be buffered out and may not affect overall tumor behavior because overall proliferation and hypoxia are relatively low in the canine spontaneous tumors studied here. In our study, the majority of the tumor cells were not labeled for either markers. When %corrected PIMO labeled area fraction (fraction of labeled tumor area) plus %PCNA was calculated, the median was 33 % (range 7.8 to 86.7%) if no overlap of staining was assumed (which may not be completely true). 67% of the tissue or cells were not labeled either PIMO or PCNA, but the biologic importance of the non-labeled tumor cells can not be ignored. Those non-labeled cells may have a significant relationship to the tumor's biologic behavior. This population could include acutely hypoxic regions and necrosis.

There was an association between tumor grade and uncorrected PIMO labeled area (figure 4.13). Uncorrected PIMO labeled area was lower in high-grade soft tissue sarcomas. This may indicate that high-grade tumors contain more "other" tissue such as necrosis. Necrosis may be the end result of tumor activity, but necrosis related factors could be the key to understanding tumor biology.

Hypoxia marker: Potential as a prognostic factor?

The measurement of tumor oxygenation using Eppendorf needle electrodes has been the only method where there was a repeatable correlation between low tumor oxygenation and poor prognosis in patients with cancer, but there are several limitations with this technique. Tumors have to be accessible for needle insertion and needle insertion is invasive. There is

no way to differentiate living from dead cells, nor chronic versus acute hypoxia in this method and there is little doubt that necrosis affects the measurement. A low oxygen concentration may be a reflection of necrosis. If this is true, necrosis may be a better indicator of tumor aggressiveness than hypoxia. Necrosis itself will have a limited effect because necrotic cells are dead, but it may be an indication of increased O_2 consumption consistent with chronic diffusion limited hypoxia and/or active tumor proliferation. In one recent study it was determined that there was a trend that the most hypoxic tumors measured by oxygen electrodes and the highest score of necrosis, had no or little PIMO binding (Nordsmark et al., 2003). This also suggests that evaluation of necrotic or prenecrotic areas will provide important biologic information about the tumor. The evaluation of necrosis will be difficult with any technique. It is wise to look for a pre-necrotic status in tumors, which may include chronic hypoxic and apoptotic cells. Other studies also suggested the correlation between necrosis and aggressive tumor behavior in breast cancer (Colpaert et al., 2003; Leek et al., 1999).

In the mouse model, there was a significant correlation between pO_2 measurement, PIMO labeling, and the radiobiological hypoxic fractions (Raleigh et al., 1999), but there has not been a good correlation reported between PIMO labeling and O_2 electrode measurements in patients (Nordsmark et al., 2003; Olive et al., 2001a) and there seems to be an agreement that PIMO labeling and O_2 electrode measurement operate in fundamentally different ways and provide substantially different information as the O_2 electrode measures tissue pO_2 in a quantitative manner while 2-nitroimidazole labeling is based on a non-linear system with indirect detection method. For example, O_2 electrode simply measures pO_2 in the inserted tissue with no discrimination and PIMO intensity may vary depending on diffusion limited or perfusion-limited hypoxia and does not dictate pO_2. Necrosis seems to be a major confounding factor in the two measurements. The O_2 electrode readings characterize necrosis as anoxic, low O_2 tension, whereas absence of nitroimidazole binding in necrotic areas may identify them as necrosis with manual evaluation or oxic with computer based automatic counting. The O_2 electrode technique may overestimate the presence of hypoxia in highly necrotic tumors, which may not be accurate to evaluate overall tumor hypoxia.

The 2-nitroimidazole marker method has greater spatial heterogeneity than electrode measurements (Jenkins et al., 2000). The potential benefit of O_2 electrode measurement is that the reading is an average value from a large volume of tumor tissue compared to the

marker method, which may represent for the entire tumor more accurately. Both systems will not allow distinction of acute versus chronic hypoxia. But it is assumed that the O_2 electrode measurement is directly affected by both forms of hypoxia. As we already discussed, one of the problems with hypoxia marker method is uncertainty of the hypoxic labeling for acutely hypoxic cells. The main difference between the two systems seems to be detectability of acute hypoxia and accounting for necrosis. Hypoxia markers could detect hypoxic cells, but it may be more important to investigate the level of the hypoxia of the labeled cells. For example, active proliferation of the tumor cells may have a more profound effect on the degree of hypoxia (pO_2) than the area or volume of hypoxia, and small areas of significant hypoxia could have great effects on the overall tumor biology.

To combine these two methods, it may be possible to study degree of hypoxia (pO_2) and volume or distribution of hypoxia using hypoxia markers methods to recognize different subgroups of tumor cells with different degrees of hypoxia.

Also, measurement of intensity of labeling using flow cytometry may provide more useful information and perhaps it may allow identification of a relationship between tumor hypoxia and proliferation with combination of several techniques. At this point there is firm evidence that O_2 electrode measurements are related to survival in some tumors. In one study the hypoxia marker, PIMO, did not predict for prognosis in human with bladder cancer (Hoskin et al., 2003). Other study showed that PIMO binding predicted for outcome in human head and neck squamous cell carcinoma (Kaanders et al., 2002c). It is too early to conclude the prognostic value of hypoxia marker methods to quantify tumor hypoxia.

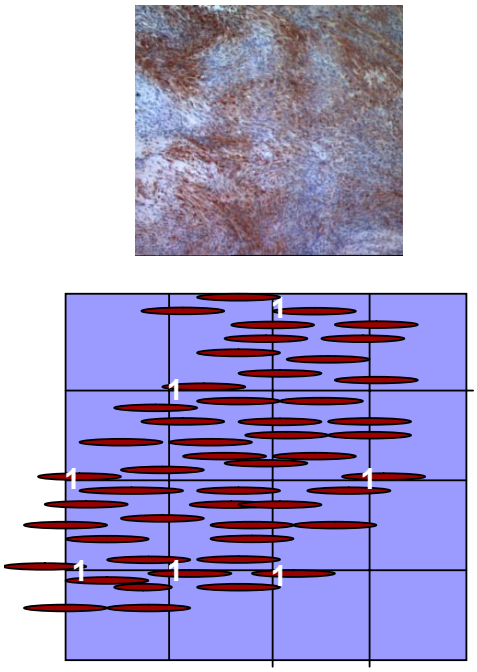

Figure 4. 16a: FSA (high grade)

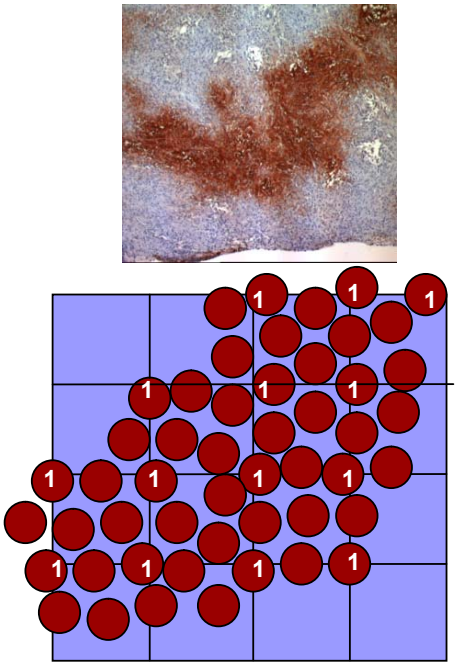

Figure 4. 16b: HPC (low grade)

Figure 4.16 Effects of histology type on PIMO labeled area fraction

Fifty labeled tumor cells (dark red) and background (contained unlabeled tumor cells and others). On these sections of tumor, fractions of uncorrected PIMO labeled area were 7/25= 0.28 in figure 4.16a and 14/25= 0.56 in figure 4.16b. Figure 4.16a represents a typical fibrosarcoma where cells are spindle shaped and the background contains large amount of connective tissue between tumor cells. Figure 4.16b represents a typical hemangiopericytoma where cells are relatively round with abundant cytoplasm and there is little connective tissue between tumor cells.

References

1999. Data Analysis Products Division, M. S-PLUS 2000 User's Guide. MathSoft, Inc., Seattle, Washington.

Aebersold, D.M., P. Burri, K.T. Beer, J. Laissue, V. Djonov, R.H. Greiner, and G.L. Semenza. 2001. Expression of hypoxia-inducible factor-1alpha: a novel predictive and prognostic parameter in the radiotherapy of oropharyngeal cancer. Cancer Res 61:2911-6.

Airley, R., J. Loncaster, S. Davidson, M. Bromley, S. Roberts, A. Patterson, R. Hunter, I. Stratford, and C. West. 2001. Glucose transporter glut-1 expression correlates with tumor hypoxia and predicts metastasis-free survival in advanced carcinoma of the cervix. Clin Cancer Res 7:928-34.

Beasley, N.J., R. Leek, M. Alam, H. Turley, G.J. Cox, K. Gatter, P. Millard, S. Fuggle, and A.L. Harris. 2002. Hypoxia-inducible factors HIF-1alpha and HIF-2alpha in head and neck cancer: relationship to tumor biology and treatment outcome in surgically resected patients. Cancer Res 62:2493-7.

Begg, A.C. 2003. Is HIF-1[alpha] a good marker for tumor hypoxia? International Journal of Radiation Oncology*Biology*Physics 56:917-919.

Birner, P., B. Gatterbauer, G. Oberhuber, M. Schindl, K. Rossler, A. Prodinger, H. Budka, and J.A. Hainfellner. 2001. Expression of hypoxia-inducible factor-1 alpha in oligodendrogliomas: its impact on prognosis and on neoangiogenesis. Cancer 92:165-71.

Bostock, D.E., and M.T. Dye. 1980. Prognosis after surgical excision of canine fibrous connective tissue sarcomas. Vet Pathol 17:581-8.

Cline, J.M., G.L. Rosner, J.A. Raleigh, and D.E. Thrall. 1997. Quantification of CCI-103F labeling heterogeneity in canine solid tumors. Int J Radiat Oncol Biol Phys 37:655-62.

Colpaert, C.G., P.B. Vermeulen, P. Van Beest, A. Soubry, G. Goovaerts, L.Y. Dirix, A.L. Harris, and E.A. Van Marck. 2003. Cutaneous breast cancer deposits show distinct growth patterns with different degrees of angiogenesis, hypoxia and fibrin deposition. Histopathology 42:530-40.

Durand, R.E., and J.A. Raleigh. 1998. Identification of nonproliferating but viable hypoxic tumor cells in vivo. Cancer Res 58:3547-50.

Durand, R.E., and C. Aquino-Parsons. 2001. Clinical relevance of intermittent tumour blood flow. Acta Oncol 40:929-36.

Evans, S.M., S.M. Hahn, D.P. Magarelli, and C.J. Koch. 2001. Hypoxic heterogeneity in human tumors: EF5 binding, vasculature, necrosis, and proliferation. Am J Clin Oncol 24:467-72.

Freyer, J.P. 1994. Rates of oxygen consumption for proliferating and quiescent cells isolated from multicellular tumor spheroids. Adv Exp Med Biol 345:335-42.

Govindarajulu, Z. 1988. Statistical Techniques in Bioassay. Karger, Basel.

Haugland, H.K., V. Vukovic, M. Pintilie, A.W. Fyles, M. Milosevic, R.P. Hill, and D.W. Hedley. 2002. Expression of hypoxia-inducible factor-1alpha in cervical carcinomas: correlation with tumor oxygenation. Int J Radiat Oncol Biol Phys 53:854-861.

Hoskin, P.J., A. Sibtain, F.M. Daley, and G.D. Wilson. 2003. GLUT1 and CAIX as intrinsic markers of hypoxia in bladder cancer: relationship with vascularity and proliferation as predictors of outcome of ARCON. Br J Cancer 89:1290-7.

Hui, E.P., A.T. Chan, F. Pezzella, H. Turley, K.F. To, T.C. Poon, B. Zee, F. Mo, P.M. Teo, D.P. Huang, K.C. Gatter, P.J. Johnson, and A.L. Harris. 2002. Coexpression of hypoxia-inducible factors 1alpha and 2alpha, carbonic anhydrase IX, and vascular endothelial growth factor in nasopharyngeal carcinoma and relationship to survival. Clin Cancer Res 8:2595-604.

Jenkins, W.T., S.M. Evans, and C.J. Koch. 2000. Hypoxia and necrosis in rat 9L glioma and Morris 7777 hepatoma tumors: comparative measurements using EF5 binding and the Eppendorf needle electrode. Int J Radiat Oncol Biol Phys 46:1005-17.

Kaanders, J.H., K.I. Wijffels, H.A. Marres, A.S. Ljungkvist, L.A. Pop, F.J. van den Hoogen, P.C. de Wilde, J. Bussink, J.A. Raleigh, and A.J. van der Kogel. 2002. Pimonidazole binding and tumor vascularity predict for treatment outcome in head and neck cancer. Cancer Res 62:7066-74.

Kennedy, A.S., J.A. Raleigh, G.M. Perez, D.P. Calkins, D.E. Thrall, D.B. Novotny, and M.A. Varia. 1997. Proliferation and hypoxia in human squamous cell carcinoma of the cervix: first report of combined immunohistochemical assays. Int J Radiat Oncol Biol Phys 37:897-905.

Leek, R.D., R.J. Landers, A.L. Harris, and C.E. Lewis. 1999. Necrosis correlates with high vascular density and focal macrophage infiltration in invasive carcinoma of the breast. Br J Cancer 79:991-5.

Ljungkvist, A.S., J. Bussink, P.F. Rijken, J.H. Kaanders, A.J. van der Kogel, and J. Denekamp. 2002. Vascular architecture, hypoxia, and proliferation in first-generation xenografts of human head-and-neck squamous cell carcinomas. Int J Radiat Oncol Biol Phys 54:215-28.

McCormick, D., C. Yu, C. Hobbs, and P.A. Hall. 1993. The relevance of antibody concentration to the immunohistological quantification of cell proliferation-associated antigens. Histopathology 22:543-7.

Nakayama, K., A. Kanzaki, K. Hata, H. Katabuchi, H. Okamura, K. Miyazaki, M. Fukumoto, and Y. Takebayashi. 2002. Hypoxia-inducible factor 1 alpha (HIF-1 alpha) gene expression in human ovarian carcinoma. Cancer Lett 176:215-23.

Nordsmark, M., J. Keller, O.S. Nielsen, E. Lundorf, and J. Overgaard. 1997. Tumour oxygenation assessed by polarographic needle electrodes and bioenergetic status measured by 31P magnetic resonance spectroscopy in human soft tissue tumours. Acta Oncol 36:565-71.

Nordsmark, M., M. Hoyer, J. Keller, O.S. Nielsen, O.M. Jensen, and J. Overgaard. 1996. The relationship between tumor oxygenation and cell proliferation in human soft tissue sarcomas. Int J Radiat Oncol Biol Phys 35:701-8.

Nordsmark, M., J. Loncaster, C. Aquino-Parsons, S.C. Chou, M. Ladekarl, H. Havsteen, J.C. Lindegaard, S.E. Davidson, M. Varia, C. West, R. Hunter, J. Overgaard, and J.A. Raleigh. 2003. Measurements of hypoxia using pimonidazole and polarographic oxygen-sensitive electrodes in human cervix carcinomas. Radiother Oncol 67:35-44.

Olive, P.L., J.P. Banath, and C. Aquino-Parsons. 2001a. Measuring hypoxia in solid tumours--is there a gold standard? Acta Oncol 40:917-23.

Olive, P.L., C. Aquino-Parsons, S.H. MacPhail, S.Y. Liao, J.A. Raleigh, M.I. Lerman, and E.J. Stanbridge. 2001b. Carbonic anhydrase 9 as an endogenous marker for hypoxic cells in cervical cancer. Cancer Res 61:8924-9.

Raleigh, J.A., S.C. Chou, G.E. Arteel, and M.R. Horsman. 1999. Comparisons among pimonidazole binding, oxygen electrode measurements, and radiation response in C3H mouse tumors. Radiat Res 151:580-9.

Schindl, M., S.F. Schoppmann, H. Samonigg, H. Hausmaninger, W. Kwasny, M. Gnant, R. Jakesz, E. Kubista, P. Birner, and G. Oberhuber. 2002. Overexpression of Hypoxia-inducible Factor 1alpha Is Associated with an Unfavorable Prognosis in Lymph Node-positive Breast Cancer. Clin Cancer Res 8:1831-7.

Searle, S.R., G. Casella, and C.E. McCulloch. 1992. Variance Components. John Wiley and Sons, Inc., New York.

Secomb, T.W., R. Hsu, E.T. Ong, J.F. Gross, and M.W. Dewhirst. 1995. Analysis of the effects of oxygen supply and demand on hypoxic fraction in tumors. Acta Oncol 34:313-6.

Shannon, A.M., D.J. Bouchier-Hayes, C.M. Condron, and D. Toomey. 2003. Tumour hypoxia, chemotherapeutic resistance and hypoxia-related therapies. Cancer Treat Rev 29:297-307.

Thrall, D.E., G.L. Rosner, C. Azuma, M.C. McEntee, and J.A. Raleigh. 1997. Hypoxia marker labeling in tumor biopsies: quantification of labeling variation and criteria for biopsy sectioning. Radiother Oncol 44:171-6.

Tsang, R.W., A.W. Fyles, M. Milosevic, A. Syed, M. Pintilie, W. Levin, and L.A. Manchul. 2000. Interrelationship of proliferation and hypoxia in carcinoma of the cervix. 46 46:95-9.

Varia, M.A., D.P. Calkins-Adams, L.H. Rinker, A.S. Kennedy, D.B. Novotny, W.C. Fowler, Jr., and J.A. Raleigh. 1998. Pimonidazole: a novel hypoxia marker for complementary study of tumor hypoxia and cell proliferation in cervical carcinoma. Gynecol Oncol 71:270-7.

Webster, L., R.J. Hodgkiss, and G.D. Wilson. 1998. Cell cycle distribution of hypoxia and progression of hypoxic tumour cells in vivo. Br J Cancer 77:227-34.

West, C.M., R.A. Cooper, J.A. Loncaster, D.P. Wilks, and M. Bromley. 2001. Tumor vascularity: a histological measure of angiogenesis and hypoxia. Cancer Res 61:2907-10.

Zeman, E.M., D.P. Calkins, J.M. Cline, D.E. Thrall, and J.A. Raleigh. 1993. The relationship between proliferative and oxygenation status in spontaneous canine tumors. Int J Radiat Oncol Biol Phys 27:891-8.

CONCLUSION

We found no clear relationship between tumor hypoxia and proliferation in canine spontaneous solid tumors. The clinical outcome of the dogs studied in the project is unknown at this time, but these results suggest tumor hypoxia and proliferation measurements are independent and potentially complementary predictive factors in canine spontaneous tumors.

PIMO is an excellent hypoxia marker to identify reductively active hypoxic cells. Adduct formation occurs within 20 minutes after injection and adducts are stable *in vivo* at least 72 hours. Classic diffusion limited hypoxia may be more related with intensive areas of PIMO labeling and transient perfusion limited hypoxia may not have been detected with our technique. Perfusion limited hypoxia being related to proliferation might be more complex because the areas of hypoxia are transient and such areas still might be actively proliferating under the transient hypoxic conditions.

FUTURE DIRECTION

Data for the treatment response and survival are immature and will be available for assessing whether the markers to have prognostic value in these canine spontaneous solid tumors. The degree of hypoxia varied significantly between different types of tumors and a reference value should be set for each type of tumor. For example, soft tissue sarcomas consist of several different histologic types including fibrosarcoma, hemangiopericytoma, neurofibrosarcoma and others, but for the marker based study, the consistency of histologic features had an influence on quantification of PIMO labeled area. Geographic Information System (GIS) analysis might be one way to examine the analysis of regional relationships systematically.

Because PIMO detects hypoxia at the cellular level, not only can the spatial patterns of hypoxia be investigated relative to adjacent histologic landmarks, but more importantly, it offers the opportunity to isolate cells for a biologic study such as gene expression in response to hypoxia. Pimonidazole can also be used a targeting agent for hypoxic cells such as for hypoxia responsible gene therapy.

APPENDICES

1. Pimonidazole study form
2. Procedure for analyzing plasma kinetics of pimonidazole
3. Pimonidazole staining procedure
4. Pimonidazole staining working sheet
5. PCNA staining procedure
6. PCNA staining working sheet
7. PCNA counting sheet

Appendix 1: Pimonidazole study form

Pimonidazole biopsy study

stamp here for patient information

Pathology number :
Tumor type:
Tumor location:
Tumor dimension:
Body Weight(kg):
BSA(m^2):

Amount of pimonidazole HCl ( ) gm
Multiply BSA ( ) m^2 x 0.5 gm/ m^2 = ( ) gm
Amount of 0.9 % NaCl ( ) ml
Amount of pimo. HCl ( ) gm / 0.28 gm x 50 ml = ( ) ml 0.9% NaCl
Pimonidazole administered iv on / / @ :
PK: Yes / No MRI date / / @ :

Biopsy time 24h post / / @ :
72h post / / @ :

Draw biopsy sites and attach Polaroid picture :

Prepared by _____ Date _____

Appendix 2: Procedure for analyzing plasma kinetics of pimonidazole

1. Collect 2 ml of blood samples in heparinized tube
2. Centrifuge samples for 10' at 3000 RPM to separate plasma and RBCs.
3. Remove plasma
4. Precipitate plasma proteins by addition of acetonitrile (1 : 1 = CAN : plasma)
5. Centrifuge samples for 15' at 5000 RPM.
6. Dry samples under stream of air.
7. Resuspend samples in 13.6 uM Etanidazole in 0.9% saline solution for use as internal standard.
8. Inject 100 ul aliquot for analysis by HPLC.

HPLC system:

- Solvent: 30% MeOH (300 ml): 69% H2O (690 ml): 1% Trifluoroacetic Acid (10 ml)
- Flow Rate: 1.0 ml/min
- Column: Alltech Alltima C18 (250 x 4.6 mm, 5 u particle size) with guard column
- Detection wavelength: 324 nm by means of a Spectra Physics model 8450 variable wavelength detector.
- Retention times:
    i. Etanidazole 3.65'
    ii. Pimonidazole 5.10'
    iii. PIMO N-Oxide 6.15'

Appendix 3: Pimonidazole staining procedure

Procedure title				Prepared by Date	
Step		**Station**	**Solution**	**Time**	**Comments**
1		1	100% xylene	10x Dip & Blot	Deparaffinize
2		2	100% Ethanol	10x D & B	Rehydrate
3		3	95% Ethanol	10x D & B	
4		4	80% Ethanol	10x D & B	
5		5	UPH2O + 0.2% BRIJ 35	10x D & B	
6		6	PBS+0.2%BRIJ	10x D & B	
7		7	3% H2O2 in H2O	15 min@hu.40°C	Inactivate
8		6	PBS+0.2%BRIJ	10x D & B	
9		10A	PRONASE	25 min @hu.40°C	Digestion
10		6	PBS+0.2%BRIJ	10x D & B	
11		10B	Blocking serum	30min @hu.40°C	Block(yellow)+A
12		11A	Primary antibody (poly#27-10) *negative control*	1 hrs@hu.40°C 1:2000	1° Ab +B in 50mM PBS
13		Flat	PBS+0.2%BRIJ	2min	
14		10C	Secondary antibody	30min @hu.40°C	2° Ab(blue)
			Prepare : ABC RGT(in PBS)	@ 37°C for30min	(grey)
15		Flat	PBS+0.2%BRIJ	2min	
16		11B	ABC RGT	30min @hu.40°C	Label(grey)
17		Flat	PBS+0.2%BRIJ	2min	
			Prepare AEC-HRP (in glass tube) Turn on SLIDE Warmer (80°C)	just before use	
18		12B	AEC-HRP	20 min@RT	Chromogen
19		Coplin	Running d H2O in Coplin Jar	2 min	
20		Flat	Aqua Hematoxylin	1.5 min	Counterstain
21		Coplin	Running d H2O in Coplin Jar	2 min	
22		Coplin	PBS+0.2%BRIJ	1 min	
23		Coplin	Running d H2O in Coplin Jar	2 min	
			Wipe back		
			Place on warmmer		
			Add 2-5 drops crystal mount		
24			Heat slides	20 min	

Appendix 4: Pimonidazole staining working sheet

DATE: EXPER.: PREPARED BY

PURPOSE:

BUFFER: 10mM PBS + 0.2%BRIJ35

KIT: VECTASTAIN ABC "ELITE" RABBIT IgG (PK-61 DATE EXP:

Block 200ul normal goat serum DATE DIL.:

10ml PBS 20 drop Avidin

1°AB: 1:2000(#27-10) DATE PREP.:

make 1:100(40ul:4000ul) (500:9500) DATE DIL.:

10ml 50mM PBS + BRIJ 20 drop Biotin

200ul normal goat serum

2°AB: 50ul Biotinylated antibody (1drop) DATE PREP.:

10ml PBS 200ul normal goat serum DATE DIL.:

SUBSTRATE AEC(RED) COUNTERSTAIN: AQUA HEMATOXYLIN

TYPE OF SECTION: Paraffine SAMPLE SPECIES: DOG

SAMPLE FIXATION: 10%NBF NUMBER OF SLIDS:

DESCRIPTION OF SLIDES:

Folder		name	patho #	sample #	slide #	comment
1	1					
	2					
2	3					
	4					
3	5					
	6					
4	7					
	8					
5	9					
	10					
6	11					
	12					
7	13					
	14					
8	15					
	16					
9	17					
	18					
10	19					
	20					

Preincubation @ 40°C(>20min) Start: End: Total :

COMMENT:

Appendix 5: PCNA staining procedure

Procedure title			Prepared by	
			Date	
Ste	Station	Solution	Time	Comments
1	Incubator	dry bath	>15min @ 40°C	
2	1	100% xylene	10x Dip & Blot	Deparaffinizing
3	2	100% Ethanol	10x D & B	Rehydrating
4	3	95% Ethanol	10x D & B	
5	4	80% Ethanol	10x D & B	
6	5	UPH2O + 0.2% BRIJ 35	10x D & B	
7	6	10 mM PBStb	10x D & B	
8	10A	Bottle #1	5 min. @ RT	Inavtivating
9	6	10 mM PBStb	10x D & B	
10	Flat	1°Ab a-PCNA1:50	15 min.	negative control
11	coplin jar	10 mM PBStb	2 min.	
12	Flat	Bottle #3	10 min.	
13	coplin jar	10 mM PBStb	2 min.	
14	Prepare DAB (Bottle #4): 1 ml #4A + 40 ul #4B / 4-5 slides			
15		Bottle #4	5 min.	DAB-HRP
16	Turn on SLIDE Warmer (80°C)			
17	coplin jar	UP H2O	2 min.	
18	Flat	Aqua Hematoxylin	35 sec.	Counterstain
19	coplin jar	running DD H2O	2 min.	
20	coplin jar	10 mM PBStb	1 min.	
21	coplin jar	running DD H2O	2 min.	
22	Slide warmer	Wipe back		Heat slides
		Place on warmmer		
		Add 2-5 drops crystal mount		

Appendix 6: PCNA staining working sheet

GENERAL PROCEDURE: **DATE:**

1 Reffer to the Microprobe Procedure Log Sheet

2 **Slide Incubation** @ 40°C ,at least 15 min.
start: stop Total time:

3 **Deparaffinizing and Rehydrating**
Station 1: 100% Xylene; Prep:
Station 2: 100% Ethanol; Prep:
Station 3: 95% Ethanol; Prep:
Station 4: 80% Ethanol; Prep:

4 **Prep Station 5: 100ml upH2O + 0.2ml BRIJ35;**
Date stock prepared:

5 **Prep Station 6: (PBStb) 200 ml of 10mM PBS**
1 tab. PBS+2ml TRITON X-100+0.4ml BRIJ35,bring to 200ml vol.
with UP H20

6 **1°AB (Monoclonal a-PCNA)**
a. Make 10ml of Primary Ab.Dilution Buffer (PADB):
10ml of 10mM PBStb + 100ul of normal horse serum
b. 1:50 dilution: 1ml PADB + 40ul PCNA stock

7 **NUMBER OF SLIDES:**

8 **DESCRIPTION OF SLIDES:**

	name & path#	tissue#		slice	memo
1					
2					
3					
4					
5					
6					
7					
8					
9					
10					
11					
12					
13					
14					
15					
16					
17					
18					
19					
20					

MEMO/COMMENT

Appendix 7: PCNA counting sheet

Patient Name: ____________________ Patient Number: ____________

Pathology Number: ____________ Pimo administration: ____________

XRT: ____________________ LH: ____________________

tissue #	date	Bx		Comments:	
1		N	P		
2		N	P		
3		N	P		
4		N	P		
5		N	P		
6		N	P	result: 1	
7		N	P	2	
8		N	P	3	
9		N	P	4	
10		N	P	sum	
11		N	P		
12		N	P		

tissue#	Count																				
	1																				
	2																				
	3																				
	4																				
	sum																				
	1																				
	2																				
	3																				
	4																				
	sum																				
	1																				
	2																				
	3																				
	4																				
	sum																				
	1																				
	2																				
	3																				
	4																				
	sum																				

Magnification: ________ Method: ____________________

Completed by: ____________________ Date Completed: ________